Minimal Admissible Control of Constrained Static Linear Systems with Applications to Power Systems

Dem Fachbereich
Elektrotechnik und Informationstechnik
der Technischen Universität Darmstadt
zur Erlangung des akademischen Grades eines Doktor-Ingenieurs (Dr.-Ing.)
genehmigte Dissertation
von

Edwin Camilo Mora Gil, M.Sc.
geboren am 9. Januar 1991 in Bogotá

Referent:	Prof. Dr. rer. nat. Florian Steinke
Korreferent:	Prof. Dr.-Ing. Timm Faulwasser
Tag der Einreichung:	30.11.2021

TECHNISCHE
UNIVERSITÄT
DARMSTADT

D 17 · Darmstadt 2021

Edwin Camilo Mora Gil
Minimal Admissible Control of Constrained Static Linear Systems with Applications to Power Systems
Darmstadt, Technische Universität Darmstadt
Tag der mündlichen Prüfung: 21.02.2022

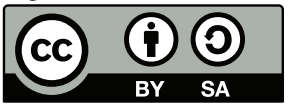

Kurzfassung

Im Zuge der Energiewende ist eine Anpassung der derzeitigen Entscheidungsalgorithmen im Stromnetzbetrieb erforderlich. Voraussetzung dafür ist die Auslegung neuartiger Regelalgorithmen, welche trotz der intrinsischen Unsicherheiten der erneuerbaren und dezentralen Stromerzeugung den Ausgleich zwischen Erzeugung und Verbrauch sicherstellen. Dabei nimmt die Anzahl der im Netz installierten Steuer- und Messgeräte rapide zu, was unvermeidbare cyber-physische Schwachstellen impliziert. Künftige Stromnetze erfordern daher eine Erhöhung der Resilienz gegenüber unerwarteten, folgenschweren Ereignissen wie Naturkatastrophen oder Cyber-Angriffen.

Vor diesem Hintergrund und unter Abstraktion des Stromnetzes als beschränktes statisches lineares System wird in dieser Arbeit ein neuartiges mathematisches Konzept für die Charakterisierung und Berechnung zulässiger Regelgesetze entwickelt. Ein zulässiges Regelgesetz wird als eine Ausgangsrückführung verstanden, welche den Messgrößen spezielle Regelungsaktionen zuordnet, die immer zu einem möglicherweise unsicheren, aber zulässigen Systemzustand führen. Ein zentraler Aspekt dieser Arbeit stellt die Untersuchung dar, wie die Existenz zulässiger Regelgesetze zu verifizieren ist. Obwohl dies im Allgemeinen einen enormen Rechenaufwand erfordert, wird gezeigt, dass dafür in einigen Spezialfällen ein endlich dimensionales Machbarkeitsproblems abzuleiten ist. Zudem wird veranschaulicht, dass unter geeigneten Annahmen ein zulässiges Regelgesetz immer als eine stückweise-affine Funktion formuliert werden kann, die ent-weder *online* mittels Methoden der linearen Optimierung oder *offline* durch Lösung eines zweistufigen multiparametrischen linearen Optimierungsproblems berechenbar ist. Darüber hinaus kann ein zulässiges affines Regelgesetz oftmals effizient durch lineare Optimierung bestimmt werden, sofern dieses existiert.

Außerdem werden im Rahmen dieser Arbeit Algorithmen vorgestellt für 1) die Berechnung von unteren/oberen Grenzen für die minimale Anzahl von Aktuatoren und Sensoren, die die Existenz eines zulässigen Regelgesetzes garantieren, 2) den Entwurf zulässiger Regelgesetze, die zusätzlich robust gegenüber unerwarteten, böswilligen Manipulationen einiger Aktuator-/Sensorsignale sind, und 3) die Berechnung zulässiger, affiner Regelgesetze für lineare, zeitinvariante Systeme mit Beschränkungen.

Schließlich wird das Potenzial der vorgestellten Ideen anhand verschiedener Anwendungen im Bereich der Lastflussregelung demonstriert. Insbesondere finden die neuartigen Methoden Anwendung zur Identifikation kritischer Generator- und Sensorsignale für eine robuste Lastflussregelung in Übertragungsnetzen. Zusätzlich wird die Entwicklung robuster Spannungs-/VAr-Regelungsstrategien für Verteilungsnetze erläutert, welche eine große Anzahl von Photovoltaikeinheiten besitzen und/oder für den Fall, dass gestörte Sensorsignale vorliegen. Die in dieser Arbeit vorgestellten neuartigen Werkzeuge werden die Netzbetreiber von Übertragungs- und Verteilnetzen bei der Entscheidungsfindung in Fragen der Netzplanung und des Netzbetriebes im Hinblick auf die Herausforderungen der Energiewende unterstützen.

Abstract

The path to the energy transition calls for adaptation of current decision-making algorithms in power grid operations. On this premise, novel control algorithms are desired such that the intrinsic uncertainty accompanying renewable/decentralized power generation does not jeopardize the balancing between power supply and demand. More challenging, the number of control and monitoring devices installed in the grid is growing rapidly, which inevitably introduces cyber-physical vulnerabilities. Future power systems must hence incorporate an enhanced operational resilience against unexpected, high-impact events like natural catastrophes or cyber-physical threats.

With the above scope, and abstracting the power network as a constrained static linear system, this thesis contributes a novel mathematical framework for the characterization and computation of admissible control laws. An admissible control law is understood as a feedback mapping that assigns measured quantities to control actions that always result in a possibly uncertain, but feasible system state. A central part of this thesis investigates how to verify the existence of admissible control laws. Although such verification task is in general computationally challenging, we show that in some special cases it turns into solving a finite dimensional feasibility problem. We also prove that, under appropriate assumptions, an admissible control law can always be chosen to be a piecewise-affine function that is computable either *online* via linear programming, or *offline* by solving a two-stage multiparametric linear optimization problem. In addition, the existence of admissible affine control laws can in many cases be verified efficiently by solving a linear optimization problem that also yields an admissible realization for the control law if one exists.

Furthermore, our framework provides algorithms for 1) the computation of lower and upper bounds for the minimal number of actuators and sensors that guarantee the existence of an admissible control law, 2) the design of admissible control laws that additionally cope with unexpected, malicious manipulation of some actuator/sensor signals, and 3) the computation of admissible affine output feedback control laws for constrained, linear time-invariant systems.

We finally illustrate the potential of our ideas with various applications in power flow control. Particularly, we apply our methods to identify critical generator and sensor devices for robust active power flow control in transmission networks. Besides, we show how to design robust voltage/VAr control policies for distribution networks having a large amount of photovoltaic generation units combined with imperfect observations. The set of novel tools presented in this thesis will assist both transmission and distribution system operators in many grid operation and planning tasks towards achieving the energy transition.

Table of Contents

Symbols and Acronyms

Symbols

Sets

$\mathbb{R}$	Real numbers
$\mathbb{C}$	Complex numbers
$\mathbb{Z}$	Integer numbers
$\mathbb{N}^+$	Natural numbers without zero
$\mathcal{C} \subset \mathbb{N}^+$	Set of actuators
$\mathcal{M} \subset \mathbb{N}^+$	Set of sensors

Scalars

$\lvert\mathcal{C}\rvert$	Cardinality of $\mathcal{C}$
$\lvert\mathcal{M}\rvert$	Cardinality of $\mathcal{M}$

Vectors

$\boldsymbol{x}$	$\in \mathbb{R}^{n_x}$	State
$\boldsymbol{u}$	$\in \mathbb{R}^{n_u}$	Action
$\boldsymbol{u}_\mathrm{c}$	$\in \mathbb{R}^{\lvert\mathcal{C}\rvert}$	Control action
$\boldsymbol{u}_\mathrm{f}$	$\in \mathbb{R}^{n_u-\lvert\mathcal{C}\rvert}$	Exogenous action
$\boldsymbol{y}$	$\in \mathbb{R}^{n_y}$	Measurable output
$\boldsymbol{y}^\mathrm{m}$	$\in \mathbb{R}^{\lvert\mathcal{M}\rvert}$	Measured output
$\boldsymbol{y}^\mathrm{u}$	$\in \mathbb{R}^{n_y-\lvert\mathcal{C}\rvert}$	Unmeasured output
$\mathbf{I}$		Identity matrix of suitable dimensions
$\mathbf{1}$		Vector of ones of suitable dimension
$\mathbf{0}$		Matrix of zeros of suitable dimensions

Acronyms

AC	Alternating Current
BMI	Bilinear Matrix Inequality
CR	Critical Region
DC	Direct Current
DER	Decentralized Energy Resources
DSO	Distribution System Operator
EMPC	Explicit Model-Predictive Control
IEEE	Institute of Electrical and Electronics Engineers
HC	Hill Climbing
KKT	Karush-Kuhn-Tucker
IEA	International Energy Agency
LMI	Linear Matrix Inequality
LP	Linear Programming
LTI	Linear Time-Invariant
LQR	Linear-Quadratic Regulator
MILP	Mixed-Integer Linear Programming
MPC	Model Predictive Control
MPP	Multiparametric Programming
MPLP	Multiparametric Linear Programming
OPF	Optimal Power Flow
OSS	Optimal Steady State
PCE	Polynomial Chaos Expansion
PV	Photovoltaic
PWA	Piecewise-affine
QCQP	Quadratically Constrained Quadratic Programming
RTO	Real-time Optimization
SDP	Semidefinite Programming
SOCP	Second-Order Cone Programming
TSO	Transmission System Operator

1 Introduction

1.1 The Big Picture

Electricity is a fundamental service for the daily life in modern human societies. According to the International Energy Agency (IEA), the total global power consumption in 2018 was about 22316 TWh [1]. This demand was covered more than half by conventional power plants fired with coal (38%), natural gas (23%), and oil (2.9%). Yet, electricity generation from renewable sources like wind (4.8%) and solar (2.1%) registered a strongly positive growth.[1] In Germany, the total combined solar and wind electricity generation (circa 183 TWh) surpassed fossil-fuel generation (ca. 178 TWh) in 2020 [2].

This transformation meets one of the most elaborate and complex technical systems ever made by humankind. A power grid has to be controlled to keep the balance between power consumption and generation at all times, independently of changes in electricity generation and demand, weather conditions, and in the event of unexpected outages of various software and/or hardware assets, among others. Assisted by monitoring systems that periodically provide information about the state of the grid (e.g., actual power demand and generation), network operators make complex decisions that are communicated as commands to local (fully) automated controllers for implementation.

Electricity was traditionally generated by a rather small number of large conventional power plants and delivered to the consumers in a unidirectional fashion. This is illustrated on the left of Fig. 1.1. In the traditional, hierarchical approach, the generated power is transported through a high voltage transmission network to electrical substations, from which the power is distributed via lower voltage grids to the final consumers.

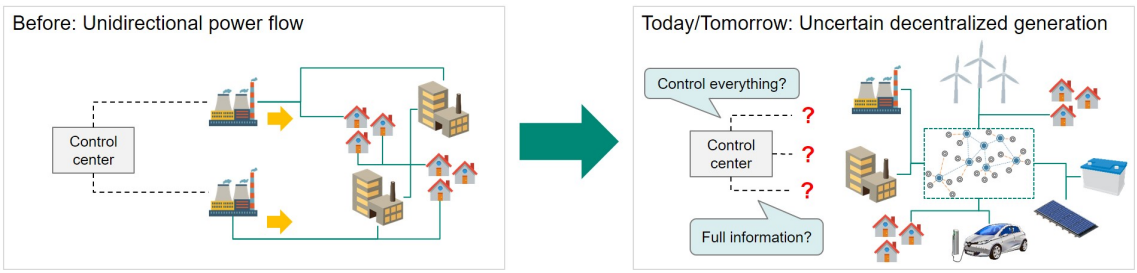

Figure 1.1: Comparison of past and current/future operation of power networks.

[1] $(+12,4\%)$ wind and $(+24.3\%)$ solar with respect to 2017.

This traditional setting allowed system operators to reliably control the power flowing through the grid with reasonable efforts, as the electricity generated by the few power plants could be coordinated globally at the transmission level based on demand forecasts. Transmission grids thus had a high degree of automation compared to distribution networks, which were operated solely to carry electricity to individual consumers.

This paradigm is, however, changing rapidly due to the rise of renewable generation as indicated above. Concretely, power grids are turning into cyber-physical networks connecting a large and growing number of rather small decentralized producers with the consumers. This is illustrated on the right side of Fig. 1.1. These decentralized generation units produce electricity by using renewable energy resources like wind and sun as their fuel, and consumers have the possibility of installing their own generation units locally.[2] All of this, together with current innovations like electromobility and storage technologies, represents new challenges for both Transmission System Operators (TSO) and Distribution System Operators (DSO) in order to maintain an uninterrupted equilibrium between power generation and demand with minimum operational costs. In particular, the volatility of renewables combined with other flexibilities (e.g., storage units, electric vehicles, power-to-heat, load management [4, 5], among others) can quickly bring current power grids to contingency situations, like overloads in power substations [6] or over/undervoltages in distribution networks [7], if the controllable generation units are not operated properly. At the same time, the number of installed sensors and controllable devices is growing fast [8] (particulary in distribution networks),[3] which on the one hand increases system efficiencies, but on the other hand introduces vulnerabilities in the automation infrastructure [12].

1.2 Scope of the Thesis

The paradigm shift in power grid operations described above clearly calls for adaptation of traditional power flow control techniques in order to cope with the uncertainty and volatility introduced by the large amount of decentralized generation units installed at all grid levels. Under this premise, the aim of the present dissertation is to provide a set of novel tools that assist both TSOs and DSOs in many decisions related to power flow control applications. More specifically, this dissertation focuses on how to solve power flow control problems for which static representations of power systems are considered. This class of control problems arises when system operators have to periodically (typically in time intervals of 15 min) decide on how to choose suitable set point signals for those

[2]The term *prosumer* is a portmanteau word coined by Alvin Toffler [3] that in the context of power systems refers to individuals being able to produce and consume electricity.

[3]According to the IEA, a record of 133 GW of PhotoVoltaic (PV) capacity was installed globally in 2020 [9]. In particular, the total number of installed PV systems in Germany reached ca. 2 million [10]. Besides, the IEA reports that the global stock of electric vehicles in a sustainable development scenario can reach more that 200 million units by 2030 [11].

quantities they can manipulate (e.g., generator power set points) based on those quantities they can measure (e.g., grid frequency) such that a set of operational constraints are fulfilled independently of the value of those quantities determined by other system users (e.g., power demand). Since the number of decentralized and uncertain prosumers connected at all grid levels is growing rapidly, the achievement of the control task above introduced is becoming more challenging for both transmission and distribution system operators.

Another central point investigated in this dissertation is how to identify those (few) critical quantities in the grid that have to be manipulated and measured by the system operator in order to solve the static control task described above. A systematic solution approach is fundamental here, since the number decentralized generation units connected to the grid is growing rapidly, and with them the number of available sensors and controllable devices. Deciding which automation devices are (not) to be accessible by the system operator is thus becoming difficult in practice. Let us now illustrate the niche of this dissertation with the following oversimplified example.

Example 1. Consider the simple microgrid depicted in Fig. 1.3 at steady state. The power system consists of three generators that should supply a constant demand of 5 MW. The small generators located at buses 1 and 2 have a maximum capacity of 1 MW and can be interpreted as decentralized generation units. Moreover, the generator located at bus 4 has a maximum capacity of 10 MW and can be interpreted as a synchronous generator with a droop constant of 4 MW/Hz.[4] The goal is to maintain the frequency deviation always within ± 0.1 Hz at steady state, which is a typical operational constraint in power flow operations. For simplicity, we intentionally set large capacity limits for the transmission lines such that only the constraint on the frequency deviation is relevant here.

In order to keep the operational costs at a minimum, the system operator has now to decide about which generators are to be manipulated or monitored by him, and which ones are to be left free to be manipulated by other users. After making this decision, the system operator has to find a control policy that always determines set points for the manipulable generators for which the constraint on the frequency deviation is fulfilled.

For this particular example, an experienced practitioner will note that at least the power set point of the large generator has to be controlled by the system operator based on measurements of the power injections at buses 1 and 2, see Fig. 1.3. The reason is that the large generator alone can supply the demand by setting a suitable power set point. However, such set point has to be chosen based on the joint power produced by the small

[4] Synchronous machines have an inherent inertia that is crucial to compensate frequency fluctuations in the short term (up to 5 s) [13]. To support this task, a *primary droop control* regulates the local generator rotational speed by proportionally adapting the active power generated by the machine based on local frequency measurements. This process takes place in a time scale of tens of seconds [14]. Remarkably, recent developments allow system operators to integrate *low inertia* generation units (e.g., batteries, wind, and solar producers connected to the grid via power electronic interfaces) into the primary control scheme [13].

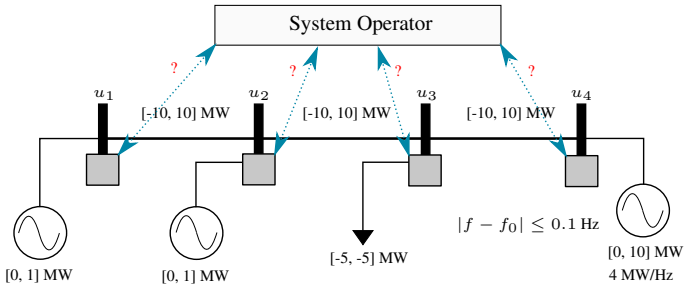

Figure 1.2: An exemplary microgrid with constant electricity demand. The generation units are subject to lower and upper bounds. To always fulfill the frequency constraint with minimum operational costs, the grid operator has to determine the smallest set of generators he has to manipulate and monitor.

decentralized units, as otherwise the total generation can surpass the demand such that the resulting frequency deviation exceeds the maximum allowed value 0.1 Hz. Note that the power injected by the decentralized generation units is not necessarily to be manipulated by the system operator and can be left free to be determined by other users.

Using the notation provided in Fig. 1.3, the system operator has now to find a control policy $u_4 = k(u_1, u_2)$ that always guarantees a frequency deviation within ± 0.1 Hz. For this simple example, an affine policy $u_4 = \alpha + \beta(u_1 + u_2)$ parametrized by $\alpha, \beta \in \mathbb{R}$ can be designed by using the parameters of the large generator together with the limits of the decentralized generators. For instance, we can set the large generator to match the demand when the small units are not producing power (i.e., $u_4 = \alpha = 5$ MW if $u_1 = u_2 = 0$ MW), and accept the maximum frequency deviation when both small generators are producing with maximum capacity. Here it is important to observe that, when the frequency deviation is maximum, the maximum allowed power deviation between generation and demand is given by 0.1 Hz $\cdot$ 4 MW/Hz = 0.4 MW, i.e., a total generation of 5 ± 0.4 MW is admissible. Thus, one possible choice for the power set point of the large generator given that $u_{1,2} = 1$ MW is $u_4 = 5 + 0.4 - 2 = 3.4$ MW.

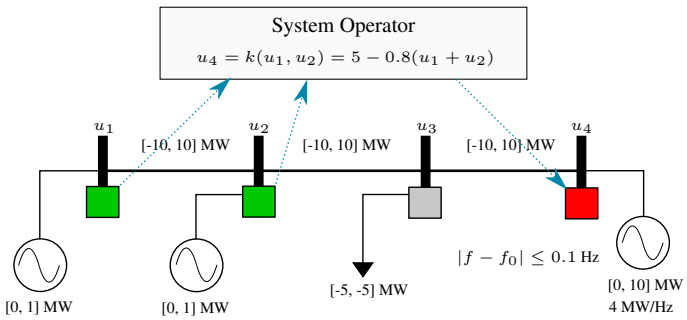

Figure 1.3: To fulfill the constraint on the grid frequency, the system operator only has to manipulate the power set point of the large generator (red box) based on measurements (green boxes) of the power generated by the small generation units. Although the electricity produced by the small generators is determined by external users, the affine policy implemented by the system operator is guaranteed to always yield a suitable power set point for the large generator.

The scalar β can therefore be obtained based on the above considered worst-case situation $u_{1,2} = 1$ MW, i.e.,

$$u_4 = 3.4 = 5 + \beta(1+1) = 5 + 2\beta \Rightarrow \beta = \frac{3.4 - 5}{2} = -0.8,$$

which yields the policy $u_4 = 5 - 0.8(u_1 + u_2)$. □

While for the demonstrated example all solutions can readily be verified manually, it shows that the situation may become much more complex in larger transmission and distribution grids. The topological location of generators and loads in the grid is important as well as their capacity and their neighborhood. An automated tool for selecting critical elements to control and/or measure is thus very beneficial for complex power networks with high penetration of renewable distributed generation and with transmission lines that are operated close to their technical limits.

In order to cope with the cyber-physical vulnerabilities introduced by the increasing number of sensors and controllable devices connected to the grid [12], future power flow control methods are also required to go beyond existing $N - \mathsf{k}$ contingency management strategies [15, 16]. This will allow system operators to keep the balance between power supply and demand even if some sensor or actuator signals are intentionally corrupted by external agents. Innovations to enhance the operational resilience of the power grid against unexpected, high-impact events are thus desired.

1.3 Research Questions

Consider a power grid at steady state being represented mathematically as a system of linear (in)equalities, such as illustrated by Example 1. Then, the following research questions emerge naturally from the above discussion:

1. Under which conditions can we guarantee the existence of an *admissible* control policy, namely a feedback mapping that, based on a set of measured quantities, always determines control actions that result in a system state that might not be uniquely determined but is guaranteed to be feasible?

2. Provided that there exists such an admissible control policy, how can we compute one efficiently?

3. What are the (few) actuator and sensor devices in the system that are critical for guaranteeing the existence of an admissible control policy?

4. How to cope with distortions of some actuator and sensor signals (accidental or malicious)?

5. How does an admissible control policy affect the stability of the overall system over time?[5]

Concerning the applications to power systems we ask:

1. In transmission networks, what is the smallest set of controllable prosumers and sensor devices allowing for the existence of an admissible control policy?

2. In distribution networks, how to always maintain admissible voltage levels despite the high penetration of renewables and the low degree of observability?

1.4 Contributions

To address the above research questions, we first introduce a **novel mathematical framework** for the control of **constrained static linear systems**, i.e., steady state systems described by a set of linear (in)equalities [20]. The proposed framework allows the system operator to determine control actions based on few measured quantities. Such control actions are guaranteed to be valid for any state that could produce such observation. Although the resulting system state is often not exactly determined, it is guaranteed to be feasible. The framework thus does not require any state estimation stage. In addition, control actions and observations being either corrupted with noise or distorted by (malicious) external agents can be integrated as well, even if the controller has no knowledge about the disturbances, but just about the possible size of these.

Throughout this thesis, we then propose **several novel algorithms** for verifying the existence of such admissible control policies under appropriate assumptions. The novel set of algorithms is built based on tools from mathematical optimization and control theory. We also show that, in some special cases, piecewise-affine admissible control policies can be computed efficiently via (multiparametric) linear optimization techniques [21]. Moreover, the **minimum number of actuators and sensors** required to guarantee the existence of an admissible control policy can in some cases be found by solving a mixed-integer linear program [20, 22]. For the general case, we also propose a heuristic minimization method based on hill climbing optimization.

We illustrate the potential of our novel framework and the associated control algorithms with many power system examples. Particularly, we demonstrate how to apply our methods to identify critical generator and sensor devices for **robust active power flow control** in transmission networks [20, 22]. We show that in many cases a small number of controlled generators and power flow measurements is sufficient to always guarantee a feasible grid state. Besides, we show how to design **robust voltage/VAr control** policies

[5] In the literature of power systems, the term *stability* has different interpretations depending on the context, e.g., frequency/voltage stability, large/small disturbance stability, short-/long-term stability, etc. [17]. To avoid misinterpretations, this thesis adopts the notion of (asymptotic) stability utilized in the study of linear time-invariant systems [18, 19]. This notion is formally introduced in Chapter 6.

for distribution networks having a large amount of photovoltaic generation units [23]. In this application, our policies keep the voltage levels across the network within a desired range of values independently of the power consumption/generation profile at each node. To this end, the proposed policies use a small number of measured voltages and power injections to manipulate the on-load-tap changer of the substation transformer together with the reactive power injected by a small number of photovoltaic units. Under some assumptions, our control algorithms additionally tolerate the exogenous distortion of a small number of actuator/sensor signals.

We finally remark that our methods are derived from abstract mathematical formulations, which extends the range of applications beyond the power system domain. Moreover, we show that our ideas are compatible with the description of constrained linear time-invariant systems at steady state. In particular, we study how to design affine output feedback control laws guaranteeing the **asymptotic stability** of the resulting closed-loop system as well as the fulfillment of a set of operational constraints at steady state [24].

Various parts of this thesis have been previously published by the author of this dissertation:

2021

[20] E. Mora and F. Steinke. "On the minimal set of controllers and sensors for linear power flow". In: *Electric Power Systems Research* 190 (2021). Presented at the 21st Power Systems Computation Conference (PSCC) 2020, p. 106647

[23] E. Mora and F. Steinke. "Robust voltage regulation for active distribution networks with imperfect observability". In: *2021 IEEE Madrid PowerTech*. 2021, pp. 1–6

2020

[24] E. Mora and F. Steinke. "Minimal Control of Constrained, Partially Controllable & Observable Linear Systems". In: *IFAC-PapersOnLine* 53.2 (2020). Presented at the 21st IFAC World Congress 2020, pp. 4521–4526

[22] E. Mora and F. Steinke. "Computing sparse affine-linear control policies for linear power flow in microgrids". In: *2020 IEEE PES Innovative Smart Grid Technologies Europe (ISGT-Europe)*. 2020, pp. 364–368

The use of elements of the publications listed above is not explicitly referred anymore in subsequent chapters.

1.5 Related Work

As mentioned previously, this thesis focuses on power flow control problems for which steady state system representations of the system are used. Power flow control problems involving dynamics and performance over time, e.g., the design of primary and secondary [14, 25, 26, 27] controllers, are not studied in great detail in this thesis.[6]

The ideas presented in this thesis are related to work on robust optimization [28], combinatorial optimization [29], and control theory [30, 12] applied to solve many power flow control problems. In the following, we briefly review the most important lines of related work. More detailed literature references are provided in the subsequent chapters of this dissertation.

Robust Optimal Power Flow. We identify two lines of research that incorporate the inherent uncertainty of decentralized renewable generation in power flow control: deterministic approaches and probabilistic approaches.

In the deterministic setting, the sources of uncertainty are supposed to be bounded by a pre-specified uncertainty set. The task is then to find a suitable control action that is valid *for all* elements in the uncertainty set [28]. This is typically achieved numerically by solving either a multilevel [31, 32] or a multi-stage optimization problem [33, 34]. Note that when the uncertainty set is convex, such formulations can in many cases be reduced to single step optimization problems [35]. Although the resulting control action, if it exists, is guaranteed to be valid for all elements in the uncertainty set, its conservativeness depends strongly on the choice of the uncertainty set [36, 37]. As we discuss later, this thesis extends current robust power flow formulations by integrating measurement-dependent uncertainties.

The second line of research models the uncertainties as random variables subject to a priori known probability distributions. The task is then to find a control action that is valid *for many* realizations of the uncertainties and/or performs well on average. Scenario-based approaches [38, 39, 40] are popular here, and various chance-constrained problem formulations have been developed specially for Gaussian-distributed uncertainties. For other probability distributions, novel techniques based on Polynomial Chaos Expansion (PCE) have been proposed [41]. Although such methods are known to be computationally expensive, an efficient implementation of PCE methods has been recently obtained by exploiting the structure of the power flow equations [42]. Another interesting technique for solving chance-constrained optimization problems that 1) combines deterministic robust optimization with scenario-based optimization, and 2) does not require prior knowledge of the underlying probability distributions has been proposed in [43]. Probabilistic approaches are not covered by the scope of thesis.

[6] Chapter 6 addresses the problem of asymptotic stability for constrained linear time-invariant systems. A detailed review on optimization and control algorithms for power system applications is given in [26].

Multiparametric Programming. MultiParametric Programming (MPP) considers optimization problems which are given in terms of (time-)varying parameters. Instead of solving the optimization problem for any given parameter realization, optimal solutions are computed as a function of the varying parameters without exhaustively enumerating the entire parametric space [44, 45]. In fact, it has been shown that the explicit solution over the parameter space can in many cases be obtained in a piecewise fashion [44, 46, 47]. To this end, the parameter space is systematically partitioned into subsets, typically called Critical Regions (CR). Then, for each critical region, a closed-form policy is computed. Multiparametric programming has found particular application in the field of Explicit Model Predictive Control (EMPC) [48, 49, 50, 51].[7] We found applications in power system operations [53, 54] as well. In this thesis, we show that admissible piecewise-affine control policies can often be computed offline via multiparametric linear optimization techniques, at least for systems having a small number of uncertainties.

Minimal Actuator and Sensor Sets. The optimal input/output selection problem [55] has recently become very attractive in the context of controlling complex networks [56] modeled as Linear Time-Invariant (LTI) systems. Here, algorithms based on (structural) controllability/observability [57, 58, 59], minimum energy control [60], properties of the controllability Gramian [61, 62], among others, have been proposed to find the minimum number of actuators. By applying the duality principle of LTI systems [63], the same ideas can be employed for determining the smallest number of sensors. Another related line of works employs a mixed-integer Bilinear Matrix Inequality (BMI) formulation to simultaneously find the smallest number of actuators and sensors required to compute an output feedback controller that guarantees closed-loop asymptotic stability [64, 65, 66]. Ideas for the synthesis of sparsity-promoting state feedback laws guaranteeing asymptotic stability have also been investigated [67, 68, 69]. We note that most of the work has been done for unconstrained LTI systems [70]. In this thesis, we integrate state and input constraints for the steady state into the actuator/sensor selection problem, and focus our investigation mainly on control policies for static systems.

Constrained Closed-loop LTI Systems and Extremum Seeking. Contrary to control techniques based on invariant sets [71, 72] with application to state feedback control, we do not require constraints on states, inputs, or outputs to be fulfilled at all times but only for the steady state. In addition, we focus on output feedback control strategies not requiring an observer.

Our research is related to the idea of *Real-Time Optimization* (RTO), a term coined in the literature of process control [73, 74, 30] that is also applied in power system operations, e.g., voltage regulation problems [26]. The idea is to design a model-based,

[7] In this thesis, the acronym EMPC is not to be associated to the term Economic Model Predictive Control, a state feedback control approach encoding economic objectives as process control objectives [52].

upper-level control system operated in closed-loop that periodically provides set points to the lower-level control systems in order to maintain the process operation as close as possible to the economic optimum [30, 75]. Since the approach uses steady state models of the plant to determine the optimal set points,[8] the time between successive optimization steps has to be large enough for the plant to reach a new steady state and a new control command can be implemented. Rather than designing economic optimal set points for the manipulable quantities, this dissertation investigates how to verify that feasible set points computed based on the observed outputs always exist.

Another related line of research aims at regulating an arbitrary output of the system to the solution of a constrained optimization problem. This method has recently been termed in the literature as *linear convex optimal steady state control* [76] and relies on encoding the Karush-Kuhn-Tucker (KKT) conditions [77, 78] of the optimization problem as a (non-linear) dynamic system. This step turns the optimal steady state problem into a tractable stabilization problem.[9]

1.6 Structure of the Thesis

Fig. 1.4 presents the building blocks of this thesis. After introducing the theory of admissible control laws for constrained linear static systems in Chapter 2, we derive in Chapter 3 a set of algorithms for verifying the existence of admissible control laws under some key assumptions. If an admissible control law exists, then one can in many cases be computed by employing the techniques proposed in this chapter.

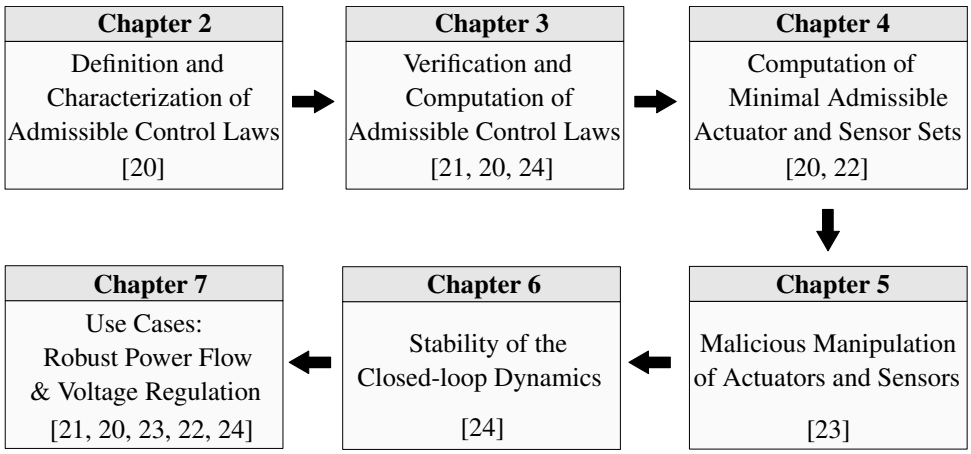

Figure 1.4: Structure of the thesis. Some contents of the chapters have been previously published.

[8] In the context of dynamic systems and control, the term *plant* refers to the system to be controlled by the system operator.

[9] The Karush-Kuhn-Tucker (KKT) conditions are first-order necessary conditions for optimality in constrained non-linear optimization problems. For linear optimization problems, the KKT conditions are also sufficient for optimality.

In Chapter 4 we present novel approaches for computing the smallest number of actuator and sensor devices required to guarantee the existence of an admissible control law. The ideas proposed in Chapters 2 and 3 are extended in Chapter 5 to handle the distortion of few actuator/sensor signals. We also provide in Chapter 6 ideas for the computation of affine output feedback control laws for LTI dynamic systems where the system state is subject to linear constraints at steady state. Finally, in Chapter 7, our ideas are applied to solve different power flow control problems.

Let us now take a closer look at the content of this thesis.

Chapter 2 – Admissible Control Laws. This chapter introduces a theoretical concept that forms the cornerstone of this thesis: The admissible control law, an output feedback control law that guarantees feasible system operation under uncertainty. This concept is developed for constrained static linear systems. In particular, we provide a set of conditions to test the existence of admissible control laws. While directly verifying the existence of an admissible control law is computationally challenging, we derive a set of related conditions which, in some special cases, allow for the derivation of efficient verification algorithms.

Chapter 3 – Verifying the Existence of Admissible Control Laws. Equipped with the admissibility conditions introduced in Chapter 2, this chapter derives efficient algorithms for 1) verifying the existence of admissible control laws and 2) computing admissible control laws (when possible). We show that, in many cases, verifying the existence of admissible affine control laws can be achieved by solving a finite dimensional linear optimization problem. Besides, the existence of admissible piecewise-affine control laws can under some assumptions be verified by solving a finite dimensional, non-convex, quadratically constrained quadratic optimization problem. Such assumptions also allow us to compute admissible piecewise-affine control laws either online via linear programming or offline by solving a two-stage multiparametric linear optimization problem.

Chapter 4 – Minimal Admissible Sets of Actuators and Sensors. The theory and the methods of previous chapters can be exploited to derive algorithms that determine the smallest number of actuators and sensors for which the existence of an admissible control law is guaranteed. In particular, mixed-integer linear optimization algorithms are derived for the computation of lower and upper bounds for the minimal actuator and sensor sets. This chapter also proposes an algorithm to compute the minimal set based on hill climbing optimization techniques.

Chapter 5 – Distortion of Actuator and Sensor Signals. This chapter extends the theory and the design techniques proposed in Chapters 2 and 3 to cases where the actuator and sensor sets are subject to exogenous, malicious manipulation. The control center thus receives potentially corrupted sensor information, and based on it determines control actions that may thereafter be manipulated by external agents, but still guarantee feasible system states.

Chapter 6 – Stability of the Closed-loop Dynamics. This chapter aims the synthesis of affine output feedback control laws for constrained LTI dynamic systems. Concretely, the control law has to guarantee the asymptotic stability of the resulting closed-loop system as well as the fulfillment of a set of linear operational constraints at steady state.

Chapter 7 – Applications to Power Systems. This chapter demonstrates how to apply the algorithmic tools proposed in previous chapters to solve various power flow control problems. Particularly, we apply our algorithms to determine the minimal number of actuators and sensors required to guarantee feasible power flow operation in transmission networks subject to uncertain generation and consumption profiles. We in addition study the problem of voltage regulation in distribution grids with high penetration of non-controllable decentralized generation units. Cases studies involving undesired manipulation of some actuator/sensor channels are also considered here.

1.7 Mathematical Background & Notation

Background. The content of this thesis is based on diverse mathematical tools from linear algebra, constrained optimization, and control theory. In this regard, the author of this thesis humbly recommends the books of Boyd [35, 79] and Bertsekas [80]. However, many other books and materials utilized in (under)graduate courses of electrical engineering [81], control theory [82, 18] and (combinatorial) optimization theory [83] shall also be adequate to understand the ideas proposed in this thesis.

Notation. If not specified otherwise, we use the notation x for a scalar, $\boldsymbol{x}$ for a vector, and $\mathbf{X}$ for a matrix quantity, all defined in an Euclidean space of appropriate dimension. Here we emphasize that bold symbols (like $\boldsymbol{x}$) are also utilized to denote quantities defined in the set of complex numbers, for instance $\boldsymbol{\lambda} \in \mathbb{C}$ may denote an eigenvalue of a predefined square matrix. Moreover, bold symbols are also used to denote vector valued functions, for instance the function $\boldsymbol{f} : \mathbb{R}^3 \to \mathbb{R}^2$.

We employ cursive uppercase symbols to denote subsets of the naturals or the reals. For instance, $\mathcal{S} \subset \mathbb{N}^+$ is a subset of the set of natural numbers without zero. The cardinality of $\mathcal{S}$ (number of elements in the set) is represented by $|\mathcal{S}|$.

Index notation is used extensively in this thesis. With a mild abuse of notation, the symbol $\mathbf{X}^j$ often denotes the jth row of the matrix $\mathbf{X}$. However, it may also denote the jth instance of a set of matrices. This notation should not be confused with the jth power of the matrix $\mathbf{X}$, which is also used in few specific parts of this thesis. However, we extensively specify the meaning of the symbols through the thesis to avoid confusion. Likewise, the symbol $\boldsymbol{x}^j \in \mathbb{R}^n$ with $j \in \{1, ..., n\}$ indicates that vector $\boldsymbol{x}$ is the jth instance of n possible instances defined by the set $\{1, ..., n\}$.

For two vectors $\boldsymbol{x}, \boldsymbol{y} \in \mathbb{R}^d$, the Hadamard product, also known as the element-wise product, is a map from $\mathbb{R}^d$ to $\mathbb{R}^d$ defined element-wise by $(\boldsymbol{x} \circ \boldsymbol{y})_i = x_i y_i$ for all $i = 1, ..., d$. Note that the scalars x_i and y_i represent the ith entries of $\boldsymbol{x}$ and $\boldsymbol{y}$, respectively. The symbol $\circ$ should thus not be confused with the composition operator of two functions. The operation $\boldsymbol{\mathcal{X}} \times \boldsymbol{\mathcal{U}}$ denotes the Cartesian product of the sets $\boldsymbol{\mathcal{X}}$ and $\boldsymbol{\mathcal{U}}$. It should not be confused with the cross product of two vectors in $\mathbb{R}^3$. The operators $<, \leq, >, \geq$ are defined element-wise for vectors and matrices.

2 Admissible Control Laws

This chapter formally defines constrained static linear systems and admissible control laws for them. As we explain in the following, verifying the existence of an admissible control law is in general computationally challenging as it turns into an infinite dimensional feasibility problem. To overcome this difficulty, we derive in this chapter a collection of related admissibility conditions that, under some assumptions, allow us to derive efficient verification algorithms in subsequent chapters.

2.1 Basic Definitions

Consider the static linear system depicted in Fig. 2.1. The vector $\boldsymbol{u} \in \boldsymbol{\mathcal{U}} \subset \mathbb{R}^{n_u}$ represents an external *action* that affects the (internal) *state* $\boldsymbol{x} \in \mathbb{R}^{n_x}$ of the system.[1] The action $\boldsymbol{u}$ influences the state $\boldsymbol{x}$ through the linear mapping $\boldsymbol{x} = \mathbf{F}\boldsymbol{u}$, where the matrix $\mathbf{F} \in \mathbb{R}^{n_x \times n_u}$ is assumed to be known in a priori.

We make the key assumption that all system transients have been settled to a stable equilibrium point, allowing us to study the system at steady state. The action $\boldsymbol{u}$ is hence to be understood as a constant signal that determines the constant equilibrium values for both the steady state $\boldsymbol{x}$ and the corresponding *measurable output* $\boldsymbol{y} \in \mathbb{R}^{n_y}$, respectively.[2] The discussion about how to dynamically bring the state of the system from any arbitrary initial position to a steady state within a desired feasible set is postponed to Chapter 6.

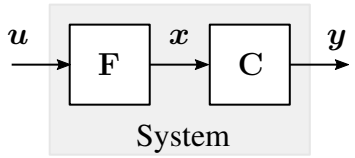

Figure 2.1: Block diagram representation of a static system. The (internal) state $\boldsymbol{x}$ of the system is influenced by the action $\boldsymbol{u}$ via $\boldsymbol{x} = \mathbf{F}\boldsymbol{u}$. The measurable output $\boldsymbol{y} = \mathbf{C}\boldsymbol{x}$ depends linearly on the state.

[1] In the field of dynamic systems and control, the notion of *state* refers to a minimum set of variables that fully describe the system and its response to any given set of external inputs [18, 84]. This is the notion adopted in this thesis.

[2] Note that the term *action*, which is used in the literature of reinforcement learning [85, 86], correspond to the term *input* used regularly in the literature of dynamic systems and control [87].

We say that the state $\boldsymbol{x}$ is *feasible* if it lies in the *feasible set* $\boldsymbol{\mathcal{X}} \subset \mathbb{R}^{n_x}$. In this thesis, we restrict our analysis to polyhedral constraints on $\boldsymbol{x}$, i.e., the feasible set $\boldsymbol{\mathcal{X}}$ is defined by a set of linear inequalities of the form $\mathbf{E}\boldsymbol{x} \leq \boldsymbol{b}$. The matrix $\mathbf{E} \in \mathbb{R}^{n_z \times n_x}$ and the vector $\boldsymbol{b} \in \mathbb{R}^{n_z}$ are supposed to be known in a priori as they are used to model both physical and operational system requirements depending on the application. Since the state of the system is related linearly to the action via $\boldsymbol{x} = \mathbf{F}\boldsymbol{u}$, we can represent constraints on the state of the system directly in terms of the action $\boldsymbol{u}$, i.e.,

$$\mathbf{E}\boldsymbol{x} \leq \boldsymbol{b} \Rightarrow \mathbf{EF}\boldsymbol{u} \leq \boldsymbol{b} \Rightarrow \mathbf{A}\boldsymbol{u} \leq \boldsymbol{b},$$

where $\mathbf{A} = \mathbf{EF}$ and $\mathbf{A} \in \mathbb{R}^{n_z \times n_u}$. We thus say that the state of the system is feasible if $\boldsymbol{u}$ adheres to the condition $\mathbf{A}\boldsymbol{u} \leq \boldsymbol{b}$.

The vector $\boldsymbol{y}$ represents a set of measurable quantities which are supposed to depend linearly on the system's state, i.e., $\boldsymbol{y} = \mathbf{C}\boldsymbol{x}$, where the matrix $\mathbf{C} \in \mathbb{R}^{n_y \times n_x}$ is given. Since $\boldsymbol{x} = \mathbf{F}\boldsymbol{u}$ holds, we can express vector $\boldsymbol{y}$ in terms of the action $\boldsymbol{u}$ via the linear mapping $\boldsymbol{y} = \mathbf{CF}\boldsymbol{u} = \mathbf{M}\boldsymbol{u}$, with $\mathbf{M} \in \mathbb{R}^{n_y \times n_u}$.

A *constrained static linear system* can then be fully expressed in terms of the action $\boldsymbol{u}$, the measurable output $\boldsymbol{y}$, and the parameters $\mathbf{A}$, $\boldsymbol{b}$, $\mathbf{M}$, and $\boldsymbol{\mathcal{U}}$ as

$$\mathbf{A}\boldsymbol{u} \leq \boldsymbol{b}, \quad \boldsymbol{y} = \mathbf{M}\boldsymbol{u}, \quad \boldsymbol{u} \in \boldsymbol{\mathcal{U}}. \tag{2.1}$$

Note in system (2.1) that polyhedral constraints on $\boldsymbol{u}$ can also be included by adding them as rows to the parameters $\mathbf{A}$ and $\boldsymbol{b}$. However, the above system representation is beneficial for the purposes of this thesis and will therefore be used extensively.

Now we introduce the *controller*, an entity that can access some (but possibly not all) entries of vector $\boldsymbol{y}$ and, based on that information, is able to influence the state of system by setting the value of some (but possibly not all) entries of $\boldsymbol{u}$. For now we consider idealized communication channels between system and controller. More specifically, the information transmitted from the system to the controller and vice versa is not distorted or manipulated in-between by some exogenous factor.[3] Note that if the controller were able to set the value of the entire vector $\boldsymbol{u}$, then no sensors would be required as the value of $\boldsymbol{x}$ would be uniquely determined by the $\boldsymbol{u}$ known to the controller. The goal of the controller is to determine control actions that always result in a feasible system state. In this thesis, we will also refer to the controller as the *system operator* or the *control center*.

Formally, we partition the entries of $\boldsymbol{u}$ into the *control action* $\boldsymbol{u}_\mathrm{c} \in \boldsymbol{\mathcal{U}}_\mathrm{c}$ and the *exogenous action* $\boldsymbol{u}_\mathrm{f} \in \boldsymbol{\mathcal{U}}_\mathrm{f}$,[4] see Fig. 2.2. The value of the control action $\boldsymbol{u}_\mathrm{c}$ is set by the controller via a suitable *control law*. In contrast, the value of the exogenous action $\boldsymbol{u}_\mathrm{f}$ is determined either by other users, cooperative or malicious, by fixed external conditions,

[3] This assumption is removed in Chapter 5.

[4] The terms *control action* and *exogenous action* are equivalent to the terms *control input* and *disturbance*, respectively. The latter terms are more common in the literature of dynamic systems and control.

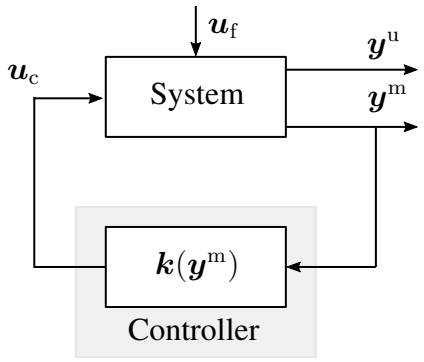

Figure 2.2: The system is influenced by the exogenous action $\boldsymbol{u}_\mathrm{f}$ as well as by the control action $\boldsymbol{u}_\mathrm{c}$, which is set by the controller according to the control law $\boldsymbol{u}_\mathrm{c} = \boldsymbol{k}(\boldsymbol{y}^\mathrm{m})$.

or at random. The indices of those entries of $\boldsymbol{u}$ associated to the control action $\boldsymbol{u}_\mathrm{c}$ are in the *actuator set* $\mathcal{C} \subseteq \{1, ..., n_u\}$. The dimensions of $\boldsymbol{u}_\mathrm{c}$ and $\boldsymbol{u}_\mathrm{f}$ are thus given in terms of the total number of controlled actuators $|\mathcal{C}|$. If not specified otherwise, the set of control actions $\boldsymbol{\mathcal{U}}_\mathrm{c} \subset \mathbb{R}^{|\mathcal{C}|}$ as well as the uncertainty set $\boldsymbol{\mathcal{U}}_\mathrm{f} \subset \mathbb{R}^{n_u - |\mathcal{C}|}$ are supposed to be bounded, convex, and fulfill $\boldsymbol{\mathcal{U}} = \boldsymbol{\mathcal{U}}_\mathrm{c} \times \boldsymbol{\mathcal{U}}_\mathrm{f}$. We also assume that the sets $\boldsymbol{\mathcal{U}}_\mathrm{c}$ and $\boldsymbol{\mathcal{U}}_\mathrm{f}$ are known to the controller.

Likewise, we partition vector $\boldsymbol{y}$ into the *measured output* $\boldsymbol{y}^\mathrm{m}$, which is accessible to the control center, and the *unmeasured output* $\boldsymbol{y}^\mathrm{u}$, which is not required by the controller and may or may not be recorded in practice. The indexes of those entries of $\boldsymbol{y}$ associated to the measured output $\boldsymbol{y}^\mathrm{m}$ are in the *sensor set* $\mathcal{M} \subseteq \{1, ..., n_y\}$.[5] The dimensions of $\boldsymbol{y}^\mathrm{m}$ and $\boldsymbol{y}^\mathrm{u}$ are thus determined by the total number of monitored sensors $|\mathcal{M}|$, i.e., $\boldsymbol{y}^\mathrm{m} \in \mathbb{R}^{|\mathcal{M}|}$ and $\boldsymbol{y}^\mathrm{u} \in \mathbb{R}^{n_y - |\mathcal{M}|}$.

The defined partitions of $\boldsymbol{u}$ and $\boldsymbol{y}$ allow us to partition the matrices $\mathbf{A}$ and $\mathbf{M}$ along their columns and rows, yielding

$$\begin{aligned} \mathbf{A}\boldsymbol{u} &= \mathbf{A}_\mathrm{c}\boldsymbol{u}_\mathrm{c} + \mathbf{A}_\mathrm{f}\boldsymbol{u}_\mathrm{f}, \\ \boldsymbol{y} = \begin{bmatrix} \boldsymbol{y}^\mathrm{m} \\ \boldsymbol{y}^\mathrm{u} \end{bmatrix} &= \begin{bmatrix} \mathbf{M}^\mathrm{m} \\ \mathbf{M}^\mathrm{u} \end{bmatrix} \boldsymbol{u} = \begin{bmatrix} \mathbf{M}^\mathrm{m}_\mathrm{c} & \mathbf{M}^\mathrm{m}_\mathrm{f} \\ \mathbf{M}^\mathrm{u}_\mathrm{c} & \mathbf{M}^\mathrm{u}_\mathrm{f} \end{bmatrix} \begin{bmatrix} \boldsymbol{u}_\mathrm{c} \\ \boldsymbol{u}_\mathrm{f} \end{bmatrix}. \end{aligned} \tag{2.2}$$

As introduced above, the controller determines the control action $\boldsymbol{u}_\mathrm{c}$ based on the measured output $\boldsymbol{y}^\mathrm{m}$ via a control law, namely a mapping $\boldsymbol{u}_\mathrm{c} = \boldsymbol{k}(\boldsymbol{y}^\mathrm{m})$. Fig. 2.2 illustrates this. If the control law $\boldsymbol{u}_\mathrm{c} = \boldsymbol{k}(\boldsymbol{y}^\mathrm{m})$ guarantees a feasible system state independently of the value of the exogenous action $\boldsymbol{u}_\mathrm{f}$, then we say that it is *admissible*. This idea is formalized as follows.

Definition 1. The control law $\boldsymbol{k} : \mathrm{M}^\mathrm{m}(\boldsymbol{\mathcal{U}}^\star) \to \boldsymbol{\mathcal{U}}_\mathrm{c}$ is admissible if

$$\forall \boldsymbol{u}_\mathrm{f} \in \boldsymbol{\mathcal{U}}_\mathrm{f} : \ \mathbf{A}_\mathrm{c}\boldsymbol{k}(\boldsymbol{y}^\mathrm{m}) + \mathbf{A}_\mathrm{f}\boldsymbol{u}_\mathrm{f} \leq \boldsymbol{b}, \tag{2.3}$$

where $\boldsymbol{y}^\mathrm{m} = \mathbf{M}^\mathrm{m}_\mathrm{c}\boldsymbol{k}(\boldsymbol{y}^\mathrm{m}) + \mathbf{M}^\mathrm{m}_\mathrm{f}\boldsymbol{u}_\mathrm{f}$ and $\mathrm{M}^\mathrm{m}(\boldsymbol{\mathcal{U}}^\star)$ is the set of all possible observations $\boldsymbol{y}^\mathrm{m}$.

[5] For simplicity, we shall use the terms *sensor* or *observation* as synonyms of *measured output*. We may also refer to $\mathcal{M}$ as *measurement set*.

Definition 2 (Admissible sets $\mathcal{C}$ and $\mathcal{M}$)**.** The actuator and sensor sets $\mathcal{C}$ and $\mathcal{M}$ are admissible if there exists an admissible control law $\boldsymbol{u}_\mathrm{c} = \boldsymbol{k}(\boldsymbol{y}^\mathrm{m})$ for those sets.

Example 2. This example illustrates how to use the proposed modeling approach in a power systems application. Consider the simple power distribution feeder shown in Fig. 2.3. The feeder has two loads, the first connected to bus 1 and the second to bus 2. The substation transformer located at bus 0 is connected to bus 1 through a transmission line. This transmission line is modeled as a series impedance with resistance $\mathrm{r}_{01} \in \mathbb{R}_{>0}$ and reactance $\mathrm{x}_{01} \in \mathbb{R}_{>0}$. Another transmission line with electrical parameters $\mathrm{r}_{12} \in \mathbb{R}_{>0}$ and $\mathrm{x}_{12} \in \mathbb{R}_{>0}$ connects buses 1 and 2. The goal of the grid operator is to keep all voltage levels always within the limits $\underline{v} \in \mathbb{R}_{>0}$ and $\overline{v} \in \mathbb{R}_{>0}$.

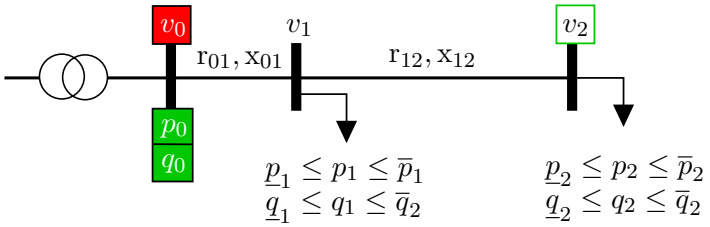

Figure 2.3: Single line diagram of a simple distribution feeder with voltage control. The control center can set the voltage level v_0 (the red box) based on measurements of the power (p_0, q_0) at the substation transformer (the boxes filled in green). While there is also a sensor recording the voltage level v_2 (the green framed box), such sensor is not connected to the control center. The loads at buses 1 and 2 are not determined by the grid operator, but by independent consumers. The grid operator can, however, assume bounds on these uncertain loads.

We model the distribution feeder by using a linearized version of the *DistFlow* equations [88, 89] that neglects the line losses. The nodal voltages $v_{1,2} \in \mathbb{R}$ are constrained to be within the limits $\underline{v}$ and $\overline{v}$, defining the feasible operating region of the system. According to the adopted linearized power flow model, the voltages v_1 and v_2 are influenced linearly by the voltage at the root node v_0 as well as by the active and reactive power injections $p_{1,2} \in \mathbb{R}$ and $q_{1,2} \in \mathbb{R}$. The resulting system of linear (in)equalities for the voltages is given by both

$$\begin{bmatrix} \underline{v} \\ \underline{v} \end{bmatrix} \leq \begin{bmatrix} v_1 \\ v_2 \end{bmatrix} \leq \begin{bmatrix} \overline{v} \\ \overline{v} \end{bmatrix} \Rightarrow \underbrace{\begin{bmatrix} \mathbf{I} \\ -\mathbf{I} \end{bmatrix}}_{\mathbf{E}} \underbrace{\begin{bmatrix} v_1 \\ v_2 \end{bmatrix}}_{\boldsymbol{x}} \leq \underbrace{\begin{bmatrix} \overline{v}\mathbf{1} \\ -\underline{v}\mathbf{1} \end{bmatrix}}_{\boldsymbol{b}} \tag{2.4}$$

and

$$\underbrace{\begin{bmatrix} v_1 \\ v_2 \end{bmatrix}}_{\boldsymbol{x}} = \underbrace{\begin{bmatrix} 1 & -\mathrm{r}_{01} & 0 & -\mathrm{x}_{01} & 0 \\ 1 & -\mathrm{r}_{01} & -\mathrm{r}_{12} & -\mathrm{x}_{01} & -\mathrm{x}_{12} \end{bmatrix}}_{\mathbf{F}} \underbrace{\begin{bmatrix} v_0 \\ p_1 \\ p_2 \\ q_1 \\ q_2 \end{bmatrix}}_{\boldsymbol{u}}, \tag{2.5}$$

where the identity matrix $\mathbf{I}$ and the vector of ones $\mathbf{1}$ have of appropriate dimensions. Further, the possible observations are given in Fig. 2.3 as the active and reactive power at the substation transformer (p_0, q_0) as well as the voltage level at node 2, yielding

$$\underbrace{\begin{bmatrix} p_0 \\ q_0 \\ v_2 \end{bmatrix}}_{\boldsymbol{y}} = \underbrace{\begin{bmatrix} 0 & -1 & -1 & 0 & 0 \\ 0 & 0 & 0 & -1 & -1 \\ 1 & -\mathrm{r}_{01} & -\mathrm{r}_{12} & -\mathrm{x}_{01} & -\mathrm{x}_{12} \end{bmatrix}}_{\mathbf{M}} \underbrace{\begin{bmatrix} v_0 \\ p_1 \\ p_2 \\ q_1 \\ q_2 \end{bmatrix}}_{\boldsymbol{u}}. \tag{2.6}$$

From the system specifications given in Fig. 2.3 together with expressions (2.4)–(2.6) we readily obtain the constrained static system representation (2.1).

As illustrated in Fig. 2.3, the system operator can manipulate the voltage at the root node ($\boldsymbol{u}_\mathrm{c} = v_0$) based on the power at the substation transformer ($\boldsymbol{y}^\mathrm{m} = [p_0 \;\; q_0]^\mathrm{T}$). From equation (2.5), the actuator and sensor sets are given by $\mathcal{C} = \{1\}$ and $\mathcal{M} = \{1, 2\}$, respectively. The power injections at nodes 1 and 2 are thus uncertain to the controller ($\boldsymbol{u}_\mathrm{f} = [p_1 \;\; p_2 \;\; q_1 \;\; q_2]^\mathrm{T}$), where the uncertainty set $\boldsymbol{\mathcal{U}}_\mathrm{f}$ is given by the Cartesian product of intervals

$$\boldsymbol{\mathcal{U}}_\mathrm{f} = [\underline{p}_1, \, \overline{p}_1] \times [\underline{p}_2, \, \overline{p}_2] \times [\underline{q}_1, \, \overline{q}_1] \times [\underline{q}_2, \, \overline{q}_2].$$

The grid operator has thus to keep all voltages levels within $\underline{v}$ and $\overline{v}$ for all possible realizations of the uncertain power injections $\boldsymbol{u}_\mathrm{f} \in \boldsymbol{\mathcal{U}}_\mathrm{f}$. To this end, an admissible control law $v_0 = \boldsymbol{k}([p_0 \;\; q_0]^\mathrm{T})$, if possible, has to be found. If such an admissible control law exists, then the actuator and sensor sets $(\mathcal{C}, \mathcal{M})$ are admissible. □

At this point, manifold interesting research questions arise naturally:

- For given actuator and sensor sets $(\mathcal{C}, \mathcal{M})$, how can we verify the existence of an admissible control law?
- What is the minimum number of actuators in $\mathcal{C}$ and sensors in $\mathcal{M}$ that guarantees the existence of an admissible control law?
- Provided there exists an admissible control law for the system, how can we design one efficiently?

The rest of the present chapter together with Chapters 3 and 4 aim at rigorously answering these questions. In order to simplify the notation in the subsequent analysis, we use the standard notation

$$\exists \boldsymbol{u}_\mathrm{c} = \boldsymbol{k}(\boldsymbol{y}^\mathrm{m}) \text{ admissible}$$

to say that there exists an admissible control law $\boldsymbol{k} : \mathrm{M}^\mathrm{m}(\boldsymbol{\mathcal{U}}^\star) \to \boldsymbol{\mathcal{U}}_\mathrm{c}$.

2.2 Alternative Characterizations

The idea behind Definition 1 is that the value of the control action $\boldsymbol{u}_\mathrm{c}$ chosen through the mapping $\boldsymbol{k}$ for the observation $\boldsymbol{y}^\mathrm{m}$ should be valid for the exogenous action $\boldsymbol{u}_\mathrm{f}$ from which $\boldsymbol{y}^\mathrm{m}$ originated. Since this should be possible for all elements in the uncertainty set $\boldsymbol{\mathcal{U}}_\mathrm{f}$, verifying the existence of an admissible mapping $\boldsymbol{k}$ turns into an infinite dimensional feasibility problem—in general a challenging task from the computational point of view. Definition 1 additionally establish a recursive relation between $\boldsymbol{u}_\mathrm{c}$ and $\boldsymbol{y}^\mathrm{m}$, which adds more complexity to the verification task.

In the following, we present some special system instances for which the recursion can be eliminated when verifying the existence of an admissible control law $\boldsymbol{u}_\mathrm{c} = \boldsymbol{k}(\boldsymbol{y}^\mathrm{m})$. Inspired by them, we then present non-recursive admissibility conditions valid for the general case. The discussion on how to tackle the infinite dimension challenge of the verification task is left for subsequent sections.

Special Cases Not Involving Recursion

There are, in fact, some special cases for which verifying the admissibility of a control law $\boldsymbol{u}_\mathrm{c} = \boldsymbol{k}(\boldsymbol{y}^\mathrm{m})$ does not involve recursion. Consider first the trivial case $\boldsymbol{\mathcal{U}}_\mathrm{f} = \emptyset$, i.e., a system with no exogenous influences. An admissible control law $\boldsymbol{u}_\mathrm{c} = \boldsymbol{k}(\boldsymbol{y}^\mathrm{m})$ should then fulfill $\mathbf{A}_\mathrm{c}\boldsymbol{k}(\boldsymbol{y}^\mathrm{m}) \leq \boldsymbol{b}$ with $\boldsymbol{y}^\mathrm{m} = \mathbf{M}_\mathrm{c}^\mathrm{m}\boldsymbol{k}(\boldsymbol{y}^\mathrm{m})$. In this case, we can eliminate recursion since

$$\boldsymbol{u}_\mathrm{c} = \boldsymbol{k}(\boldsymbol{y}^\mathrm{m}) = \boldsymbol{k}(\mathbf{M}_\mathrm{c}^\mathrm{m}\boldsymbol{u}_\mathrm{c}) = \check{\boldsymbol{k}}(\boldsymbol{u}_\mathrm{c}),$$

i.e., $\check{\boldsymbol{k}}(\boldsymbol{u}_\mathrm{c})$ is the identity function. The admissibility condition is thus reduced to checking whether the control action $\boldsymbol{u}_\mathrm{c} \in \boldsymbol{\mathcal{U}}_\mathrm{c}$ chosen by the controller fulfills $\mathbf{A}_\mathrm{c}\boldsymbol{u}_\mathrm{c} \leq \boldsymbol{b}$. Note that in this case the there is no necessity of any feedback observation $\boldsymbol{y}^\mathrm{m}$ as the vector $\boldsymbol{u} = \boldsymbol{u}_\mathrm{c}$ is completely known to the controller.

Another special case occurs when $\mathbf{M}_\mathrm{c}^\mathrm{m} = \mathbf{0}$, i.e., the observation fed back to the controller depends only on the exogenous action $\boldsymbol{u}_\mathrm{f}$ and is given by $\boldsymbol{y}^\mathrm{m} = \mathbf{M}_\mathrm{f}^\mathrm{m}\boldsymbol{u}_\mathrm{f}$. In this case, an admissible control law $\boldsymbol{u}_\mathrm{c} = \boldsymbol{k}(\boldsymbol{y}^\mathrm{m})$ should fulfill

$$\forall \boldsymbol{u}_\mathrm{f} \in \boldsymbol{\mathcal{U}}_\mathrm{f} : \mathbf{A}_\mathrm{c}\boldsymbol{k}(\mathbf{M}_\mathrm{f}^\mathrm{m}\boldsymbol{u}_\mathrm{f}) + \mathbf{A}_\mathrm{f}\boldsymbol{u}_\mathrm{f} \leq \boldsymbol{b}. \tag{2.7}$$

Again, the resulting admissibility condition does not involve recursion. If in addition the matrix $\mathbf{M}_\mathrm{f}^\mathrm{m}$ has full column rank, i.e., $\mathrm{rank}(\mathbf{M}_\mathrm{f}^\mathrm{m}) = n_u - |\mathcal{C}|$, then the (overdetermined) system of linear equations $\mathbf{M}_\mathrm{f}^\mathrm{m}\boldsymbol{u}_\mathrm{f} = \boldsymbol{y}^\mathrm{m}$ has unique solution and the controller can determine the value of $\boldsymbol{u}_\mathrm{f}$ by using the pseudo-inverse of $\mathbf{M}_\mathrm{f}^\mathrm{m}$, i.e.,

$$\boldsymbol{y}^\mathrm{m} = \mathbf{M}_\mathrm{f}^\mathrm{m}\boldsymbol{u}_\mathrm{f} \Rightarrow \boldsymbol{u}_\mathrm{f} = \mathbf{M}_\mathrm{f}^{\mathrm{m}+}\boldsymbol{y}^\mathrm{m}. \tag{2.8}$$

Thus, the controller can employ the value of $\boldsymbol{u}_\mathrm{f}$ to choose the control action $\boldsymbol{u}_\mathrm{c}$ via some mapping $\boldsymbol{u}_\mathrm{c} = \tilde{\boldsymbol{k}}(\boldsymbol{u}_\mathrm{f})$ fulfilling

$$\forall \boldsymbol{u}_\mathrm{f} \in \boldsymbol{\mathcal{U}}_\mathrm{f} : \mathbf{A}_\mathrm{c}\tilde{\boldsymbol{k}}(\boldsymbol{u}_\mathrm{f}) + \mathbf{A}_\mathrm{f}\boldsymbol{u}_\mathrm{f} \leq \boldsymbol{b}. \tag{2.9}$$

While the above special cases may find practical application, they are not the focus of this thesis. Still, they are important to understand how to remove the recursion when verifying the admissibility of control law $\boldsymbol{u}_\mathrm{c} = \boldsymbol{k}(\boldsymbol{y}^\mathrm{m})$ in the general case. The relevance of expressions (2.7) and (2.9) will become clear in the following.

The General Case

Now we center our investigation in verifying the existence of an admissible control law $\boldsymbol{u}_\mathrm{c} = \boldsymbol{k}(\boldsymbol{y}^\mathrm{m})$ for systems in which the uncertainty set $\boldsymbol{\mathcal{U}}_\mathrm{f}$ is not empty and the dimension of $\boldsymbol{u}_\mathrm{f}$ is large compared to the dimensions of $\boldsymbol{u}_\mathrm{c}$ and $\boldsymbol{y}^\mathrm{m}$. For this kind of systems the matrix $\mathrm{M}_\mathrm{f}^\mathrm{m}$ has not full rank, i.e., the system of linear equations $\mathrm{M}_\mathrm{f}^\mathrm{m}\boldsymbol{u}_\mathrm{f} = \boldsymbol{y}^\mathrm{m}$ is underdetermined and (2.8) cannot be used. Condition (2.9) can therefore not be used to verify the existence of an admissible control law and we should address the verification task from another point of view.[6]

Inspired by the special cases mentioned in the previous section, we now consider two alternative control laws, namely the mapping $\boldsymbol{u}_\mathrm{c} = \hat{\boldsymbol{k}}(\boldsymbol{y}_\mathrm{f}^\mathrm{m})$, with $\boldsymbol{y}_\mathrm{f}^\mathrm{m} = \mathrm{M}_\mathrm{f}^\mathrm{m}\boldsymbol{u}_\mathrm{f}$, and the mapping $\boldsymbol{u}_\mathrm{c} = \tilde{\boldsymbol{k}}(\boldsymbol{u}_\mathrm{f})$.[7] Fig. 2.4 illustrates these alternative control concepts by using block diagrams. Note that other control structures are possible, e.g., one could aim at estimating $\boldsymbol{u}_\mathrm{f}$ based on $\boldsymbol{y}^\mathrm{m}$ and then use the estimation to compute the control action $\boldsymbol{u}_\mathrm{c}$. However, we restrict the scope of this thesis to the study of the artificial control laws $\boldsymbol{u}_\mathrm{c} = \hat{\boldsymbol{k}}(\boldsymbol{y}_\mathrm{f}^\mathrm{m})$ and $\boldsymbol{u}_\mathrm{c} = \tilde{\boldsymbol{k}}(\boldsymbol{u}_\mathrm{f})$.

Although the control laws $\boldsymbol{u}_\mathrm{c} = \hat{\boldsymbol{k}}(\boldsymbol{y}_\mathrm{f}^\mathrm{m})$ and $\boldsymbol{u}_\mathrm{c} = \tilde{\boldsymbol{k}}(\boldsymbol{u}_\mathrm{f})$ may not be implementable in practice as only the observation $\boldsymbol{y}^\mathrm{m}$ is available to the controller, we can constrain them such that they *emulate* the behavior of an admissible control law $\boldsymbol{u}_\mathrm{c} = \boldsymbol{k}(\boldsymbol{y}^\mathrm{m})$. In other words, we can restrict these control laws such that—for each exogenous action $\boldsymbol{u}_\mathrm{f} \in \boldsymbol{\mathcal{U}}_\mathrm{f}$—the control action $\boldsymbol{u}_\mathrm{c} \in \boldsymbol{\mathcal{U}}_\mathrm{c}$ generated from $\boldsymbol{y}_\mathrm{f}^\mathrm{m}$ (or $\boldsymbol{u}_\mathrm{f}$) guarantees the fulfillment of the constraints of the system and is the same for all other points in the uncertainty set $\boldsymbol{\mathcal{U}}_\mathrm{f}$ that yield the same observation $\boldsymbol{y}^\mathrm{m}$. This is advantageous since verifying the existence of such constrained control laws does not involve recursion. More interesting, we show in the following that the existence of a control law $\boldsymbol{u}_\mathrm{c} = \hat{\boldsymbol{k}}(\boldsymbol{y}_\mathrm{f}^\mathrm{m})$ (or $\boldsymbol{u}_\mathrm{c} = \tilde{\boldsymbol{k}}(\boldsymbol{u}_\mathrm{f})$) being able to mimic the behavior of an admissible control law $\boldsymbol{u}_\mathrm{c} = \boldsymbol{k}(\boldsymbol{y}^\mathrm{m})$ implies the existence of an admissible control law $\boldsymbol{u}_\mathrm{c} = \boldsymbol{k}(\boldsymbol{y}^\mathrm{m})$, and vice versa. For this reason and with a mild abuse of notation, we coin the term "admissible" also to those constrained alternative control laws $\boldsymbol{u}_\mathrm{c} = \hat{\boldsymbol{k}}(\boldsymbol{y}_\mathrm{f}^\mathrm{m})$ and $\boldsymbol{u}_\mathrm{c} = \tilde{\boldsymbol{k}}(\boldsymbol{u}_\mathrm{f})$ emulating the admissibility property of the control law $\boldsymbol{u}_\mathrm{c} = \boldsymbol{k}(\boldsymbol{y}^\mathrm{m})$.

[6] Note that ideas of, e.g., compressive sensing [90] could be useful here. However, we leave the analysis about under which conditions the matrix $\mathrm{M}_\mathrm{f}^\mathrm{m}$ allows us to recover the value of $\boldsymbol{u}_\mathrm{f}$ from $\boldsymbol{y}^\mathrm{m}$ for future work.

[7] According to the literature of control theory, the control laws $\boldsymbol{u}_\mathrm{c} = \hat{\boldsymbol{k}}(\boldsymbol{y}_\mathrm{f}^\mathrm{m})$ and $\boldsymbol{u}_\mathrm{c} = \tilde{\boldsymbol{k}}(\boldsymbol{u}_\mathrm{f})$ are cast as disturbance feedforward control laws [91].

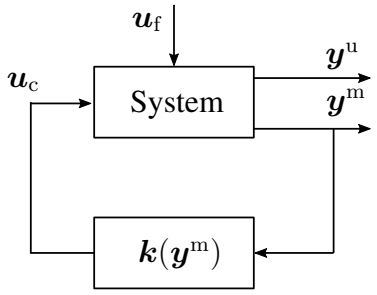

(a) The control law $\boldsymbol{u}_\mathrm{c} = \boldsymbol{k}(\boldsymbol{y}^\mathrm{m})$.

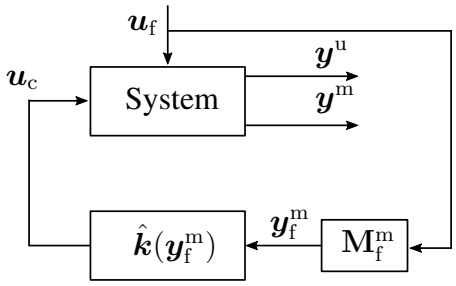

(b) The control law $\boldsymbol{u}_\mathrm{c} = \hat{\boldsymbol{k}}(\boldsymbol{y}_\mathrm{f}^\mathrm{m})$.

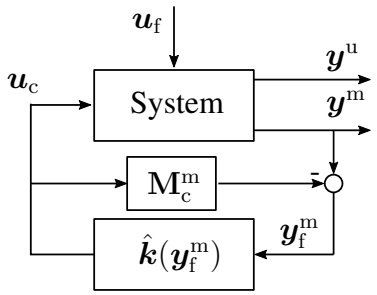

(c) Another implementation of the control law $\boldsymbol{u}_\mathrm{c} = \hat{\boldsymbol{k}}(\boldsymbol{y}_\mathrm{f}^\mathrm{m})$.

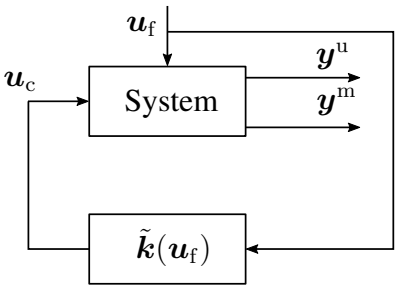

(d) The control law $\boldsymbol{u}_\mathrm{c} = \tilde{\boldsymbol{k}}(\boldsymbol{u}_\mathrm{f})$.

Figure 2.4: Block diagram representation of (a) the original control law $\boldsymbol{u}_\mathrm{c} = \boldsymbol{k}(\boldsymbol{y}^\mathrm{m})$, and (b)–(d) the alternative control laws $\boldsymbol{u}_\mathrm{c} = \hat{\boldsymbol{k}}(\boldsymbol{y}_\mathrm{f}^\mathrm{m})$ and $\boldsymbol{u}_\mathrm{c} = \tilde{\boldsymbol{k}}(\boldsymbol{u}_\mathrm{f})$.

Admissible Control Law $\boldsymbol{u}_\mathrm{c} = \hat{\boldsymbol{k}}(\boldsymbol{y}_\mathrm{f}^\mathrm{m})$

Instead of defining the control law as a function of $\boldsymbol{y}^\mathrm{m}$, we now consider the control law $\boldsymbol{u}_\mathrm{c} = \hat{\boldsymbol{k}}(\boldsymbol{y}_\mathrm{f}^\mathrm{m})$ that maps the elements in the set $\mathrm{M}_\mathrm{f}^\mathrm{m}(\boldsymbol{\mathcal{U}}_\mathrm{f})$ to control actions in $\boldsymbol{\mathcal{U}}_\mathrm{c}$, see Figs. 2.4 (b) and (c). In order to emulate the behavior of an admissible control law $\boldsymbol{u}_\mathrm{c} = \boldsymbol{k}(\boldsymbol{y}^\mathrm{m})$, the control law $\boldsymbol{u}_\mathrm{c} = \hat{\boldsymbol{k}}(\boldsymbol{y}_\mathrm{f}^\mathrm{m})$ must guarantee that for each $\boldsymbol{u}_\mathrm{f} \in \boldsymbol{\mathcal{U}}_\mathrm{f}$ there exist a control action $\boldsymbol{u}_\mathrm{c} \in \boldsymbol{\mathcal{U}}_\mathrm{c}$ generated from $\boldsymbol{y}_\mathrm{f}^\mathrm{m} = \mathrm{M}_\mathrm{f}^\mathrm{m}\boldsymbol{u}_\mathrm{f}$ that fulfills the constraints of the system.

Definition 3. The control law $\hat{\boldsymbol{k}} : \mathrm{M}_\mathrm{f}^\mathrm{m}(\boldsymbol{\mathcal{U}}_\mathrm{f}) \to \boldsymbol{\mathcal{U}}_\mathrm{c}$ is admissible if

$$\forall \boldsymbol{u}_\mathrm{f} \in \boldsymbol{\mathcal{U}}_\mathrm{f} : \ \mathbf{A}_\mathrm{c}\hat{\boldsymbol{k}}(\boldsymbol{y}_\mathrm{f}^\mathrm{m}) + \mathbf{A}_\mathrm{f}\boldsymbol{u}_\mathrm{f} \leq \boldsymbol{b},$$

with $\boldsymbol{y}_\mathrm{f}^\mathrm{m} = \mathrm{M}_\mathrm{f}^\mathrm{m}\boldsymbol{u}_\mathrm{f}$.

Theorem 1. The following two statements are equivalent:

1. $\exists \boldsymbol{u}_\mathrm{c} = \boldsymbol{k}(\boldsymbol{y}^\mathrm{m})$ admissible.
2. $\exists \boldsymbol{u}_\mathrm{c} = \hat{\boldsymbol{k}}(\boldsymbol{y}_\mathrm{f}^\mathrm{m})$ admissible.

Proof. First, we recall that $\boldsymbol{y}^\mathrm{m} = \mathrm{M}_\mathrm{c}^\mathrm{m}\boldsymbol{u}_\mathrm{c} + \mathrm{M}_\mathrm{f}^\mathrm{m}\boldsymbol{u}_\mathrm{f} = \mathrm{M}_\mathrm{c}^\mathrm{m}\boldsymbol{u}_\mathrm{c} + \boldsymbol{y}_\mathrm{f}^\mathrm{m}$. We now suppose that an admissible control law $\boldsymbol{u}_\mathrm{c} = \boldsymbol{k}(\boldsymbol{y}^\mathrm{m})$ exists. Then, for all possible $\boldsymbol{y}^\mathrm{m} \in \mathrm{M}^\mathrm{m}(\boldsymbol{\mathcal{U}}^\star)$, we

can map the pair $(\boldsymbol{y}^{\mathrm{m}}, \boldsymbol{k}(\boldsymbol{y}^{\mathrm{m}}))$ to a pair $(\boldsymbol{y}_{\mathrm{f}}^{\mathrm{m}}, \boldsymbol{u}_{\mathrm{c}})$, namely

$$\begin{bmatrix} \boldsymbol{y}_{\mathrm{f}}^{\mathrm{m}} \\ \boldsymbol{u}_{\mathrm{c}} \end{bmatrix} = \begin{bmatrix} \mathbf{I} & -\mathrm{M}_{\mathrm{c}}^{\mathrm{m}} \\ \mathbf{0} & \mathbf{I} \end{bmatrix} \begin{bmatrix} \boldsymbol{y}^{\mathrm{m}} \\ \boldsymbol{k}(\boldsymbol{y}^{\mathrm{m}}) \end{bmatrix}.$$

Note that the pairs $(\boldsymbol{y}_{\mathrm{f}}^{\mathrm{m}}, \boldsymbol{u}_{\mathrm{c}})$ generated from $(\boldsymbol{y}^{\mathrm{m}}, \boldsymbol{k}(\boldsymbol{y}^{\mathrm{m}}))$ imply an admissible control law $\boldsymbol{u}_{\mathrm{c}} = \hat{\boldsymbol{k}}(\boldsymbol{y}_{\mathrm{f}}^{\mathrm{m}})$. Now we assume there exist an admissible control law $\boldsymbol{u}_{\mathrm{c}} = \hat{\boldsymbol{k}}(\boldsymbol{y}_{\mathrm{f}}^{\mathrm{m}})$. Then, for all possible $\boldsymbol{y}_{\mathrm{f}}^{\mathrm{m}} \in \mathrm{M}_{\mathrm{f}}^{\mathrm{m}}(\boldsymbol{\mathcal{U}}_{\mathrm{f}})$, we can map the pair $(\boldsymbol{y}_{\mathrm{f}}^{\mathrm{m}}, \hat{\boldsymbol{k}}(\boldsymbol{y}_{\mathrm{f}}^{\mathrm{m}}))$ to a pair $(\boldsymbol{y}^{\mathrm{m}}, \boldsymbol{u}_{\mathrm{c}})$, i.e.,

$$\begin{bmatrix} \boldsymbol{y}^{\mathrm{m}} \\ \boldsymbol{u}_{\mathrm{c}} \end{bmatrix} = \begin{bmatrix} \mathbf{I} & \mathrm{M}_{\mathrm{c}}^{\mathrm{m}} \\ \mathbf{0} & \mathbf{I} \end{bmatrix} \begin{bmatrix} \boldsymbol{y}_{\mathrm{f}}^{\mathrm{m}} \\ \hat{\boldsymbol{k}}(\boldsymbol{y}_{\mathrm{f}}^{\mathrm{m}}) \end{bmatrix}.$$

Observe that the pairs $(\boldsymbol{y}^{\mathrm{m}}, \boldsymbol{u}_{\mathrm{c}})$ generated from $(\boldsymbol{y}_{\mathrm{f}}^{\mathrm{m}}, \hat{\boldsymbol{k}}(\boldsymbol{y}_{\mathrm{f}}^{\mathrm{m}}))$ readily imply an admissible mapping $\boldsymbol{u}_{\mathrm{c}} = \boldsymbol{k}(\boldsymbol{y}^{\mathrm{m}})$. □

Contrary to the more natural control law $\boldsymbol{u}_{\mathrm{c}} = \boldsymbol{k}(\boldsymbol{y}^{\mathrm{m}})$, verifying the existence of an admissible control law $\boldsymbol{u}_{\mathrm{c}} = \hat{\boldsymbol{k}}(\boldsymbol{y}_{\mathrm{f}}^{\mathrm{m}})$ does not involve recursion since the observation $\boldsymbol{y}_{\mathrm{f}}^{\mathrm{m}}$ is only determined by exogenous action $\boldsymbol{u}_{\mathrm{f}}$.[8] The proof of Theorem 1 also provides a method to map an admissible control law $\boldsymbol{u}_{\mathrm{c}} = \hat{\boldsymbol{k}}(\boldsymbol{y}_{\mathrm{f}}^{\mathrm{m}})$ to an admissible control law $\boldsymbol{u}_{\mathrm{c}} = \boldsymbol{k}(\boldsymbol{y}^{\mathrm{m}})$ and vice versa.

Admissible Control Law $\boldsymbol{u}_{\mathrm{c}} = \tilde{\boldsymbol{k}}(\boldsymbol{u}_{\mathrm{f}})$

As illustrated in Fig. 2.4 (d), another option is to define the control law directly as a function of $\boldsymbol{u}_{\mathrm{f}}$, namely a mapping $\boldsymbol{u}_{\mathrm{c}} = \tilde{\boldsymbol{k}}(\boldsymbol{u}_{\mathrm{f}})$. To mimic the behavior of an admissible control law $\boldsymbol{u}_{\mathrm{c}} = \boldsymbol{k}(\boldsymbol{y}^{\mathrm{m}})$, we restrict the mapping $\tilde{\boldsymbol{k}}$ such that, for each exogenous action $\boldsymbol{u}_{\mathrm{f}} \in \boldsymbol{\mathcal{U}}_{\mathrm{f}}$, it maps $\boldsymbol{u}_{\mathrm{f}}$ to a control action $\boldsymbol{u}_{\mathrm{c}} \in \boldsymbol{\mathcal{U}}_{\mathrm{c}}$ that not only fulfills the constraints of the system but also is invariant for all elements in the uncertainty set $\boldsymbol{\mathcal{U}}_{\mathrm{f}}$ that yield the same observation $\boldsymbol{y}^{\mathrm{m}}$ (or equivalently the same $\boldsymbol{y}_{\mathrm{f}}^{\mathrm{m}}$). This results in the following definition.

Definition 4. The control law $\tilde{\boldsymbol{k}} : \boldsymbol{\mathcal{U}}_{\mathrm{f}} \to \boldsymbol{\mathcal{U}}_{\mathrm{c}}$ is admissible if

$$\forall \boldsymbol{u}_{\mathrm{f}} \in \boldsymbol{\mathcal{U}}_{\mathrm{f}} : \ \forall \boldsymbol{u}'_{\mathrm{f}} \in \hat{\boldsymbol{\mathcal{U}}}_{\mathrm{f}}(\boldsymbol{u}_{\mathrm{f}}) : \ \mathbf{A}_{\mathrm{c}} \tilde{\boldsymbol{k}}(\boldsymbol{u}_{\mathrm{f}}) + \mathbf{A}_{\mathrm{f}} \boldsymbol{u}'_{\mathrm{f}} \leq \boldsymbol{b},$$

where $\hat{\boldsymbol{\mathcal{U}}}_{\mathrm{f}}(\boldsymbol{u}_{\mathrm{f}}) = \{\boldsymbol{u}'_{\mathrm{f}} \in \boldsymbol{\mathcal{U}}_{\mathrm{f}} : \mathrm{M}_{\mathrm{f}}^{\mathrm{m}} \boldsymbol{u}'_{\mathrm{f}} = \mathrm{M}_{\mathrm{f}}^{\mathrm{m}} \boldsymbol{u}_{\mathrm{f}}\}$ is a family of sets.

Theorem 2. The following two statements are equivalent:

1. $\exists \boldsymbol{u}_{\mathrm{c}} = \hat{\boldsymbol{k}}(\boldsymbol{y}_{\mathrm{f}}^{\mathrm{m}})$ admissible.
2. $\exists \boldsymbol{u}_{\mathrm{c}} = \tilde{\boldsymbol{k}}(\boldsymbol{u}_{\mathrm{f}})$ admissible.

[8] With a mild abuse of notation, we extensively use the term *observation* when referring to vector $\boldsymbol{y}_{\mathrm{f}}^{\mathrm{m}} \in \mathrm{M}_{\mathrm{f}}^{\mathrm{m}}(\boldsymbol{\mathcal{U}}_{\mathrm{f}})$ in this thesis.

Proof. Suppose that an admissible control law $\boldsymbol{u}_\mathrm{c} = \hat{\boldsymbol{k}}(\boldsymbol{y}_\mathrm{f}^\mathrm{m})$ exists. Then, there also exists an admissible control law $\boldsymbol{u}_\mathrm{c} = \tilde{\boldsymbol{k}}(\boldsymbol{u}_\mathrm{f})$, namely

$$\boldsymbol{u}_\mathrm{c} = \tilde{\boldsymbol{k}}(\boldsymbol{u}_\mathrm{f}) = \hat{\boldsymbol{k}}(\mathrm{M}_\mathrm{f}^\mathrm{m}\boldsymbol{u}_\mathrm{f}).$$

Now assume that there exists an admissible control law $\boldsymbol{u}_\mathrm{c} = \tilde{\boldsymbol{k}}(\boldsymbol{u}_\mathrm{f})$. Then, there also exists an admissible control law $\boldsymbol{u}_\mathrm{c} = \hat{\boldsymbol{k}}(\boldsymbol{y}_\mathrm{f}^\mathrm{m})$, namely the one constructed by mapping all possible pairs $(\boldsymbol{u}_\mathrm{f}, \tilde{\boldsymbol{k}}(\boldsymbol{u}_\mathrm{f}))$ to pairs of the form $(\boldsymbol{y}_\mathrm{f}^\mathrm{m}, \boldsymbol{u}_\mathrm{c})$, i.e.,

$$\begin{bmatrix} \boldsymbol{y}_\mathrm{f}^\mathrm{m} \\ \boldsymbol{u}_\mathrm{c} \end{bmatrix} = \begin{bmatrix} \mathrm{M}_\mathrm{f}^\mathrm{m} & \mathbf{0} \\ \mathbf{0} & \mathbf{I} \end{bmatrix} \begin{bmatrix} \boldsymbol{u}_\mathrm{f} \\ \tilde{\boldsymbol{k}}(\boldsymbol{u}_\mathrm{f}) \end{bmatrix}.$$

□

The admissibility of the control law $\boldsymbol{u}_\mathrm{c} = \tilde{\boldsymbol{k}}(\boldsymbol{u}_\mathrm{f})$ can also be characterized in terms of the null-space of $\mathrm{M}_\mathrm{f}^\mathrm{m}$. Specifically, each exogenous action $\boldsymbol{u}_\mathrm{f} \in \boldsymbol{\mathcal{U}}_\mathrm{f}$ can be decomposed as $\boldsymbol{u}_\mathrm{f} = \boldsymbol{u}_\mathrm{fm} + \boldsymbol{u}_\mathrm{fu}$, where $\boldsymbol{u}_\mathrm{fm}$ belongs to the orthogonal complement of the null-space of $\mathrm{M}_\mathrm{f}^\mathrm{m}$ and $\boldsymbol{u}_\mathrm{fu}$ belongs to the null-space of $\mathrm{M}_\mathrm{f}^\mathrm{m}$. The control action $\boldsymbol{u}_\mathrm{c}$ should therefore be invariant with respect to $\boldsymbol{u}_\mathrm{fu}$.

Note that the control law $\boldsymbol{u}_\mathrm{c} = \tilde{\boldsymbol{k}}(\boldsymbol{u}_\mathrm{f})$ can in general not be implemented in practice since the controller can only access $\boldsymbol{y}^\mathrm{m}$. However, verifying the existence of an admissible mapping $\boldsymbol{u}_\mathrm{c} = \tilde{\boldsymbol{k}}(\boldsymbol{u}_\mathrm{f})$ does not involve recursion, allowing us to verify indirectly the existence of an admissible control law $\boldsymbol{u}_\mathrm{c} = \boldsymbol{k}(\boldsymbol{y}^\mathrm{m})$ by combining Theorems 1 and 2. Summarizing, we obtain the equivalence

$$\exists \boldsymbol{u}_\mathrm{c} = \boldsymbol{k}(\boldsymbol{y}^\mathrm{m}) \text{ admissible} \Leftrightarrow \exists \boldsymbol{u}_\mathrm{c} = \hat{\boldsymbol{k}}(\boldsymbol{y}_\mathrm{f}^\mathrm{m}) \text{ admissible} \Leftrightarrow \exists \boldsymbol{u}_\mathrm{c} = \tilde{\boldsymbol{k}}(\boldsymbol{u}_\mathrm{f}) \text{ admissible}.$$

Let us illustrate the above equivalence with the following simple example.

Example 3. Consider the three dimensional system parametrized by

$$\mathbf{A} = \begin{bmatrix} 1 & 1 & 0 \\ 1 & -1 & -1 \end{bmatrix}, \quad \boldsymbol{b} = \begin{bmatrix} 1.25 \\ 1 \end{bmatrix}, \quad \mathbf{M} = \begin{bmatrix} 1 & 1 & 1 \\ 1 & 1 & 0 \end{bmatrix}, \quad \begin{bmatrix} 0 \\ -1 \\ 0 \end{bmatrix} \leq \boldsymbol{u} \leq \begin{bmatrix} 1 \\ 1 \\ 1 \end{bmatrix}.$$

We analyze the case when $\mathcal{C} = \{2\}$ and $\mathcal{M} = \{1\}$. According to Definition 3, we have to test for the existence of a mapping $\boldsymbol{u}_\mathrm{c} = \hat{\boldsymbol{k}}(\boldsymbol{y}_\mathrm{f}^\mathrm{m})$ such that, for all $\boldsymbol{u}_\mathrm{f} \in [\mathbf{0}, \mathbf{1}]$:

$$-1 \leq \hat{\boldsymbol{k}}(\boldsymbol{y}_\mathrm{f}^\mathrm{m}) \leq 1 \text{ and } \underbrace{\begin{bmatrix} 1 \\ -1 \end{bmatrix}}_{\mathbf{A}_\mathrm{c}} \hat{\boldsymbol{k}}(\boldsymbol{y}_\mathrm{f}^\mathrm{m}) + \underbrace{\begin{bmatrix} 1 & 0 \\ 1 & -1 \end{bmatrix}}_{\mathbf{A}_\mathrm{f}} \boldsymbol{u}_\mathrm{f} \leq \underbrace{\begin{bmatrix} 1.25 \\ 1 \end{bmatrix}}_{\boldsymbol{b}}, \tag{2.10}$$

where $\boldsymbol{y}_\mathrm{f}^\mathrm{m} = \mathrm{M}_\mathrm{f}^\mathrm{m}\boldsymbol{u}_\mathrm{f} = \begin{bmatrix} 1 & 1 \end{bmatrix} \boldsymbol{u}_\mathrm{f}$.

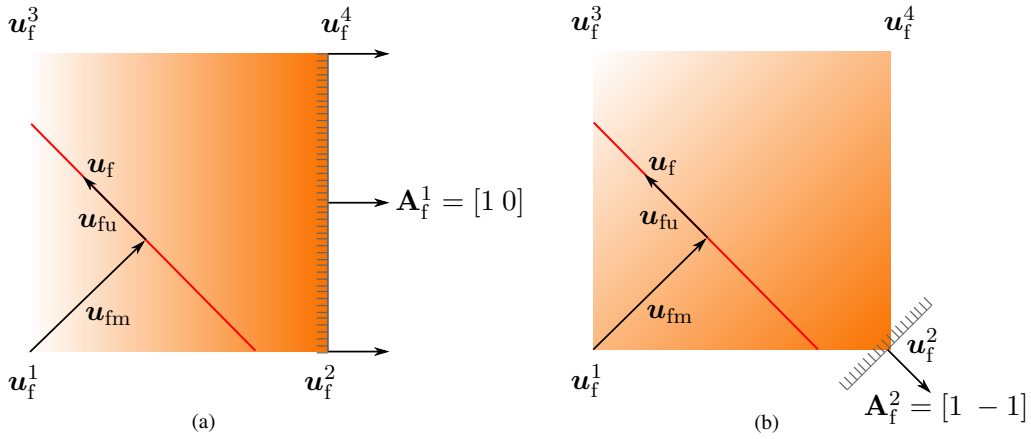

Figure 2.5: Color-coded visualization of the effect of $\boldsymbol{u}_\mathrm{f} \in \mathcal{U}_\mathrm{f}$ on each constraint of the system (2.10). (a) and (b) The red line represents all points in $\mathcal{U}_\mathrm{f}$ that yield the same observation $\boldsymbol{y}_\mathrm{f}^\mathrm{m}$. (a) Any point along the line connecting the points $\boldsymbol{u}_\mathrm{f}^2$ and $\boldsymbol{u}_\mathrm{f}^4$ maximizes the impact on the first constraint. (b) Only the point $\boldsymbol{u}_\mathrm{f}^2$ maximizes the impact on the second constraint.

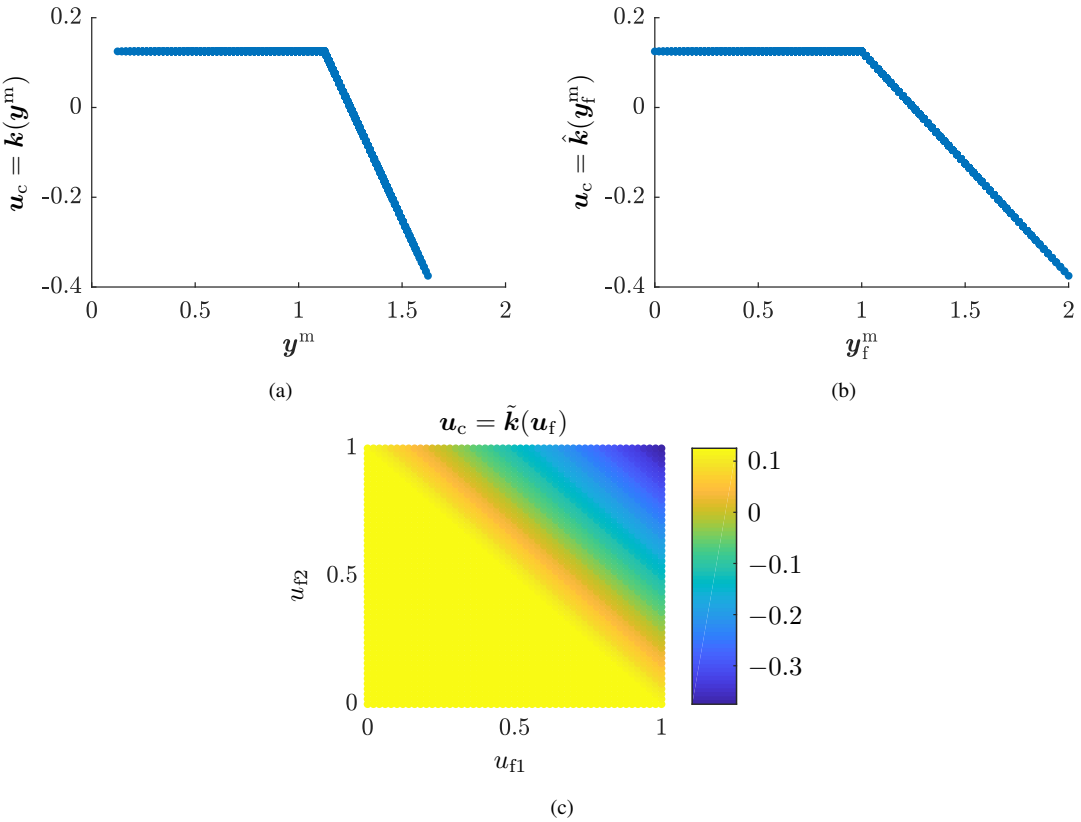

Figure 2.6: (a) An admissible control law $\boldsymbol{u}_\mathrm{c} = \boldsymbol{k}(\boldsymbol{y}^\mathrm{m})$ for the system (2.10) can be chosen as a piecewise-affine function. (b) The same admissible control law expressed as $\boldsymbol{u}_\mathrm{c} = \hat{\boldsymbol{k}}(\boldsymbol{y}_\mathrm{f}^\mathrm{m})$. (c) Color-coding of the same admissible control law expressed as $\boldsymbol{u}_\mathrm{c} = \tilde{\boldsymbol{k}}(\boldsymbol{u}_\mathrm{f})$. Note that the values of $\boldsymbol{u}_\mathrm{c}$ along the component $\boldsymbol{u}_\mathrm{fu}$ of $\boldsymbol{u}_\mathrm{f}$ are the same.

Fig. 2.5 (a) shows the uncertainty set $\boldsymbol{\mathcal{U}}_\mathrm{f}$, a rectangle, together with the components $\boldsymbol{u}_\mathrm{fm}$ and $\boldsymbol{u}_\mathrm{fu}$ of $\boldsymbol{u}_\mathrm{f}$ in the orthogonal complement of the null-space of $\mathrm{M}_\mathrm{f}^\mathrm{m}$ and the kernel of $\mathrm{M}_\mathrm{f}^\mathrm{m}$, respectively. For a given $\boldsymbol{y}_\mathrm{f}^\mathrm{m}$, the control action $\boldsymbol{u}_\mathrm{c}$ has thus to be the same for all elements spanned by the kernel of $\mathrm{M}_\mathrm{f}^\mathrm{m}$, i.e., all $\boldsymbol{u}_\mathrm{f}$ having the same $\boldsymbol{u}_\mathrm{fm}$ value.

Observe in Fig. 2.5 (a) that there is an infinite set of points in $\boldsymbol{\mathcal{U}}_\mathrm{f}$ maximizing the impact on the first constraint, but with different measurements $\boldsymbol{y}_\mathrm{f}^\mathrm{m}$. For the second constraint, see Fig. 2.5 (b), the maximum impact occurs at only one point, namely $\boldsymbol{u}_\mathrm{f}^2$.

By employing the techniques proposed in this thesis, we can show that there exists an admissible control law $\boldsymbol{u}_\mathrm{c} = \hat{\boldsymbol{k}}(\boldsymbol{y}_\mathrm{f}^\mathrm{m})$ for this system. From Theorems 1 and 2, there also exist admissible control laws $\boldsymbol{u}_\mathrm{c} = \boldsymbol{k}(\boldsymbol{y}^\mathrm{m})$, with $\boldsymbol{y}^\mathrm{m} = \mathbf{1}^\mathrm{T}\boldsymbol{u}$, and $\boldsymbol{u}_\mathrm{c} = \tilde{\boldsymbol{k}}(\boldsymbol{u}_\mathrm{f})$, respectively. A possible realization of such admissible control laws is pictured in Fig. 2.6. Since there exists an admissible control law $\boldsymbol{u}_\mathrm{c} = \boldsymbol{k}(\boldsymbol{y}^\mathrm{m})$ for this system, the actuator and sensor sets $\mathcal{C} = \{2\}$ and $\mathcal{M} = \{1\}$ are admissible. □

The previous introductory example exposes an interesting property about admissible control laws, namely that they can always be chosen to be piecewise-affine (PWA) functions in case the sets $\boldsymbol{\mathcal{U}}_\mathrm{c}$ and $\boldsymbol{\mathcal{U}}_\mathrm{f}$ are convex polytopes. We prove this property of admissible control laws in Section 2.3. We additionally provide in Chapter 3 a method to compute closed-form expressions for admissible PWA control laws based on multi-parametric linear optimization techniques, again under the assumption that $\boldsymbol{\mathcal{U}}_\mathrm{c}$ and $\boldsymbol{\mathcal{U}}_\mathrm{f}$ are convex polytopes. Now, let us discuss further about the characteristics of admissible control laws.

2.2.1 Worst-case Characterization of the Uncertainty

The admissibility conditions for $\boldsymbol{u}_\mathrm{c} = \tilde{\boldsymbol{k}}(\boldsymbol{u}_\mathrm{f})$ provided in Definition 4 can be simplified by noting that, for a given exogenous action $\boldsymbol{u}_\mathrm{f}$, it is not necessary to check for the existence of a suitable control action for all elements in the set $\hat{\boldsymbol{\mathcal{U}}}_\mathrm{f}(\boldsymbol{u}_\mathrm{f})$, but only for those elements in $\hat{\boldsymbol{\mathcal{U}}}_\mathrm{f}(\boldsymbol{u}_\mathrm{f})$ that maximize the impact on the constraints of the system.

Theorem 3. The control law $\tilde{\boldsymbol{k}} : \boldsymbol{\mathcal{U}}_\mathrm{f} \to \boldsymbol{\mathcal{U}}_\mathrm{c}$ is admissible if and only if

$$\forall \boldsymbol{u}_\mathrm{f} \in \boldsymbol{\mathcal{U}}_\mathrm{f} : \ \mathbf{A}_c\tilde{\boldsymbol{k}}(\boldsymbol{u}_\mathrm{f}) + \tilde{\boldsymbol{z}}(\boldsymbol{u}_\mathrm{f}) \leq \boldsymbol{b}, \tag{2.11}$$

where the mapping $\tilde{\boldsymbol{z}} : \boldsymbol{\mathcal{U}}_\mathrm{f} \to \mathbb{R}^{n_z}$ is defined by

$$\tilde{\boldsymbol{z}}(\boldsymbol{u}_\mathrm{f}) = \begin{bmatrix} \max_{\boldsymbol{u}'_\mathrm{f} \in \boldsymbol{\mathcal{U}}_\mathrm{f}} \ \mathbf{A}_\mathrm{f}^1\boldsymbol{u}'_\mathrm{f} \text{ s.t. } \mathrm{M}_\mathrm{f}^\mathrm{m}\boldsymbol{u}'_\mathrm{f} = \mathrm{M}_\mathrm{f}^\mathrm{m}\boldsymbol{u}_\mathrm{f} \\ \vdots \\ \max_{\boldsymbol{u}'_\mathrm{f} \in \boldsymbol{\mathcal{U}}_\mathrm{f}} \ \mathbf{A}_\mathrm{f}^{n_z}\boldsymbol{u}'_\mathrm{f} \text{ s.t. } \mathrm{M}_\mathrm{f}^\mathrm{m}\boldsymbol{u}'_\mathrm{f} = \mathrm{M}_\mathrm{f}^\mathrm{m}\boldsymbol{u}_\mathrm{f} \end{bmatrix}, \tag{2.12}$$

and $\mathbf{A}_\mathrm{f}^j$ represents the jth row of $\mathbf{A}_\mathrm{f}$, with $j = 1, ..., n_z$.

Proof. If the control law $\boldsymbol{u}_\mathrm{c} = \tilde{\boldsymbol{k}}(\boldsymbol{u}_\mathrm{f})$ is admissible, then (2.11) also holds since for each $\boldsymbol{u}_\mathrm{f} \in \boldsymbol{\mathcal{U}}_\mathrm{f}$ there is a control action $\boldsymbol{u}_\mathrm{c}$ valid for all elements in the set $\hat{\boldsymbol{\mathcal{U}}}_\mathrm{f}(\boldsymbol{u}_\mathrm{f})$, which includes the points in $\boldsymbol{\mathcal{U}}_\mathrm{f}$ solving the maximization problems in (2.12).

To show that the converse implication also holds, we first note that

$$\forall \boldsymbol{u}_\mathrm{f} \in \boldsymbol{\mathcal{U}}_\mathrm{f} : \ \forall \boldsymbol{u}'_\mathrm{f} \in \hat{\boldsymbol{\mathcal{U}}}_\mathrm{f}(\boldsymbol{u}_\mathrm{f}) : \ \mathbf{A}_\mathrm{f}\boldsymbol{u}'_\mathrm{f} \leq \tilde{\boldsymbol{z}}(\boldsymbol{u}_\mathrm{f}).$$

Assuming that the control law $\boldsymbol{u}_\mathrm{c} = \tilde{\boldsymbol{k}}(\boldsymbol{u}_\mathrm{f})$ fulfills (2.11), we obtain that

$$\forall \boldsymbol{u}_\mathrm{f} \in \boldsymbol{\mathcal{U}}_\mathrm{f} : \ \forall \boldsymbol{u}'_\mathrm{f} \in \hat{\boldsymbol{\mathcal{U}}}_\mathrm{f}(\boldsymbol{u}_\mathrm{f}) : \ \mathbf{A}_\mathrm{c}\tilde{\boldsymbol{k}}(\boldsymbol{u}_\mathrm{f}) + \mathbf{A}_\mathrm{f}\boldsymbol{u}'_\mathrm{f} \leq \mathbf{A}_\mathrm{c}\tilde{\boldsymbol{k}}(\boldsymbol{u}_\mathrm{f}) + \tilde{\boldsymbol{z}}(\boldsymbol{u}_\mathrm{f}) \leq \boldsymbol{b},$$

i.e., the control law $\boldsymbol{u}_\mathrm{c} = \tilde{\boldsymbol{k}}(\boldsymbol{u}_\mathrm{f})$ is admissible. □

Theorem 4. The control law $\hat{\boldsymbol{k}} : \mathrm{M}_\mathrm{f}^\mathrm{m}(\boldsymbol{\mathcal{U}}_\mathrm{f}) \mapsto \boldsymbol{\mathcal{U}}_\mathrm{c}$ is admissible if and only if

$$\forall \boldsymbol{y}_\mathrm{f}^\mathrm{m} \in \mathrm{M}_\mathrm{f}^\mathrm{m}(\boldsymbol{\mathcal{U}}_\mathrm{f}) : \ \mathbf{A}_\mathrm{c}\hat{\boldsymbol{k}}(\boldsymbol{y}_\mathrm{f}^\mathrm{m}) + \hat{\boldsymbol{z}}(\boldsymbol{y}_\mathrm{f}^\mathrm{m}) \leq \boldsymbol{b}, \tag{2.13}$$

where the mapping $\hat{\boldsymbol{z}} : \mathrm{M}_\mathrm{f}^\mathrm{m}(\boldsymbol{\mathcal{U}}_\mathrm{f}) \to \mathbb{R}^{n_z}$ is defined by

$$\hat{\boldsymbol{z}}(\boldsymbol{y}_\mathrm{f}^\mathrm{m}) = \begin{bmatrix} \max_{\boldsymbol{u}_\mathrm{f} \in \boldsymbol{\mathcal{U}}_\mathrm{f}} \ \mathbf{A}_\mathrm{f}^1\boldsymbol{u}_\mathrm{f} \text{ s.t. } \mathrm{M}_\mathrm{f}^\mathrm{m}\boldsymbol{u}_\mathrm{f} = \boldsymbol{y}_\mathrm{f}^\mathrm{m} \\ \vdots \\ \max_{\boldsymbol{u}_\mathrm{f} \in \boldsymbol{\mathcal{U}}_\mathrm{f}} \ \mathbf{A}_\mathrm{f}^{n_z}\boldsymbol{u}_\mathrm{f} \text{ s.t. } \mathrm{M}_\mathrm{f}^\mathrm{m}\boldsymbol{u}_\mathrm{f} = \boldsymbol{y}_\mathrm{f}^\mathrm{m} \end{bmatrix}, \tag{2.14}$$

and $\mathbf{A}_\mathrm{f}^j$ represents the jth row of $\mathbf{A}_\mathrm{f}$, with $j = 1, ..., n_z$.

Proof. Omitted as it is similar to the proof of Theorem 3. □

Remark 1. In Theorem 3, the mapping $\tilde{\boldsymbol{z}}(\boldsymbol{u}_\mathrm{f})$ is defined in terms of n_z convex maximization problems. However, the mapping $\tilde{\boldsymbol{z}}(\boldsymbol{u}_\mathrm{f})$ can be re-expressed in terms of the single, but larger, convex maximization problem

$$\begin{aligned} \tilde{\boldsymbol{z}}(\boldsymbol{u}_\mathrm{f}) = \arg\max_{\tilde{\boldsymbol{z}} \in \mathbb{R}^{n_z}} \max_{\boldsymbol{u}_\mathrm{f}^{1,\ldots,n_z} \in \boldsymbol{\mathcal{U}}_\mathrm{f}} & \ \mathbf{1}^\mathrm{T}\tilde{\boldsymbol{z}} \\ \text{s.t. } \tilde{\boldsymbol{z}} = & \begin{bmatrix} \mathbf{A}_\mathrm{f}^1\boldsymbol{u}_\mathrm{f}^1 \\ \vdots \\ \mathbf{A}_\mathrm{f}^{n_z}\boldsymbol{u}_\mathrm{f}^{n_z} \end{bmatrix}, \\ & \mathrm{M}_\mathrm{f}^\mathrm{m}\boldsymbol{u}_\mathrm{f}^{1,\ldots,n_z} = \mathrm{M}_\mathrm{f}^\mathrm{m}\boldsymbol{u}_\mathrm{f}. \end{aligned} \tag{2.15}$$

Note that a similar formulation for the mapping $\hat{\boldsymbol{z}}(\boldsymbol{y}_\mathrm{f}^\mathrm{m})$ defined in Theorem 4 can be obtained by simply replacing the term $\mathrm{M}_\mathrm{f}^\mathrm{m}\boldsymbol{u}_\mathrm{f}$ with $\boldsymbol{y}_\mathrm{f}^\mathrm{m}$ in the equality constraints of maximization problem (2.15). As we show in Chapter 3, the above formulation of the mapping $\tilde{\boldsymbol{z}}(\boldsymbol{u}_\mathrm{f})$ (or $\hat{\boldsymbol{z}}(\boldsymbol{y}_\mathrm{f}^\mathrm{m})$) is beneficial for computing the closed-form expression of an admissible PWA control law $\boldsymbol{u}_\mathrm{c} = \tilde{\boldsymbol{k}}(\boldsymbol{u}_\mathrm{f})$ (or $\boldsymbol{u}_\mathrm{c} = \hat{\boldsymbol{k}}(\boldsymbol{y}_\mathrm{f}^\mathrm{m})$) in case $\boldsymbol{\mathcal{U}}_\mathrm{f}$ is a convex polytope.

Theorems 3 and 4 provide equivalent conditions for the existence of admissible control laws $\boldsymbol{u}_\mathrm{c} = \tilde{\boldsymbol{k}}(\boldsymbol{u}_\mathrm{f})$ and $\boldsymbol{u}_\mathrm{c} = \hat{\boldsymbol{k}}(\boldsymbol{y}_\mathrm{f}^\mathrm{m})$, respectively. Specifically, we obtain the equivalences

- $\exists \boldsymbol{u}_\mathrm{c} = \tilde{\boldsymbol{k}}(\boldsymbol{u}_\mathrm{f})$ admissible $\Leftrightarrow \exists \boldsymbol{u}_\mathrm{c} = \tilde{\boldsymbol{k}}(\boldsymbol{u}_\mathrm{f})$ fulfilling (2.11).
- $\exists \boldsymbol{u}_\mathrm{c} = \hat{\boldsymbol{k}}(\boldsymbol{y}_\mathrm{f}^\mathrm{m})$ admissible $\Leftrightarrow \exists \boldsymbol{u}_\mathrm{c} = \hat{\boldsymbol{k}}(\boldsymbol{y}_\mathrm{f}^\mathrm{m})$ fulfilling (2.13).

Although conditions (2.11) and (2.13) are non-recursive and simpler to analyze in comparison to the conditions given in Definition 1, verifying the existence of admissible control laws $\boldsymbol{u}_\mathrm{c} = \tilde{\boldsymbol{k}}(\boldsymbol{u}_\mathrm{f})$ and/or $\boldsymbol{u}_\mathrm{c} = \hat{\boldsymbol{k}}(\boldsymbol{y}_\mathrm{f}^\mathrm{m})$ still is a challenging infinite dimensional feasibility problem. In the subsequent section we show that, if the uncertainty set $\boldsymbol{\mathcal{U}}_\mathrm{f}$ is a convex polytope, then it is possible to simplify the admissibility condition to a condition involving only a finite number of linear inequalities.

2.3 Special Case: Polytopic Uncertainty Sets

As mentioned in Section 2.2, verifying the existence of an admissible control law is in general a challenging task as it turns into an infinite dimensional feasibility problem. There are, however, important cases in which we can simplify the verification task into a finite dimensional feasibility problem. This section studies the particular case where the uncertainty set $\boldsymbol{\mathcal{U}}_\mathrm{f}$ is a convex polytope.

Assumption 1. The uncertainty set $\boldsymbol{\mathcal{U}}_\mathrm{f}$ is a convex polytope, i.e., each point $\boldsymbol{u}_\mathrm{f} \in \boldsymbol{\mathcal{U}}_\mathrm{f}$ can be represented as a *convex combination* of the *corners* of $\boldsymbol{\mathcal{U}}_\mathrm{f}$,[9] namely,

$$\boldsymbol{u}_\mathrm{f} = \sum_{i=1}^{R} \boldsymbol{u}_\mathrm{f}^i \lambda_i, \quad \text{with } \sum_{i=1}^{R} \lambda_i = 1, \quad \lambda_i \in \mathbb{R}_{\geq 0}, \quad i \in \{1, ..., R\},$$

where $\boldsymbol{u}_\mathrm{f}^i$ denotes the ith corner of $\boldsymbol{\mathcal{U}}_\mathrm{f}$, and $R \in \mathbb{N}^+$ is the total number of corners.

To start our analysis, we again center our investigation in systems for which $\mathcal{M} \neq \emptyset$, $\boldsymbol{\mathcal{U}}_\mathrm{f} \neq \emptyset$, and $\mathrm{rank}(\mathrm{M}_\mathrm{f}^\mathrm{m}) < n_u - |\mathcal{C}|$ apply. We also recall from Theorem 3 that the control law $\boldsymbol{u}_\mathrm{c} = \tilde{\boldsymbol{k}}(\boldsymbol{u}_\mathrm{f})$ is admissible if and only if

$$\forall \boldsymbol{u}_\mathrm{f} \in \boldsymbol{\mathcal{U}}_\mathrm{f} : \ \mathbf{A}_\mathrm{c} \tilde{\boldsymbol{k}}(\boldsymbol{u}_\mathrm{f}) + \tilde{\boldsymbol{z}}(\boldsymbol{u}_\mathrm{f}) \leq \boldsymbol{b},$$

where $\tilde{\boldsymbol{z}}(\boldsymbol{u}_\mathrm{f})$ is given by

$$\tilde{\boldsymbol{z}}(\boldsymbol{u}_\mathrm{f}) = \begin{bmatrix} \max_{\boldsymbol{u}_\mathrm{f}' \in \boldsymbol{\mathcal{U}}_\mathrm{f}} \ \mathbf{A}_\mathrm{f}^1 \boldsymbol{u}_\mathrm{f}' \text{ s.t. } \mathrm{M}_\mathrm{f}^\mathrm{m} \boldsymbol{u}_\mathrm{f}' = \mathrm{M}_\mathrm{f}^\mathrm{m} \boldsymbol{u}_\mathrm{f} \\ \vdots \\ \max_{\boldsymbol{u}_\mathrm{f}' \in \boldsymbol{\mathcal{U}}_\mathrm{f}} \ \mathbf{A}_\mathrm{f}^{n_z} \boldsymbol{u}_\mathrm{f}' \text{ s.t. } \mathrm{M}_\mathrm{f}^\mathrm{m} \boldsymbol{u}_\mathrm{f}' = \mathrm{M}_\mathrm{f}^\mathrm{m} \boldsymbol{u}_\mathrm{f} \end{bmatrix}.$$

[9] A corner is a vertex, also known as extreme point, of a polyhedron.

In the following, we show that under Assumption 1 the mapping $\tilde{\boldsymbol{z}}(\boldsymbol{u}_\mathrm{f})$ has a set of properties that allow us to 1) transform the above admissibility condition into an equivalent condition that involves a finite number of linear inequalities, and 2) show that an admissible control law can always be chosen as a PWA function.

Under Assumption 1, the maximization problems defining the entries of $\tilde{\boldsymbol{z}}(\boldsymbol{u}_\mathrm{f})$ are linear. More interesting, for each $j \in \{1, ..., n_z\}$ the function

$$\tilde{z}_j(\boldsymbol{u}_\mathrm{f}) = \max_{\boldsymbol{u}'_\mathrm{f} \in \boldsymbol{\mathcal{U}}_\mathrm{f}} \ \mathbf{A}_\mathrm{f}^j \boldsymbol{u}'_\mathrm{f} \text{ s.t. } \mathbf{M}_\mathrm{f}^\mathrm{m} \boldsymbol{u}'_\mathrm{f} = \mathbf{M}_\mathrm{f}^\mathrm{m} \boldsymbol{u}_\mathrm{f},$$

is continuous, concave, and piecewise-affine.

Corollary 1 ([92, Corollary 6.3.2])**.** If $\boldsymbol{\mathcal{U}}_\mathrm{f}$ is a convex polytope, then the mapping $\tilde{z}_j(\boldsymbol{u}_\mathrm{f})$ is continuous, piecewise-affine, and concave for each $j \in \{1, ..., n_z\}$.

Now, from Corollary 1 and recalling that the mapping $\tilde{\boldsymbol{z}}(\boldsymbol{u}_\mathrm{f})$ can be expressed in terms of the single (and in this case also linear) maximization problem (2.15), we deduce that the mapping $\tilde{\boldsymbol{z}}(\boldsymbol{u}_\mathrm{f})$ is continuous and PWA.

Corollary 2. If $\boldsymbol{\mathcal{U}}_\mathrm{f}$ is a convex polytope, then the mapping $\tilde{\boldsymbol{z}}(\boldsymbol{u}_\mathrm{f})$ is continuous and piecewise-affine.

The mapping $\tilde{\boldsymbol{z}}(\boldsymbol{u}_\mathrm{f})$ has one additional property that allows us to re-express condition (2.11) as a finite number of linear inequalities, namely that each piece of $\tilde{\boldsymbol{z}}(\boldsymbol{u}_\mathrm{f})$ is valid in a so-called *critical region* (CR) defined by a convex polytope.

Corollary 3 ([93])**.** The *critical regions* of $\boldsymbol{\mathcal{U}}_\mathrm{f}$ associated to the PWA mapping $\tilde{\boldsymbol{z}}(\boldsymbol{u}_\mathrm{f})$ are convex polytopes.

The above introduced properties of $\tilde{\boldsymbol{z}}(\boldsymbol{u}_\mathrm{f})$ allow us to re-express condition (2.11) as a finite number of linear inequalities as follows. First, note that under Assumption 1 we can partition the polytopic uncertainty set $\boldsymbol{\mathcal{U}}_\mathrm{f}$ into $\hat{\kappa} \in \mathbb{N}^+$ polytopic critical regions associated to the PWA mapping $\tilde{\boldsymbol{z}}(\boldsymbol{u}_\mathrm{f})$. We can thus not only express any realization of $\boldsymbol{u}_\mathrm{f} \in \boldsymbol{\mathcal{U}}_\mathrm{f}$ as a convex combination of the corners of its associated polytopic critical region, but also the values mapped by $\tilde{\boldsymbol{z}}$ at those corners. The following theorem formalize this.[10]

Theorem 5. Let $\tilde{\boldsymbol{z}}(\boldsymbol{u}_\mathrm{f})$ be given as in (2.15). Also let $\mathcal{R}^\kappa(\boldsymbol{\mathcal{U}}_\mathrm{f})$ denote the κth critical region of $\boldsymbol{\mathcal{U}}_\mathrm{f}$ associated to the mapping $\tilde{\boldsymbol{z}}(\boldsymbol{u}_\mathrm{f})$, where $\kappa \in \{1, ..., \hat{\kappa}\}$ and $\hat{\kappa} \in \mathbb{N}^+$ is the total number of critical regions. Further, let $C^\kappa_{\boldsymbol{\mathcal{U}}_\mathrm{f}} \subset \mathcal{R}^\kappa(\boldsymbol{\mathcal{U}}_\mathrm{f})$ be the set containing the corners of $\mathcal{R}^\kappa(\boldsymbol{\mathcal{U}}_\mathrm{f})$, $|C^\kappa_{\boldsymbol{\mathcal{U}}_\mathrm{f}}|$ be the number of corners of $\mathcal{R}^\kappa(\boldsymbol{\mathcal{U}}_\mathrm{f})$, and $\boldsymbol{u}_\mathrm{f}^{\kappa i} \in C^\kappa_{\boldsymbol{\mathcal{U}}_\mathrm{f}}$ be the ith corner of $\mathcal{R}^\kappa(\boldsymbol{\mathcal{U}}_\mathrm{f})$, for all $i \in \{1, ..., |C^\kappa_{\boldsymbol{\mathcal{U}}_\mathrm{f}}|\}$, for all $\kappa \in \{1, ..., \hat{\kappa}\}$. Then, for all $\kappa \in \{1, ..., \hat{\kappa}\}$ and for all $\boldsymbol{u}_\mathrm{f} \in \mathcal{R}^\kappa(\boldsymbol{\mathcal{U}}_\mathrm{f})$, the κth piece of $\tilde{\boldsymbol{z}}(\boldsymbol{u}_\mathrm{f})$, here denoted by $\tilde{\boldsymbol{z}}^\kappa(\boldsymbol{u}_\mathrm{f})$, can be expressed as

$$\tilde{\boldsymbol{z}}^\kappa(\boldsymbol{u}_\mathrm{f}) = \sum_{i=1}^{|C^\kappa_{\boldsymbol{\mathcal{U}}_\mathrm{f}}|} \tilde{\boldsymbol{z}}(\boldsymbol{u}_\mathrm{f}^{\kappa i}) \mu_i^\kappa(\boldsymbol{u}_\mathrm{f}), \tag{2.16}$$

[10] A mapping having this property is known in the literature as a *convex combination mapping* [94].

where

$$\mu_i^\kappa(\boldsymbol{u}_\mathrm{f}) \geq 0 \;\text{ and }\; \sum_{i=1}^{|C^\kappa_{\boldsymbol{\mathcal{U}}_\mathrm{f}}|} \mu_i^\kappa(\boldsymbol{u}_\mathrm{f}) = 1. \tag{2.17}$$

Proof. From Corollaries 2 and 3, the κth piece of $\tilde{\boldsymbol{z}}(\boldsymbol{u}_\mathrm{f})$ is an affine function of the form

$$\tilde{\boldsymbol{z}}^\kappa(\boldsymbol{u}_\mathrm{f}) = \mathbf{S}^\kappa \boldsymbol{u}_\mathrm{f} + \boldsymbol{n}^\kappa, \quad \forall \boldsymbol{u}_\mathrm{f} \in \mathcal{R}^\kappa(\boldsymbol{\mathcal{U}}_\mathrm{f}),$$

with $\mathbf{S}^\kappa \in \mathbb{R}^{n_z \times (n_u - |\mathcal{C}|)}$ and $\boldsymbol{n}^\kappa \in \mathbb{R}^{n_z}$. Since $\mathcal{R}^\kappa(\boldsymbol{\mathcal{U}}_\mathrm{f})$ is a convex polytope, we can express any exogenous action $\boldsymbol{u}_\mathrm{f} \in \mathcal{R}^\kappa(\boldsymbol{\mathcal{U}}_\mathrm{f})$ in terms of a convex combination of the corners of $\mathcal{R}^\kappa(\boldsymbol{\mathcal{U}}_\mathrm{f})$, namely $\boldsymbol{u}_\mathrm{f} = \sum_{i=1}^{|C^\kappa_{\boldsymbol{\mathcal{U}}_\mathrm{f}}|} \boldsymbol{u}_\mathrm{f}^{\kappa i} \mu_i^\kappa(\boldsymbol{u}_\mathrm{f})$, with $\mu_i^\kappa(\boldsymbol{u}_\mathrm{f}) \geq 0$ and $\sum_{i=1}^{|C^\kappa_{\boldsymbol{\mathcal{U}}_\mathrm{f}}|} \mu_i^\kappa(\boldsymbol{u}_\mathrm{f}) = 1$. Then,

$$\tilde{\boldsymbol{z}}^\kappa(\boldsymbol{u}_\mathrm{f}) = \mathbf{S}^\kappa \boldsymbol{u}_\mathrm{f} + \boldsymbol{n}^\kappa = \mathbf{S}^\kappa \sum_{i=1}^{|C^\kappa_{\boldsymbol{\mathcal{U}}_\mathrm{f}}|} \boldsymbol{u}_\mathrm{f}^{\kappa i} \mu_i^\kappa + \boldsymbol{n}^\kappa = \sum_{i=1}^{|C^\kappa_{\boldsymbol{\mathcal{U}}_\mathrm{f}}|} \underbrace{(\mathbf{S}^\kappa \boldsymbol{u}_\mathrm{f}^{\kappa i} + \boldsymbol{n}^\kappa)}_{\tilde{\boldsymbol{z}}^\kappa(\boldsymbol{u}_\mathrm{f}^{\kappa i}) = \tilde{\boldsymbol{z}}(\boldsymbol{u}_\mathrm{f}^{\kappa i})} \mu_i^\kappa,$$

which holds for all $\kappa \in \{1, ..., \hat{\kappa}\}$. □

Theorem 5 is the key to reduce the admissibility condition (2.11) for the mapping $\boldsymbol{u}_\mathrm{c} = \tilde{\boldsymbol{k}}(\boldsymbol{u}_\mathrm{f})$ to a condition comprising a finite number of linear inequalities. This is because, provided that the corners of $\mathcal{R}^\kappa(\boldsymbol{\mathcal{U}}_\mathrm{f})$ for all $\kappa \in \{1, ..., \hat{\kappa}\}$ are available, we can precompute the values $\tilde{\boldsymbol{z}}^{\kappa i} = \tilde{\boldsymbol{z}}^\kappa(\boldsymbol{u}_\mathrm{f}^{\kappa i}) = \tilde{\boldsymbol{z}}(\boldsymbol{u}_\mathrm{f}^{\kappa i})$, with $i \in \{1, ..., |C^\kappa_{\boldsymbol{\mathcal{U}}_\mathrm{f}}|\}$ and then, for each $i \in \{1, ..., |C^\kappa_{\boldsymbol{\mathcal{U}}_\mathrm{f}}|\}$ and for each $\kappa \in \{1, ..., \hat{\kappa}\}$, check if for the ith corner of $\mathcal{R}^\kappa(\boldsymbol{\mathcal{U}}_\mathrm{f})$ there exists a control action $\boldsymbol{u}_\mathrm{c}^{\kappa i} \in \boldsymbol{\mathcal{U}}_\mathrm{c}$ such that the inequality $\mathbf{A}_\mathrm{c} \boldsymbol{u}_\mathrm{c}^{\kappa i} + \tilde{\boldsymbol{z}}^{\kappa i} \leq \boldsymbol{b}$ holds.

Theorem 6. Let $\tilde{\boldsymbol{z}}(\boldsymbol{u}_\mathrm{f})$, $\mathcal{R}^\kappa(\boldsymbol{\mathcal{U}}_\mathrm{f})$, $C^\kappa_{\boldsymbol{\mathcal{U}}_\mathrm{f}}$, and $\boldsymbol{u}_\mathrm{f}^{\kappa i} \in \mathcal{R}^\kappa(\boldsymbol{\mathcal{U}}_\mathrm{f})$ be defined as in Theorem 5, and let $\tilde{\boldsymbol{z}}^{\kappa i} = \tilde{\boldsymbol{z}}(\boldsymbol{u}_\mathrm{f}^{\kappa i})$, for all $i \in \{1, ..., |C^\kappa_{\boldsymbol{\mathcal{U}}_\mathrm{f}}|\}$ and for all $\kappa \in \{1, ..., \hat{\kappa}\}$. Then, the following two statements are equivalent:

1. $\exists \boldsymbol{u}_\mathrm{c} = \tilde{\boldsymbol{k}}(\boldsymbol{u}_\mathrm{f})$ admissible.

2. The condition

$$\exists \boldsymbol{u}_\mathrm{c}^{\kappa i} \in \boldsymbol{\mathcal{U}}_\mathrm{c} : \; \mathbf{A}_\mathrm{c} \boldsymbol{u}_\mathrm{c}^{\kappa i} + \tilde{\boldsymbol{z}}^{\kappa i} \leq \boldsymbol{b}, \quad \forall i \in \{1, ..., |C^\kappa_{\boldsymbol{\mathcal{U}}_\mathrm{f}}|\}, \; \forall \kappa \in \{1, ..., \hat{\kappa}\} \tag{2.18}$$

is fulfilled.

Proof. If an admissible control law $\boldsymbol{u}_\mathrm{c} = \tilde{\boldsymbol{k}}(\boldsymbol{u}_\mathrm{f})$ exists, then there exist valid values of $\boldsymbol{u}_\mathrm{c}$ for each point in $\boldsymbol{\mathcal{U}}_\mathrm{f}$, including the corners of each critical region of $\boldsymbol{\mathcal{U}}_\mathrm{f}$ associated to the PWA mapping $\tilde{\boldsymbol{z}}(\boldsymbol{u}_\mathrm{f})$.

To prove the converse implication, let the points $\boldsymbol{u}_\mathrm{c}^{\kappa i}$, $\boldsymbol{u}_\mathrm{f}^{\kappa i}$, and $\tilde{\boldsymbol{z}}^{\kappa i} = \tilde{\boldsymbol{z}}(\boldsymbol{u}_\mathrm{f}^{\kappa i})$, with $i \in \{1, ..., |C^\kappa_{\boldsymbol{\mathcal{U}}_\mathrm{f}}|\}$ and $\kappa \in \{1, ..., \hat{\kappa}\}$ be given and fulfill (2.18). Then, for the κth piece of $\tilde{\boldsymbol{z}}(\boldsymbol{u}_\mathrm{f})$, we can construct a control law

$$\boldsymbol{u}_\mathrm{c} = \tilde{\boldsymbol{k}}^\kappa(\boldsymbol{u}_\mathrm{f}) = \sum_{i=1}^{|C^\kappa_{\boldsymbol{\mathcal{U}}_\mathrm{f}}|} \boldsymbol{u}_\mathrm{c}^{\kappa i} \mu_i^\kappa(\boldsymbol{u}_\mathrm{f}), \quad \forall \boldsymbol{u}_\mathrm{f} \in \mathcal{R}^\kappa(\boldsymbol{\mathcal{U}}_\mathrm{f}), \tag{2.19}$$

where the functions $\mu_i^\kappa(\boldsymbol{u}_\mathrm{f})$ fulfill (in)equalities (2.17). The control action $\boldsymbol{u}_\mathrm{c}$ is thus a convex combination of the precomputed control values $\boldsymbol{u}_\mathrm{c}^{\kappa i}$, with $i \in \{1, ..., |C^\kappa_{\boldsymbol{\mathcal{U}}_\mathrm{f}}|\}$ and $\kappa \in \{1, ..., \hat{\kappa}\}$. From Theorem 5, we know that the κth piece of the mapping $\tilde{\boldsymbol{z}}(\boldsymbol{u}_\mathrm{f})$ can be expressed as in (2.16). Then,

$$\begin{aligned}\forall \boldsymbol{u}_\mathrm{f} \in \mathcal{R}^\kappa(\boldsymbol{\mathcal{U}}_\mathrm{f}) :\ \mathbf{A}_\mathrm{c}\tilde{\boldsymbol{k}}^\kappa(\boldsymbol{u}_\mathrm{f}) + \tilde{\boldsymbol{z}}^\kappa(\boldsymbol{u}_\mathrm{f}) &= \mathbf{A}_\mathrm{c}\sum_{i=1}^{|C^\kappa_{\boldsymbol{\mathcal{U}}_\mathrm{f}}|} \boldsymbol{u}_\mathrm{c}^{\kappa i}\mu_i^\kappa(\boldsymbol{u}_\mathrm{f}) + \sum_{i=1}^{|C^\kappa_{\boldsymbol{\mathcal{U}}_\mathrm{f}}|} \tilde{\boldsymbol{z}}^{\kappa i}\mu_i^\kappa(\boldsymbol{u}_\mathrm{f}) \\ &= \sum_{i=1}^{|C^\kappa_{\boldsymbol{\mathcal{U}}_\mathrm{f}}|} \underbrace{\left(\mathbf{A}_\mathrm{c}\boldsymbol{u}_\mathrm{c}^{\kappa i} + \tilde{\boldsymbol{z}}^{\kappa i}\right)}_{\leq \boldsymbol{b}} \mu_i^\kappa(\boldsymbol{u}_\mathrm{f}) \leq \boldsymbol{b},\end{aligned}$$

which holds for all $\kappa \in \{1, ..., \hat{\kappa}\}$ and thus for all $\boldsymbol{u}_\mathrm{f} \in \boldsymbol{\mathcal{U}}_\mathrm{f} = \cup_{\kappa=1}^{\hat{\kappa}} \mathcal{R}^\kappa(\boldsymbol{\mathcal{U}}_\mathrm{f})$. The piecewise control law (2.19) hence fulfills the admissibility condition provided in Theorem 3. □

Theorem 7. The control law (2.19) is a piecewise-affine function.

Proof. It follows from the facts that 1) both $\tilde{\boldsymbol{z}}(\boldsymbol{u}_\mathrm{f})$ and $\tilde{\boldsymbol{k}}(\boldsymbol{u}_\mathrm{f})$ are expressed in terms of the functions $\mu_i^\kappa(\boldsymbol{u}_\mathrm{f})$ fulfilling conditions (2.17) and 2) $\tilde{\boldsymbol{z}}(\boldsymbol{u}_\mathrm{f})$ is piecewise-affine. □

Note that an admissible PWA control law $\boldsymbol{u}_\mathrm{c} = \hat{\boldsymbol{k}}(\boldsymbol{y}_\mathrm{f}^\mathrm{m})$ can also be constructed by following similar approaches as the proposed in Theorems 5 and 6. The reason is that the set of all possible observations $\mathrm{M}_\mathrm{f}^\mathrm{m}(\boldsymbol{\mathcal{U}}_\mathrm{f})$ generated by the convex polytope $\boldsymbol{\mathcal{U}}_\mathrm{f}$ is also a convex polytope. The mapping $\hat{\boldsymbol{z}}(\boldsymbol{y}_\mathrm{f}^\mathrm{m})$ is thus a PWA mapping defined in polytopic critical regions of the set $\mathrm{M}_\mathrm{f}^\mathrm{m}(\boldsymbol{\mathcal{U}}_\mathrm{f})$, allowing for the derivation of an admissibility condition given in terms of a finite number of linear inequalities. More detailed derivations and proofs in this regard are omitted as they are very similar to the approaches of Theorems 5 and 6.

From Theorem 6, we have the equivalence

$\boldsymbol{\mathcal{U}}_\mathrm{f}$ is a convex polytope: $\exists \boldsymbol{u}_\mathrm{c} = \tilde{\boldsymbol{k}}(\boldsymbol{u}_\mathrm{f})$ admissible $\Leftrightarrow$ Condition (2.18) is fulfilled.

Note that if 1) Assumption 1 holds, 2) the corners of the critical regions of $\boldsymbol{\mathcal{U}}_\mathrm{f}$ associated to $\tilde{\boldsymbol{z}}(\boldsymbol{u}_\mathrm{f})$ are available, and 3) there exists an admissible control law $\boldsymbol{u}_\mathrm{c} = \tilde{\boldsymbol{k}}(\boldsymbol{u}_\mathrm{f})$, then we can compute the admissible control law (2.17)–(2.19) as indicated in the proof of Theorem 6. Unfortunately, the number of critical regions of $\boldsymbol{\mathcal{U}}_\mathrm{f}$ associated to $\tilde{\boldsymbol{z}}(\boldsymbol{u}_\mathrm{f})$ often grows exponentially with the dimension of $\boldsymbol{u}_\mathrm{f}$, limiting the approach to small applications.

On a Necessary Admissibility Condition

Instead of using all corners of the critical regions of $\boldsymbol{\mathcal{U}}_\mathrm{f}$ associated to the mapping $\tilde{\boldsymbol{z}}(\boldsymbol{u}_\mathrm{f})$, we now focus on a subset of corners only, namely those corners of $\boldsymbol{\mathcal{U}}_\mathrm{f}$ that maximize the impact on the constraints of the system. To this end, let $C^\star_{\boldsymbol{\mathcal{U}}_\mathrm{f}} \subseteq \boldsymbol{\mathcal{U}}_\mathrm{f}$ denote such

subset or corners. A point $\boldsymbol{u}_\mathrm{f} \in \boldsymbol{\mathcal{U}}_\mathrm{f}$ belongs to $C^\star_{\boldsymbol{\mathcal{U}}_\mathrm{f}}$ if there exists $j \in \{1, ..., n_z\}$ such that $\boldsymbol{u}_\mathrm{f}$ is an optimal solution for

$$\boldsymbol{u}_\mathrm{f} = \underset{\boldsymbol{u}'_\mathrm{f} \in C^\star_{\boldsymbol{\mathcal{U}}_\mathrm{f}}}{\arg\max}\, \mathbf{A}_\mathrm{f}^j \boldsymbol{u}'_\mathrm{f}. \tag{2.20}$$

Remark 2. In many cases the optimal solutions of (2.20) for different rows of $\mathbf{A}_\mathrm{f}$ will coincide and $|C^\star_{\boldsymbol{\mathcal{U}}_\mathrm{f}}|$ is even smaller than its maximum possible value n_z.

Remark 3. The maximizer of problem (2.20) is not unique in general. In particular, problem (2.20) has unique maximizer only if the direction $\mathbf{A}_\mathrm{f}^i$ is not parallel to the normal vector associated to any hyperplane of the convex polytope $\boldsymbol{\mathcal{U}}_\mathrm{f} \neq \emptyset$. See for instance Fig. 2.6 where both $\boldsymbol{u}_\mathrm{f}^2$ and $\boldsymbol{u}_\mathrm{f}^4$ solve problem (2.20) for $j = 1$.

Although the total number of corners in $C^\star_{\boldsymbol{\mathcal{U}}_\mathrm{f}}$ is often significantly smaller than R, using the subset $C^\star_{\boldsymbol{\mathcal{U}}_\mathrm{f}}$ instead of using all corners of $\boldsymbol{\mathcal{U}}_\mathrm{f}$ is not sufficient to conclude about the existence of an admissible control law $\boldsymbol{u}_\mathrm{c} = \tilde{\boldsymbol{k}}(\boldsymbol{u}_\mathrm{f})$. More specifically, the fulfillment of the condition

$$\exists \boldsymbol{u}_\mathrm{c}^j \in \boldsymbol{\mathcal{U}}_\mathrm{c} \text{ s.t. } \mathbf{A}_\mathrm{c}\boldsymbol{u}_\mathrm{c}^j + \tilde{\boldsymbol{z}}(\boldsymbol{u}_\mathrm{f}^j) \leq \boldsymbol{b}, \quad \text{where } \boldsymbol{u}_\mathrm{f}^j \in C^\star_{\boldsymbol{\mathcal{U}}_\mathrm{f}},\ \forall j \in \{1, ..., n_z\} \tag{2.21}$$

does not imply the existence of an admissible control law $\boldsymbol{u}_\mathrm{c} = \tilde{\boldsymbol{k}}(\boldsymbol{u}_\mathrm{f})$ per se. In fact, there are many constrained static linear systems for which suitable control actions associated to the elements of $C^\star_{\boldsymbol{\mathcal{U}}_\mathrm{f}}$ exist, but there are no suitable control actions for all points $\boldsymbol{u}_\mathrm{f} \in \boldsymbol{\mathcal{U}}_\mathrm{f}$. The following example illustrates this.

Example 4. Consider the system

$$\mathbf{A}_\mathrm{c} = \begin{bmatrix} 1 \\ -1 \end{bmatrix}, \mathbf{A}_\mathrm{f} = \begin{bmatrix} 0 & 1 \\ -1 & 0 \end{bmatrix}, \boldsymbol{b} = \begin{bmatrix} 1 \\ -1 \end{bmatrix}, \mathbf{M}_\mathrm{f}^\mathrm{m} = \begin{bmatrix} 1 & 0 \\ 0 & 1 \end{bmatrix}, \mathbf{0} \leq \boldsymbol{u} \leq \mathbf{1}.$$

For the above setting, an admissible control law $\boldsymbol{u}_\mathrm{c} = \tilde{\boldsymbol{k}}(\boldsymbol{u}_\mathrm{f})$ does not exist. To see this, take for instance the point $\boldsymbol{u}_\mathrm{f} = \begin{bmatrix} 0.5 & 1 \end{bmatrix}^\mathrm{T}$. Then, we have that

$$\tilde{\boldsymbol{z}}\left(\begin{bmatrix} 0.5 \\ 1 \end{bmatrix} \right) = \begin{bmatrix} 1 \\ -0.5 \end{bmatrix}$$

and hence the associated value of $\boldsymbol{u}_\mathrm{c} = \tilde{\boldsymbol{k}}(\boldsymbol{u}_\mathrm{f})$ should fulfill

$$\begin{bmatrix} \boldsymbol{u}_\mathrm{c} + 1 \\ -\boldsymbol{u}_\mathrm{c} - 0.5 \end{bmatrix} \leq \begin{bmatrix} 1 \\ -1 \end{bmatrix}.$$

The above inequalities imply that $\boldsymbol{u}_\mathrm{c} \leq 0 \wedge \boldsymbol{u}_\mathrm{c} \geq 0.5$, which is impossible. However, the following set $C^\star_{\boldsymbol{\mathcal{U}}_\mathrm{f}}$ can be constructed based on maximization problem (2.20)

$$C^\star_{\boldsymbol{\mathcal{U}}_\mathrm{f}} = \left\{ \underbrace{\begin{bmatrix} 1 \\ 1 \end{bmatrix}}_{\boldsymbol{u}_\mathrm{f}^1}, \underbrace{\begin{bmatrix} 0 \\ 0 \end{bmatrix}}_{\boldsymbol{u}_\mathrm{f}^2} \right\}.$$

Thus, the values $\tilde{\boldsymbol{z}}^1$ and $\tilde{\boldsymbol{z}}^2$ are given by

$$\tilde{\boldsymbol{z}}^1 = \tilde{\boldsymbol{z}}\left(\begin{bmatrix}1\\1\end{bmatrix}\right) = \begin{bmatrix}1\\-1\end{bmatrix}, \quad \tilde{\boldsymbol{z}}^2 = \tilde{\boldsymbol{z}}\left(\begin{bmatrix}0\\0\end{bmatrix}\right) = \begin{bmatrix}0\\0\end{bmatrix}.$$

Note that in this case condition (2.21) can be fulfilled, since

$$\begin{bmatrix}\boldsymbol{u}_\mathrm{c}^1 + 1\\ -\boldsymbol{u}_\mathrm{c}^1 - 1\end{bmatrix} \leq \begin{bmatrix}1\\-1\end{bmatrix} \Rightarrow \boldsymbol{u}_\mathrm{c}^1 = 0, \qquad \begin{bmatrix}\boldsymbol{u}_\mathrm{c}^2\\ -\boldsymbol{u}_\mathrm{c}^2\end{bmatrix} \leq \begin{bmatrix}1\\-1\end{bmatrix} \Rightarrow \boldsymbol{u}_\mathrm{c}^2 = 1.$$

However, this is not sufficient to conclude about the existence of an admissible control law for the system. □

From the above analysis, also illustrated with Example 4, we obtain the implication

> $\boldsymbol{\mathcal{U}}_\mathrm{f}$ is a convex polytope: $\exists \boldsymbol{u}_\mathrm{c} = \tilde{\boldsymbol{k}}(\boldsymbol{u}_\mathrm{f})$ admissible $\Rightarrow$ Condition (2.21) is fulfilled.

Although using condition (2.21) is not sufficient to verify the existence of an admissible control law, it involves a finite set of linear inequalities that scales linearly with the number of constraints n_z. As we discuss in Chapter 4, this property allows us to compute a lower bound for the minimal admissible actuator and sensor sets $(\mathcal{C}, \mathcal{M})$.

2.4 Special Case: Affine Control Laws

So far we have defined conditions for the existence of admissible control laws without prespecifying any closed-form expression for computing the values of $\boldsymbol{u}_\mathrm{c}$. In this section, we provide a set of admissibility conditions for cases in which the control law is assumed to be an affine function of $\boldsymbol{y}^\mathrm{m}$, $\boldsymbol{y}_\mathrm{f}^\mathrm{m}$, or $\boldsymbol{u}_\mathrm{f}$. Admissible affine control laws are interesting because they can be computed and implemented efficiently as we will show in Chapter 3. However, the existence of an admissible control law **does not** imply the existence of an admissible **affine** control law in general as we show in the following.

As previously mentioned, we are interested in static systems for which $\mathcal{M} \neq \emptyset$, $\boldsymbol{\mathcal{U}}_\mathrm{f} \neq \emptyset$, and $\mathrm{rank}(\mathrm{M}_\mathrm{f}^\mathrm{m}) < n_u - |\mathcal{C}|$ hold. We in addition remove Assumption 1 in this section, i.e., we now require the uncertainty set $\boldsymbol{\mathcal{U}}_\mathrm{f}$ only to be bounded and convex.

From Definitions 1, 3, and 4, and by assuming that the control laws $\boldsymbol{u}_\mathrm{c} = \boldsymbol{k}(\boldsymbol{y}^\mathrm{m})$, $\boldsymbol{u}_\mathrm{c} = \hat{\boldsymbol{k}}(\boldsymbol{y}_\mathrm{f}^\mathrm{m})$, and $\boldsymbol{u}_\mathrm{c} = \tilde{\boldsymbol{k}}(\boldsymbol{u}_\mathrm{f})$ are affine mappings, we readily derive the following admissibility conditions.

Corollary 4. Let $\mathbf{K} \in \mathbb{R}^{|\mathcal{C}|\times|\mathcal{M}|}$ and $\boldsymbol{w} \in \mathbb{R}^{|\mathcal{C}|}$ be given. The affine control law defined by $\boldsymbol{u}_\mathrm{c} = \mathbf{K}\boldsymbol{y}^\mathrm{m} + \boldsymbol{w}$ is admissible if

$$\forall \boldsymbol{u}_\mathrm{f} \in \boldsymbol{\mathcal{U}}_\mathrm{f} : \mathbf{A}_\mathrm{c}\mathbf{K}\boldsymbol{y}^\mathrm{m} + \mathbf{A}_\mathrm{c}\boldsymbol{w} + \mathbf{A}_\mathrm{f}\boldsymbol{u}_\mathrm{f} \leq \boldsymbol{b} \ \wedge \ \mathbf{K}\boldsymbol{y}^\mathrm{m} + \boldsymbol{w} \in \boldsymbol{\mathcal{U}}_\mathrm{c},$$

with $\boldsymbol{y}^\mathrm{m} = \mathrm{M}_\mathrm{c}^\mathrm{m}\mathbf{K}\boldsymbol{y}^\mathrm{m} + \mathrm{M}_\mathrm{c}^\mathrm{m}\boldsymbol{w} + \mathrm{M}_\mathrm{f}^\mathrm{m}\boldsymbol{u}_\mathrm{f}$.

Corollary 5. Let $\hat{\mathbf{K}} \in \mathbb{R}^{|\mathcal{C}|\times|\mathcal{M}|}$ and $\hat{\boldsymbol{w}} \in \mathbb{R}^{|\mathcal{C}|}$ be given. The affine control law defined by $\boldsymbol{u}_\mathrm{c} = \hat{\mathbf{K}}\boldsymbol{y}_\mathrm{f}^\mathrm{m} + \hat{\boldsymbol{w}}$ is admissible if

$$\forall \boldsymbol{u}_\mathrm{f} \in \boldsymbol{\mathcal{U}}_\mathrm{f} : \ \mathbf{A}_\mathrm{c}\hat{\mathbf{K}}\boldsymbol{y}_\mathrm{f}^\mathrm{m} + \mathbf{A}_\mathrm{c}\hat{\boldsymbol{w}} + \mathbf{A}_\mathrm{f}\boldsymbol{u}_\mathrm{f} \leq \boldsymbol{b} \wedge \ \hat{\mathbf{K}}\boldsymbol{y}_\mathrm{f}^\mathrm{m} + \hat{\boldsymbol{w}} \in \boldsymbol{\mathcal{U}}_\mathrm{c},$$

with $\boldsymbol{y}_\mathrm{f}^\mathrm{m} = \mathbf{M}_\mathrm{f}^\mathrm{m}\boldsymbol{u}_\mathrm{f}$.

Corollary 6. Let $\tilde{\mathbf{K}} \in \mathbb{R}^{|\mathcal{C}|\times n_u - |\mathcal{C}|}$ and $\tilde{\boldsymbol{w}} \in \mathbb{R}^{|\mathcal{C}|}$ be given. The affine control law defined by $\boldsymbol{u}_\mathrm{c} = \tilde{\mathbf{K}}\boldsymbol{u}_\mathrm{f} + \tilde{\boldsymbol{w}}$ is admissible if

$$\forall \boldsymbol{u}_\mathrm{f} \in \boldsymbol{\mathcal{U}}_\mathrm{f} : \ \forall \boldsymbol{u}'_\mathrm{f} \in \hat{\boldsymbol{\mathcal{U}}}_\mathrm{f}(\boldsymbol{u}_\mathrm{f}) : \ \mathbf{A}_\mathrm{c}\tilde{\mathbf{K}}\boldsymbol{u}_\mathrm{f} + \mathbf{A}_\mathrm{c}\tilde{\boldsymbol{w}} + \mathbf{A}_\mathrm{f}\boldsymbol{u}'_\mathrm{f} \leq \boldsymbol{b} \ \wedge \ \tilde{\mathbf{K}}\boldsymbol{u}_\mathrm{f} + \tilde{\boldsymbol{w}} \in \boldsymbol{\mathcal{U}}_\mathrm{c},$$

where $\hat{\boldsymbol{\mathcal{U}}}_\mathrm{f}(\boldsymbol{u}_\mathrm{f}) = \{\boldsymbol{u}'_\mathrm{f} \in \boldsymbol{\mathcal{U}}_\mathrm{f} : \mathbf{M}_\mathrm{f}^\mathrm{m}\boldsymbol{u}'_\mathrm{f} = \mathbf{M}_\mathrm{f}^\mathrm{m}\boldsymbol{u}_\mathrm{f}\}$.

In many cases, the above presented statements are equivalent to each other as established by the following theorems.

Theorem 8. Let both $(\mathbf{I} - \mathbf{K}\mathbf{M}_\mathrm{c}^\mathrm{m}) \in \mathbb{R}^{|\mathcal{C}|\times|\mathcal{C}|}$ and $(\mathbf{I} + \hat{\mathbf{K}}\mathbf{M}_\mathrm{c}^\mathrm{m}) \in \mathbb{R}^{|\mathcal{C}|\times|\mathcal{C}|}$ be invertible matrices. Then, the following two statements are equivalent:

1. $\exists \boldsymbol{u}_\mathrm{c} = \mathbf{K}\boldsymbol{y}^\mathrm{m} + \boldsymbol{w}$ admissible.
2. $\exists \boldsymbol{u}_\mathrm{c} = \hat{\mathbf{K}}\boldsymbol{y}_\mathrm{f}^\mathrm{m} + \hat{\boldsymbol{w}}$ admissible.

Proof. First, assume that there exists an admissible control law $\boldsymbol{u}_\mathrm{c} = \mathbf{K}\boldsymbol{y}^\mathrm{m} + \boldsymbol{w}$. We can then construct an admissible control law $\boldsymbol{u}_\mathrm{c} = \hat{\mathbf{K}}\boldsymbol{y}_\mathrm{f}^\mathrm{m} + \hat{\boldsymbol{w}}$ by employing the parameters $\mathbf{K}$ and $\boldsymbol{w}$ as follows. By noting that,

$$\boldsymbol{u}_\mathrm{c} = \mathbf{K}\boldsymbol{y}^\mathrm{m} + \boldsymbol{w} = \mathbf{K}(\mathbf{M}_\mathrm{c}^\mathrm{m}\boldsymbol{u}_\mathrm{c} + \mathbf{M}_\mathrm{f}^\mathrm{m}\boldsymbol{u}_\mathrm{f}) + \boldsymbol{w},$$

we obtain,

$$(\mathbf{I} - \mathbf{K}\mathbf{M}_\mathrm{c}^\mathrm{m})\boldsymbol{u}_\mathrm{c} = \mathbf{K}\mathbf{M}_\mathrm{f}^\mathrm{m}\boldsymbol{u}_\mathrm{f} + \boldsymbol{w} \Rightarrow \boldsymbol{u}_\mathrm{c} = (\mathbf{I} - \mathbf{K}\mathbf{M}_\mathrm{c}^\mathrm{m})^{\text{-}1}(\mathbf{K}\mathbf{M}_\mathrm{f}^\mathrm{m}\boldsymbol{u}_\mathrm{f} + \boldsymbol{w}).$$

Therefore,

$$\boldsymbol{u}_\mathrm{c} = \underbrace{(\mathbf{I} - \mathbf{K}\mathbf{M}_\mathrm{c}^\mathrm{m})^{\text{-}1}\mathbf{K}}_{\hat{\mathbf{K}}}\boldsymbol{y}_\mathrm{f}^\mathrm{m} + \underbrace{(\mathbf{I} - \mathbf{K}\mathbf{M}_\mathrm{c}^\mathrm{m})^{\text{-}1}\boldsymbol{w}}_{\hat{\boldsymbol{w}}}. \tag{2.22}$$

Now assume that there exists an admissible control law $\boldsymbol{u}_\mathrm{c} = \hat{\mathbf{K}}\boldsymbol{y}_\mathrm{f}^\mathrm{m} + \hat{\boldsymbol{w}}$. Then, we can use the parameters $\hat{\mathbf{K}}$ and $\hat{\boldsymbol{w}}$ to construct an admissible control law $\boldsymbol{u}_\mathrm{c} = \mathbf{K}\boldsymbol{y}^\mathrm{m} + \boldsymbol{w}$ as follows. We first note that,

$$\boldsymbol{u}_\mathrm{c} = \hat{\mathbf{K}}\boldsymbol{y}_\mathrm{f}^\mathrm{m} + \hat{\boldsymbol{w}} = \hat{\mathbf{K}}\mathbf{M}_\mathrm{f}^\mathrm{m}\boldsymbol{u}_\mathrm{f} + \hat{\boldsymbol{w}} \Rightarrow \hat{\mathbf{K}}\mathbf{M}_\mathrm{f}^\mathrm{m}\boldsymbol{u}_\mathrm{f} = \boldsymbol{u}_\mathrm{c} - \hat{\boldsymbol{w}}.$$

Since $\boldsymbol{y}^\mathrm{m} = \mathbf{M}_\mathrm{c}^\mathrm{m}\boldsymbol{u}_\mathrm{c} + \mathbf{M}_\mathrm{f}^\mathrm{m}\boldsymbol{u}_\mathrm{f}$, we have

$$\begin{aligned}\hat{\mathbf{K}}\boldsymbol{y}^\mathrm{m} &= \hat{\mathbf{K}}\mathbf{M}_\mathrm{c}^\mathrm{m}\boldsymbol{u}_\mathrm{c} + \hat{\mathbf{K}}\mathbf{M}_\mathrm{f}^\mathrm{m}\boldsymbol{u}_\mathrm{f} \\ &= \hat{\mathbf{K}}\mathbf{M}_\mathrm{c}^\mathrm{m}\boldsymbol{u}_\mathrm{c} + \boldsymbol{u}_\mathrm{c} - \hat{\boldsymbol{w}} \\ &= (\hat{\mathbf{K}}\mathbf{M}_\mathrm{c}^\mathrm{m} + \mathbf{I})\boldsymbol{u}_\mathrm{c} - \hat{\boldsymbol{w}}.\end{aligned}$$

Therefore,

$$\boldsymbol{u}_\mathrm{c} = \underbrace{(\hat{\mathbf{K}}\mathbf{M}_\mathrm{c}^\mathrm{m} + \mathbf{I})^{-1}\hat{\mathbf{K}}}_{\mathbf{K}}\boldsymbol{y}^\mathrm{m} + \underbrace{(\hat{\mathbf{K}}\mathbf{M}_\mathrm{c}^\mathrm{m} + \mathbf{I})^{-1}\hat{\boldsymbol{w}}}_{\boldsymbol{w}}. \tag{2.23}$$

□

Theorem 9. The following two statements are equivalent:

1. $\exists \boldsymbol{u}_\mathrm{c} = \hat{\mathbf{K}}\boldsymbol{y}_\mathrm{f}^\mathrm{m} + \hat{\boldsymbol{w}}$ admissible.
2. $\exists \boldsymbol{u}_\mathrm{c} = \tilde{\mathbf{K}}\boldsymbol{u}_\mathrm{f} + \tilde{\boldsymbol{w}}$ admissible.

Proof. If there exists an admissible control law $\boldsymbol{u}_\mathrm{c} = \hat{\mathbf{K}}\boldsymbol{y}_\mathrm{f}^\mathrm{m} + \hat{\boldsymbol{w}}$, then we can construct an admissible control law $\boldsymbol{u}_\mathrm{c} = \tilde{\mathbf{K}}\boldsymbol{u}_\mathrm{f} + \tilde{\boldsymbol{w}}$, i.e.,

$$\boldsymbol{u}_\mathrm{c} = \hat{\mathbf{K}}\boldsymbol{y}_\mathrm{f}^\mathrm{m} + \hat{\boldsymbol{w}} = \underbrace{\hat{\mathbf{K}}\mathbf{M}_\mathrm{f}^\mathrm{m}}_{\tilde{\mathbf{K}}}\boldsymbol{u}_\mathrm{f} + \underbrace{\hat{\boldsymbol{w}}}_{\tilde{\boldsymbol{w}}}.$$

Now assume that there exists an admissible control law $\boldsymbol{u}_\mathrm{c} = \tilde{\mathbf{K}}\boldsymbol{u}_\mathrm{f} + \tilde{\boldsymbol{w}}$, i.e., the matrix $\tilde{\mathbf{K}}$ fulfills

$$\forall \boldsymbol{u}_\mathrm{f} \in \boldsymbol{\mathcal{U}}_\mathrm{f} : \forall \boldsymbol{u}'_\mathrm{f} \in \boldsymbol{\mathcal{U}}_\mathrm{f}\tilde{\boldsymbol{k}}(\boldsymbol{u}_\mathrm{f}) : \tilde{\mathbf{K}}\boldsymbol{u}_\mathrm{f} = \tilde{\mathbf{K}}\boldsymbol{u}'_\mathrm{f},$$

which also means that $\mathrm{null}(\tilde{\mathbf{K}}) \supseteq \mathrm{null}(\mathbf{M}_\mathrm{f}^\mathrm{m})$. We can thus obtain the value of $\hat{\mathbf{K}}$ by using the pseudo-inverse of $\mathbf{M}_\mathrm{f}^\mathrm{m}$, i.e.,

$$\tilde{\mathbf{K}} = \hat{\mathbf{K}}\mathbf{M}_\mathrm{f}^\mathrm{m} \Rightarrow \tilde{\mathbf{K}}\mathbf{M}_\mathrm{f}^{\mathrm{m}+} = \hat{\mathbf{K}}\mathbf{M}_\mathrm{f}^\mathrm{m}\mathbf{M}_\mathrm{f}^{\mathrm{m}+} = \hat{\mathbf{K}}\mathbf{M}_\mathrm{f}^\mathrm{m}\mathbf{M}_\mathrm{f}^{\mathrm{m}\mathrm{T}}(\mathbf{M}_\mathrm{f}^\mathrm{m}\mathbf{M}_\mathrm{f}^{\mathrm{m}\mathrm{T}})^{-1} = \hat{\mathbf{K}}.$$

The control law $\boldsymbol{u}_\mathrm{c} = \hat{\mathbf{K}}\boldsymbol{y}_\mathrm{f}^\mathrm{m} + \hat{\boldsymbol{w}}$ is therefore given by

$$\boldsymbol{u}_\mathrm{c} = \underbrace{\tilde{\mathbf{K}}\mathbf{M}_\mathrm{f}^{\mathrm{m}+}}_{\hat{\mathbf{K}}}\boldsymbol{y}_\mathrm{f}^\mathrm{m} + \underbrace{\tilde{\boldsymbol{w}}}_{\hat{\boldsymbol{w}}}.$$

□

From Theorems 8 and 9, we obtain the implications

- $\exists \boldsymbol{u}_\mathrm{c} = \mathbf{K}\boldsymbol{y}^\mathrm{m} + \boldsymbol{w}$ admissible $\wedge\ \mathrm{rank}(\mathbf{I} - \mathbf{K}\mathbf{M}_\mathrm{c}^\mathrm{m}) = |\mathcal{C}| \Rightarrow \exists \boldsymbol{u}_\mathrm{c} = \hat{\mathbf{K}}\boldsymbol{y}_\mathrm{f}^\mathrm{m} + \hat{\boldsymbol{w}}$ admissible.
- $\exists \boldsymbol{u}_\mathrm{c} = \hat{\mathbf{K}}\boldsymbol{y}_\mathrm{f}^\mathrm{m} + \hat{\boldsymbol{w}}$ admissible $\wedge\ \mathrm{rank}(\mathbf{I} + \hat{\mathbf{K}}\mathbf{M}_\mathrm{c}^\mathrm{m}) = |\mathcal{C}| \Rightarrow \exists \boldsymbol{u}_\mathrm{c} = \mathbf{K}\boldsymbol{y}^\mathrm{m} + \boldsymbol{w}$ admissible.
- $\exists \boldsymbol{u}_\mathrm{c} = \hat{\mathbf{K}}\boldsymbol{y}_\mathrm{f}^\mathrm{m} + \hat{\boldsymbol{w}}$ admissible $\Leftrightarrow \exists \boldsymbol{u}_\mathrm{c} = \tilde{\mathbf{K}}\boldsymbol{u}_\mathrm{f} + \tilde{\boldsymbol{w}}$ admissible.

Here it is important to note that the existence of an admissible control law does not imply the existence of an admissible affine control law in general. In fact, there are many constrained static systems for which an admissible control law exists, but an admissible affine control law is impossible.

Example 5. Consider the system defined by

$$\mathbf{A}_\mathrm{c} = \begin{bmatrix} 1 \\ -1 \\ -1 \\ -2 \end{bmatrix}, \mathbf{A}_\mathrm{f} = \begin{bmatrix} -1 & -1 \\ -1 & 1 \\ 1 & -1 \\ 1 & 1 \end{bmatrix}, \boldsymbol{b} = \begin{bmatrix} 0 \\ 0 \\ 0 \\ 0 \end{bmatrix}, \tag{2.24}$$
$$\mathbf{M}_\mathrm{f} = \begin{bmatrix} 1 & 1 \\ 1 & 0 \\ 0 & 1 \end{bmatrix}, \ \mathbf{0} \leq \boldsymbol{u}_\mathrm{f} \leq \mathbf{1}, \ 0 \leq \boldsymbol{u}_\mathrm{c} \leq 1.$$

We study two particular realizations of the sensor set $\mathcal{M}$, namely $\mathcal{M}_1 = \{1\}$ and $\mathcal{M}_2 = \{2, 3\}$. The system requires that the value of the control actions fulfills $\boldsymbol{u}_\mathrm{c} = 0$ if $\boldsymbol{u}_\mathrm{f} = \mathbf{0}$, and $\boldsymbol{u}_\mathrm{c} = 1$ if $\boldsymbol{u}_\mathrm{f} \in \{[0\ 1]^\mathrm{T}, [1\ 0]^\mathrm{T}, [1\ 1]^\mathrm{T}\}$. In both cases, the constraints (2.24) cannot be fulfilled by any affine control law $\boldsymbol{u}_\mathrm{c} = \tilde{\mathbf{K}}\boldsymbol{u}_\mathrm{f} + \tilde{\boldsymbol{w}}$ subject to the conditions of Corollary 6. Such maps have only three degrees of freedom and the constraints are not co-linear here. However, there exists an admissible control law for both sensor sets $\mathcal{M}_1$ and $\mathcal{M}_2$, namely the PWA control laws depicted in Fig. 2.7.

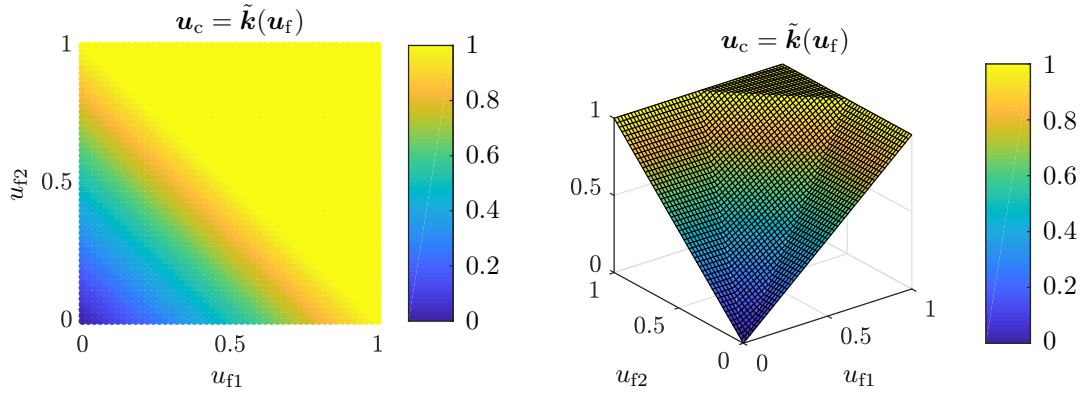

(a) Sensor set $\mathcal{M}_1 = \{1\}$.

(b) Sensor set $\mathcal{M}_2 = \{2, 3\}$.

Figure 2.7: Admissible PWA control laws (color-coded in the space of $\boldsymbol{u}_\mathrm{f}$) for the system defined by (2.24). The system constrains $\boldsymbol{u}_\mathrm{c} = \tilde{\boldsymbol{k}}(\boldsymbol{u}_\mathrm{f})$ to be zero if $\boldsymbol{u}_\mathrm{f} = \mathbf{0}$ and one at the remaining vertices of $\boldsymbol{\mathcal{U}}_\mathrm{f}$. These constraints cannot be fulfilled by any affine control law, but admissible PWA control laws actually exist. □

From the above analysis, also illustrated with Example 5, we obtain the implication

$$\exists \boldsymbol{u}_\mathrm{c} = \tilde{\mathbf{K}}\boldsymbol{u}_\mathrm{f} + \tilde{\boldsymbol{w}} \text{ admissible} \Rightarrow \exists \boldsymbol{u}_\mathrm{c} = \tilde{\boldsymbol{k}}(\boldsymbol{u}_\mathrm{f}) \text{ admissible.}$$

Note that the above implication also holds if either the control law $\boldsymbol{u}_\mathrm{c} = \hat{\boldsymbol{k}}(\boldsymbol{y}_\mathrm{f}^\mathrm{m})$ or $\boldsymbol{u}_\mathrm{c} = \boldsymbol{k}(\boldsymbol{y}^\mathrm{m})$ were used instead. In Chapter 4, we explain how to exploit the above implication to obtain a computable upper bound for the minimal admissible actuator and sensor sets $(\mathcal{C}, \mathcal{M})$. In addition, we show in Section 3.1 that an affine control law can be computed very efficiently and with admissibility guarantees provided that both $\boldsymbol{\mathcal{U}}_\mathrm{c}$ and $\boldsymbol{\mathcal{U}}_\mathrm{f}$ are hypercubes.

2.5 Discussion

In this chapter, we defined constrained static linear systems and presented a set of conditions for the existence of admissible control laws for this system class. After introducing the notions of admissible control law and admissible actuator and sensor sets, we studied the existence of admissible control laws in detail, which is accompanied by various illustrative examples.

Verifying the existence of an admissible control law $\boldsymbol{u}_\mathrm{c} = \boldsymbol{k}(\boldsymbol{y}^\mathrm{m})$ turns generally into an infinite dimensional feasibility problem that also involves recursion. However, it is possible to eliminate recursion by verifying the existence of other admissible control laws, namely the alternative mappings $\boldsymbol{u}_\mathrm{c} = \hat{\boldsymbol{k}}(\boldsymbol{y}_\mathrm{f}^\mathrm{m})$ and/or $\boldsymbol{u}_\mathrm{c} = \tilde{\boldsymbol{k}}(\boldsymbol{u}_\mathrm{f})$. This is because the existence of one those alternative control laws being admissible also implies the existence of an admissible control law $\boldsymbol{u}_\mathrm{c} = \boldsymbol{k}(\boldsymbol{y}^\mathrm{m})$ per se—and the converse implication is also true. In other words, it is always possible to map an admissible control law $\boldsymbol{u}_\mathrm{c} = \hat{\boldsymbol{k}}(\boldsymbol{y}_\mathrm{f}^\mathrm{m})$ (or $\boldsymbol{u}_\mathrm{c} = \tilde{\boldsymbol{k}}(\boldsymbol{u}_\mathrm{f})$) to an admissible control law $\boldsymbol{u}_\mathrm{c} = \boldsymbol{k}(\boldsymbol{y}^\mathrm{m})$ and vice versa.

We further examined the computational complexity of the derived conditions, finding that some of them can be expressed in terms of a finite number of linear inequalities when the uncertainty set $\boldsymbol{\mathcal{U}}_\mathrm{f}$ is a convex polytope. An overview of the whole collection of conditions and their relations with each other is depicted in Fig. 2.8.

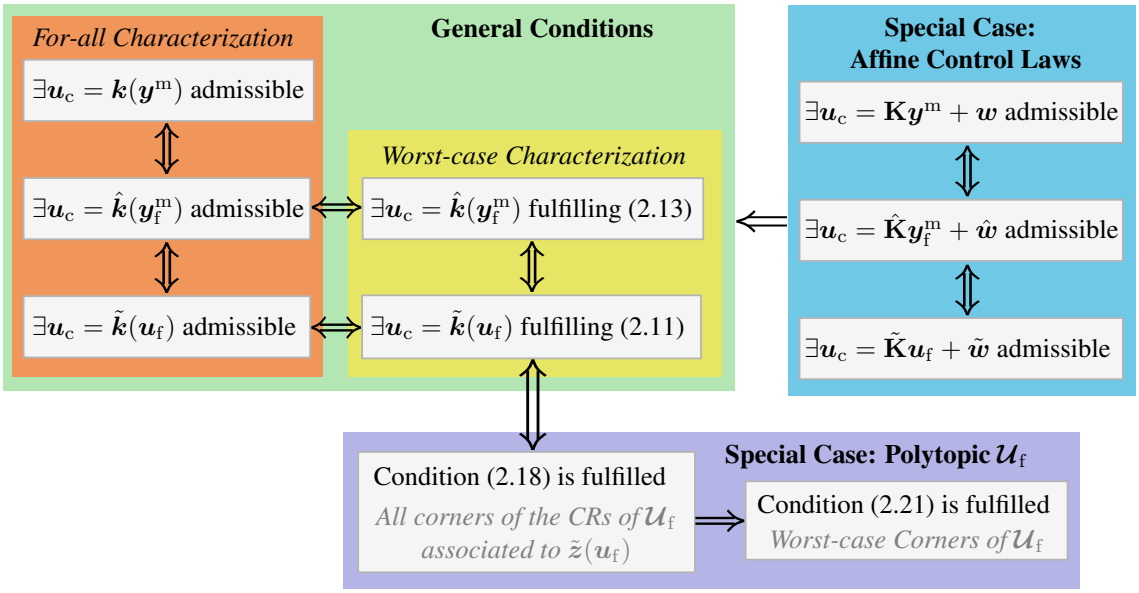

Figure 2.8: Relation of general admissibility conditions (green, orange, and yellow) to the derived conditions based on the corners of $\boldsymbol{\mathcal{U}}_\mathrm{f}$ (purple) and the assumption of affine control laws (blue). The existence of an admissible control law per se does not imply the existence of an admissible affine control law in general. Moreover, if the uncertainty set $\boldsymbol{\mathcal{U}}_\mathrm{f}$ is a convex polytope, then the existence of an admissible control law $\boldsymbol{u}_\mathrm{c} = \tilde{\boldsymbol{k}}(\boldsymbol{u}_\mathrm{f})$ can be verified by using all corners of the CRs of $\boldsymbol{\mathcal{U}}_\mathrm{f}$ associated to $\tilde{\boldsymbol{z}}(\boldsymbol{u}_\mathrm{f})$ and condition (2.18). If instead only the subset of corners $C^\star_{\boldsymbol{\mathcal{U}}_\mathrm{f}}$ is utilized together with condition (2.21), then nothing can be concluded about the existence of an admissible control law $\boldsymbol{u}_\mathrm{c} = \tilde{\boldsymbol{k}}(\boldsymbol{u}_\mathrm{f})$.

3 Verifying the Existence of Admissible Control Laws

The admissibility conditions introduced in Chapter 2 are now exploited to derive a set of algorithms that find, if possible, an admissible control law for given actuator and sensor sets $(\mathcal{C}, \mathcal{M})$. Under the assumption that both $\boldsymbol{\mathcal{U}}_{\mathrm{c}}$ and $\boldsymbol{\mathcal{U}}_{\mathrm{f}}$ are convex polytopes, the verification and computation of both affine and PWA admissible control laws can be done offline with the help of (multiparametric) linear optimization techniques.

3.1 Admissible Affine Control Laws

In this section, we derive a set of algorithms for the verification and computation of admissible affine control laws of the form $\boldsymbol{u}_{\mathrm{c}} = \hat{\mathbf{K}}\boldsymbol{y}_{\mathrm{f}}^{\mathrm{m}} + \hat{\boldsymbol{w}}$. The algorithms proposed below are based on the admissibility condition provided in Corollary 5 for given actuator and sensor sets $(\mathcal{C}, \mathcal{M})$, and apply to constrained static linear systems for which $\mathcal{M} \neq \emptyset$, $\boldsymbol{\mathcal{U}}_{\mathrm{f}} \neq \emptyset$, and $\mathrm{rank}(\mathbf{M}_{\mathrm{f}}^{\mathrm{m}}) < n_u - |\mathcal{C}|$ hold.

Here we recall that the non-existence of an admissible affine control law of the form $\boldsymbol{u}_{\mathrm{c}} = \hat{\mathbf{K}}\boldsymbol{y}_{\mathrm{f}}^{\mathrm{m}} + \hat{\boldsymbol{w}}$ does not imply the non-existence of an admissible control law $\boldsymbol{u}_{\mathrm{c}} = \hat{\boldsymbol{k}}(\boldsymbol{y}_{\mathrm{f}}^{\mathrm{m}})$ of arbitrary form. However, if there exist suitable controller parameters $(\hat{\mathbf{K}}, \hat{\boldsymbol{w}})$ for which the control law $\boldsymbol{u}_{\mathrm{c}} = \hat{\mathbf{K}}\boldsymbol{y}_{\mathrm{f}}^{\mathrm{m}} + \hat{\boldsymbol{w}}$ is admissible, then the existence of an admissible control law of arbitrary form is guaranteed.

Although we limit our algorithms to the verification and computation of admissible affine control laws of the form $\boldsymbol{u}_{\mathrm{c}} = \hat{\mathbf{K}}\boldsymbol{y}_{\mathrm{f}}^{\mathrm{m}} + \hat{\boldsymbol{w}}$, corresponding affine control laws of the form $\boldsymbol{u}_{\mathrm{c}} = \mathbf{K}\boldsymbol{y}^{\mathrm{m}} + \boldsymbol{w}$, which are directly implementable in practice, can be computed straightforwardly by using Theorem 8 once suitable parameters $\hat{\mathbf{K}}$ and $\hat{\boldsymbol{w}}$ are found.

Provided there exists an admissible affine control law $\boldsymbol{u}_{\mathrm{c}} = \hat{\mathbf{K}}\boldsymbol{y}_{\mathrm{f}}^{\mathrm{m}} + \hat{\boldsymbol{w}}$, the verification algorithms presented in the following can be easily extended to compute optimal admissible affine control laws, i.e., admissible control laws that minimize (for instance) linear and/or quadratic functions of $\boldsymbol{u}_{\mathrm{c}}$ depending on the application. Our verification algorithms can also be extended to verify the existence of admissible distributed/decentralized affine control laws, which can be achieved in a straightforward manner by additionally

constraining the structure of the controller parameters $(\hat{\mathbf{K}}, \hat{\boldsymbol{w}})$. Such extensions are out of the scope of this thesis.

3.1.1 Formulation of the Verification Task

From Corollary 5, the existence of an admissible affine control law $\boldsymbol{u}_\mathrm{c} = \hat{\mathbf{K}}\boldsymbol{y}_\mathrm{f}^\mathrm{m} + \hat{\boldsymbol{w}}$ is guaranteed if there exist parameters $\hat{\mathbf{K}} \in \mathbb{R}^{|\mathcal{C}|\times|\mathcal{M}|}$ and $\hat{\boldsymbol{w}} \in \mathbb{R}^{|\mathcal{C}|}$, such that

$$\forall \boldsymbol{u}_\mathrm{f} \in \boldsymbol{\mathcal{U}}_\mathrm{f} : \ (\mathbf{A}_\mathrm{c}\hat{\mathbf{K}}\mathbf{M}_\mathrm{f}^\mathrm{m} + \mathbf{A}_\mathrm{f})\boldsymbol{u}_\mathrm{f} + \mathbf{A}_\mathrm{c}\hat{\boldsymbol{w}} \leq \boldsymbol{b} \ \wedge \ \hat{\mathbf{K}}\mathbf{M}_\mathrm{f}^\mathrm{m}\boldsymbol{u}_\mathrm{f} + \hat{\boldsymbol{w}} \in \boldsymbol{\mathcal{U}}_\mathrm{c}. \tag{3.1}$$

Assumption 2. The set of control actions $\boldsymbol{\mathcal{U}}_\mathrm{c}$ is a convex polytope, i.e.,

$$\boldsymbol{\mathcal{U}}_\mathrm{c} = \{\boldsymbol{u}_\mathrm{c} \in \mathbb{R}^{|\mathcal{C}|} : \mathbf{Q}_\mathrm{c}\boldsymbol{u}_\mathrm{c} \leq \boldsymbol{q}_\mathrm{c}\},$$

with $\mathbf{Q}_\mathrm{c} \in \mathbb{R}^{l_\mathrm{c}\times|\mathcal{C}|}$ and $\boldsymbol{q}_\mathrm{c} \in \mathbb{R}^{l_\mathrm{c}}$.

Under Assumption 2—which is not strictly necessary but simplifies the following analysis and is also realistic in many practical applications—the infinite set of linear inequalities (3.1) can be expressed in the compact form

$$\forall \boldsymbol{u}_\mathrm{f} \in \boldsymbol{\mathcal{U}}_\mathrm{f} : \ \hat{\mathbf{A}}(\hat{\mathbf{K}})\boldsymbol{u}_\mathrm{f} + \hat{\mathbf{A}}_\mathrm{c}\hat{\boldsymbol{w}} \leq \hat{\boldsymbol{b}}, \tag{3.2}$$

where $\hat{\mathbf{A}}(\hat{\mathbf{K}}) = \hat{\mathbf{A}}_\mathrm{c}\hat{\mathbf{K}}\mathbf{M}_\mathrm{f}^\mathrm{m} + \hat{\mathbf{A}}_\mathrm{f}$ and

$$\hat{\mathbf{A}}_\mathrm{c} = \begin{bmatrix}\mathbf{A}_\mathrm{c}\\ \mathbf{Q}_\mathrm{c}\end{bmatrix}, \quad \hat{\mathbf{A}}_\mathrm{f} = \begin{bmatrix}\mathbf{A}_\mathrm{f}\\ \mathbf{0}\end{bmatrix}, \quad \hat{\boldsymbol{b}} = \begin{bmatrix}\boldsymbol{b}\\ \boldsymbol{q}_\mathrm{c}\end{bmatrix}. \tag{3.3}$$

Moreover, (in)equalities (3.2) and (3.3) allow us to find controller parameters $(\hat{\mathbf{K}}, \hat{\boldsymbol{w}})$ guaranteeing the existence of an admissible control law $\boldsymbol{u}_\mathrm{c} = \hat{\mathbf{K}}\boldsymbol{y}_\mathrm{f}^\mathrm{m} + \hat{\boldsymbol{w}}$ by solving the constrained, infinite dimensional feasibility problem

$$\begin{aligned} &\min_{\hat{\mathbf{K}},\hat{\boldsymbol{w}},\eta} \ \eta \\ &\text{s.t. } \hat{\mathbf{A}}(\hat{\mathbf{K}})\boldsymbol{u}_\mathrm{f} + \hat{\mathbf{A}}_\mathrm{c}\hat{\boldsymbol{w}} \leq \hat{\boldsymbol{b}} + \eta\mathbf{1}, \quad \forall \boldsymbol{u}_\mathrm{f} \in \boldsymbol{\mathcal{U}}_\mathrm{f}, \\ &\quad \hat{\mathbf{K}} \in \mathbb{R}^{|\mathcal{C}|\times|\mathcal{M}|}, \quad \hat{\boldsymbol{w}} \in \mathbb{R}^{|\mathcal{C}|}, \quad \eta \in \mathbb{R}, \end{aligned} \tag{3.4}$$

In the above minimization task, $\mathbf{1}$ is a vector of ones of suitable dimension, and the variable $\eta \in \mathbb{R}$ works as an indicator of how far is the system from violating an operational constraint. An admissible affine control law $\boldsymbol{u}_\mathrm{c} = \hat{\mathbf{K}}\boldsymbol{y}_\mathrm{f}^\mathrm{m} + \hat{\boldsymbol{w}}$ is thus obtained if the optimal value of η fulfills $\eta \leq 0$. Otherwise there is no admissible affine control law for the given actuator and sensor sets $(\mathcal{C}, \mathcal{M})$ and nothing can be said about the existence of an admissible control law $\boldsymbol{u}_\mathrm{c} = \hat{\boldsymbol{k}}(\boldsymbol{y}_\mathrm{f}^\mathrm{m})$ in general.

Note that, in its current form, feasibility problem (3.4) is intractable as the cost function is subject to an infinite number of inequality constraints.[1] In the following, we show that there are important instances of problem (3.4) which can be solved as finite dimensional feasibility problems, in particular if the uncertainty set $\boldsymbol{\mathcal{U}}_\mathrm{f}$ is shaped either by a convex polytope, or shaped by a $\mathsf{p}-$norm.[2]

3.1.2 Special Case: Convex Polytopic Uncertainty

When assuming that $\boldsymbol{\mathcal{U}}_\mathrm{f}$ is a convex polytope, i.e., it can be represented either by a finite set of linear inequalities ($\mathcal{H}$-representation), or by using convex combinations of its corners ($\mathcal{V}$-representation) [95], feasibility problem (3.4) turns into a finite dimensional feasibility problem. In the following we derive verification algorithms that exploit both the $\mathcal{V}$-representation and the $\mathcal{H}$-representation of $\boldsymbol{\mathcal{U}}_\mathrm{f}$.

$\mathcal{V}$–representation of $\boldsymbol{\mathcal{U}}_\mathrm{f}$. In case the uncertainty set $\boldsymbol{\mathcal{U}}_\mathrm{f}$ is a convex polytope and the corners of $\boldsymbol{\mathcal{U}}_\mathrm{f}$ are available, we can test for the existence of controller parameters $(\hat{\mathbf{K}}, \hat{\boldsymbol{w}})$ valid for the corners of $\boldsymbol{\mathcal{U}}_\mathrm{f}$ only. This guarantees that, if those controller parameters exist, they are also valid for all exogenous actions $\boldsymbol{u}_\mathrm{f} \in \boldsymbol{\mathcal{U}}_\mathrm{f}$, i.e., the affine control law $\boldsymbol{u}_\mathrm{c} = \hat{\mathbf{K}}\boldsymbol{y}_\mathrm{f}^\mathrm{m} + \hat{\boldsymbol{w}}$ is admissible. To show this, let $C_{\boldsymbol{\mathcal{U}}_\mathrm{f}}$ be the set containing the corners of $\boldsymbol{\mathcal{U}}_\mathrm{f}$. Also let $|C_{\boldsymbol{\mathcal{U}}_\mathrm{f}}|$ denote the cardinality of $C_{\boldsymbol{\mathcal{U}}_\mathrm{f}}$ and $\boldsymbol{u}_\mathrm{f}^i$ with $i \in \{1, ..., |C_{\boldsymbol{\mathcal{U}}_\mathrm{f}}|\}$, represent the ith corner of $\boldsymbol{\mathcal{U}}_\mathrm{f}$. Now assume that the parameters $(\hat{\mathbf{K}}, \hat{\boldsymbol{w}})$ fulfill

$$\hat{\mathbf{A}}(\hat{\mathbf{K}})\boldsymbol{u}_\mathrm{f}^i + \hat{\mathbf{A}}_\mathrm{c}\hat{\boldsymbol{w}} \leq \hat{\boldsymbol{b}}, \quad \forall i \in \{1, ..., |C_{\boldsymbol{\mathcal{U}}_\mathrm{f}}|\}.$$

Then, since any exogenous action $\boldsymbol{u}_\mathrm{f} \in \boldsymbol{\mathcal{U}}_\mathrm{f}$ can be expressed as a convex combination of the corners of $\boldsymbol{\mathcal{U}}_\mathrm{f}$, i.e., $\boldsymbol{u}_\mathrm{f} = \sum_{i=1}^{|C_{\boldsymbol{\mathcal{U}}_\mathrm{f}}|} \boldsymbol{u}_\mathrm{f}^i \lambda_i$, with $\lambda_i \in \mathbb{R}_{\geq 0}, \sum_{i=1}^{|C_{\boldsymbol{\mathcal{U}}_\mathrm{f}}|} \lambda_i = 1$, we obtain

$$\hat{\mathbf{A}}(\hat{\mathbf{K}})\boldsymbol{u}_\mathrm{f} + \hat{\mathbf{A}}_\mathrm{c}\hat{\boldsymbol{w}} = \hat{\mathbf{A}}(\hat{\mathbf{K}}) \sum_{i=1}^{|C_{\boldsymbol{\mathcal{U}}_\mathrm{f}}|} \boldsymbol{u}_\mathrm{f}^i \lambda_i + \hat{\mathbf{A}}_\mathrm{c}\hat{\boldsymbol{w}} = \sum_{i=1}^{|C_{\boldsymbol{\mathcal{U}}_\mathrm{f}}|} \underbrace{\left(\hat{\mathbf{A}}(\hat{\mathbf{K}})\boldsymbol{u}_\mathrm{f}^i + \hat{\mathbf{A}}_\mathrm{c}\hat{\boldsymbol{w}}\right)}_{\leq \hat{\boldsymbol{b}}} \lambda_i \leq \hat{\boldsymbol{b}}.$$

With this in mind, we can use the corners of $\boldsymbol{\mathcal{U}}_\mathrm{f}$ to equivalently express feasibility problem (3.4) as the finite dimensional LP

$$\begin{aligned} \min_{\hat{\mathbf{K}}, \hat{\boldsymbol{w}}, \eta} \ & \eta \\ \text{s.t. } & \hat{\mathbf{A}}(\hat{\mathbf{K}})\boldsymbol{u}_\mathrm{f}^i + \hat{\mathbf{A}}_\mathrm{c}\hat{\boldsymbol{w}} \leq \hat{\boldsymbol{b}} + \eta\mathbf{1}, \quad \forall i \in \{1, ..., |C_{\boldsymbol{\mathcal{U}}_\mathrm{f}}|\}, \\ & \hat{\mathbf{K}} \in \mathbb{R}^{|\mathcal{C}|\times|\mathcal{M}|}, \quad \hat{\boldsymbol{w}} \in \mathbb{R}^{|\mathcal{C}|}, \quad \eta \in \mathbb{R}. \end{aligned} \tag{3.5}$$

[1] Nevertheless, an upper bound for the feasibility indicator can be obtained by, for instance, the following three-step approach. First, we approximate the uncertainty set $\boldsymbol{\mathcal{U}}_\mathrm{f}$ from the exterior as the union of a finite number of polytopes. We subsequently enumerate those polytopes and seek for a unique realization of the controller parameters valid over all polytopes. To this end, the verification algorithms presented in subsequent sections can be extended in a straightforward manner. A similar technique can be used to find a lower bound for the feasibility indicator η. The derivation of those bounds is out of the scope of this thesis.

[2] The p-norm of a vector $\boldsymbol{x} \in \mathbb{R}^{n_x}$ is defined as $\|\boldsymbol{x}\|_\mathsf{p} := \left(\sum_{i=1}^{n_x} |x_i|^\mathsf{p}\right)^{1/\mathsf{p}}$, with $\mathsf{p} \in \mathbb{N}^+$.

Although feasibility problem (3.5) is a LP where the objective function is subject to a finite number of constraints, the number of corners of $\boldsymbol{\mathcal{U}}_{\mathrm{f}}$ grows in general exponentially with the dimension of $\boldsymbol{u}_{\mathrm{f}}$, which limits the application of this verification approach to small- and medium-scale problem instances depending on the computing equipment.

$\mathcal{H}$–representation of $\boldsymbol{\mathcal{U}}_{\mathrm{f}}$. In case the polytopic uncertainty set $\boldsymbol{\mathcal{U}}_{\mathrm{f}}$ is defined by a set of linear inequalities, i.e.,

$$\boldsymbol{\mathcal{U}}_{\mathrm{f}} = \{\boldsymbol{u}_{\mathrm{f}} \in \mathbb{R}^{n_u-|\mathcal{C}|} : \mathbf{Q}_{\mathrm{f}}\boldsymbol{u}_{\mathrm{f}} \leq \boldsymbol{q}_{\mathrm{f}}\}, \tag{3.6}$$

where $\mathbf{Q}_{\mathrm{f}} \in \mathbb{R}^{l_{\mathrm{f}}\times(n_u-|\mathcal{C}|)}$ and $\boldsymbol{q}_{\mathrm{f}} \in \mathbb{R}^{l_{\mathrm{f}}}$ are given, we can reduce the complexity of solving problem (3.4) as follows. First, note in condition (3.2) that it is not necessary to consider all points in $\boldsymbol{\mathcal{U}}_{\mathrm{f}}$, but only those ones that maximize the impact on each row of the term $\hat{\mathbf{A}}(\hat{\mathbf{K}})\boldsymbol{u}_{\mathrm{f}}$, i.e., the worst-case realizations of $\boldsymbol{u}_{\mathrm{f}} \in \boldsymbol{\mathcal{U}}_{\mathrm{f}}$. To see this, let $\hat{\mathbf{A}}^{j}(\hat{\mathbf{K}}) \in \mathbb{R}^{1\times(n_u-|\mathcal{C}|)}$ represent the jth row of the matrix $\hat{\mathbf{A}}(\hat{\mathbf{K}}) \in \mathbb{R}^{\hat{n}_z\times(n_u-|\mathcal{C}|)}$, with $j \in \{1,...,\hat{n}_z\}$.[3] The worst-case realizations of $\boldsymbol{u}_{\mathrm{f}} \in \boldsymbol{\mathcal{U}}_{\mathrm{f}}$ can then be found by solving for each $j \in \{1,...,\hat{n}_z\}$

$$\max_{\boldsymbol{u}_{\mathrm{f}}\in\mathbb{R}^{n_u-|\mathcal{C}|}} \ \hat{\mathbf{A}}^{j}(\hat{\mathbf{K}})\boldsymbol{u}_{\mathrm{f}} \text{ s.t. } \mathbf{Q}_{\mathrm{f}}\boldsymbol{u}_{\mathrm{f}} \leq \boldsymbol{q}_{\mathrm{f}}, \tag{3.7}$$

which is a LP. Since for all $j \in \{1,...,\hat{n}_z\}$ and for all exogenous actions $\boldsymbol{u}_{\mathrm{f}} \in \boldsymbol{\mathcal{U}}_{\mathrm{f}}$ the inequality

$$\hat{\mathbf{A}}^{j}(\hat{\mathbf{K}})\boldsymbol{u}_{\mathrm{f}} \leq \max_{\boldsymbol{u}_{\mathrm{f}}\in\boldsymbol{\mathcal{U}}_{\mathrm{f}}} \ \hat{\mathbf{A}}^{j}(\hat{\mathbf{K}})\boldsymbol{u}_{\mathrm{f}}$$

holds, we readily obtain that

$$\forall \boldsymbol{u}_{\mathrm{f}} \in \boldsymbol{\mathcal{U}}_{\mathrm{f}} : \hat{\mathbf{A}}^{j}(\hat{\mathbf{K}})\boldsymbol{u}_{\mathrm{f}} + \hat{\mathbf{A}}_{\mathrm{c}}^{j}\hat{\boldsymbol{w}} \leq \max_{\boldsymbol{u}_{\mathrm{f}}\in\boldsymbol{\mathcal{U}}_{\mathrm{f}}} \hat{\mathbf{A}}^{j}(\hat{\mathbf{K}})\boldsymbol{u}_{\mathrm{f}} + \hat{\mathbf{A}}_{\mathrm{c}}^{j}\hat{\boldsymbol{w}} \leq \hat{\boldsymbol{b}}, \quad j \in \{1,...,\hat{n}_z\}.$$

Feasibility problem (3.4) is therefore equivalent to the finite dimensional feasibility problem

$$\begin{aligned} &\min_{\hat{\mathbf{K}},\hat{\boldsymbol{w}},\eta} \ \eta \\ &\text{s.t. } \left(\max_{\boldsymbol{u}_{\mathrm{f}}\in\boldsymbol{\mathcal{U}}_{\mathrm{f}}} \hat{\mathbf{A}}^{j}(\hat{\mathbf{K}})\boldsymbol{u}_{\mathrm{f}}\right) + \hat{\mathbf{A}}_{\mathrm{c}}^{j}\hat{\boldsymbol{w}} \leq \hat{b}_j + \eta, \quad \forall j \in \{1,...,\hat{n}_z\}, \\ &\quad \hat{\mathbf{K}} \in \mathbb{R}^{|\mathcal{C}|\times|\mathcal{M}|}, \quad \hat{\boldsymbol{w}} \in \mathbb{R}^{|\mathcal{C}|}, \quad \eta \in \mathbb{R}, \end{aligned} \tag{3.8}$$

Compared to problem (3.4), problem (3.8) is defined by a total of $\hat{n}_z$ inequality constraints, each of them embedding linear maximization problem (3.7). Under the assumption that $\boldsymbol{\mathcal{U}}_{\mathrm{f}}$ is a convex polytope, feasibility problem (3.8) has a special form that can be re-expressed as single linear minimization problem by applying strong duality theory. Concretely, we can dualize LP (3.7) to obtain a linear minimization problem that has the

[3] Note the mild abuse of notation used for the symbol $\hat{\mathbf{A}}^{j}(\hat{\mathbf{K}})$. Such symbol is not to be confused with the jth power of a matrix, which is however defined for squared matrices only.

same objective value as LP (3.7) at the optimum, and then substitute LP (3.7) with its dual in problem (3.8). This yields a feasibility problem given only in terms of minimization operators that in addition can be transformed into a single LP as we explain next.

The dual of LP (3.7) is given for fixed $\hat{\mathbf{K}}$ and for each $j \in \{1, ..., \hat{n}_z\}$ by

$$\begin{aligned} \min_{\boldsymbol{\nu}^j \in \mathbb{R}_{\geq 0}} \ & \boldsymbol{q}_{\mathrm{f}}^{\mathrm{T}} \boldsymbol{\nu}^j \\ \text{s.t. } & \mathbf{Q}_{\mathrm{f}}^{\mathrm{T}} \boldsymbol{\nu}^j = \hat{\mathbf{A}}^{j\mathrm{T}}(\hat{\mathbf{K}}), \end{aligned}$$

where vector $\boldsymbol{\nu}^j$ represents the dual variable associated to the inequality constraints $\mathbf{Q}_{\mathrm{f}} \boldsymbol{u}_{\mathrm{f}} \leq \boldsymbol{q}_{\mathrm{f}}$ of the jth dual LP. By replacing LP (3.7) with its dual in problem (3.8), we obtain

$$\begin{aligned} \min_{\hat{\mathbf{K}}, \hat{\boldsymbol{w}}, \eta} \ & \eta \\ \text{s.t. } & \left(\min_{\boldsymbol{\nu}^j \in \mathbb{R}_{\geq 0}} \ \boldsymbol{q}_{\mathrm{f}}^{\mathrm{T}} \boldsymbol{\nu}^j \text{ s.t. } \mathbf{Q}_{\mathrm{f}}^{\mathrm{T}} \boldsymbol{\nu}^j = \hat{\mathbf{A}}^{j\mathrm{T}}(\hat{\mathbf{K}}) \right) + \hat{\mathbf{A}}_{\mathrm{c}}^{j} \hat{\boldsymbol{w}} \leq \hat{b}_j + \eta, \quad \forall j \in \{1, ..., \hat{n}_z\}, \\ & \hat{\mathbf{K}} \in \mathbb{R}^{|\mathcal{C}| \times |\mathcal{M}|}, \quad \hat{\boldsymbol{w}} \in \mathbb{R}^{|\mathcal{C}|}, \quad \eta \in \mathbb{R}, \end{aligned}$$

which can equivalently be rewritten as

$$\begin{aligned} \min_{\hat{\mathbf{K}}, \hat{\boldsymbol{w}}, \eta, \boldsymbol{\nu}^j} \ & \eta \\ \text{s.t. } & \boldsymbol{q}_{\mathrm{f}}^{\mathrm{T}} \boldsymbol{\nu}^j + \hat{\mathbf{A}}_{\mathrm{c}}^{j} \hat{\boldsymbol{w}} \leq \hat{b}_j + \eta, \quad \forall j \in \{1, ..., \hat{n}_z\}, \\ & \mathbf{Q}_{\mathrm{f}}^{\mathrm{T}} \boldsymbol{\nu}^j = \hat{\mathbf{A}}^{j\mathrm{T}}(\hat{\mathbf{K}}), \quad \forall j \in \{1, ..., \hat{n}_z\}, \\ & \boldsymbol{\nu}^j \geq \mathbf{0}, \quad \forall j \in \{1, ..., \hat{n}_z\}, \\ & \hat{\mathbf{K}} \in \mathbb{R}^{|\mathcal{C}| \times |\mathcal{M}|}, \quad \hat{\boldsymbol{w}} \in \mathbb{R}^{|\mathcal{C}|}, \quad \eta \in \mathbb{R}. \end{aligned} \tag{3.9}$$

Note that moving the inner minimization operator over $\boldsymbol{\nu}^j$ to the outer level leads to an equivalent formulation since any optimal solution of (3.9) is feasible for both the dual of LP (3.7) and problem (3.8) yielding the same objective value, and vice versa. Feasibility problem (3.9) is a finite dimensional LP, which means that the existence of an admissible affine control law $\boldsymbol{u}_{\mathrm{c}} = \hat{\mathbf{K}} \boldsymbol{y}_{\mathrm{f}}^{\mathrm{m}} + \hat{\boldsymbol{w}}$ can be verified efficiently.

3.1.3 Special Case: p-norm Shaped Uncertainty

Now we derive verification algorithms for the case where the uncertainty set $\boldsymbol{\mathcal{U}}_{\mathrm{f}}$ is shaped by a p-norm, see Fig. 3.1. In this particular case, the maximum effect of the exogenous actions $\boldsymbol{u}_{\mathrm{f}} \in \boldsymbol{\mathcal{U}}_{\mathrm{f}}$ on each system constraint can be determined analytically for given controller parameters $(\hat{\mathbf{K}}, \hat{\boldsymbol{w}})$. This fact can be exploited to reduce the infinite dimensional feasibility problem (3.4) to one involving a finite number of (linear) inequalities only. As in previous section, $\hat{\mathbf{A}}^{j}(\hat{\mathbf{K}})$ represents the jth row of the matrix $\hat{\mathbf{A}}(\hat{\mathbf{K}})$ with $j \in \{1, ..., \hat{n}_z\}$. In addition, let $\boldsymbol{u}_{\mathrm{f}} = \boldsymbol{u}_{\mathrm{f0}} + \mathbf{P}_{\mathrm{f}} \hat{\boldsymbol{u}}_{\mathrm{f}}$, where $\boldsymbol{u}_{\mathrm{f0}} \in \mathbb{R}^{n_u - |\mathcal{C}|}$ is a constant

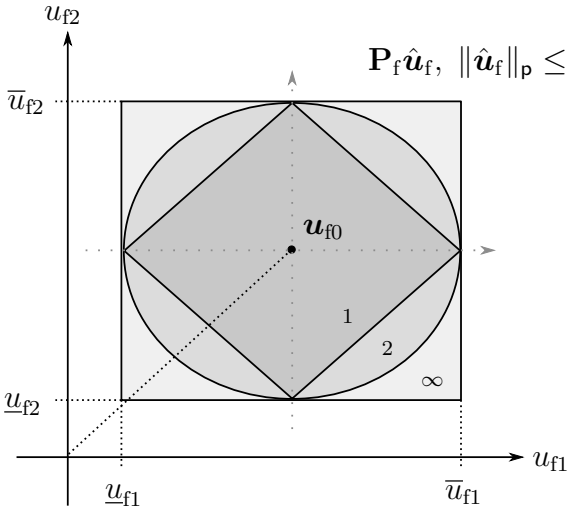

Figure 3.1: Two dimensional representation of the p–norm-bounded uncertainty set $\boldsymbol{\mathcal{U}}_{\mathrm{f}}$ in terms of the affine transformation $\boldsymbol{u}_{\mathrm{f}} = \boldsymbol{u}_{\mathrm{f}0} + \mathbf{P}\hat{\boldsymbol{u}}_{\mathrm{f}}$, $\|\hat{\boldsymbol{u}}_{\mathrm{f}}\|_{\mathsf{p}} \leq 1$, for $\mathsf{p} = \{1, 2\}$ and $\mathsf{p} \to \infty$.

vector, $\mathbf{P}_{\mathrm{f}} \in \mathbb{R}^{(n_u - |\mathcal{C}|)\times(n_u-|\mathcal{C}|)}$ is a diagonal, positive definite matrix, and $\hat{\boldsymbol{u}}_{\mathrm{f}} \in \mathbb{R}^{n_u-|\mathcal{C}|}$ is an uncertain term that fulfills $\|\hat{\boldsymbol{u}}_{\mathrm{f}}\|_{\mathsf{p}} \leq 1$. Notice that the parameters $\boldsymbol{u}_{\mathrm{f}0}$ and $\mathbf{P}_{\mathrm{f}}$ are readily determined by the given bounds of $\boldsymbol{u}_{\mathrm{f}}$.

Then, from Corollary 5 and expressions (3.2)–(3.3), the controller parameters $(\hat{\mathbf{K}}, \hat{\boldsymbol{w}})$ have to fulfill

$$\forall \hat{\boldsymbol{u}}_{\mathrm{f}} \text{ s.t. } \|\hat{\boldsymbol{u}}_{\mathrm{f}}\|_{\mathsf{p}} \leq 1 :\ \hat{\mathbf{A}}^{j}(\hat{\mathbf{K}})\boldsymbol{u}_{\mathrm{f}0} + \hat{\mathbf{A}}^{j}(\hat{\mathbf{K}})\mathbf{P}_{\mathrm{f}}\hat{\boldsymbol{u}}_{\mathrm{f}} + \hat{\mathbf{A}}_{\mathrm{c}}^{j}\hat{\boldsymbol{w}} \leq \hat{b}_j, \quad \forall j \in \{1, ..., \hat{n}_z\} \tag{3.10}$$

in order to guarantee the existence of an admissible affine control law $\boldsymbol{u}_{\mathrm{c}} = \hat{\mathbf{K}}\boldsymbol{y}_{\mathrm{f}}^{\mathrm{m}} + \hat{\boldsymbol{w}}$. While condition (3.10) is still given in terms of an infinite number of inequalities, we can reduce the number of inequalities to $\hat{n}_z$ (i.e., the number of rows of $\hat{\mathbf{A}}(\hat{\mathbf{K}})$) as follows.

Observe in condition (3.10) that it is not necessary to consider all elements in the set $\{\hat{\boldsymbol{u}}_{\mathrm{f}} \text{ s.t. } \|\hat{\boldsymbol{u}}_{\mathrm{f}}\|_{\mathsf{p}} \leq 1\}$, but only those points that maximize the term $\hat{\mathbf{A}}^{j}(\hat{\mathbf{K}})\mathbf{P}_{\mathrm{f}}\hat{\boldsymbol{u}}_{\mathrm{f}}$ for each $j \in \{1, ..., \hat{n}_z\}$ and a given matrix $\hat{\mathbf{K}}$. Those worst-case realizations of $\hat{\boldsymbol{u}}_{\mathrm{f}}$ can be found by solving for each $j \in \{1, ..., \hat{n}_z\}$

$$\max_{\|\hat{\boldsymbol{u}}_{\mathrm{f}}\|_{\mathsf{p}} \leq 1} \hat{\mathbf{A}}^{j}(\hat{\mathbf{K}})\mathbf{P}_{\mathrm{f}}\hat{\boldsymbol{u}}_{\mathrm{f}}. \tag{3.11}$$

Remarkably, the above constrained maximization problem has a special form that allows us to solve it analytically. By applying the ideas proposed in [35], the analytical solution of problem (3.11) is given by

$$\max_{\|\hat{\boldsymbol{u}}_{\mathrm{f}}\|_{\mathsf{p}} \leq 1} \hat{\mathbf{A}}^{j}(\hat{\mathbf{K}})\mathbf{P}_{\mathrm{f}}\hat{\boldsymbol{u}}_{\mathrm{f}} = \|\hat{\mathbf{A}}^{j}(\hat{\mathbf{K}})\mathbf{P}_{\mathrm{f}}\|_{\mathsf{p}^*},$$

where $\mathsf{p}^* \in \mathbb{N}^+$ fulfills $\mathsf{p}^{-1} + \mathsf{p}^{*-1} = 1$.[4] Inequalities (3.10) are thus equivalent to

$$\hat{\mathbf{A}}^{j}(\hat{\mathbf{K}})\boldsymbol{u}_{\mathrm{f}0} + \|\hat{\mathbf{A}}^{j}(\hat{\mathbf{K}})\mathbf{P}_{\mathrm{f}}\|_{\mathsf{p}^*} + \hat{\mathbf{A}}_{\mathrm{c}}^{j}\hat{\boldsymbol{w}} \leq \hat{b}_j, \quad \forall j \in \{1, ..., \hat{n}_z\}.$$

[4]For any p–norm defined in an Euclidean space of dimension d, its dual norm is the mapping $\mathbb{R}^d \mapsto \mathbb{R}$ defined by $\|\boldsymbol{y}\|_{\mathsf{p}^*} := \max_{\|\boldsymbol{x}\|_{\mathsf{p}} \leq 1} \boldsymbol{x}^{\mathrm{T}}\boldsymbol{y}$.

Equipped with the above inequalities, we can equivalently express feasibility problem (3.4) in terms of $\hat{n}_z$ inequality constraints as

$$\begin{aligned}
&\min_{\hat{\mathbf{K}},\hat{\boldsymbol{w}},\eta} \ \eta \\
&\text{s.t. } \hat{\mathbf{A}}^j(\hat{\mathbf{K}})\boldsymbol{u}_{\mathrm{f0}} + \|\hat{\mathbf{A}}^j(\hat{\mathbf{K}})\mathbf{P}_{\mathrm{f}}\|_{\mathsf{p}^*} + \hat{\mathbf{A}}_{\mathrm{c}}^j\hat{\boldsymbol{w}} \leq \hat{b}_j + \eta, \quad \forall j \in \{1,...,\hat{n}_z\}, \\
&\quad \hat{\mathbf{K}} \in \mathbb{R}^{|\mathcal{C}|\times|\mathcal{M}|}, \quad \hat{\boldsymbol{w}} \in \mathbb{R}^{|\mathcal{C}|}, \quad \eta \in \mathbb{R}.
\end{aligned} \tag{3.12}$$

Note that feasibility problem (3.12) is convex for $\mathsf{p} \geq 1$, i.e., it can be solved efficiently by using, e.g., interior point methods [96, 35]. In particular, problem (3.12) turns into a LP when $\mathsf{p} = 1$ or $\mathsf{p} \to \infty$, and into a SOCP when $\mathsf{p} = 2$.

Example 6 (Formulation for $\mathsf{p} \to \infty$)**.** In case $\mathsf{p} \to \infty$ we have that $\mathsf{p}^* = 1$, which results in the LP formulation

$$\begin{aligned}
&\min_{\hat{\mathbf{K}},\hat{\boldsymbol{w}},\eta} \ \eta \\
&\text{s.t. } \hat{\mathbf{A}}^j(\hat{\mathbf{K}})\boldsymbol{u}_{\mathrm{f0}} + \|\hat{\mathbf{A}}^j(\hat{\mathbf{K}})\mathbf{P}_{\mathrm{f}}\|_1 + \hat{\mathbf{A}}_{\mathrm{c}}^j\hat{\boldsymbol{w}} \leq \hat{b}_j + \eta, \quad \forall j \in \{1,...,\hat{n}_z\}, \\
&\quad \hat{\mathbf{K}} \in \mathbb{R}^{|\mathcal{C}|\times|\mathcal{M}|}, \quad \hat{\boldsymbol{w}} \in \mathbb{R}^{|\mathcal{C}|}, \quad \eta \in \mathbb{R}.
\end{aligned} \tag{3.13}$$

The above feasibility problem is a LP because, for each $j \in \{1,...,\hat{n}_z\}$, we can substitute the 1–norm term with the expression $\boldsymbol{r}_j^{\mathrm{T}}\mathbf{1}$, where $\boldsymbol{r}_j \in \mathbb{R}^{n_u-|\mathcal{C}|}$ is an auxiliary vector subject to the linear inequalities

$$\begin{aligned}
\boldsymbol{r}_j^{\mathrm{T}} &\geq \ \ \hat{\mathbf{A}}^j(\hat{\mathbf{K}})\mathbf{P}_{\mathrm{f}}, \\
\boldsymbol{r}_j^{\mathrm{T}} &\geq -\hat{\mathbf{A}}^j(\hat{\mathbf{K}})\mathbf{P}_{\mathrm{f}}.
\end{aligned} \tag{3.14}$$

In this manner, formulation (3.13) is equivalent to

$$\begin{aligned}
&\min_{\hat{\mathbf{K}},\hat{\boldsymbol{w}},\eta,\boldsymbol{r}_j} \ \eta \\
&\quad \text{s.t. } \hat{\mathbf{A}}^j(\hat{\mathbf{K}})\boldsymbol{u}_{\mathrm{f0}} + \boldsymbol{r}_j^{\mathrm{T}}\mathbf{1} + \hat{\mathbf{A}}_{\mathrm{c}}^j\hat{\boldsymbol{w}} \leq \hat{b}_j + \eta, \quad \forall j \in \{1,...,\hat{n}_z\}, \\
&\qquad \boldsymbol{r}_j^{\mathrm{T}} \geq \ \ \hat{\mathbf{A}}^j(\hat{\mathbf{K}})\mathbf{P}_{\mathrm{f}}, \quad \forall j \in \{1,...,\hat{n}_z\}, \\
&\qquad \boldsymbol{r}_j^{\mathrm{T}} \geq -\hat{\mathbf{A}}^j(\hat{\mathbf{K}})\mathbf{P}_{\mathrm{f}}, \quad \forall j \in \{1,...,\hat{n}_z\}, \\
&\qquad \hat{\mathbf{K}} \in \mathbb{R}^{|\mathcal{C}|\times|\mathcal{M}|}, \quad \hat{\boldsymbol{w}} \in \mathbb{R}^{|\mathcal{C}|}, \quad \eta \in \mathbb{R}, \quad \boldsymbol{r}_j \in \mathbb{R}^{n_u-|\mathcal{C}|}.
\end{aligned} \tag{3.15}$$

The existence of an admissible control law $\boldsymbol{u}_{\mathrm{c}} = \hat{\mathbf{K}}\boldsymbol{y}_{\mathrm{f}}^{\mathrm{m}} + \hat{\boldsymbol{w}}$ is thus guaranteed if the optimal value of η fulfills $\eta \leq 0$. Note that the above linear feasibility problem requires the introduction of $\hat{n}_z$ auxiliary vector variables together with $2\hat{n}_z$ vector inequality constraints, which means that the number of auxiliary constraints grows quadratically with the number of rows of the matrix $\hat{\mathbf{A}}(\hat{\mathbf{K}})$.

Equivalent Formulation for ∞-norm Shaped Uncertainty

In case the uncertainty set $\boldsymbol{\mathcal{U}}_\mathrm{f}$ is shaped by an ∞-norm, we found another formulation to determine the existence of controller parameters $(\hat{\mathbf{K}}, \hat{\boldsymbol{w}})$ guaranteeing the existence of an admissible affine control law $\boldsymbol{u}_\mathrm{c} = \hat{\mathbf{K}}\boldsymbol{y}_\mathrm{f}^\mathrm{m} + \hat{\boldsymbol{w}}$. Contrary to the technique resulting in feasibility problem (3.13), the method we present next does not rely in the transformation $\boldsymbol{u}_\mathrm{f} = \boldsymbol{u}_\mathrm{f0} + \mathbf{P}_\mathrm{f}\hat{\boldsymbol{u}}_\mathrm{f}$ to model the worst-case effect of $\boldsymbol{u}_\mathrm{f} \in [\underline{\boldsymbol{u}}_\mathrm{f}, \overline{\boldsymbol{u}}_\mathrm{f}]$ on each system constraint. However, we show later that the resulting formulation can also be transformed into LP (3.15) in a straightforward manner.

The method proposed here is based on the analytical solution of the LP

$$\boldsymbol{u}_\mathrm{f}^j = \underset{\underline{\boldsymbol{u}}_\mathrm{f} \leq \boldsymbol{u}_\mathrm{f} \leq \overline{\boldsymbol{u}}_\mathrm{f}}{\arg\max}\, \hat{\mathbf{A}}^j(\hat{\mathbf{K}})\boldsymbol{u}_\mathrm{f},$$

where $\hat{\mathbf{A}}^j(\hat{\mathbf{K}})$ represents the jth row of $\hat{\mathbf{A}}(\hat{\mathbf{K}})$ and $\boldsymbol{u}_\mathrm{f}^j$ is the worst-case realization of $\boldsymbol{u}_\mathrm{f} \in \boldsymbol{\mathcal{U}}_\mathrm{f}$ on the jth constraint of the system for each $j \in \{1, ..., \hat{n}_z\}$. Note that the above LP is an instance of LP (3.7) for the case where $\boldsymbol{\mathcal{U}}_\mathrm{f}$ is shaped by an ∞–norm. For each $j \in \{1, ..., \hat{n}_z\}$, the value of $\boldsymbol{u}_\mathrm{f}^j$ is readily given element-wise by

$$u_{\mathrm{f}k}^j = \begin{cases} \overline{u}_{\mathrm{f}k} & \text{if } \hat{A}_{jk}(\hat{\mathbf{K}}) \geq 0 \\ \underline{u}_{\mathrm{f}k} & \text{else} \end{cases}.$$

With this in mind and recalling admissibility condition (3.2), we now introduce a tight upper bound on $\hat{\mathbf{A}}(\hat{\mathbf{K}})\boldsymbol{u}_\mathrm{f}$ via the auxiliary matrix $\mathbf{H} \in \mathbb{R}^{\hat{n}_z \times (n_u - |\mathcal{C}|)}$ whose entries fulfill for all $j \in \{1, ..., \hat{n}_z\}$ and for all $k \in \{1, ..., n_u - |\mathcal{C}|\}$

$$\begin{aligned} H_{jk} &\geq \hat{A}_{jk}(\hat{\mathbf{K}})\overline{u}_{\mathrm{f}k}, \\ H_{jk} &\geq \hat{A}_{jk}(\hat{\mathbf{K}})\underline{u}_{\mathrm{f}k}. \end{aligned} \tag{3.16}$$

The tight upper bound of $\hat{\mathbf{A}}(\hat{\mathbf{K}})\boldsymbol{u}_\mathrm{f}$ is thus given by $\mathbf{H}\,\mathbf{1}$ and condition (3.2) can equivalently be re-expressed in terms of both the linear inequalities (3.16) and

$$\mathbf{H}\,\mathbf{1} + \hat{\mathbf{A}}_\mathrm{c}\hat{\boldsymbol{w}} \leq \hat{\boldsymbol{b}}. \tag{3.17}$$

The existence of controller parameters $(\hat{\mathbf{K}}, \hat{\boldsymbol{w}})$ for which the resulting affine control law $\boldsymbol{u}_\mathrm{c} = \hat{\mathbf{K}}\boldsymbol{y}_\mathrm{f}^\mathrm{m} + \hat{\boldsymbol{w}}$ is admissible can hence be verified efficiently by solving the linear feasibility problem

$$
\begin{aligned}
\min_{\hat{\mathbf{K}},\hat{\boldsymbol{w}},\mathbf{H},\eta} \quad & \eta \\
\text{s.t. } & \mathbf{H}\,\mathbf{1} + \hat{\mathbf{A}}_{\mathrm{c}}\hat{\boldsymbol{w}} \leq \hat{\boldsymbol{b}} + \eta\mathbf{1}, \\
& H_{jk} \geq \hat{A}_{jk}(\hat{\mathbf{K}})\overline{u}_{\mathrm{f}k}, \quad \forall j \in \{1,...,\hat{n}_z\},\ \forall k \in \{1,...,n_u - |\mathcal{C}|\}, \\
& H_{jk} \geq \hat{A}_{jk}(\hat{\mathbf{K}})\underline{u}_{\mathrm{f}k}, \quad \forall j \in \{1,...,\hat{n}_z\},\ \forall k \in \{1,...,n_u - |\mathcal{C}|\}, \\
& \hat{\mathbf{K}} \in \mathbb{R}^{|\mathcal{C}|\times|\mathcal{M}|}, \quad \hat{\boldsymbol{w}} \in \mathbb{R}^{|\mathcal{C}|}, \\
& \mathbf{H} \in \mathbb{R}^{\hat{n}_z \times n_u - |\mathcal{C}|}, \quad \eta \in \mathbb{R}.
\end{aligned}
\tag{3.18}
$$

Remark 4. LP (3.18) can be transformed into LP (3.15) via the following steps. First note that, since the matrix $\mathbf{P}_{\mathrm{f}}$ is diagonal, we have that

$$
\begin{aligned}
\overline{u}_{\mathrm{f}k} &= u_{\mathrm{f}0k} + P_{\mathrm{f}kk}, \\
\underline{u}_{\mathrm{f}k} &= u_{\mathrm{f}0k} - P_{\mathrm{f}kk}.
\end{aligned}
$$

Then, by replacing the above expressions for the lower and upper bounds of $u_{\mathrm{f}k}$ into inequalities (3.16), we obtain for all $j \in \{1,...,\hat{n}_z\}$ and for all $k \in \{1,...,n_u - |\mathcal{C}|\}$

$$
\begin{aligned}
H_{jk} &\geq \hat{A}_{jk}(\hat{\mathbf{K}})u_{\mathrm{f}0k} + \hat{A}_{jk}(\hat{\mathbf{K}})P_{\mathrm{f}kk}, \\
H_{jk} &\geq \hat{A}_{jk}(\hat{\mathbf{K}})u_{\mathrm{f}0k} - \hat{A}_{jk}(\hat{\mathbf{K}})P_{\mathrm{f}kk}.
\end{aligned}
$$

Now observe that, at the optimum of (3.18), the above inequalities can be expressed for all $j \in \{1,...,\hat{n}_z\}$ and for all $k \in \{1,...,n_u - |\mathcal{C}|\}$ as an equality given in terms of the sign of $\hat{A}_{jk}(\hat{\mathbf{K}})$,[5] i.e.,

$$
H_{jk} = \hat{A}_{jk}(\hat{\mathbf{K}})u_{\mathrm{f}0k} + \operatorname{sign}\left(\hat{A}_{jk}(\hat{\mathbf{K}})\right)\hat{A}_{jk}(\hat{\mathbf{K}})P_{\mathrm{f}kk}.
$$

For each $j \in \{1,...,\hat{n}_z\}$, we can now construct a feasible solution for vector $\boldsymbol{r}_j$ in LP (3.15) in terms of matrix $\mathbf{H}$. This is because, by letting $\mathbf{H}^j$ be the jth row of $\mathbf{H}$, we obtain for all $j \in \{1,...,\hat{n}_z\}$

$$
\begin{aligned}
\mathbf{H}^j\mathbf{1} &= \sum_{k=1}^{n_u-|\mathcal{C}|} \hat{A}_{jk}(\hat{\mathbf{K}})u_{\mathrm{f}0k} + \sum_{k=1}^{n_u-|\mathcal{C}|} \operatorname{sign}\left(\hat{A}_{jk}(\hat{\mathbf{K}})\right)\hat{A}_{jk}(\hat{\mathbf{K}})P_{\mathrm{f}kk} \\
&= \hat{\mathbf{A}}^{j}(\hat{\mathbf{K}})\boldsymbol{u}_{\mathrm{f}0} + \sum_{k=1}^{n_u-|\mathcal{C}|} |\hat{A}_{jk}(\hat{\mathbf{K}})P_{\mathrm{f}kk}| \\
&= \hat{\mathbf{A}}^{j}(\hat{\mathbf{K}})\boldsymbol{u}_{\mathrm{f}0} + \|\hat{\mathbf{A}}^{j}(\hat{\mathbf{K}})\mathbf{P}_{\mathrm{f}}\|_1 \\
&= \hat{\mathbf{A}}^{j}(\hat{\mathbf{K}})\boldsymbol{u}_{\mathrm{f}0} + \boldsymbol{r}_j^{\mathrm{T}}\mathbf{1}.
\end{aligned}
$$

[5] The function $\operatorname{sign}(x)$ maps $x \in \mathbb{R}$ to 1 if x is non-negative, and to -1 otherwise.

3.1.4 Summary

The efficient algorithmic techniques presented in this section are suitable for verifying the existence of admissible affine control laws of the form $\boldsymbol{u}_\mathrm{c} = \hat{\mathbf{K}}\boldsymbol{y}_\mathrm{f}^\mathrm{m} + \hat{\boldsymbol{w}}$, provided that the uncertainty set $\boldsymbol{\mathcal{U}}_\mathrm{f}$ is either a convex polytope or is shaped by a p–norm. The proposed verification algorithms are derived from Corollary 5 and also yield, if possible, an admissible realization for the affine control law. As computing the controller parameters $(\hat{\mathbf{K}}, \hat{\boldsymbol{w}})$ can be done offline, the implementation of this class of control laws is very efficient in practice.

3.2 Admissible PWA Control Laws

The verification and computation techniques proposed in previous section are suitable under the assumption that the control law has an affine structure. However, we showed in Chapter 2 that the existence of an admissible control law in general does not necessarily imply the existence of admissible affine control laws. With this in mind, we derive in this section a set of algorithms that (assuming that the sets $\boldsymbol{\mathcal{U}}_\mathrm{c}$ and $\boldsymbol{\mathcal{U}}_\mathrm{f}$ are convex polytopes) verify the existence of an admissible PWA control law $\boldsymbol{u}_\mathrm{c} = \hat{\boldsymbol{k}}(\boldsymbol{y}_\mathrm{f}^\mathrm{m})$. Our verification algorithms are based on Theorems 3 and 4. Without loss of generality, we derive verification algorithms for the control law $\boldsymbol{u}_\mathrm{c} = \hat{\boldsymbol{k}}(\boldsymbol{y}_\mathrm{f}^\mathrm{m})$ only. This is because if the control law $\boldsymbol{u}_\mathrm{c} = \hat{\boldsymbol{k}}(\boldsymbol{y}_\mathrm{f}^\mathrm{m})$ is guaranteed to be admissible, then we can apply Theorem 1 to map it to the more natural control law $\boldsymbol{u}_\mathrm{c} = \boldsymbol{k}(\boldsymbol{y}^\mathrm{m})$.

After introducing the verification task for the general case where both the control and exogenous action spaces are convex sets, we investigate the special case where the sets $\boldsymbol{\mathcal{U}}_\mathrm{f}$ and $\boldsymbol{\mathcal{U}}_\mathrm{c}$ are convex polytopes.

3.2.1 Formulation of the Verification Task

In the following, the set of control actions $\boldsymbol{\mathcal{U}}_\mathrm{c}$ as well as the set of exogenous actions $\boldsymbol{\mathcal{U}}_\mathrm{f}$ are supposed to be bounded and convex and to have arbitrary shape. We additionally recall from Chapter 2 our particular interest in constrained static systems for which both the uncertainty set $\boldsymbol{\mathcal{U}}_\mathrm{f}$ and the sensor set $\mathcal{M}$ are not empty, and $\mathrm{rank}(\mathrm{M}_\mathrm{f}^\mathrm{m}) < n_u - |\mathcal{C}|$ holds. From Theorem 4, an admissible control law $\hat{\boldsymbol{k}} : \mathrm{M}_\mathrm{f}^\mathrm{m}(\boldsymbol{\mathcal{U}}_\mathrm{f}) \to \boldsymbol{\mathcal{U}}_\mathrm{c}$ should fulfill

$$\forall \boldsymbol{y}_\mathrm{f}^\mathrm{m} \in \mathrm{M}_\mathrm{f}^\mathrm{m}(\boldsymbol{\mathcal{U}}_\mathrm{f}) : \ \mathbf{A}_\mathrm{c}\hat{\boldsymbol{k}}(\boldsymbol{y}_\mathrm{f}^\mathrm{m}) + \hat{\boldsymbol{z}}(\boldsymbol{y}_\mathrm{f}^\mathrm{m}) \leq \boldsymbol{b},$$

where

$$\hat{\boldsymbol{z}}(\boldsymbol{y}_\mathrm{f}^\mathrm{m}) = \begin{bmatrix} \max_{\boldsymbol{u}_\mathrm{f} \in \boldsymbol{\mathcal{U}}_\mathrm{f}} \ \mathbf{A}_\mathrm{f}^1 \boldsymbol{u}_\mathrm{f} \text{ s.t. } \mathrm{M}_\mathrm{f}^\mathrm{m}\boldsymbol{u}_\mathrm{f} = \boldsymbol{y}_\mathrm{f}^\mathrm{m} \\ \vdots \\ \max_{\boldsymbol{u}_\mathrm{f} \in \boldsymbol{\mathcal{U}}_\mathrm{f}} \ \mathbf{A}_\mathrm{f}^{n_z} \boldsymbol{u}_\mathrm{f} \text{ s.t. } \mathrm{M}_\mathrm{f}^\mathrm{m}\boldsymbol{u}_\mathrm{f} = \boldsymbol{y}_\mathrm{f}^\mathrm{m} \end{bmatrix}$$

and $\boldsymbol{y}_\mathrm{f}^\mathrm{m} = \mathrm{M}_\mathrm{f}^\mathrm{m}\boldsymbol{u}_\mathrm{f}$. Hence, a possible method to verify the existence of an admissible control law $\boldsymbol{u}_\mathrm{c} = \hat{\boldsymbol{k}}(\boldsymbol{y}_\mathrm{f}^\mathrm{m})$ comprises the following two steps. For all possible observation $\boldsymbol{y}_\mathrm{f}^\mathrm{m} \in \mathrm{M}_\mathrm{f}^\mathrm{m}(\boldsymbol{\mathcal{U}}_\mathrm{f})$, we first solve the feasibility problem

$$\begin{aligned} &\min_{\boldsymbol{u}_\mathrm{c}\in\boldsymbol{\mathcal{U}}_\mathrm{c},\eta\in\mathbb{R}} \ \eta \\ &\quad \text{s.t. } \mathbf{A}_\mathrm{c}\boldsymbol{u}_\mathrm{c} + \hat{\boldsymbol{z}}(\boldsymbol{y}_\mathrm{f}^\mathrm{m}) \leq \boldsymbol{b} + \eta\mathbf{1}, \\ &\qquad \hat{\boldsymbol{z}}(\boldsymbol{y}_\mathrm{f}^\mathrm{m}) = \begin{bmatrix} \max_{\boldsymbol{u}_\mathrm{f}\in\boldsymbol{\mathcal{U}}_\mathrm{f}} \mathbf{A}_\mathrm{f}^1\boldsymbol{u}_\mathrm{f} \text{ s.t. } \mathbf{M}_\mathrm{f}^\mathrm{m}\boldsymbol{u}_\mathrm{f} = \boldsymbol{y}_\mathrm{f}^\mathrm{m} \\ \vdots \\ \max_{\boldsymbol{u}_\mathrm{f}\in\boldsymbol{\mathcal{U}}_\mathrm{f}} \mathbf{A}_\mathrm{f}^{n_z}\boldsymbol{u}_\mathrm{f} \text{ s.t. } \mathbf{M}_\mathrm{f}^\mathrm{m}\boldsymbol{u}_\mathrm{f} = \boldsymbol{y}_\mathrm{f}^\mathrm{m} \end{bmatrix}, \end{aligned} \tag{3.19}$$

where $\mathbf{1}$ is a vector of ones of appropriate dimension. Note that under the considerations for $\boldsymbol{\mathcal{U}}_\mathrm{c}$ and $\boldsymbol{\mathcal{U}}_\mathrm{f}$ introduced above, the optimal value of η is always bounded. Subsequently, we check whether the optimal value of the feasibility indicator η fulfills $\eta \leq 0$. Clearly, an admissible control law $\boldsymbol{u}_\mathrm{c} = \hat{\boldsymbol{k}}(\boldsymbol{y}_\mathrm{f}^\mathrm{m})$ exists if and only if the solution of (3.19) yields $\eta \leq 0$ for all possible observations $\boldsymbol{y}_\mathrm{f}^\mathrm{m} \in \mathrm{M}_\mathrm{f}^\mathrm{m}(\boldsymbol{\mathcal{U}}_\mathrm{f})$.

However, this approach for verifying the existence of an admissible control law $\boldsymbol{u}_\mathrm{c} = \hat{\boldsymbol{k}}(\boldsymbol{y}_\mathrm{f}^\mathrm{m})$ is still an infinite dimensional feasibility task as we have to solve feasibility problem (3.19) for all possible observations $\boldsymbol{y}_\mathrm{f}^\mathrm{m} \in \mathrm{M}_\mathrm{f}^\mathrm{m}(\boldsymbol{\mathcal{U}}_\mathrm{f})$.[6] In the next section, we show to how to reduce the verification task to a finite dimensional feasibility problem, given that the sets $\boldsymbol{\mathcal{U}}_\mathrm{c}$ and $\boldsymbol{\mathcal{U}}_\mathrm{f}$ are both convex polytopes.

3.2.2 Special Case: Convex Polytopic Uncertainty

Instead of using the corners of the uncertainty set $\boldsymbol{\mathcal{U}}_\mathrm{f}$ for verifying the existence of an admissible PWA control law, cf. Theorem 6, we now derive a verification algorithm for the case where control and exogenous action spaces $\boldsymbol{\mathcal{U}}_\mathrm{c}$ and $\boldsymbol{\mathcal{U}}_\mathrm{f}$ are convex polytopes given in the $\mathcal{H}$-representation, i.e.,

$$\begin{aligned} \boldsymbol{\mathcal{U}}_\mathrm{c} &= \{\boldsymbol{u}_\mathrm{c} \in \mathbb{R}^{|\mathcal{C}|} : \mathbf{Q}_\mathrm{c}\boldsymbol{u}_\mathrm{c} \leq \boldsymbol{q}_\mathrm{c}\}, \\ \boldsymbol{\mathcal{U}}_\mathrm{f} &= \{\boldsymbol{u}_\mathrm{f} \in \mathbb{R}^{n_u-|\mathcal{C}|} : \mathbf{Q}_\mathrm{f}\boldsymbol{u}_\mathrm{f} \leq \boldsymbol{q}_\mathrm{f}\}. \end{aligned}$$

For this particular case, we can verify the existence of an admissible PWA control law $\boldsymbol{u}_\mathrm{c} = \hat{\boldsymbol{k}}(\boldsymbol{y}_\mathrm{f}^\mathrm{m})$ by solving a single, non-convex, quadratically constrained quadratic program (QCQP) as explained next.

Given that both $\boldsymbol{\mathcal{U}}_\mathrm{c}$ and $\boldsymbol{\mathcal{U}}_\mathrm{f}$ have the representation indicated above, the set of possible observations $\mathrm{M}_\mathrm{f}^\mathrm{m}(\boldsymbol{\mathcal{U}}_\mathrm{f})$ is also a convex polytope, i.e.,

$$\mathrm{M}_\mathrm{f}^\mathrm{m}(\boldsymbol{\mathcal{U}}_\mathrm{f}) = \left\{\boldsymbol{y}_\mathrm{f}^\mathrm{m} \in \mathbb{R}^{|\mathcal{M}|}, \boldsymbol{u}_\mathrm{f} \in \boldsymbol{\mathcal{U}}_\mathrm{f} : \boldsymbol{y}_\mathrm{f}^\mathrm{m} = \mathrm{M}_\mathrm{f}^\mathrm{m}\boldsymbol{u}_\mathrm{f}\right\}, \tag{3.20}$$

[6] As mentioned previously, a lower/upper bound for the feasibility indicator η can still be obtained by approximating the set of exogenous actions $\boldsymbol{\mathcal{U}}_\mathrm{f}$ from the interior/exterior using, for instance, a finite union of convex polytopes. The derivation of those bounds is out of the scope of this thesis.

Furthermore, feasibility problem (3.19) turns for each given observation $\boldsymbol{y}_{\mathrm{f}}^{\mathrm{m}} \in \mathrm{M}_{\mathrm{f}}^{\mathrm{m}}(\boldsymbol{\mathcal{U}}_{\mathrm{f}})$ into

$$\begin{aligned} &\min_{\boldsymbol{u}_{\mathrm{c}},\eta} \ \eta \\ &\text{s.t. } \mathbf{A}_{\mathrm{c}}^{j}\boldsymbol{u}_{\mathrm{c}} + \left(\max_{\mathbf{Q}_{\mathrm{f}}\boldsymbol{u}_{\mathrm{f}} \leq \boldsymbol{q}_{\mathrm{f}}} \mathbf{A}_{\mathrm{f}}^{j}\boldsymbol{u}_{\mathrm{f}} \text{ s.t. } \mathbf{M}_{\mathrm{f}}^{\mathrm{m}}\boldsymbol{u}_{\mathrm{f}} = \boldsymbol{y}_{\mathrm{f}}^{\mathrm{m}} \right) \leq b_j + \eta, \quad \forall j \in \{1,...,n_z\}, \\ &\quad \mathbf{Q}_{\mathrm{c}}\boldsymbol{u}_{\mathrm{c}} \leq \boldsymbol{q}_{\mathrm{c}}, \end{aligned} \tag{3.21}$$

where $\mathbf{A}_{\mathrm{c}}^{j}$ and $\mathbf{A}_{\mathrm{f}}^{j}$ denote the jth row of $\mathbf{A}_{\mathrm{c}}$ and $\mathbf{A}_{\mathrm{f}}$, respectively. Feasibility problem (3.21) has a special structure that allows us to remove the inner linear maximization problems to obtain a single linear minimization problem. More specifically, we can apply strong duality theory here to replace the jth inner LP with its dual (which is a minimization LP), and then move the inner minimization operator to the outer level. This technique is valid because the set of exogenous actions $\boldsymbol{\mathcal{U}}_{\mathrm{f}}$ is bounded and has no empty interior, which means that the optimal solution of the inner LPs is bounded for all possible observations $\boldsymbol{y}_{\mathrm{f}}^{\mathrm{m}} \in \mathrm{M}_{\mathrm{f}}^{\mathrm{m}}(\boldsymbol{\mathcal{U}}_{\mathrm{f}})$ and, therefore, each dualized LP has the same optimal objective value as its primal counterpart. For each $j \in \{1,...,n_z\}$, the dual of the jth inner LP in feasibility problem (3.21) is given by

$$\begin{aligned} &\min_{\substack{\boldsymbol{\rho}^j \in \mathbb{R}^{|\mathcal{M}|}, \\ \boldsymbol{\lambda}^j \in \mathbb{R}^{l_{\mathrm{f}}}_{\geq 0}}} \ \boldsymbol{\rho}^{j\mathrm{T}}\boldsymbol{y}_{\mathrm{f}}^{\mathrm{m}} + \boldsymbol{\lambda}^{j\mathrm{T}}\boldsymbol{q}_{\mathrm{f}} \\ &\quad \text{s.t. } \begin{bmatrix} \mathbf{M}_{\mathrm{f}}^{\mathrm{m}\mathrm{T}} & \mathbf{Q}_{\mathrm{f}}^{\mathrm{T}} \end{bmatrix} \begin{bmatrix} \boldsymbol{\rho}^j \\ \boldsymbol{\lambda}^j \end{bmatrix} = \mathbf{A}_{\mathrm{f}}^{j\mathrm{T}}, \end{aligned}$$

where $\boldsymbol{\rho}^j \in \mathbb{R}^{|\mathcal{M}|}$ and $\boldsymbol{\lambda}^j \in \mathbb{R}^{l_{\mathrm{f}}}_{\geq 0}$ symbolize the dual variables associated to the constraints $\mathbf{M}_{\mathrm{f}}^{\mathrm{m}}\boldsymbol{u}_{\mathrm{f}} = \boldsymbol{y}_{\mathrm{f}}^{\mathrm{m}}$ and $\mathbf{Q}_{\mathrm{f}}\boldsymbol{u}_{\mathrm{f}} \leq \boldsymbol{q}_{\mathrm{f}}$, respectively. By substituting each inner maximization LP in with its dual and moving each resulting inner minimization to the outer level, we obtain the linear feasibility problem

$$\begin{aligned} &\min_{\substack{\boldsymbol{u}_{\mathrm{c}} \in \mathbb{R}^{|\mathcal{C}|}, \eta \in \mathbb{R}, \\ \boldsymbol{\rho}^j \in \mathbb{R}^{|\mathcal{M}|}, \boldsymbol{\lambda}^j \in \mathbb{R}^{l_{\mathrm{f}}}_{\geq 0}}} \ \eta \\ &\quad \text{s.t. } \mathbf{A}_{\mathrm{c}}^{j}\boldsymbol{u}_{\mathrm{c}} + \boldsymbol{\rho}^{j\mathrm{T}}\boldsymbol{y}_{\mathrm{f}}^{\mathrm{m}} + \boldsymbol{\lambda}^{j\mathrm{T}}\boldsymbol{q}_{\mathrm{f}} - \eta \leq b_j, \quad \forall j \in \{1,...,n_z\}, \\ &\qquad \begin{bmatrix} \mathbf{M}_{\mathrm{f}}^{\mathrm{m}\mathrm{T}} & \mathbf{Q}_{\mathrm{f}}^{\mathrm{T}} \end{bmatrix} \begin{bmatrix} \boldsymbol{\rho}^j \\ \boldsymbol{\lambda}^j \end{bmatrix} = \mathbf{A}_{\mathrm{f}}^{j\mathrm{T}}, \quad \forall j \in \{1,...,n_z\}, \\ &\qquad \mathbf{Q}_{\mathrm{c}}\boldsymbol{u}_{\mathrm{c}} \leq \boldsymbol{q}_{\mathrm{c}}. \end{aligned} \tag{3.22}$$

As already mentioned in previous section, the existence of an admissible control law $\boldsymbol{u}_{\mathrm{c}} = \hat{\boldsymbol{k}}(\boldsymbol{y}_{\mathrm{f}}^{\mathrm{m}})$ is guaranteed if and only if the optimal value of the feasibility indicator η fulfills $\eta \leq 0$ for all possible observations $\boldsymbol{y}_{\mathrm{f}}^{\mathrm{m}} \in \mathrm{M}_{\mathrm{f}}^{\mathrm{m}}(\boldsymbol{\mathcal{U}}_{\mathrm{f}})$. Now observe that, instead

of solving feasibility problem (3.22) for each element in the set $\mathrm{M}_{\mathrm{f}}^{\mathrm{m}}(\boldsymbol{\mathcal{U}}_{\mathrm{f}})$, we can seek for the observation that maximizes the optimal value of η over all possible observations in $\mathrm{M}_{\mathrm{f}}^{\mathrm{m}}(\boldsymbol{\mathcal{U}}_{\mathrm{f}})$. In this manner, the existence of an admissible control law $\boldsymbol{u}_{\mathrm{c}} = \hat{\boldsymbol{k}}(\boldsymbol{y}_{\mathrm{f}}^{\mathrm{m}})$ is guaranteed if and only if the maximum value of the feasibility indicator η over all possible $\boldsymbol{y}_{\mathrm{f}}^{\mathrm{m}} \in \mathrm{M}_{\mathrm{f}}^{\mathrm{m}}(\boldsymbol{\mathcal{U}}_{\mathrm{f}})$ is at most zero. Verifying the existence of an admissible control law $\boldsymbol{u}_{\mathrm{c}} = \hat{\boldsymbol{k}}(\boldsymbol{y}_{\mathrm{f}}^{\mathrm{m}})$ is thus equivalent to solve the max-min feasibility problem

$$
\begin{aligned}
\eta^{\star} = \max_{\boldsymbol{y}_{\mathrm{f}}^{\mathrm{m}} \in \mathrm{M}_{\mathrm{f}}^{\mathrm{m}}(\boldsymbol{\mathcal{U}}_{\mathrm{f}})} \; & \min_{\substack{\boldsymbol{u}_{\mathrm{c}} \in \mathbb{R}^{|\mathcal{C}|}, \eta \in \mathbb{R}, \\ \boldsymbol{\rho}^j \in \mathbb{R}^{|\mathcal{M}|}, \boldsymbol{\lambda}^j \in \mathbb{R}^{l_{\mathrm{f}}}_{\geq 0}}} \quad \eta \\
& \text{s.t. } \mathbf{A}_{\mathrm{c}}^j \boldsymbol{u}_{\mathrm{c}} + \boldsymbol{\rho}^{j\mathrm{T}} \boldsymbol{y}_{\mathrm{f}}^{\mathrm{m}} + \boldsymbol{\lambda}^{j\mathrm{T}} \boldsymbol{q}_{\mathrm{f}} \leq b_j + \eta, \quad \forall j \in \{1, ..., n_z\}, \\
& \quad \begin{bmatrix} \mathbf{M}_{\mathrm{f}}^{\mathrm{m}\mathrm{T}} & \mathbf{Q}_{\mathrm{f}}^{\mathrm{T}} \end{bmatrix} \begin{bmatrix} \boldsymbol{\rho}^j \\ \boldsymbol{\lambda}^j \end{bmatrix} = \mathbf{A}_{\mathrm{f}}^{j\mathrm{T}}, \quad \forall j \in \{1, ..., n_z\}, \\
& \quad \mathbf{Q}_{\mathrm{c}} \boldsymbol{u}_{\mathrm{c}} \leq \boldsymbol{q}_{\mathrm{c}}.
\end{aligned}
$$

Instead of solving the above max-min feasibility problem, we propose to dualize LP (3.22) to obtain a maximization LP that is thereafter exploited to derive a single, non-convex (QCQP) verification algorithm. To this end, first note that LP (3.22) is always feasible for each given observation $\boldsymbol{y}_{\mathrm{f}}^{\mathrm{m}} \in \mathrm{M}_{\mathrm{f}}^{\mathrm{m}}(\boldsymbol{\mathcal{U}}_{\mathrm{f}})$. Then, by strong duality, the dual formulation of LP (3.22) corresponds to an always feasible maximization LP whose optimal cost equals the optimal value of the feasibility indicator η. To derive the dual maximization LP, we now introduce the dual variables $\boldsymbol{\alpha} \in \mathbb{R}^{n_z}_{\leq 0}$, $\boldsymbol{\beta}^{1,...,n_z} \in \mathbb{R}^{n_u - |\mathcal{C}|}$, and $\boldsymbol{\gamma} \in \mathbb{R}^{l_{\mathrm{c}}}_{\leq 0}$, which correspond to the first, second, and third constraint of (3.22), respectively. Each primal variable in LP (3.22) thus receives a dual constraint, which yields the following set of dual (in)equality constraints:

$$
\begin{aligned}
(\eta): \quad & -\mathbf{1}^{\mathrm{T}} \boldsymbol{\alpha} = 1, \\
(\boldsymbol{u}_{\mathrm{c}}): \quad & \mathbf{A}_{\mathrm{c}}^{\mathrm{T}} \boldsymbol{\alpha} + \mathbf{Q}_{\mathrm{c}}^{\mathrm{T}} \boldsymbol{\gamma} = 0, \\
(\boldsymbol{\rho}^j): \quad & \alpha_j \boldsymbol{y}_{\mathrm{f}}^{\mathrm{m}} + \mathbf{M}_{\mathrm{f}}^{\mathrm{m}} \boldsymbol{\beta}^j = \mathbf{0}, \quad \forall j \in \{1, ..., n_z\}, \\
(\boldsymbol{\lambda}^j): \quad & \alpha_j \boldsymbol{q}_{\mathrm{f}} + \mathbf{Q}_{\mathrm{f}} \boldsymbol{\beta}^j \leq \mathbf{0}, \quad \forall j \in \{1, ..., n_z\}.
\end{aligned}
\tag{3.23}
$$

Moreover, the dual cost to be maximized is given by

$$
\text{dual cost of LP (3.22)} = \boldsymbol{b}^{\mathrm{T}} \boldsymbol{\alpha} + \sum_{j=1}^{n_z} \mathbf{A}_{\mathrm{f}}^j \boldsymbol{\beta}^j + \boldsymbol{q}_{\mathrm{c}}^{\mathrm{T}} \boldsymbol{\gamma}, \tag{3.24}
$$

which is readily obtained from the parameters of the right-hand side of the constraints in LP (3.22). Remember that the optimal dual cost (3.24) equals the optimal value of η.

By using the dual constraints (3.23) and the dual cost (3.24), we readily obtain the dual of feasibility problem (3.22), namely a linear maximization problem over $(\boldsymbol{\alpha}, \boldsymbol{\beta}^j, \boldsymbol{\gamma})$ that (apparently) should be solved for all possible observations $\boldsymbol{y}_{\mathrm{f}}^{\mathrm{m}} \in \mathrm{M}_{\mathrm{f}}^{\mathrm{m}}(\boldsymbol{\mathcal{U}}_{\mathrm{f}})$ in order to verify the existence of an admissible control law $\boldsymbol{u}_{\mathrm{c}} = \hat{\boldsymbol{k}}(\boldsymbol{y}_{\mathrm{f}}^{\mathrm{m}})$. However, we know

from the previous analysis that we only have to find the observation in $\mathrm{M}_{\mathrm{f}}^{\mathrm{m}}(\boldsymbol{\mathcal{U}}_{\mathrm{f}})$ that maximizes the value of the feasibility indicator η. It is at this point when the dual LP of feasibility problem (3.22) gains paramount importance. This is because the desired worst-case realization of $\boldsymbol{y}_{\mathrm{f}}^{\mathrm{m}} \in \mathrm{M}_{\mathrm{f}}^{\mathrm{m}}(\boldsymbol{\mathcal{U}}_{\mathrm{f}})$ that maximizes η can be found by considering the observation $\boldsymbol{y}_{\mathrm{f}}^{\mathrm{m}} \in \mathrm{M}_{\mathrm{f}}^{\mathrm{m}}(\boldsymbol{\mathcal{U}}_{\mathrm{f}})$ also as an optimization variable in the dual formulation of feasibility problem (3.22). The existence of an admissible control law $\boldsymbol{u}_{\mathrm{c}} = \hat{\boldsymbol{k}}(\boldsymbol{y}_{\mathrm{f}}^{\mathrm{m}})$ can therefore be verified by first solving

$$\begin{aligned}
\eta^{\star} = \max_{\substack{\boldsymbol{\alpha}\in\mathbb{R}^{n_z}_{\leq 0},\ \boldsymbol{\beta}^j\in\mathbb{R}^{n_u-|\mathcal{C}|},\\ \boldsymbol{\gamma}\in\mathbb{R}^{l_{\mathrm{c}}}_{\leq 0},\ \boldsymbol{y}_{\mathrm{f}}^{\mathrm{m}}\in\mathbf{M}_{\mathrm{f}}^{\mathrm{m}}(\boldsymbol{\mathcal{U}}_{\mathrm{f}})}} & \boldsymbol{b}^{\mathrm{T}}\boldsymbol{\alpha} + \sum_{j=1}^{n_z} \mathbf{A}_{\mathrm{f}}^{j}\boldsymbol{\beta}^{j} + \boldsymbol{q}_{\mathrm{c}}^{\mathrm{T}}\boldsymbol{\gamma} \\
\text{s.t. } & -\mathbf{1}^{\mathrm{T}}\boldsymbol{\alpha} = 1, \\
& \mathbf{A}_{\mathrm{c}}^{\mathrm{T}}\boldsymbol{\alpha} + \mathbf{Q}_{\mathrm{c}}^{\mathrm{T}}\boldsymbol{\gamma} = 0, \\
& \alpha_j \boldsymbol{y}_{\mathrm{f}}^{\mathrm{m}} + \mathbf{M}_{\mathrm{f}}^{\mathrm{m}}\boldsymbol{\beta}^{j} = \mathbf{0},\ \forall j \in \{1,...,n_z\}, \\
& \alpha_j \boldsymbol{q}_{\mathrm{f}} + \mathbf{Q}_{\mathrm{f}}\boldsymbol{\beta}^{j} \leq \mathbf{0},\ \forall j \in \{1,...,n_z\},
\end{aligned} \tag{3.25}$$

and thereafter checking whether $\eta^{\star} \leq 0$. In affirmative case, the existence of an admissible control law $\boldsymbol{u}_{\mathrm{c}} = \hat{\boldsymbol{k}}(\boldsymbol{y}_{\mathrm{f}}^{\mathrm{m}})$ is guaranteed. Otherwise, an admissible control law for the constrained static system is impossible and the actuator and sensor sets $(\mathcal{C}, \mathcal{M})$ have to be adapted. Note in feasibility problem (3.25) that the bilinear equalities involving the optimization variables α_j and $\boldsymbol{y}_{\mathrm{f}}^{\mathrm{m}}$ make the feasibility set not-convex. Feasibility problem (3.25) is concretely a non-convex QCQP and has by definition worst-case exponential complexity. However, we found that a special implementation of the QCQP (3.25) yields the global optimal solution efficiently in practice.

Implementation of the QCQP Verification Algorithm

We could establish experimentally that the efficiency of solving QCQP (3.25) can be significantly improved by exploiting the characteristics of Gurobi 9.1.1 [97], the non-convex QCQP solver of our choice. The simple, but key step consists of isolating the bilinear terms from the linear conditions by introducing new auxiliary optimization variables $\boldsymbol{\psi}^j \in \mathbb{R}^{|\mathcal{M}|}$ which are restricted by

$$\boldsymbol{\psi}^j = \alpha_j \boldsymbol{y}_{\mathrm{f}}^{\mathrm{m}}, \quad j = 1,...,n_z. \tag{3.26}$$

This allows us to partition the constraints of QCQP (3.25) into a block of pure linear constraints, and the set of bilinear constraints (3.26) which are handled systematically in Gurobi by employing a technique based on McCornick envelopes [98] and a spatial branching [99] strategy. By recalling that $\mathrm{M}_{\mathrm{f}}^{\mathrm{m}}(\boldsymbol{\mathcal{U}}_{\mathrm{f}})$ is given by (3.20), the QCQP verification algorithm (3.25) is thus equivalent to

$$
\begin{aligned}
\eta^\star = \max_{\substack{\boldsymbol{\alpha},\, \boldsymbol{\beta}^j,\, \boldsymbol{\gamma},\\ \boldsymbol{u}_\mathrm{f}, \boldsymbol{y}_\mathrm{f}^\mathrm{m}, \boldsymbol{\psi}^j}} \; & \boldsymbol{b}^\mathrm{T}\boldsymbol{\alpha} + \sum_{j=1}^{n_z} \mathbf{A}_\mathrm{f}^j \boldsymbol{\beta}^j + \boldsymbol{q}_\mathrm{c}^\mathrm{T}\boldsymbol{\gamma} \\
\text{s.t.} \; & -\mathbf{1}^\mathrm{T}\boldsymbol{\alpha} = 1, \\
& \mathbf{A}_\mathrm{c}^\mathrm{T}\boldsymbol{\alpha} + \mathbf{Q}_\mathrm{c}^\mathrm{T}\boldsymbol{\gamma} = 0, \\
& \alpha_j \boldsymbol{q}_\mathrm{f} + \mathbf{Q}_\mathrm{f}\boldsymbol{\beta}^j \leq \mathbf{0}, \; \forall j \in \{1, ..., n_z\}, \\
& \boldsymbol{\alpha} \leq \mathbf{0}, \\
& \boldsymbol{\gamma} \leq \mathbf{0}, \\
& \mathbf{Q}_\mathrm{f}\boldsymbol{u}_\mathrm{f} \leq \boldsymbol{q}_\mathrm{f}, \\
& \boldsymbol{y}_\mathrm{f}^\mathrm{m} = \mathbf{M}_\mathrm{f}^\mathrm{m}\boldsymbol{u}_\mathrm{f}, \\
& \boldsymbol{\psi}^j + \mathbf{M}_\mathrm{f}^\mathrm{m}\boldsymbol{\beta}^j = \mathbf{0}, \; \forall j \in \{1, ..., n_z\}, \\
& \boldsymbol{\psi}^j = \alpha_j \boldsymbol{y}_\mathrm{f}^\mathrm{m}, \quad \forall j \in \{1, ..., n_z\}.
\end{aligned}
\tag{3.27}
$$

We validate experimentally that providing the explicit partitioning to the solver reduces the solver time by 1–2 orders of magnitude, making QCQP (3.27) efficient for practical use cases as we illustrate in Chapter 7.

We also remark that in many cases it is not necessary to solve QCQP (3.27) to global optimality. This is because an upper bound for the optimal cost fulfilling $\overline{\eta}^\star \leq 0$ is sufficient to prove the existence of an admissible PWA control law, and a lower bound satisfying $\underline{\eta}^\star > 0$ is sufficient to show that an admissible control law does not exist.

3.3 Computing Admissible PWA Control Laws

QCQP (3.27) provides an efficient method to verify the existence an admissible control law $\boldsymbol{u}_\mathrm{c} = \hat{\boldsymbol{k}}(\boldsymbol{y}_\mathrm{f}^\mathrm{m})$, provided that the set of control actions $\boldsymbol{\mathcal{U}}_\mathrm{c}$ as well as the set of exogenous actions $\boldsymbol{\mathcal{U}}_\mathrm{f}$ are convex polytopes. Under these assumptions, we present in this section a set of algorithms to compute an admissible control law $\boldsymbol{u}_\mathrm{c} = \hat{\boldsymbol{k}}(\boldsymbol{y}_\mathrm{f}^\mathrm{m})$ once its existence has been verified.

As we learned from Chapter 2, an admissible control law $\boldsymbol{u}_\mathrm{c} = \hat{\boldsymbol{k}}(\boldsymbol{y}_\mathrm{f}^\mathrm{m})$ can always be chosen as a piecewise affine function if the set $\boldsymbol{\mathcal{U}}_\mathrm{f}$ is a convex polytope. While it is possible to compute an admissible PWA control law based on the corners of $\boldsymbol{\mathcal{U}}_\mathrm{f}$, such approach is not always viable as the number of corners of $\boldsymbol{\mathcal{U}}_\mathrm{f}$ grows in general exponentially. However, there are alternative, more efficient methods for computing an admissible PWA control law that do not require the corners of $\boldsymbol{\mathcal{U}}_\mathrm{f}$. For instance, feasibility problem (3.22) already yields an *online* method for mapping a given observation $\boldsymbol{y}_\mathrm{f}^\mathrm{m} \in \mathrm{M}_\mathrm{f}^\mathrm{m}(\boldsymbol{\mathcal{U}}_\mathrm{f})$ to a suitable control action $\boldsymbol{u}_\mathrm{c} \in \boldsymbol{\mathcal{U}}_\mathrm{c}$. In the following, we show that the control law $\boldsymbol{u}_\mathrm{c} = \hat{\boldsymbol{k}}(\boldsymbol{y}_\mathrm{f}^\mathrm{m})$ implied by feasibility problem (3.22) is a PWA function whose closed-form expression can also be computed *offline* by using multiparametric linear optimization techniques.

Although the algorithms proposed below compute admissible PWA control laws $\boldsymbol{u}_\mathrm{c} = \hat{\boldsymbol{k}}(\boldsymbol{y}_\mathrm{f}^\mathrm{m})$ that minimize the value of the feasibility indicator η, such algorithms can easily be extended to compute admissible PWA control laws minimizing, e.g., linear or quadratic objective functions of the control action $\boldsymbol{u}_\mathrm{c}$.

3.3.1 Online Two-stage Approach

For reasons that will become clearer later, it is beneficial to express the control law $\boldsymbol{u}_\mathrm{c} = \hat{\boldsymbol{k}}(\boldsymbol{y}_\mathrm{f}^\mathrm{m})$ implied by feasibility problem (3.22) as an equivalent two-step algorithm. In the first step, we evaluate the function $\hat{\boldsymbol{z}}(\boldsymbol{y}_\mathrm{f}^\mathrm{m})$, cf. Theorem 4, using the observation $\boldsymbol{y}_\mathrm{f}^\mathrm{m}$ which is assumed to be available to the controller. Instead of evaluating $\hat{\boldsymbol{z}}(\boldsymbol{y}_\mathrm{f}^\mathrm{m})$ element-wise as indicated in (2.14), we adopt here the single equivalent maximization LP

$$\begin{aligned} \hat{\boldsymbol{z}}(\boldsymbol{y}_\mathrm{f}^\mathrm{m}) = \underset{\tilde{\boldsymbol{z}}\in\mathbb{R}^{n_z}}{\arg\max} \; \max_{\boldsymbol{u}_\mathrm{f}^{1,\ldots,n_z}\in\boldsymbol{\mathcal{U}}_\mathrm{f}} \; & \mathbf{1}^\mathrm{T}\tilde{\boldsymbol{z}} \\ \text{s.t. } \tilde{\boldsymbol{z}} = & \begin{bmatrix} \mathbf{A}_\mathrm{f}^1\boldsymbol{u}_\mathrm{f}^1 \\ \vdots \\ \mathbf{A}_\mathrm{f}^{n_z}\boldsymbol{u}_\mathrm{f}^{n_z} \end{bmatrix}, \\ & \mathbf{M}_\mathrm{f}^\mathrm{m}\boldsymbol{u}_\mathrm{f}^{1,\ldots,n_z} = \boldsymbol{y}_\mathrm{f}^\mathrm{m}, \end{aligned} \tag{3.28}$$

which can be derived by using an approach similar to the explained in Remark 1. In this manner, we obtain the worst-case impact of those exogenous actions $\boldsymbol{u}_\mathrm{f} \in \boldsymbol{\mathcal{U}}_\mathrm{f}$—which yield the same observation $\boldsymbol{y}_\mathrm{f}^\mathrm{m}$—on each constraint of the system. In the second step, we compute the control action $\boldsymbol{u}_\mathrm{c}$ associated to the observation $\boldsymbol{y}_\mathrm{f}^\mathrm{m}$ by using the value of $\hat{\boldsymbol{z}}(\boldsymbol{y}_\mathrm{f}^\mathrm{m})$ in the LP formulation

$$\begin{aligned} \boldsymbol{u}_\mathrm{c} = \hat{\boldsymbol{k}}(\boldsymbol{y}_\mathrm{f}^\mathrm{m}) = \underset{\boldsymbol{u}_\mathrm{c}\in\boldsymbol{\mathcal{U}}_\mathrm{c}}{\arg\min} \min_{\eta\in\mathbb{R}} \; & \eta \\ \text{s.t. } & \mathbf{A}_\mathrm{c}\boldsymbol{u}_\mathrm{c} + \hat{\boldsymbol{z}}(\boldsymbol{y}_\mathrm{f}^\mathrm{m}) \leq \boldsymbol{b} + \eta\mathbf{1}. \end{aligned} \tag{3.29}$$

If an admissible control law $\boldsymbol{u}_\mathrm{c} = \hat{\boldsymbol{k}}(\boldsymbol{y}_\mathrm{f}^\mathrm{m})$ exists, then the optimal value of the feasibility indicator η is guaranteed to be at most zero for all possible observations $\boldsymbol{y}_\mathrm{f}^\mathrm{m} \in \mathrm{M}_\mathrm{f}^\mathrm{m}(\boldsymbol{\mathcal{U}}_\mathrm{f})$ and therefore the constraints of the system are always fulfilled.

Remark 5. LP (3.29) can easily be modified to minimize, for instance, linear or (convex) quadratic objective functions of $\boldsymbol{u}_\mathrm{c}$. Concretely, we can simply remove the feasibility indicator η from LP (3.29) and replace the cost function η with an objective of the form $\boldsymbol{c}^\mathrm{T}\boldsymbol{u}_\mathrm{c} + \boldsymbol{u}_\mathrm{c}^\mathrm{T}\mathbf{R}\boldsymbol{u}_\mathrm{c}$. Here, the linear costs are parametrized by the vector $\boldsymbol{c} \in \mathbb{R}^{|\mathcal{C}|}$, and the quadratic costs by the (positive semidefinite) matrix $\mathbf{R} \in \mathbb{R}^{|\mathcal{C}|\times|\mathcal{C}|}$.[7]

[7] A positive semidefinite matrix is a symmetric square matrix whose eigenvalues are real, non-negative numbers.

An interesting aspect of computing the control action $\boldsymbol{u}_\mathrm{c}$ via LPs (3.28)–(3.29) is that, for each given observation $\boldsymbol{y}_\mathrm{f}^\mathrm{m} \in \mathrm{M}_\mathrm{f}^\mathrm{m}(\boldsymbol{\mathcal{U}}_\mathrm{f})$, the resulting control action $\boldsymbol{u}_\mathrm{c}$ may still be valid for another observation $\boldsymbol{y}_\mathrm{f}^{\mathrm{m}\prime}$ yielding another $\hat{\boldsymbol{z}}(\boldsymbol{y}_\mathrm{f}^{\mathrm{m}\prime})$, as long as the inequality $\mathbf{A}_\mathrm{c}\boldsymbol{u}_\mathrm{c} + \hat{\boldsymbol{z}}(\boldsymbol{y}_\mathrm{f}^{\mathrm{m}\prime}) \leq \boldsymbol{b}$ holds. This property is exploited next to compute the control action $\boldsymbol{u}_\mathrm{c}$ for a given $\boldsymbol{y}_\mathrm{f}^\mathrm{m}$ over time.

Minimal Action Sequential Control Law

In practice, the control action $\boldsymbol{u}_\mathrm{c}$ is often computed periodically based on the current observation $\boldsymbol{y}_\mathrm{f}^\mathrm{m}$ in order to adjust the system to new situations. However, it may be not desired to adapt the value of $\boldsymbol{u}_\mathrm{c}$ at each iteration, which may be undesirable due to economic and technical reasons. We therefore propose to adapt an existing $\boldsymbol{u}_\mathrm{c}$ *only* if its current value leads to a possible constraint violation for the incoming observation $\boldsymbol{y}_\mathrm{f}^\mathrm{m}$.

In each iteration, the controller receives a new observation $\boldsymbol{y}^\mathrm{m}$ from which the value of $\boldsymbol{y}_\mathrm{f}^\mathrm{m}$ can be computed based on the previous control action $\boldsymbol{u}_\mathrm{c}$, i.e., $\boldsymbol{y}_\mathrm{f}^\mathrm{m} = \boldsymbol{y}^\mathrm{m} - \mathrm{M}_\mathrm{c}^\mathrm{m}\boldsymbol{u}_\mathrm{c}$. After evaluating $\hat{\boldsymbol{z}}(\boldsymbol{y}_\mathrm{f}^\mathrm{m})$ via LP (3.28), we compute an indicator of how far each constraint of the system is from being violated, i.e., we calculate

$$\eta = \phi(\boldsymbol{y}_\mathrm{f}^\mathrm{m}) = \max_{j\in\{1,\dots,n_z\}} (\mathbf{A}_\mathrm{c}^j\boldsymbol{u}_\mathrm{c} + \hat{z}_j(\boldsymbol{y}_\mathrm{f}^\mathrm{m}) - b_j).$$

If $\eta \leq 0$ holds, then the existent control action $\boldsymbol{u}_\mathrm{c}$ still fulfills the constraints of the system and no adaptation step is required. Otherwise, $\boldsymbol{u}_\mathrm{c}$ is adapted by solving LP (3.29) using the new value of $\hat{\boldsymbol{z}}(\boldsymbol{y}_\mathrm{f}^\mathrm{m})$.

A further option to speed up the iterative control loop in cases where $\boldsymbol{y}_\mathrm{f}^\mathrm{m}$ is low-dimensional is to discretize the space $\mathrm{M}_\mathrm{f}^\mathrm{m}(\boldsymbol{\mathcal{U}}_\mathrm{f})$ and subsequently pre-compute the corresponding values for $\boldsymbol{u}_\mathrm{c} = \hat{\boldsymbol{k}}(\boldsymbol{y}_\mathrm{f}^\mathrm{m})$. These values can then be stored as a look-up table for practical implementation.

3.3.2 Offline Two-stage Approach

Instead of computing either the admissible control law implied by LP (3.22) or LPs (3.28)–(3.29) online, we now focus on finding the closed-form representation of an admissible PWA control law $\boldsymbol{u}_\mathrm{c} = \hat{\boldsymbol{k}}(\boldsymbol{y}_\mathrm{f}^\mathrm{m})$ offline. This is beneficial since it reduces the online computation effort from solving a LP to a function evaluation, which can significantly reduce the computation time and allow for guaranteed execution times.

Closed-form expressions of $\boldsymbol{u}_\mathrm{c} = \hat{\boldsymbol{k}}(\boldsymbol{y}_\mathrm{f}^\mathrm{m})$ can be computed by solving LP (3.22) for any possible observation $\boldsymbol{y}_\mathrm{f}^\mathrm{m}$. This task corresponds to computing an explicit solution of a Multi-Parametric Linear Program (MPLP) where the system matrix is parametric, since the parameter $\boldsymbol{y}_\mathrm{f}^\mathrm{m}$ is multiplied with the LP variable $\boldsymbol{\rho}^j$ in a constraint of LP (3.22).

When the right-hand side or the objective of a MPLP are parametric it is known that the solution functions are PWA [92] and the associated regions in the parameter space, the so-called critical regions, convex polyhedra [93]. If the system matrix is parametric, as in

our case, both characterizations are not necessarily fulfilled as can be deduced from [100, Theorem 4.3]. This makes computing and storing an explicit solution representation not easy in general.

However, we can show that for our special problem instance the two properties are still fulfilled. This allows us to compute and store an explicit representation of $\boldsymbol{u}_\mathrm{c} = \hat{\boldsymbol{k}}(\boldsymbol{y}_\mathrm{f}^\mathrm{m})$ with known tools.

Theorem 10. The paramatric solution $\boldsymbol{u}_\mathrm{c} = \hat{\boldsymbol{k}}(\boldsymbol{y}_\mathrm{f}^\mathrm{m})$ of (3.22) is PWA and the critical regions are all convex polyhedra.

To proof this, we return to the two-stage algorithm (3.28)–(3.29) for computing the control law $\boldsymbol{u}_\mathrm{c} = \hat{\boldsymbol{k}}(\boldsymbol{y}_\mathrm{f}^\mathrm{m})$, but now in a parametric fashion.

Closed-form of the Mapping $\hat{\boldsymbol{z}}(\boldsymbol{y}_\mathrm{f}^\mathrm{m})$

In order to determine the closed-form of the mapping $\hat{\boldsymbol{z}}(\boldsymbol{y}_\mathrm{f}^\mathrm{m})$, observe that LP (3.28) is a MPLP with right-hand side parameter $\boldsymbol{y}_\mathrm{f}^\mathrm{m} \in \mathrm{M}_\mathrm{f}^\mathrm{m}(\boldsymbol{\mathcal{U}}_\mathrm{f})$. Since $\boldsymbol{\mathcal{U}}_\mathrm{f}$ is a convex polytope, the set $\mathrm{M}_\mathrm{f}^\mathrm{m}(\boldsymbol{\mathcal{U}}_\mathrm{f})$ is also a convex polytope and, from the the analysis of Chapter 2, we know that in this particular case the mapping $\hat{\boldsymbol{z}}(\boldsymbol{y}_\mathrm{f}^\mathrm{m})$ is continuous and PWA in critical regions defined by convex polytopes.

Now let $\mathcal{R}^\kappa(\mathrm{M}_\mathrm{f}^\mathrm{m}(\boldsymbol{\mathcal{U}}_\mathrm{f}))$ be the κth critical region of $\mathrm{M}_\mathrm{f}^\mathrm{m}(\boldsymbol{\mathcal{U}}_\mathrm{f})$, with $\kappa \in \{1, ..., \hat{\kappa}\}$. Then, the κth piece of $\hat{\boldsymbol{z}}(\boldsymbol{y}_\mathrm{f}^\mathrm{m})$, here denoted by $\hat{\boldsymbol{z}}^\kappa(\boldsymbol{y}_\mathrm{f}^\mathrm{m})$, can be expressed as an affine function of the form

$$\hat{\boldsymbol{z}}^\kappa(\boldsymbol{y}_\mathrm{f}^\mathrm{m}) = \boldsymbol{\Pi}^\kappa \boldsymbol{y}_\mathrm{f}^\mathrm{m} + \boldsymbol{r}^\kappa, \quad \forall \boldsymbol{y}_\mathrm{f}^\mathrm{m} \in \mathcal{R}^\kappa(\mathrm{M}_\mathrm{f}^\mathrm{m}(\boldsymbol{\mathcal{U}}_\mathrm{f})). \tag{3.30}$$

The parameters $\boldsymbol{\Pi}^\kappa \in \mathbb{R}^{n_z \times |\mathcal{C}|}$ and $\boldsymbol{r}^\kappa \in \mathbb{R}^{n_z}$ are valid for the critical region $\mathcal{R}^\kappa(\mathrm{M}_\mathrm{f}^\mathrm{m}(\boldsymbol{\mathcal{U}}_\mathrm{f}))$ and can be readily determined for each $\kappa = 1, ..., \hat{\kappa}$ by using off-the-shelf multiparametric linear optimization software, e.g., the Multiparametric Programming Toolbox (MPT) [101]. Note that the values that $\hat{\boldsymbol{z}}^\kappa$ maps from the elements of $\mathcal{R}^\kappa(\mathrm{M}_\mathrm{f}^\mathrm{m}(\boldsymbol{\mathcal{U}}_\mathrm{f}))$ lay also in a convex polyhedron.

Closed-form of the Mapping $\boldsymbol{u}_\mathrm{c} = \hat{\boldsymbol{k}}(\boldsymbol{y}_\mathrm{f}^\mathrm{m})$

For the κth critical region $\mathcal{R}^\kappa(\mathrm{M}_\mathrm{f}^\mathrm{m}(\boldsymbol{\mathcal{U}}_\mathrm{f}))$ with $\kappa \in \{1, ..., \hat{\kappa}\}$, we now construct the mapping $\hat{\boldsymbol{k}}^\kappa : \mathcal{R}^\kappa(\mathrm{M}_\mathrm{f}^\mathrm{m}(\boldsymbol{\mathcal{U}}_\mathrm{f})) \to \boldsymbol{\mathcal{U}}_\mathrm{c}$ by replacing expression (3.30) on the second stage LP (3.29). We obtain

$$\begin{aligned} \hat{\boldsymbol{k}}^\kappa(\boldsymbol{y}_\mathrm{f}^\mathrm{m}) = & \arg\min_{\boldsymbol{u}_\mathrm{c} \in \boldsymbol{\mathcal{U}}_\mathrm{c}} \min_{\eta \in \mathbb{R}} \eta \\ & \text{s.t. } \mathbf{A}_\mathrm{c}\boldsymbol{u}_\mathrm{c} + \underbrace{\boldsymbol{\Pi}^\kappa \boldsymbol{y}_\mathrm{f}^\mathrm{m} + \boldsymbol{r}^\kappa}_{\hat{\boldsymbol{z}}^\kappa(\boldsymbol{y}_\mathrm{f}^\mathrm{m})} \leq \boldsymbol{b} + \eta \mathbf{1}. \end{aligned} \tag{3.31}$$

The above problem formulation can be interpreted as a MPLP with right-hand side parameter $\boldsymbol{y}_\mathrm{f}^\mathrm{m} \in \mathcal{R}^\kappa(\mathrm{M}_\mathrm{f}^\mathrm{m}(\boldsymbol{\mathcal{U}}_\mathrm{f}))$. This means that the mapping $\hat{\boldsymbol{k}}^\kappa(\boldsymbol{y}_\mathrm{f}^\mathrm{m})$ is PWA for

$\boldsymbol{y}_{\mathrm{f}}^{\mathrm{m}} \in \mathcal{R}^{\kappa}(\mathrm{M}_{\mathrm{f}}^{\mathrm{m}}(\boldsymbol{\mathcal{U}}_{\mathrm{f}}))$ and its associated critical regions of $\mathcal{R}^{\kappa}(\mathrm{M}_{\mathrm{f}}^{\mathrm{m}}(\boldsymbol{\mathcal{U}}_{\mathrm{f}}))$ are convex polytopes.

Now let $\mathcal{R}^{l\kappa}(\mathrm{M}_{\mathrm{f}}^{\mathrm{m}}(\boldsymbol{\mathcal{U}}_{\mathrm{f}}))$ denote the lth critical region of the critical region $\mathcal{R}^{\kappa}(\mathrm{M}_{\mathrm{f}}^{\mathrm{m}}(\boldsymbol{\mathcal{U}}_{\mathrm{f}}))$, with $l \in \{1, ..., \hat{l}_{\kappa}\}$. Then, for each $\kappa = 1, ..., \hat{\kappa}$, the lth piece of $\hat{\boldsymbol{k}}^{\kappa}(\boldsymbol{y}_{\mathrm{f}}^{\mathrm{m}})$, here denoted by $\hat{\boldsymbol{k}}^{l\kappa}(\boldsymbol{y}_{\mathrm{f}}^{\mathrm{m}})$, has the affine form

$$\hat{\boldsymbol{k}}^{l\kappa}(\boldsymbol{y}_{\mathrm{f}}^{\mathrm{m}}) = \mathbf{W}^{l\kappa}\boldsymbol{y}_{\mathrm{f}}^{\mathrm{m}} + \boldsymbol{v}^{l\kappa}, \quad \forall \boldsymbol{y}_{\mathrm{f}}^{\mathrm{m}} \in \mathcal{R}^{l\kappa}(\mathrm{M}_{\mathrm{f}}^{\mathrm{m}}(\boldsymbol{\mathcal{U}}_{\mathrm{f}})), \tag{3.32}$$

where $\mathbf{W}^{l\kappa} \in \mathbb{R}^{|\mathcal{C}|\times|\mathcal{M}|}$ and $\boldsymbol{v}^{l\kappa} \in \mathbb{R}^{|\mathcal{C}|}$ are fixed parameters valid for the critical region $\mathcal{R}^{l\kappa}(\mathrm{M}_{\mathrm{f}}^{\mathrm{m}}(\boldsymbol{\mathcal{U}}_{\mathrm{f}}))$. As before, the parameters $\mathbf{W}^{l\kappa}$, $\boldsymbol{v}^{l\kappa}$, and the critical regions $\mathcal{R}^{l\kappa}(\mathrm{M}_{\mathrm{f}}^{\mathrm{m}}(\boldsymbol{\mathcal{U}}_{\mathrm{f}}))$ can be computed for given κ and for each $l \in \{1, ..., \hat{l}_{\kappa}\}$ by using off-the-shelf optimization software such like MPT. Note that the resulting admissible control law $\boldsymbol{u}_{\mathrm{c}} = \hat{\boldsymbol{k}}(\boldsymbol{y}_{\mathrm{f}}^{\mathrm{m}})$ has a total of $D = \sum_{\kappa=1}^{\hat{\kappa}} \hat{l}_{\kappa}\hat{\kappa}$ affine pieces.

From the above derivations we conclude that the two-stage control law (3.28)–(3.29) is PWA. Moreover, the admissible control law implied by LP (3.22) is also PWA as formulations (3.28)–(3.29) and (3.22) are equivalent. If QCQP (3.27) outputs that there exists an admissible PWA control law, the multiparametric solution of η over $\boldsymbol{y}_{\mathrm{f}}^{\mathrm{m}} \in \mathrm{M}_{\mathrm{f}}^{\mathrm{m}}(\boldsymbol{\mathcal{U}}_{\mathrm{f}})$ always fulfills $\eta \leq 0$, for all $\kappa \in \{1, ..., \hat{\kappa}\}$. In summary, an admissible PWA control law $\boldsymbol{u}_{\mathrm{c}} = \hat{\boldsymbol{k}}(\boldsymbol{y}_{\mathrm{f}}^{\mathrm{m}})$ can be computed offline via the following algorithm.

Compute Closed-form Expression of an Admissible PWA Control Law. Using an off-the-shelf multiparametric linear optimization solver:

1. Compute the closed-form of mapping $\hat{\boldsymbol{z}}(\boldsymbol{y}_{\mathrm{f}}^{\mathrm{m}})$ by solving MPLP (3.28) over $\boldsymbol{y}_{\mathrm{f}}^{\mathrm{m}} \in \mathrm{M}_{\mathrm{f}}^{\mathrm{m}}(\boldsymbol{\mathcal{U}}_{\mathrm{f}})$. This outputs a total of $\hat{\kappa} \geq 1$ CRs of $\mathrm{M}_{\mathrm{f}}^{\mathrm{m}}(\boldsymbol{\mathcal{U}}_{\mathrm{f}})$ with corresponding local parameters $\boldsymbol{\Pi}^{\kappa}$ and $\boldsymbol{r}^{\kappa}$ for the kth affine mapping (3.30), $\kappa \in \{1, ..., \hat{\kappa}\}$.

2. For each $\kappa = 1, ..., \hat{\kappa}$: Compute the mapping $\hat{\boldsymbol{k}}^{l\kappa}(\boldsymbol{y}_{\mathrm{f}}^{\mathrm{m}})$ by solving MPLP (3.31) over $\boldsymbol{y}_{\mathrm{f}}^{\mathrm{m}} \in \mathcal{R}^{\kappa}(\mathrm{M}_{\mathrm{f}}^{\mathrm{m}}(\boldsymbol{\mathcal{U}}_{\mathrm{f}}))$. This yields a total of $\hat{l}_{\kappa} \geq 1$ CRs of $\mathcal{R}^{\kappa}(\mathrm{M}_{\mathrm{f}}^{\mathrm{m}}(\boldsymbol{\mathcal{U}}_{\mathrm{f}}))$ with corresponding local parameters $\mathbf{W}^{l\kappa}$ and $\boldsymbol{v}^{l\kappa}$ for the $l\kappa$th affine mapping (3.32), $l \in \{1, ..., \hat{l}_{\kappa}\}$.

A well-known result in multiparametric programming is that the total number of critical regions may grow exponentially with the dimension of the parameter vector [93]. We therefore recommend the offline computation of the admissible PWA control law only for small-sized problem instances. For larger applications, the efficient online computation techniques proposed above should be utilized.

The example below illustrates the correctness of the proposed algorithm for the computation of the closed-form of PWA admissible control laws.

Example 7. Consider the system defined by

$$\mathbf{A}_\mathrm{c} = \begin{bmatrix} 1 \\ -1 \\ 1 \\ -1 \end{bmatrix}, \quad \mathbf{A}_\mathrm{f} = \begin{bmatrix} 1 & 1 & 1 \\ -1 & 1 & -1 \\ 1 & -1 & -1 \\ 1 & 0 & -0.5 \end{bmatrix}, \quad \boldsymbol{b} = \begin{bmatrix} 3 \\ 1 \\ 1 \\ 1 \end{bmatrix}, \tag{3.33}$$
$$\mathbf{M}_\mathrm{f}^\mathrm{m} = \begin{bmatrix} 1 & -2 & 0.5 \end{bmatrix}, \quad 0 \leq \boldsymbol{u}_\mathrm{c} \leq 0.5, \quad \mathbf{0} \leq \boldsymbol{u}_\mathrm{f} \leq \mathbf{1}.$$

This exemplary system should fulfill four constraints and the uncertainty set $\boldsymbol{\mathcal{U}}_\mathrm{f}$ is a three dimensional cube, i.e., it has eight corners. Moreover, the exogenous actions in $\boldsymbol{\mathcal{U}}_\mathrm{f}$ yield a set of one-dimensional observations $\boldsymbol{y}_\mathrm{f}^\mathrm{m} \in [-2,\ 1.5]$.

After running the QCQP verification algorithm (3.27) we obtain $\eta^\star = 0$, i.e., there exists an admissible PWA control law $\boldsymbol{u}_\mathrm{c} = \hat{\boldsymbol{k}}(\boldsymbol{y}_\mathrm{f}^\mathrm{m})$. Since for this exemplary system the uncertainty set $\boldsymbol{\mathcal{U}}_\mathrm{f}$ has eight corners, we also verify the existence of an admissible control law by applying Theorem 6, cf. Section 2.3. As expected, condition (2.18) is fulfilled.

Now we compute the functions $\hat{z}_j(\boldsymbol{y}_\mathrm{f}^\mathrm{m})$ with $j \in \{1, ..., 4\}$ over all observations $\boldsymbol{y}_\mathrm{f}^\mathrm{m} \in [-2,\ 1.5]$ online by using LP (3.28). The values mapped by $\hat{\boldsymbol{z}}(\boldsymbol{y}_\mathrm{f}^\mathrm{m})$ are depicted in Fig. 3.2 (a). Note that, as expected, the observation-dependent worst-case for each

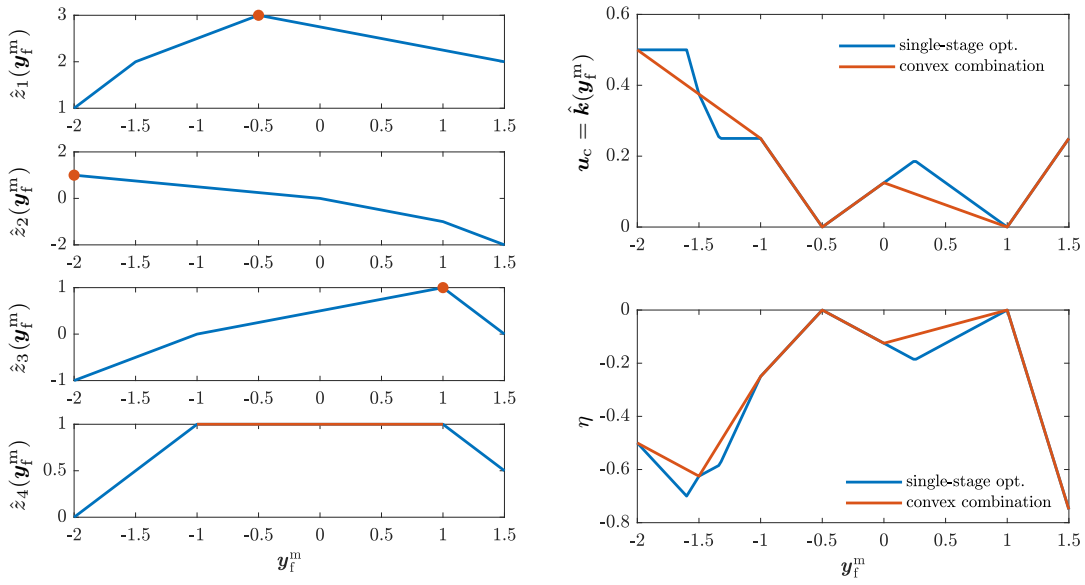

(a) (b)

Figure 3.2: (a) Observation-dependent worst-cases for each constraint of the system (3.33). The maximum impact of $\boldsymbol{u}_\mathrm{f} \in \boldsymbol{\mathcal{U}}_\mathrm{f}$ on each constraint over all observations is highlighted in red. (b) Plots of the single-stage online control law (3.22) (in blue) and the control law (2.19) (in red). Note that both control laws are continous, non-convex, and PWA. As predicted by both QCQP (3.27) and condition (2.18), admissible PWA control laws of the form $\boldsymbol{u}_\mathrm{c} = \hat{\boldsymbol{k}}(\boldsymbol{y}_\mathrm{f}^\mathrm{m})$ exist. This is corroborated experimentally by looking at the value of η over all observations, whose maximum possible value is zero. Observe that the breakpoints of η (interpreted as a function of $\boldsymbol{y}_\mathrm{f}^\mathrm{m}$) do not necessarily occur at observations related to corners of $\boldsymbol{\mathcal{U}}_\mathrm{f}$.

constraint is given by a continuous, concave, piecewise-affine function. In Fig. 3.2 (b) we plot the control laws $\boldsymbol{u}_\mathrm{c} = \hat{\boldsymbol{k}}(\boldsymbol{y}_\mathrm{f}^\mathrm{m})$ resulting from 1) the single-stage LP (3.22) and 2) the control law implied by (2.19), both computed online over all $\boldsymbol{y}_\mathrm{f}^\mathrm{m} \in \mathrm{M}_\mathrm{f}^\mathrm{m}(\boldsymbol{\mathcal{U}}_\mathrm{f})$. As expected, both control laws are continuous (non-convex) piecewise-affine functions of the observation $\boldsymbol{y}_\mathrm{f}^\mathrm{m}$.

For the single-stage control law implied by LP (3.22), we further depict in Fig. 3.2 (b) the behavior of the feasibility indicator η for both admissible PWA control laws. In both cases, the mapping $\boldsymbol{y}_\mathrm{f}^\mathrm{m} \mapsto \eta$ is non-convex, PWA and reaches its maximum value zero for the observations $\boldsymbol{y}_\mathrm{f}^{\mathrm{m}1} = -0.5$ and $\boldsymbol{y}_\mathrm{f}^{\mathrm{m}2} = 1$. Such observations are associated to the corners $\boldsymbol{u}_\mathrm{f}^1 = [1\ 1\ 1]^\mathrm{T}$ and $\boldsymbol{u}_\mathrm{f}^2 = [1\ 0\ 0]^\mathrm{T}$ of $\boldsymbol{\mathcal{U}}_\mathrm{f}$. However, the breakpoints of both mappings $\boldsymbol{u}_\mathrm{c} = \hat{\boldsymbol{k}}(\boldsymbol{y}_\mathrm{f}^\mathrm{m})$ and $\boldsymbol{y}_\mathrm{f}^\mathrm{m} \mapsto \eta$ do not necessary occur at corners of $\boldsymbol{\mathcal{U}}_\mathrm{f}$ in general.

Now we compute the closed-form of the admissible control law $\boldsymbol{u}_\mathrm{c} = \hat{\boldsymbol{k}}(\boldsymbol{y}_\mathrm{f}^\mathrm{m})$ offline by applying the algorithm proposed above. Since the observation $\boldsymbol{y}_\mathrm{f}^\mathrm{m}$ is one-dimensional, the critical regions of $\mathrm{M}_\mathrm{f}^\mathrm{m}(\boldsymbol{\mathcal{U}}_\mathrm{f})$ are one-dimensional intervals. First, we compute the closed-form expression of the PWA mapping $\hat{\boldsymbol{z}}(\boldsymbol{y}_\mathrm{f}^\mathrm{m})$ by using MPT. We obtain

$$\hat{\boldsymbol{z}}^\mathrm{T}(y_\mathrm{f}^\mathrm{m}) = \begin{cases} \begin{bmatrix} 2 & -0.5 & 1 & 1 \end{bmatrix} y_\mathrm{f}^\mathrm{m} + \begin{bmatrix} 5 & 0 & 1 & 2 \end{bmatrix} & \text{if } -2 \leq y_\mathrm{f}^\mathrm{m} \leq -1.5, \\ \begin{bmatrix} 1 & -0.5 & 1 & 1 \end{bmatrix} y_\mathrm{f}^\mathrm{m} + \begin{bmatrix} 3.5 & 0 & 1 & 2 \end{bmatrix} & \text{if } -1.5 \leq y_\mathrm{f}^\mathrm{m} \leq -1, \\ \begin{bmatrix} 1 & -0.5 & 0.5 & 0 \end{bmatrix} y_\mathrm{f}^\mathrm{m} + \begin{bmatrix} 3.5 & 0 & 0.5 & 1 \end{bmatrix} & \text{if } -1 \leq y_\mathrm{f}^\mathrm{m} \leq -0.5, \\ \begin{bmatrix} -0.5 & -0.5 & 0.5 & 0 \end{bmatrix} y_\mathrm{f}^\mathrm{m} + \begin{bmatrix} 2.75 & 0 & 0.5 & 1 \end{bmatrix} & \text{if } -0.5 \leq y_\mathrm{f}^\mathrm{m} \leq 0, \\ \begin{bmatrix} -0.5 & -1 & 0.5 & 0 \end{bmatrix} y_\mathrm{f}^\mathrm{m} + \begin{bmatrix} 2.75 & 0 & 0.5 & 1 \end{bmatrix} & \text{if } 0 \leq y_\mathrm{f}^\mathrm{m} \leq 1, \\ \begin{bmatrix} -0.5 & -2 & -2 & -1 \end{bmatrix} y_\mathrm{f}^\mathrm{m} + \begin{bmatrix} 2.75 & 1 & 3 & 2 \end{bmatrix} & \text{if } 1 \leq y_\mathrm{f}^\mathrm{m} \leq 1.5. \end{cases}$$

The mapping $\tilde{\boldsymbol{z}}(\boldsymbol{y}_\mathrm{f}^\mathrm{m})$ has thus six pieces. For each piece of the function $\hat{\boldsymbol{z}}(\boldsymbol{y}_\mathrm{f}^\mathrm{m})$, we then compute the parametric solution of $\boldsymbol{u}_\mathrm{c} = \hat{\boldsymbol{k}}(\boldsymbol{y}_\mathrm{f}^\mathrm{m})$, also using MPT. We thus obtain the admissible PWA control law

$$\hat{\boldsymbol{k}}(y_{\mathrm{f}}^{\mathrm{m}}) = \begin{cases} \hat{\boldsymbol{k}}^{11}(y_{\mathrm{f}}^{\mathrm{m}}) = 0.5 & \text{if } -2 \leq y_{\mathrm{f}}^{\mathrm{m}} \leq -1.6, \\ \hat{\boldsymbol{k}}^{21}(y_{\mathrm{f}}^{\mathrm{m}}) = -1.25y_{\mathrm{f}}^{\mathrm{m}} - 1.5 & \text{if } -1.6 \leq y_{\mathrm{f}}^{\mathrm{m}} \leq -1.5, \\ \hat{\boldsymbol{k}}^{12}(y_{\mathrm{f}}^{\mathrm{m}}) = -0.75y_{\mathrm{f}}^{\mathrm{m}} - 0.75 & \text{if } -1.5 \leq y_{\mathrm{f}}^{\mathrm{m}} \leq -1.\overline{33}, \\ \hat{\boldsymbol{k}}^{22}(y_{\mathrm{f}}^{\mathrm{m}}) = 0.25 & \text{if } -1.\overline{33} \leq y_{\mathrm{f}}^{\mathrm{m}} \leq -1, \\ \hat{\boldsymbol{k}}^{13}(y_{\mathrm{f}}^{\mathrm{m}}) = -0.5y_{\mathrm{f}}^{\mathrm{m}} - 0.25 & \text{if } -1 \leq y_{\mathrm{f}}^{\mathrm{m}} \leq -0.5, \\ \hat{\boldsymbol{k}}^{14}(y_{\mathrm{f}}^{\mathrm{m}}) = 0.25y_{\mathrm{f}}^{\mathrm{m}} + 0.125 & \text{if } -0.5 \leq y_{\mathrm{f}}^{\mathrm{m}} \leq 0, \\ \hat{\boldsymbol{k}}^{15}(y_{\mathrm{f}}^{\mathrm{m}}) = 0.25y_{\mathrm{f}}^{\mathrm{m}} + 0.125 & \text{if } 0 \leq y_{\mathrm{f}}^{\mathrm{m}} \leq 0.25, \\ \hat{\boldsymbol{k}}^{25}(y_{\mathrm{f}}^{\mathrm{m}}) = -0.25y_{\mathrm{f}}^{\mathrm{m}} + 0.25 & \text{if } 0.25 \leq y_{\mathrm{f}}^{\mathrm{m}} \leq 1, \\ \hat{\boldsymbol{k}}^{16}(y_{\mathrm{f}}^{\mathrm{m}}) = 0.5y_{\mathrm{f}}^{\mathrm{m}} - 0.5 & \text{if } 1 \leq y_{\mathrm{f}}^{\mathrm{m}} \leq 1.5. \end{cases}$$

Observe that for the 3th, 4th, and 6th piece of $\hat{\boldsymbol{z}}(\boldsymbol{y}_{\mathrm{f}}^{\mathrm{m}})$ no additional partitioning of the set $\mathrm{M}_{\mathrm{f}}^{\mathrm{m}}(\boldsymbol{\mathcal{U}}_{\mathrm{f}})$ is required when computing the associated closed-form expression for the control law. Also note that the PWA mappings $\hat{\boldsymbol{z}}(\boldsymbol{y}_{\mathrm{f}}^{\mathrm{m}})$ and $\boldsymbol{u}_{\mathrm{c}} = \hat{\boldsymbol{k}}(\boldsymbol{y}_{\mathrm{f}}^{\mathrm{m}})$ computed offline are identical to the online mappings depicted in Fig. 3.2, respectively.

3.3.3 Summary

In this section, we proposed a set of algorithms that compute admissible PWA control laws $\boldsymbol{u}_{\mathrm{c}} = \hat{\boldsymbol{k}}(\boldsymbol{y}_{\mathrm{f}}^{\mathrm{m}})$, given that their existence has been verified in a priori, and that the sets of control and exogenous actions $(\boldsymbol{\mathcal{U}}_{\mathrm{c}}, \boldsymbol{\mathcal{U}}_{\mathrm{f}})$ are both convex polytopes. In particular, we showed that admissible PWA control laws can be computed efficiently, either online by using LP (3.22) or LPs (3.28)–(3.29), or offline by employing multiparametric linear optimization techniques. The decision of taking the online or the offline approach depends on the problem setting (number of constraints, dimensions of $\boldsymbol{u}_{\mathrm{c}}$, $\boldsymbol{u}_{\mathrm{f}}$, and $\boldsymbol{y}^{\mathrm{m}}$) and the available computing equipment.

3.4 Discussion

Exploiting the theory of admissible control laws for constrained static linear systems presented in Chapter 2, we derived in the present chapter a collection of algorithms that, under some assumptions on the control and exogenous action spaces $\boldsymbol{\mathcal{U}}_{\mathrm{c}}$ and $\boldsymbol{\mathcal{U}}_{\mathrm{f}}$, verify the existence of an admissible control law $\boldsymbol{u}_{\mathrm{c}} = \hat{\boldsymbol{k}}(\boldsymbol{y}_{\mathrm{f}}^{\mathrm{m}})$ in an efficient manner.

We centered particular attention on the existence of admissible affine control laws of the form $\boldsymbol{u}_{\mathrm{c}} = \hat{\mathbf{K}}\boldsymbol{y}_{\mathrm{f}}^{\mathrm{m}} + \hat{\boldsymbol{w}}$, showing that in many cases the verification task is reduced to a convex, finite dimensional feasibility problem. For instance, the feasibility problem turns into a finite dimensional LP if the sets $(\boldsymbol{\mathcal{U}}_{\mathrm{c}}, \boldsymbol{\mathcal{U}}_{\mathrm{f}})$ are both convex polytopes. When the set of exogenous actions $\boldsymbol{\mathcal{U}}_{\mathrm{f}}$ is shaped by a p–norm, the verification task turns in general into a finite dimensional convex feasibility problem solvable via, e.g., interior point methods.

For these specific cases, the solution of the feasibility problem also yields an admissible realization for the control law $\boldsymbol{u}_\mathrm{c} = \hat{\mathbf{K}}\boldsymbol{y}_\mathrm{f}^\mathrm{m} + \hat{\boldsymbol{w}}$ in case one exists. Since the controller parameters $(\hat{\mathbf{K}}, \hat{\boldsymbol{w}})$ can be computed prior to the implementation of the controller, computing the control action $\boldsymbol{u}_\mathrm{c}$ via an admissible affine control law is straightforward and very efficient in practical applications.

For those problem instances where an admissible affine control law of the form $\boldsymbol{u}_\mathrm{c} = \hat{\mathbf{K}}\boldsymbol{y}_\mathrm{f}^\mathrm{m} + \hat{\boldsymbol{w}}$ is impossible, the existence of an admissible control law $\boldsymbol{u}_\mathrm{c} = \hat{\boldsymbol{k}}(\boldsymbol{y}_\mathrm{f}^\mathrm{m})$ of arbitrary form should be verified. While this verification task turns in general into a challenging infinite dimensional feasibility problem, we still can verify the existence of admissible PWA affine control laws by solving a non-convex QCQP for those cases where the sets $(\mathcal{U}_\mathrm{c}, \mathcal{U}_\mathrm{f})$ are convex polytopes. This particular class of admissible control laws are computable either online as linear programs, or offline by solving a two-stage multiparametric linear optimization problem. Since the number of pieces of the resulting control law grows in general exponentially with the dimension of the exogenous action $\boldsymbol{u}_\mathrm{f}$, computing the closed-form expression for the PWA control law is recommended only for small- and medium-sized problem instances depending on the computing equipment.

The verification and computation algorithms derived in this chapter are summarized in Figs. 3.3 and 3.4, respectively.

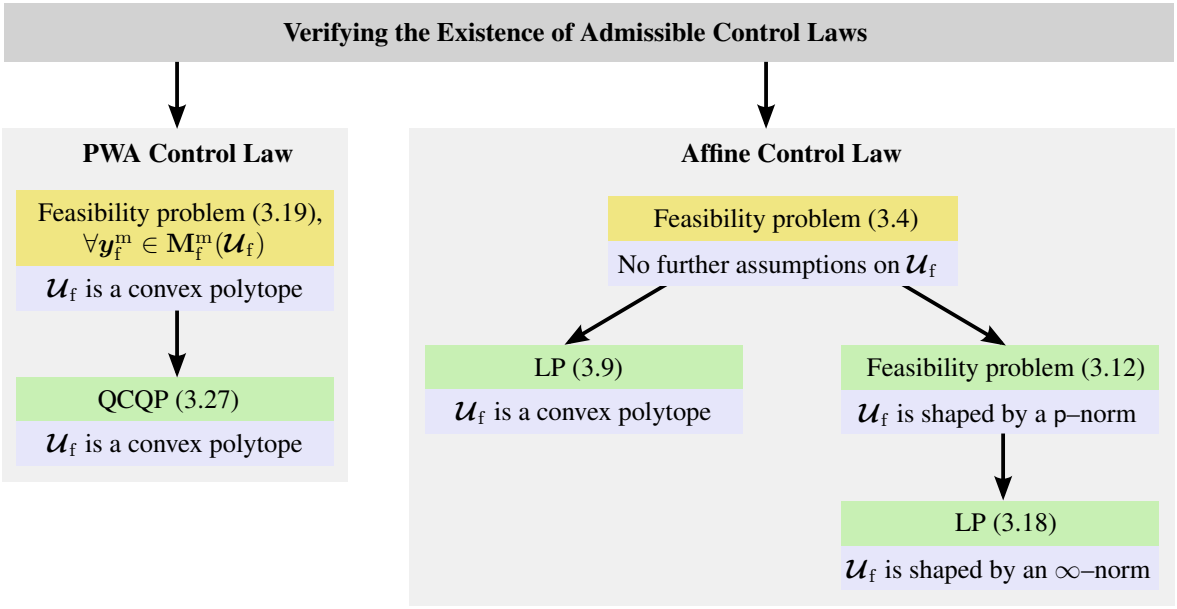

Figure 3.3: Algorithms for verifying the existence of admissible control laws of the form $\boldsymbol{u}_\mathrm{c} = \hat{\boldsymbol{k}}(\boldsymbol{y}_\mathrm{f}^\mathrm{m})$ under particular assumptions on the shape of the uncertainty set $\mathcal{U}_\mathrm{f}$. For all algorithms, it is supposed that the action space $\mathcal{U}_\mathrm{c}$ is a convex polytope. Algorithms colored in yellow/green correspond to infinite/finite dimensional feasibility problems, respectively.

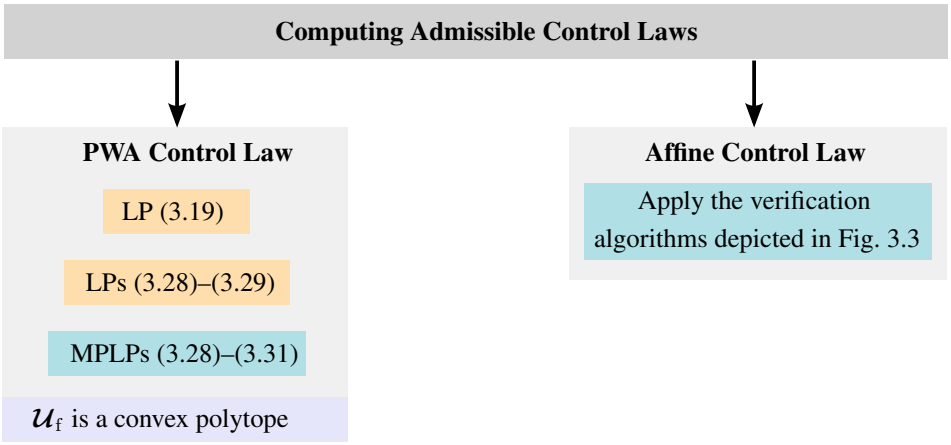

Figure 3.4: Algorithms for computing admissible control laws of the form $\boldsymbol{u}_\mathrm{c} = \hat{\boldsymbol{k}}(\boldsymbol{y}_\mathrm{f}^\mathrm{m})$ under particular assumptions on the shape of the uncertainty set $\mathcal{U}_\mathrm{f}$. For all algorithms, it is supposed that the action space $\mathcal{U}_\mathrm{c}$ is a convex polytope. Algorithms colored in blue/orange correspond to offline/online approaches, respectively.

4 Minimal Admissible Sets of Actuators and Sensors

Equipped with the theory of admissible control laws proposed in Chapter 2 together with the verification algorithms derived in Chapter 3, the present chapter addresses the task of finding the smallest possible number of actuators and sensors that guarantee the existence of an admissible control law. Although this combinatorial minimization task is computationally challenging, we show that lower and upper bounds for the minimal admissible sets $(\mathcal{C}, \mathcal{M})$ can in some special cases be found by employing mixed-integer linear optimization techniques. For the general case, we also propose a greedy optimization approach based on hill climbing optimization.

So far we investigated how to verify the existence of admissible control laws for cases where the actuator and sensor sets $(\mathcal{C}, \mathcal{M})$ are known. However, what is to be done if an admissible control law is impossible for such actuator and sensor sets? The natural answer to this question is to increase the degrees of freedom of the controller until the existence of an admissible control law is guaranteed. To this end, the elements in the sensor set $\mathcal{M}$ and/or the actuator set $\mathcal{C}$ have to be adapted based on the expertise of the practitioner, a heuristic rule, or (as proposed in this chapter) the solution of an optimization problem.

Without loss of generality, this chapter aims at finding the minimal admissible sets $(\mathcal{C}, \mathcal{M})$, i.e., the smallest number of actuators and sensors for which the existence of an admissible control law is guaranteed. After commenting on the relevance of finding the minimal sets $(\mathcal{C}, \mathcal{M})$ in power system applications, we propose a set of algorithms that compute (lower and upper bounds for) them. The proposed algorithms are derived from the theory and verification algorithms introduced in Chapters 2 and 3.

Relevance in Power Flow Control

In power networks, volatile renewable energies are transforming classical power grids with few large generators into complex cyber-physical networks. These contain a large number of distributed generators and controllable loads, and power lines are often operated close to their limits. In this context, what is the smallest set of generators and/or

loads that must be controlled based on the values of a minimal number of measurements, such that the entire system state is feasible for all possible values of the remaining elements?

Being able to identify the (optimally small) set of critical elements in complex power grids reduces the cost and effort for their control. Moreover, it is an important ingredient to reduce such systems' potentially high vulnerability with respect to natural disasters or cyber-attacks [102], enhancing their operational resilience. An increased protection status could be mandated for the identified critical elements, to keep the number of outages and failures in this group at a minimum, see [103] where the hardening of power systems to minimize system damage in case of disasters is examined.

Existing Approaches

The question on finding the minimal admissible sets $(\mathcal{C}, \mathcal{M})$ is an instance of the well-known optimal input/output selection problem, also known as the optimal actuator/sensor placement problem. Starting with classical work on controllability [87] this problem has attracted long-term research attention, in particular, for linear time-invariant dynamic systems. The problem has recently become very active again in the study of complex networks, see, e.g., [104]. While most formulations of the problem are NP-Hard due to its combinatorial nature, finding only the minimum set of actuators is possible in polynomial-time [57]. This finding is based on structural controllability theory [105] and can be used to develop distributed algorithms for finding the minimum number of controlled and measured nodes [104].

Structural controllability theory can also be used to analyze cyber-security aspects in distributed power grids [12], e.g., for evaluating the detectability and identifiability of hacked nodes. Another line of research aims at designing control structures that minimize the control effort, using controllability metrics derived from the controllability Gramian of the system [60]. Many of the related input/ouput selection problems are submodular which implies that greedy algorithms using these metrics, e.g., for the optimal placement of High-Voltage direct current lines in a simplified model of the European power transmission network, have provable suboptimality bounds [62]. Time-varying minimal configurations of sensors and actuators can be computed with the help of semi-definite programming [66].

Another research venue aims at the synthesis of sparsity-promoting static state feedback control laws for unconstrained LTI systems [67, 106, 107, 69]. The idea is to use ℓ_1-norm approximations to determine a gain matrix with sparse structure (i.e., a large number of zero entries). An upper bound for the minimal number of actuators is thus determined by the total number of rows of the gain matrix having at least one non-zero entry.

The above related works are valid for linear (dynamic, algebraic) systems without state or input/output restrictions. In this chapter, we propose an alternative, novel approach based on the steady state representation of the system only, but considering constrained variables.

4.1 Formulation of the Minimization Problem

Consider a constrained static linear system (2.1) given in terms of the action $\boldsymbol{u} \in \mathbb{R}^{n_u}$, the (possible) observation $\boldsymbol{y} \in \mathbb{R}^{n_y}$ and known parameters $(\mathbf{A}, \boldsymbol{b}, \mathrm{M}, \boldsymbol{\mathcal{U}})$. As explained in Chapter 2, the actuator and sensor sets $(\mathcal{C}, \mathcal{M})$ determine those entries of $\boldsymbol{u}$ and $\boldsymbol{y}$ which are accessible to the controller and can be used to compute an admissible control law. In the following, we make the key assumption that each dimension of the action $\boldsymbol{u} \in \boldsymbol{\mathcal{U}}$ belongs to an interval-bounded set. The action space $\boldsymbol{\mathcal{U}}$ is thus a hypercube (also known as Cartesian product of intervals or ∞-norm-shaped set).

Assumption 3. $\boldsymbol{\mathcal{U}} = \boldsymbol{\mathcal{U}}_{\mathrm{c}} \times \boldsymbol{\mathcal{U}}_{\mathrm{f}}$, where

$$\boldsymbol{\mathcal{U}}_{\mathrm{c}} = \{\boldsymbol{u}_{\mathrm{c}} \in \mathbb{R}^{|\mathcal{C}|} : \underline{\boldsymbol{u}}_{\mathrm{c}} \leq \boldsymbol{u}_{\mathrm{c}} \leq \overline{\boldsymbol{u}}_{\mathrm{c}}\}, \quad \boldsymbol{\mathcal{U}}_{\mathrm{f}} = \{\boldsymbol{u}_{\mathrm{f}} \in \mathbb{R}^{n_u - |\mathcal{C}|} : \underline{\boldsymbol{u}}_{\mathrm{f}} \leq \boldsymbol{u}_{\mathrm{f}} \leq \overline{\boldsymbol{u}}_{\mathrm{f}}\},$$

$\underline{\boldsymbol{u}}_{\mathrm{c}}, \overline{\boldsymbol{u}}_{\mathrm{c}} \in \mathbb{R}^{|\mathcal{C}|}$ and $\underline{\boldsymbol{u}}_{\mathrm{f}}, \overline{\boldsymbol{u}}_{\mathrm{f}} \in \mathbb{R}^{n_u - |\mathcal{C}|}$ are the lower and upper bounds of vectors $\boldsymbol{u}_{\mathrm{c}}$ and $\boldsymbol{u}_{\mathrm{f}}$, respectively.

Assumption 3 ensures consistency during the partitioning of $\boldsymbol{u}$ into the control $\boldsymbol{u}_{\mathrm{c}}$ and exogenous action $\boldsymbol{u}_{\mathrm{f}}$ in the algorithms below. With this in mind, the optimization task we aim to solve in this chapter reads as follows.

Problem 1. Find the set of actuators $\mathcal{C}$ and sensors $\mathcal{M}$ that solves

$$\begin{aligned} &\min_{\mathcal{C},\mathcal{M}} \ |\mathcal{C}| + \gamma|\mathcal{M}| \\ &\text{s.t. } \mathcal{C} \text{ and } \mathcal{M} \text{ are admissible,} \\ &\quad \mathcal{C} \subseteq \{1, ..., n_u\}, \\ &\quad \mathcal{M} \subseteq \{1, ..., n_y\}. \end{aligned}$$

The cost of placing a sensor is weighted by $0 \leq \gamma \leq 1$ since it will typically be smaller than implementing a full actuator. One could additionally incorporate into the objective the varying efforts and costs for controlling certain elements or acquiring certain measurements. Instead of just weighting the total number of actuators and sensors, one would then determine an individual weight for each element separately. While this idea is not developed below, all algorithms could straightforwardly be adapted.

Remark 6. The solution of Problem 1 also outputs the entries of $\boldsymbol{u}$ to be considered as exogenous actions. This is because the dimensions of both the control action $\boldsymbol{u}_{\mathrm{c}} \in \mathbb{R}^{|\mathcal{C}|}$ and the exogenous action $\boldsymbol{u}_{\mathrm{f}} \in \mathbb{R}^{n_u - |\mathcal{C}|}$ are complementary.

Remark 7. Particularly in large scale applications, there may be several constraints, i.e., rows of $\mathbf{A}$ and corresponding entries of $\boldsymbol{b}$, that are not violated for any realization of $\boldsymbol{u}$. Hence, our optimization techniques only take into account those rows of $\mathbf{A}$ for which a violation of $\mathbf{A}\boldsymbol{u} \leq \boldsymbol{b}$ is possible.

In this thesis, we propose two optimization approaches for addressing Problem 1, namely mixed-integer linear optimization and hill climbing optimization. The former approach consist of re-expressing Problem 1 as MILP, which is possible under some assumptions as we discuss subsequently. The latter approach iteratively verifies the existence of an admissible control law for a fixed instance of $(\mathcal{C}, \mathcal{M})$ and adapt it until a (local) minimum for the objective function of Problem 1 is reached. A more detailed introduction of the approaches is provided next.

Mixed-integer Linear Optimization Approaches. We show that Problem 1 can be reformulated as a mixed-integer linear program derived from Corollary 5, i.e., the control law is assumed to be an affine mapping. Since the existence of an admissible control law of arbitrary form does in general not imply the existence of an admissible affine control law, the resulting minimal actuator and sensor sets will be potentially too large but guaranteed to be admissible. In the case of admissible PWA control laws, we found that condition (2.21) can be exploited to derive a MILP formulation of Problem 1 for the special case where the matrix of possible observations $\mathbf{M}$ is the identity matrix, $\boldsymbol{y} = \boldsymbol{u}$. By recalling that verifying condition (2.21) is not sufficient to conclude about the existence of an admissible control law, the obtained minimal sets $(\mathcal{C}, \mathcal{M})$ will be potentially too small to be admissible. However, we verified experimentally that minimal admissible sets are obtained in many cases. Although condition (2.21) does not provide any guarantee about the admissibility of $\mathcal{C}$ and $\mathcal{M}$, the resulting minimal sets can be used as a starting point for the following optimization approach.

Hill Climbing Approaches. Instead of trying to formulate Problem 1 as a mixed-integer linear optimization problem, we can solve Problem 1 using a local search optimization approach. The approach we propose in the following has two routines, a mean routine and a subroutine. The mean routine fixes the values of $\mathcal{C}$ and $\mathcal{M}$ for which the existence of an admissible control law is to be verified by the subroutine. It also adapts the actuator and sensor sets until an at least locally minimal solution for Problem 1 is obtained. The adaptation process can be designed based on a problem-specific heuristic. On the other hand, the subroutine verifies the existence of an admissible control law for a fixed instance of $(\mathcal{C}, \mathcal{M})$ by running one of the finite dimensional feasibility problems proposed in Chapter 3. Although alternative heuristic optimization techniques based on evolutionary algorithms [108], e.g., particle swarm optimization, could be utilized for addressing Problem 1, in this thesis we focus on hill climbing optimization approaches [109] only.

Let us now describe the obtained algorithms in detail.

4.2 Mixed-integer Linear Optimization Approaches

In the following formulations, we consider the binary decision variables $\boldsymbol{v}_{\mathrm{c}} \in \{0,1\}^{n_u}$ and $\boldsymbol{v}_{\mathrm{m}} \in \{0,1\}^{n_y}$ defined element-wise as

$$v_{\mathrm{c}j} = \begin{cases} 1 & j \in \mathcal{C} \\ 0 & \text{else} \end{cases}, \; v_{\mathrm{m}k} = \begin{cases} 1 & k \in \mathcal{M} \\ 0 & \text{else} \end{cases},$$

for all $j \in \{1, ..., n_u\}$ and $k \in \{1, ..., n_y\}$. The decision variables $\boldsymbol{v}_{\mathrm{c}}$ and $\boldsymbol{v}_{\mathrm{m}}$ encode the indices of the entries of $\boldsymbol{u}$ belonging to $\mathcal{C}$ and the of $\boldsymbol{y}$ belonging to $\mathcal{M}$, respectively. Thus, finding the minimal actuator and sensor sets $\mathcal{C}$ and $\mathcal{M}$ is equivalent to minimizing the cost $\mathbf{1}^{\mathrm{T}}\boldsymbol{v}_{\mathrm{c}} + \gamma \mathbf{1}^{\mathrm{T}}\boldsymbol{v}_{\mathrm{m}}$.

4.2.1 Admissible Affine Control Law

As explained in Section 3.1, verifying the existence of an admissible affine control law $\boldsymbol{u}_{\mathrm{c}} = \hat{\mathbf{K}}\boldsymbol{y}_{\mathrm{f}}^{\mathrm{m}} + \hat{\boldsymbol{w}}$ can be tested in an efficient manner via LP (3.18) if $\boldsymbol{\mathcal{U}}$ is a hypercube. This finite dimensional LP is now exploited to derive a mixed-integer linear formulation that finds a suboptimal solution to Problem 1. Recalling that the existence of an admissible control law of arbitrary form does not imply the existence of an admissible affine control law, the obtained minimal sets $(\mathcal{C}, \mathcal{M})$ may be possibly too large, but are guaranteed to be admissible.

Now let $\tilde{\boldsymbol{u}}_{\mathrm{c}}, \tilde{\boldsymbol{u}}_{\mathrm{f}} \in \mathbb{R}^{n_u}$ be vectors encoding the partitions of $\boldsymbol{u}$ associated to the control action $\boldsymbol{u}_{\mathrm{c}}$ and the exogenous action $\boldsymbol{u}_{\mathrm{f}}$, i.e., for $j \in \{1, ..., n_u\}$,

$$\tilde{u}_{\mathrm{c}j} = \begin{cases} u_j & j \in \mathcal{C} \\ 0 & \text{else} \end{cases}, \; \tilde{u}_{\mathrm{f}j} = \begin{cases} u_j & j \notin \mathcal{C} \\ 0 & \text{else} \end{cases}.$$

The key for obtaining a MILP that solves Problem 1 is the introduction of a fictitious affine control law

$$\tilde{\boldsymbol{u}}_{\mathrm{c}} = \hat{\mathbf{K}}\mathbf{M}\tilde{\boldsymbol{u}}_{\mathrm{f}} + \hat{\mathbf{w}}, \tag{4.1}$$

where the structure (rows and columns) of the parameters $\hat{\mathbf{K}} \in \mathbb{R}^{n_u \times n_y}$ and $\hat{\mathbf{w}} \in \mathbb{R}^{n_u}$ is determined by the value of $\boldsymbol{v}_{\mathrm{c}}$ and $\boldsymbol{v}_{\mathrm{m}}$ according to the following conditions:

1. If u_j is chosen as an exogenous action, i.e., $v_{\mathrm{c}j} = 0$, then the jth row of both $\hat{\mathbf{K}}$ and $\hat{\mathbf{w}}$ is zero.

2. If y_k is chosen as an unmeasured output, i.e., $v_{\mathrm{m}k} = 0$, then the kth column $\hat{\mathbf{K}}$ is zero.

3. If both $v_{\mathrm{c}j} = 1$ and $u_{\mathrm{m}k} = 1$, then suitable values for the entries $\hat{\mathsf{K}}_{jk}$ and $\hat{\mathsf{w}}_j$ are to be found.

Observe that for fixed $\boldsymbol{v}_{\mathrm{c}}$ and $\boldsymbol{v}_{\mathrm{m}}$ we can obtain the parameters $\hat{\mathbf{K}} \in \mathbb{R}^{|\mathcal{C}|\times|\mathcal{M}|}$ and $\hat{\boldsymbol{w}} \in \mathbb{R}^{|\mathcal{C}|}$ of the affine control law $\boldsymbol{u}_{\mathrm{c}} = \hat{\mathbf{K}}\boldsymbol{y}_{\mathrm{f}}^{\mathrm{m}} + \hat{\boldsymbol{w}}$ by extracting those columns and rows of $\hat{\mathbf{K}}$ and $\hat{\mathbf{w}}$ for which both $v_{\mathrm{c}j} = 1$ and $u_{\mathrm{m},k} = 1$ hold.

The above conditions on the structure of the controller parameters can be modeled as a set of linear inequalities as we show next.

Structural Constraints. Denote by $\hat{\mathbf{K}}_{j\cdot}$ the jth row of $\hat{\mathbf{K}}$ and by $\hat{\mathbf{K}}_{\cdot k}$ its kth column. By noting that the entry $\hat{\mathsf{K}}_{jk}$ is selected only if both $v_{\mathrm{c}j} = 1$ and $v_{\mathrm{c}j} = 1$ hold simultaneously, we obtain the linear constraints

$$\begin{aligned} \underline{\mathbf{K}}_{\cdot k} \circ \boldsymbol{v}_{\mathrm{c}} \leq \hat{\mathbf{K}}_{\cdot k} \leq \overline{\mathbf{K}}_{\cdot k} \circ \boldsymbol{v}_{\mathrm{c}}, \quad \forall k \in \{1, ..., n_y\}, \\ \underline{\mathbf{K}}_{j\cdot} \circ \boldsymbol{v}_{\mathrm{m}}^{\mathrm{T}} \leq \hat{\mathbf{K}}_{j\cdot} \leq \overline{\mathbf{K}}_{j\cdot} \circ \boldsymbol{v}_{\mathrm{m}}^{\mathrm{T}}, \quad \forall j \in \{1, ..., n_u\}, \end{aligned} \tag{4.2}$$

where the operator $\circ$ denotes the Hadamard product.[1] The parameters $\underline{\mathbf{K}}_{\cdot k}, \overline{\mathbf{K}}_{\cdot k}, \underline{\mathbf{K}}_{j\cdot}, \overline{\mathbf{K}}_{j\cdot}$ have to be chosen *suitably* according to the problem specifications. Similarly, the entries of the vector $\hat{\mathbf{w}}$ associated to the exogenous action have to be zero, which results in

$$\underline{\boldsymbol{w}} \circ \boldsymbol{v}_{\mathrm{c}} \leq \hat{\mathbf{w}} \leq \overline{\boldsymbol{w}} \circ \boldsymbol{v}_{\mathrm{c}}, \tag{4.3}$$

with suitably chosen parameters $\underline{\boldsymbol{w}}$ and $\overline{\boldsymbol{w}}$.

Admissibility Constraints. The affine control law (4.1) has to fulfill the constraints of the system for all possible realizations of the exogenous actions, i.e.,

$$\begin{aligned} \mathbf{A}(\hat{\mathbf{K}}\mathbf{M}\tilde{\boldsymbol{u}}_{\mathrm{f}} + \hat{\mathbf{w}} + \tilde{\boldsymbol{u}}_{\mathrm{f}}) \leq \boldsymbol{b}, \quad \forall \tilde{\boldsymbol{u}}_{\mathrm{f}} \in \tilde{\boldsymbol{\mathcal{U}}}_{\mathrm{f}}(\boldsymbol{v}_{\mathrm{c}}), \\ \underline{\boldsymbol{u}} \circ \boldsymbol{v}_{\mathrm{c}} \leq \hat{\mathbf{K}}\mathbf{M}\tilde{\boldsymbol{u}}_{\mathrm{f}} + \hat{\mathbf{w}} \leq \overline{\boldsymbol{u}} \circ \boldsymbol{v}_{\mathrm{c}}, \quad \forall \tilde{\boldsymbol{u}}_{\mathrm{f}} \in \tilde{\boldsymbol{\mathcal{U}}}_{\mathrm{f}}(\boldsymbol{v}_{\mathrm{c}}), \end{aligned} \tag{4.4}$$

where $\tilde{\boldsymbol{\mathcal{U}}}_{\mathrm{f}}(\boldsymbol{v}_{\mathrm{c}}) = \{\tilde{\boldsymbol{u}}_{\mathrm{f}} \in \mathbb{R}^{n_u} : \underline{\boldsymbol{u}} \circ (\mathbf{1} - \boldsymbol{v}_{\mathrm{c}}) \leq \tilde{\boldsymbol{u}}_{\mathrm{f}} \leq \overline{\boldsymbol{u}} \circ (\mathbf{1} - \boldsymbol{v}_{\mathrm{c}})\}$. Note that the above expressions can be written compactly as

$$\tilde{\mathbf{A}}(\hat{\mathbf{K}})\tilde{\boldsymbol{u}}_{\mathrm{f}} + \tilde{\mathbf{A}}_{\mathrm{c}}\hat{\mathbf{w}} \leq \tilde{\boldsymbol{b}}(\boldsymbol{v}_{\mathrm{c}}), \quad \forall \tilde{\boldsymbol{u}}_{\mathrm{f}} \in \tilde{\boldsymbol{\mathcal{U}}}_{\mathrm{f}}(\boldsymbol{v}_{\mathrm{c}}), \tag{4.5}$$

with

$$\begin{aligned} \tilde{\mathbf{A}}(\hat{\mathbf{K}}) &= \tilde{\mathbf{A}}_{\mathrm{c}}\hat{\mathbf{K}}\mathbf{M} + \tilde{\mathbf{A}}_{\mathrm{f}}, \\ \tilde{\mathbf{A}}_{\mathrm{c}} &= \begin{bmatrix} \mathbf{A} \\ \mathbf{I} \\ -\mathbf{I} \end{bmatrix}, \quad \tilde{\mathbf{A}}_{\mathrm{f}} = \begin{bmatrix} \mathbf{A} \\ \mathbf{0} \\ \mathbf{0} \end{bmatrix}, \quad \tilde{\boldsymbol{b}}(\boldsymbol{v}_{\mathrm{c}}) = \begin{bmatrix} \boldsymbol{b} \\ \overline{\boldsymbol{u}} \circ \boldsymbol{v}_{\mathrm{c}} \\ -\underline{\boldsymbol{u}} \circ \boldsymbol{v}_{\mathrm{c}} \end{bmatrix}. \end{aligned} \tag{4.6}$$

[1] For two vectors $\boldsymbol{x}, \boldsymbol{y} \in \mathbb{R}^d$, the Hadamard product, also known as the element-wise product, is a map from $\mathbb{R}^d$ to $\mathbb{R}^d$ defined element-wise by $(\boldsymbol{x} \circ \boldsymbol{y})_i = x_i y_i$.

To reduce the expression (4.5) to a finite set of linear inequalities, we now apply the technique explained in Section 3.1.3 for interval-bounded uncertainty sets, i.e., we replace the term $\tilde{\mathbf{A}}(\hat{\mathbf{K}})\tilde{\boldsymbol{u}}_{\mathrm{f}}$ with the tight upper bound $\tilde{\mathbf{H}}\,\mathbf{1}$ that covers all worst-case realizations of $\tilde{\boldsymbol{u}}_{\mathrm{f}} \in \tilde{\boldsymbol{\mathcal{U}}}_{\mathrm{f}}(\boldsymbol{v}_{\mathrm{c}})$. The ijth entry of the matrix $\tilde{\mathbf{H}} \in \mathbb{R}^{(n_z+2n_u)\times n_u}$ has to be chosen such that it is zero if the jth entry of $\boldsymbol{u}$ is selected as a control action. Otherwise u_j is an exogenous action and $\tilde{H}_{ij} = \max(\tilde{A}_{ij}(\hat{\mathbf{K}})\underline{u}_j, \tilde{A}_{ij}(\hat{\mathbf{K}})\overline{u}_j)$ should hold according to (3.16). These constraints on $\tilde{H}_{ij}$ can be modeled via the linear inequalities

$$\begin{aligned} -\Pi_{ij}(1-v_{\mathrm{c}j}) \le \tilde{H}_{ij} \le \Pi_{ij}(1-v_{\mathrm{c}j}),\ \forall i \in \{1,...,n_z+2n_u\},\ \forall j \in \{1,...,n_u\},\\ \tilde{H}_{ij} \ge \tilde{A}_{ij}(\hat{\mathbf{K}})\overline{u}_j - \Pi_{ij}v_{\mathrm{c}j},\ \forall i \in \{1,...,n_z+2n_u\},\ \forall j \in \{1,...,n_u\},\\ \tilde{H}_{ij} \ge \tilde{A}_{ij}(\hat{\mathbf{K}})\underline{u}_j - \Pi_{ij}v_{\mathrm{c}j},\ \forall i \in \{1,...,n_z+2n_u\},\ \forall j \in \{1,...,n_u\}. \end{aligned} \tag{4.7}$$

were Π_{ij} is a *sufficiently large* positive constant. Inequalities (4.5) can thus be replaced with both (4.7) and

$$\tilde{\mathbf{H}}\mathbf{1} + \tilde{\mathbf{A}}_{\mathrm{c}}\hat{\mathbf{w}} \le \tilde{\boldsymbol{b}}(\boldsymbol{v}_{\mathrm{c}}). \tag{4.8}$$

Summarizing, inequalities (4.2), (4.3), (4.6), (4.7), and (4.8) allow us to find the minimal admissible sets of actuators and sensors by solving the MILP

$$\begin{aligned} \min_{\substack{\boldsymbol{v}_{\mathrm{c}},\boldsymbol{v}_{\mathrm{m}},\\ \hat{\mathbf{K}},\tilde{\mathbf{H}},\hat{\mathbf{w}}}}\ & \mathbf{1}^{\mathrm{T}}\boldsymbol{v}_{\mathrm{c}} + \gamma\mathbf{1}^{\mathrm{T}}\boldsymbol{v}_{\mathrm{m}} \\ \text{s.t. } & \tilde{\mathbf{H}}\mathbf{1} + \tilde{\mathbf{A}}_{\mathrm{c}}\hat{\mathbf{w}} \le \tilde{\boldsymbol{b}}, \\ & \Pi_{ij}(1-v_{\mathrm{c}j}) \le \tilde{H}_{ij} \le \Pi_{ij}(1-v_{\mathrm{c}j}), \quad \forall i \in \{1,...,n_z+2n_u\}, \forall j \in \{1,...,n_u\}, \\ & \tilde{H}_{ij} \ge \tilde{A}_{ij}(\hat{\mathbf{K}})\overline{u}_j - \Pi_{ij}v_{\mathrm{c}j}, \quad \forall i \in \{1,...,n_z+2n_u\}, \forall j \in \{1,...,n_u\}, \\ & \tilde{H}_{ij} \ge \tilde{A}_{ij}(\hat{\mathbf{K}})\underline{u}_j - \Pi_{ij}v_{\mathrm{c}j}, \quad \forall i \in \{1,...,n_z+2n_u\}, \forall j \in \{1,...,n_u\}, \\ & \underline{\mathbf{K}}_{\cdot k} \circ \boldsymbol{v}_{\mathrm{c}} \le \hat{\mathbf{K}}_{\cdot k} \le \overline{\mathbf{K}}_{\cdot k} \circ \boldsymbol{v}_{\mathrm{c}}, \quad \forall k \in \{1,...,n_y\}, \\ & \underline{\mathbf{K}}_{j\cdot} \circ \boldsymbol{v}_{\mathrm{m}}^{\mathrm{T}} \le \hat{\mathbf{K}}_{j\cdot} \le \overline{\mathbf{K}}_{j\cdot} \circ \boldsymbol{v}_{\mathrm{m}}^{\mathrm{T}}, \quad \forall j \in \{1,...,n_u\}, \\ & \underline{\boldsymbol{w}} \circ \boldsymbol{v}_{\mathrm{c}} \le \hat{\mathbf{w}} \le \overline{\boldsymbol{w}} \circ \boldsymbol{v}_{\mathrm{c}}, \\ & \boldsymbol{v}_{\mathrm{c}} \in \{0,1\}^{n_u}, \quad \boldsymbol{v}_{\mathrm{m}} \in \{0,1\}^{n_y}, \\ & \hat{\mathbf{K}} \in \mathbb{R}^{n_u\times n_y}, \quad \hat{\mathbf{w}} \in \mathbb{R}^{n_u}, \quad \tilde{\mathbf{H}} \in \mathbb{R}^{(n_z+2n_u)\times n_u}. \end{aligned} \tag{4.9}$$

After solving MILP (4.9), the parameters of the resulting minimal admissible affine control law $\boldsymbol{u}_{\mathrm{c}} = \hat{\mathbf{K}}\boldsymbol{y}_{\mathrm{f}}^{\mathrm{m}} + \hat{\boldsymbol{w}}$ are obtained by taking those partitions of $\hat{\mathbf{K}}$ and $\hat{\mathbf{w}}$ selected by the optimal values of $\boldsymbol{v}_{\mathrm{c}}$ and $\boldsymbol{v}_{\mathrm{m}}$. Such admissible affine control law can be implemented either by bringing the control law $\boldsymbol{u}_{\mathrm{c}} = \hat{\mathbf{K}}\boldsymbol{y}_{\mathrm{f}}^{\mathrm{m}} + \hat{\boldsymbol{w}}$ into the form $\boldsymbol{u}_{\mathrm{c}} = \mathbf{K}\boldsymbol{y}^{\mathrm{m}} + \boldsymbol{w}$ via equations (2.22), or by pre-computing $\boldsymbol{y}_{\mathrm{f}}^{\mathrm{m}} = \boldsymbol{y}^{\mathrm{m}} - \mathbf{M}_{\mathrm{c}}^{\mathrm{m}}\boldsymbol{u}_{\mathrm{c}}$ using the previous value of $\boldsymbol{u}_{\mathrm{c}}$.

The proposed MILP involves the introduction of the variable $\tilde{\mathbf{H}}$ together with a total of $(n_z + 2n_u)n_u$ auxiliary constraints that model the worst-case realizations of $\boldsymbol{u}_{\mathrm{f}}$. This

issue combined with the additional constraints on the structure of $\hat{\mathbf{K}}$ and $\hat{\mathbf{w}}$ make the implementation of MILP (4.9) only applicable to small to medium problem instances.

4.2.2 Admissible PWA Control Law

Contrary to MILP (4.9), which is derived by assuming an affine form for the control law, we derive in this section a MILP that, by exploiting condition (2.21), finds a lower bound solution for the smallest admissible sets $\mathcal{C}$ and $\mathcal{M}$. Note that this condition does not involve any assumption about the structure of the control law. However, the set $\boldsymbol{\mathcal{U}}$ is a hypercube (a convex polytope), which means that the minimal admissible sets $(\mathcal{C}, \mathcal{M})$ allow for the existence of an admissible PWA control law computable by using the tools proposed in Chapter 3.

In the following, we make the key assumption that the matrix of possible observations $\mathbf{M} \in \mathbb{R}^{n_u \times n_u}$ is the identity matrix, i.e., $\boldsymbol{y} = \boldsymbol{u}$. Note that, for this particular case, the binary decision variables $\boldsymbol{v}_\mathrm{c}$ and $\boldsymbol{v}_\mathrm{m}$ have the same dimension n_u. This assumption thus allows us to select which entries of $\boldsymbol{u}$ are to be chosen as control actions, observed exogenous actions, and unobserved exogenous actions.

The key for deriving the MILP algorithm is to formulate condition (2.21) as a set of linear inequalities that holds for all choices of sets $\mathcal{C}$ and $\mathcal{M}$. To this end, let $\tilde{\boldsymbol{u}}^i \in \boldsymbol{\mathcal{U}}$ with $i \in \{1, ..., n_z\}$, be defined element-wise as

$$\tilde{u}^i_j = \begin{cases} \overline{u}_j & \text{if } A_{ij} \geq 0 \\ \underline{u}_j & \text{if else} \end{cases}.$$

In other words, $\tilde{\boldsymbol{u}}^i$ solves, for each $i \in \{1, ..., n_z\}$

$$\max_{\underline{\boldsymbol{u}}_\mathrm{f} \leq \boldsymbol{u}_\mathrm{f} \leq \overline{\boldsymbol{u}}_\mathrm{f}} \mathbf{A}^i_\mathrm{f} \boldsymbol{u}_\mathrm{f}$$

for the case when all entries of $\boldsymbol{u}$ are assumed to be exogenous actions. Moreover, for any given set of actuators $\mathcal{C}$, the corners of the uncertainty set $\boldsymbol{\mathcal{U}}_\mathrm{f}$ that maximize the impact on the constraints of the system can be identified for each $i \in \{1, ..., n_z\}$ with $\tilde{\boldsymbol{u}}^i_\mathrm{f} = \tilde{\boldsymbol{u}}^i \circ (\mathbf{1} - \boldsymbol{v}_\mathrm{c})$, where $\mathbf{1}$ is a vector of ones of appropriate dimension and $\circ$ represents the Hadamard product. Since it is assumed here that $\mathbf{M} = \mathbf{I}$, one can further partition the exogenous actions into observed and unobserved exogenous actions, i.e., one can write

$$\mathbf{1} - \boldsymbol{v}_\mathrm{c} = \boldsymbol{v}_\mathrm{m} + \boldsymbol{v}_\mathrm{u}, \tag{4.10}$$

with $\boldsymbol{v}_\mathrm{u} \in \{0, 1\}^{n_u}$ being the binary vector that encodes the elements of the unobserved exogenous actions. The maximum impact on the ith constraint of the system due to the unobserved dimensions of $\boldsymbol{u}$ can then be identified with $\mathbf{A}\ (\tilde{\boldsymbol{u}}^i \circ \boldsymbol{v}_\mathrm{u})$, for all $i \in \{1, ..., n_z\}$.

Admissibility Constraints. Similarly to $\tilde{\boldsymbol{u}}^i \circ \boldsymbol{v}_\mathrm{m}$, a vector of length n_u whose unobserved entries are zero, an associated control vector $\tilde{\boldsymbol{u}}_\mathrm{c}^i \in \boldsymbol{\mathcal{U}}$ is now considered for which

$$\underline{\boldsymbol{u}} \circ \boldsymbol{v}_\mathrm{c} \leq \tilde{\boldsymbol{u}}_\mathrm{c}^i \leq \overline{\boldsymbol{u}} \circ \boldsymbol{v}_\mathrm{c}, \quad \forall i \in \{1, ..., n_z\}, \tag{4.11}$$

should hold. $\tilde{\boldsymbol{u}}_\mathrm{c}^i$ is thus a vector of length n_u whose entries related to $\mathcal{C}$ are subject to lower and upper bounds, and whose entries associated to exogenous actions are zero.

Condition (2.21) states that for all $i \in \{1, ..., n_z\}$, the control action $\tilde{\boldsymbol{u}}_\mathrm{c}^i$ for the corner $\tilde{\boldsymbol{u}}_\mathrm{f}^i = \tilde{\boldsymbol{u}}^i \circ (\mathbf{1} - \boldsymbol{v}_\mathrm{c})$ should be valid and that it should be identical to the control action mapped from all other corners that cannot be distinguished given the observations. By considering the worst-case realization of the corners of $\boldsymbol{\mathcal{U}}_\mathrm{f}$ on the constraints of the system, we obtain the set of linear inequalities

$$\mathbf{A}(\tilde{\boldsymbol{u}}_\mathrm{c}^i + \tilde{\boldsymbol{u}}^i \circ \boldsymbol{v}_\mathrm{m}) + \overline{\mathbf{A}}\boldsymbol{v}_\mathrm{u} \leq \boldsymbol{b}, \quad \forall i \in \{1, ..., n_z\}, \tag{4.12}$$

where $\overline{\mathbf{A}} \in \mathbb{R}^{n_z \times n_u}$ is defined element-wise by

$$\overline{A}_{ij} = A_{ij}\tilde{u}_j^i.$$

In summary, (in)equalities (4.10), (4.11), and (4.12) allow us to compute a lower bound solution for Problem 1 (assuming that $\mathbf{M} = \mathbf{I}$) by solving the MILP

$$\begin{aligned} \min_{\substack{\boldsymbol{v}_\mathrm{c}, \boldsymbol{v}_\mathrm{m}, \boldsymbol{v}_\mathrm{u} \in \{0,1\}^{n_u}, \\ \tilde{\boldsymbol{u}}_\mathrm{c}^i \in \mathbb{R}^{n_u}}} \quad & \mathbf{1}^\mathrm{T}\boldsymbol{v}_\mathrm{c} + \gamma \mathbf{1}^\mathrm{T}\boldsymbol{v}_\mathrm{m} \\ \text{s.t. } & \mathbf{A}(\tilde{\boldsymbol{u}}_\mathrm{c}^i + \tilde{\boldsymbol{u}}^i \circ \boldsymbol{v}_\mathrm{m}) + \overline{\mathbf{A}}\boldsymbol{v}_\mathrm{u} \leq \boldsymbol{b}, \quad \forall i \in \{1, ..., n_z\}, \\ & \underline{\boldsymbol{u}} \circ \boldsymbol{v}_\mathrm{c} \leq \tilde{\boldsymbol{u}}_\mathrm{c}^i \leq \overline{\boldsymbol{u}} \circ \boldsymbol{v}_\mathrm{c}, \quad \forall i \in \{1, ..., n_z\}, \\ & \boldsymbol{v}_\mathrm{c} + \boldsymbol{v}_\mathrm{m} + \boldsymbol{v}_\mathrm{u} = \mathbf{1}. \end{aligned} \tag{4.13}$$

The minimal sets of actuators and sensors resulting from MILP (4.13) are not guaranteed to yield an admissible control law. However, we verified both experimentally and by employing the technique proposed in Section 3.2 that these minimal sets are also admissible in many cases. In addition, MILP (4.13) scales linearly with the number of rows of $\mathbf{A} \in \mathbb{R}^{n_z \times n_u}$, making the approach reasonable for large-scale problem instances depending on the available computing equipment.

In case the resulting minimal sets are admissible, which can be verified by using QCQP (3.27), we can then compute an admissible PWA control law by applying the algorithms proposed in Chapter 3. Otherwise, the actuator and sensor sets should be adapted by, for instance, applying the hill climbing optimization approach proposed below.

4.3 Hill Climbing Optimization Approach

In this section, we describe an iterative algorithm to choose and adapt the actuator and sensor sets in order to find minimal admissible actuator and sensor sets. The key of the

proposed optimization technique is to use a subroutine that determines whether for the current instances of $\mathcal{C}$ and $\mathcal{M}$ there exists an admissible control law. Possible subroutines comprise, for instance, LP verification algorithm (3.18) being valid for affine control laws, or QCQP verification algorithm (3.27) being valid for PWA control laws.

In order to solve Problem 1, we proceed iteratively from initial sets $\mathcal{C}$ and $\mathcal{M}$ adapting them one element at a time. Since we want to measure the optimization progress also for non-admissible combinations $\mathcal{C}$ and $\mathcal{M}$, we extend the minimization objective to

$$J(\mathcal{C}, \mathcal{M}) = |\mathcal{C}| + \gamma|\mathcal{M}| + \mu \max(\eta, 0), \tag{4.14}$$

where η is the feasibility indicator obtained from solving either LP (3.18) or QCQP (3.27). The scalar $\mu > 0$ is a weighting factor that penalizes the non-admissibility of $\mathcal{C}$ and $\mathcal{M}$. We choose $\mu \gg 1$ to steer the iteration quickly towards feasible solutions.

The cost function (4.14) is minimized via a greedy hill climbing procedure. In each iteration we compute the objective value for all sets $\mathcal{M}'$ or $\mathcal{C}'$ that can be generated by adding one element to either $\mathcal{M}$ or $\mathcal{C}$. We then choose the step which yields the largest improvement of the objective value (4.14). As soon as the sets of actuators and sensors are admissible, we stop the iteration.

It is well known that the solution of this greedy approach depends on the selection of the starting point [109]. A natural option is to start with empty sets, selecting the most important controllers and measurements during the first iterations. Alternatively, we propose to use the solution of MILP (4.13) as an initial guess. More specifically, we solve MILP (4.13) for $\mathbf{M} = \mathbf{I}$ first. We then use the obtained lower bound solution for the actuator set as a starting point for the greedy approach, while disregarding the sensor set. Instead, we start with an empty instance of $\mathcal{M}$. In this manner, the observations resulting from a general $\mathbf{M}$, which potentially allow for more compact control laws than using the identity matrix, can be integrated well, but the critical controllers are already identified.

4.4 Discussion

In this chapter, we addressed the problem of finding the smallest number of actuators and sensors for which the existence of an admissible control law is guaranteed. By exploting the theory and algorithms presented in Chapters 2 and 3, we proposed to solve this problem by using optimization approaches based on mixed-integer linear programming and/or hill climbing. We could establish that the problem of finding the minimal admissible sets $(\mathcal{C}, \mathcal{M})$ can in some special cases be expressed as a MILP, for instance when either the control law is assumed to have an affine form or when we suppose the matrix of possible observations to be the identity matrix. For those special cases, the obtained minimal sets $(\mathcal{C}, \mathcal{M})$ correspond to upper and lower bounds with respect to the optimal solution of Problem 1, respectively. Since general MILP has exponential worst-case time complexity, this is an upper bound on the complexity of our first optimization approach.

In contrast, the proposed hill climbing optimization approach incorporates a verification subroutine with exponential/polynomial worst-case complexity for PWA/affine control laws, respectively, and the hill climbing procedure itself only adds polynomial factors. Moreover, the computation time of the hill climbing procedure depends strongly on the starting point.

For the realistic examples discussed in Chapter 7, we found the MILP (4.13) to be more efficient than the hill climbing procedure. However, the hill climbing approach allowed us to find small, guaranteed to be admissible solutions for $\mathcal{C}$ and $\mathcal{M}$ with very reasonable efforts also for the examined medium to large problem instances. For cases when $\mathbf{M} = \mathbf{I}$ is assumed, the solution of MILP (4.13) could often be verified to be admissible (and thus also optimal) by solving QCQP (3.27) only once without further adaptation of $\mathcal{C}$ or $\mathcal{M}$. We thus see both optimization approaches as an important contribution for solving real actuator/sensor selection problems with constraints on both the state of the system and the control action.

5 Distortion of Actuator and Sensor Signals

So far we assumed that neither the information provided by the sensors nor the control commands that the system receives from the control center have been altered in any manner. In this chapter, we remove such assumption and focus on admissible control laws that can tolerate the exogenous, malicious manipulation of the actuator/sensor signals. We show that such control laws can be computed by applying the framework introduced in previous chapters. Particularly, we extend the online, two-stage control law (2.14)–(3.29) to define special observation-dependent uncertainty sets for the distortion of at most $\mathsf{k} \in \mathbb{Z}_{\geq 0}$ actuator/sensor signals.

The $N - \mathsf{k}$ problem in power networks, i.e., the problem of finding if a power system tolerates the failure/malfunction of at most k unknown assets from a total of N assets, has gained increasing importance due to the cyber-physical vulnerabilities introduced by the rapidly growing number of installed automation and communication devices into the power network [110]. The number k is an indicator of the operational resilience of the system, since the larger the value of k, the more attacks/contingencies can be tolerated by the control center. Note that finding the maximum value of k is challenging as the number combinations of compromised actuators/sensors grows exponentially. Typical approaches assume a fixed k and employ interdiction models to determine if the system solves the $N - \mathsf{k}$ problem. An interdiction model can be understood as an attacker-defender Stackelberg game [111], and can be set up using either deterministic or probabilistic bilevel optimization models [112, 110, 113, 114, 115].

Another line of research focuses on the detection or identification of the attack/contingency, which can then be used to determine adequate reactive decisions [116, 117, 118, 119]. The attack detection task consists of finding if the system is being attacked or not. In contrast, the attack identification task aims at finding the location and nature of the attack and is known to be NP-hard due to its combinatorial nature [120].

In what follows, we assume that the number k is given and aim at the design of admissible control laws that do not require any attack detection or identification stage. Instead, we treat the attack vectors as additional observation-dependent uncertainties and

exploit the ideas provided in Chapters 2 and 3 to compute admissible control laws control laws that tolerate the distortion of at most k actuator/sensor signals.

5.1 Modeling Considerations

Consider the block diagram depicted in Fig. 5.1. The control center receives the uncertain observation $\hat{\boldsymbol{y}}^{\mathrm{m}} \neq \boldsymbol{y}^{\mathrm{m}}$ and based on it should compute the control action $\hat{\boldsymbol{u}}_{\mathrm{c}} \neq \boldsymbol{u}_{\mathrm{c}}$ according to a pre-specified control law $\hat{\boldsymbol{u}}_{\mathrm{c}} = \boldsymbol{k}(\hat{\boldsymbol{y}}^{\mathrm{m}})$. Such control law has to guarantee that the unknown, distorted control action $\boldsymbol{u}_{\mathrm{c}}$ results in a feasible system state independently of the value of the exogenous action $\boldsymbol{u}_{\mathrm{f}}$, and the distortion vectors $\Delta\boldsymbol{u}_{\mathrm{c}}$, $\Delta\boldsymbol{y}^{\mathrm{m}}$.

In this thesis, we assume that the actuator/sensor signals are manipulated additively, i.e.,

$$\boldsymbol{u}_{\mathrm{c}} = \hat{\boldsymbol{u}}_{\mathrm{c}} + \Delta\boldsymbol{u}_{\mathrm{c}}, \quad \hat{\boldsymbol{y}}^{\mathrm{m}} = \boldsymbol{y}^{\mathrm{m}} + \Delta\boldsymbol{y}^{\mathrm{m}}, \tag{5.1}$$

where $\hat{\boldsymbol{u}}_{\mathrm{c}} \in \mathbb{R}^{|\mathcal{C}|}$, $\hat{\boldsymbol{y}}^{\mathrm{m}} \in \mathbb{R}^{|\mathcal{M}|}$, $\Delta\boldsymbol{u}_{\mathrm{c}} \in \Delta\boldsymbol{\mathcal{U}}_{\mathrm{c}} \subset \mathbb{R}^{|\mathcal{C}|}$, and $\Delta\boldsymbol{y}^{\mathrm{m}} \in \Delta\boldsymbol{\mathcal{Y}}^{\mathrm{m}} \subset \mathbb{R}^{|\mathcal{M}|}$. Contrary to standard approaches in which small perturbations (e.g., noise) are typically considered, we focus on large perturbations of at most k actuator/sensor signals caused by external (malicious) agents. The non-negative integer k is assumed to be small compared to the total number of actuator and sensor devices available to the controller, i.e., $\mathsf{k} \ll |\mathcal{C}| + |\mathcal{M}|$. For this reason, the vectors $\Delta\boldsymbol{u}_{\mathrm{c}}$ and $\Delta\boldsymbol{y}^{\mathrm{m}}$ affect only a small number of (possibly unknown) entries of $\hat{\boldsymbol{u}}_{\mathrm{c}}$ and $\boldsymbol{y}^{\mathrm{m}}$, respectively.

To model such behavior, let $\boldsymbol{a}_{\mathrm{c}} \in \{0,1\}^{|\mathcal{C}|}$ and $\boldsymbol{a}_{\mathrm{m}}, \in \{0,1\}^{|\mathcal{M}|}$ be the *attack vectors* that determine which actuators and sensors are undesirably manipulated, respectively. Concretely, the attack vectors $\boldsymbol{a}_{\mathrm{c}}$ and $\boldsymbol{a}_{\mathrm{m}}$ are defined element-wise as

$$a_{\mathrm{c}j} = \begin{cases} 1 & \text{if } u_{\mathrm{c}j} \text{ is distorted} \\ 0 & \text{else} \end{cases}, \quad a_{\mathrm{m}k} = \begin{cases} 1 & \text{if } y^{\mathrm{m}}_k \text{ is distorted} \\ 0 & \text{else} \end{cases}.$$

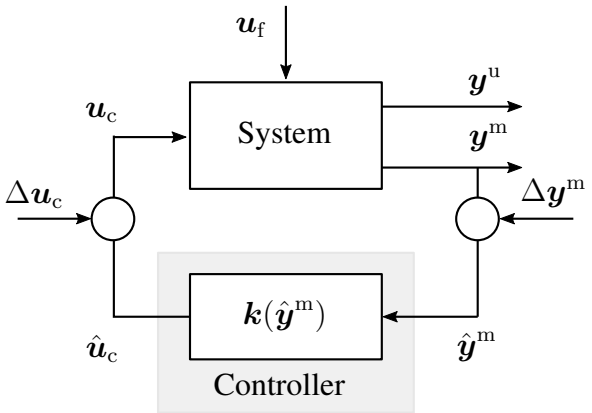

Figure 5.1: Block diagram of a controlled static linear system with distorted actuator/sensor signals. The control law $\hat{\boldsymbol{u}}_{\mathrm{c}} = \boldsymbol{k}(\hat{\boldsymbol{y}}^{\mathrm{m}})$ maps a malicious manipulated observation $\hat{\boldsymbol{y}}^{\mathrm{m}}$ to a control action $\hat{\boldsymbol{u}}_{\mathrm{c}}$ that is also prone to malicious manipulation, but still guarantees that the control action $\boldsymbol{u}_{\mathrm{c}}$ influencing the system always yields a feasible system state.

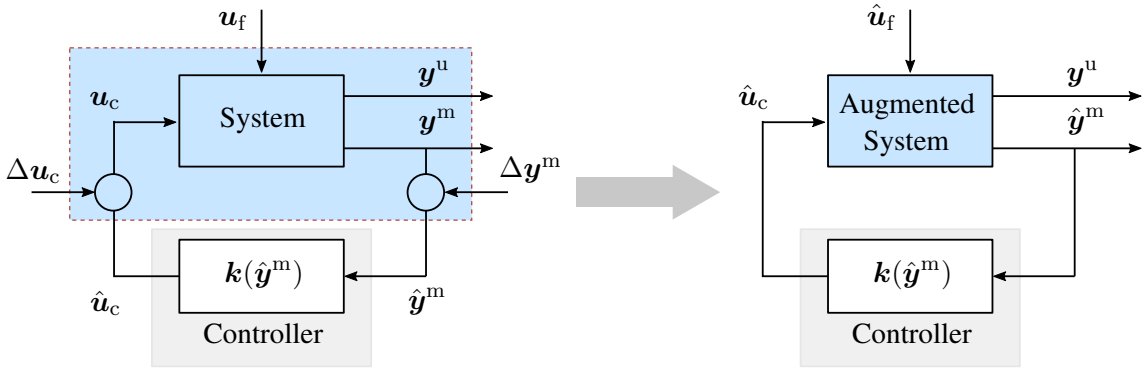

Figure 5.2: The control center treats the distortion vectors $\Delta \boldsymbol{u}_c$ and $\Delta \boldsymbol{y}^m$ as uncertain, but bounded exogenous actions. This allows us to apply the algorithms proposed in previous chapters for the computation of admissible control laws $\hat{\boldsymbol{u}}_c = \boldsymbol{k}(\hat{\boldsymbol{y}}^m)$.

Note that the actuator attack vector $\boldsymbol{a}_c$ as well as the observation attack vector $\boldsymbol{a}_m$, which may or may not be known to the controller depending on the application, are subject to

$$\mathbf{1}^T \boldsymbol{a}_c + \mathbf{1}^T \boldsymbol{a}_m \leq k. \tag{5.2}$$

An important assumption made in this chapter is that the distortion vectors $\Delta \boldsymbol{u}_c$ and $\Delta \boldsymbol{y}^m$ lie in interval-bounded uncertainty sets, which we denote by $\Delta \boldsymbol{\mathcal{U}}_c$ and $\Delta \boldsymbol{\mathcal{Y}}^m$, respectively. Since we suppose that only a few number of actuators and sensors are affected by the attack vectors $(\boldsymbol{a}_c, \boldsymbol{a}_m)$, the uncertainty sets $\Delta \boldsymbol{\mathcal{U}}_c$ and $\Delta \boldsymbol{\mathcal{Y}}^m$ are given in terms of the value of the attack vectors, i.e.,

$$\begin{aligned} \Delta \boldsymbol{\mathcal{U}}_c(\boldsymbol{a}_c) &= \{\Delta \boldsymbol{u}_c \in \mathbb{R}^{|\mathcal{C}|} : \underline{\Delta \boldsymbol{u}}_c \circ \boldsymbol{a}_c \leq \Delta \boldsymbol{u}_c \leq \overline{\Delta \boldsymbol{u}}_c \circ \boldsymbol{a}_c\}, \\ \Delta \boldsymbol{\mathcal{Y}}^m(\boldsymbol{a}_m) &= \{\Delta \boldsymbol{y}^m \in \mathbb{R}^{|\mathcal{M}|} : \underline{\Delta \boldsymbol{y}}^m \circ \boldsymbol{a}_m \leq \Delta \boldsymbol{y}^m \leq \overline{\Delta \boldsymbol{y}}^m \circ \boldsymbol{a}_m\}. \end{aligned} \tag{5.3}$$

where $\circ$ represents the Hadamard product (also known as element-wise product), and the parameters $\underline{\Delta \boldsymbol{u}}_c, \overline{\Delta \boldsymbol{u}}_c \in \mathbb{R}^{|\mathcal{C}|}$ and $\underline{\Delta \boldsymbol{y}}^m, \overline{\Delta \boldsymbol{y}}^m \in \mathbb{R}^{|\mathcal{M}|}$ symbolize the lower and upper bounds of $\Delta \boldsymbol{u}_c$ and $\Delta \boldsymbol{y}^m$, respectively. Such boundaries represent minimum and maximum plausible deviations and can be computed using the constraints of system (2.2).

With the uncertainty sets introduced above, we show in the following how apply the techniques developed in previous chapters for the computation of admissible control laws. To this end, we now consider the *augmented system* illustrated on the right of Fig. 5.2. In this new setting, the exogenous actions $\hat{\boldsymbol{u}}_f$ are given by the vector

$$\hat{\boldsymbol{u}}_f = \begin{bmatrix} \boldsymbol{u}_f^T & \Delta \boldsymbol{u}_c^T & \Delta \boldsymbol{y}^{mT} \end{bmatrix} \in \hat{\boldsymbol{\mathcal{U}}}_f(\boldsymbol{a}_c, \boldsymbol{a}_m) = \boldsymbol{\mathcal{U}}_f \times \Delta \boldsymbol{\mathcal{U}}_c(\boldsymbol{a}_c) \times \Delta \boldsymbol{\mathcal{Y}}^m(\boldsymbol{a}_m), \tag{5.4}$$

where $\hat{\boldsymbol{\mathcal{U}}}_f(\boldsymbol{a}_c, \boldsymbol{a}_m)$ symbolizes the uncertainty set associated to the augmented exogenous action $\hat{\boldsymbol{u}}_f$. Note in (5.4) that for all possible realizations of the attack vectors $\boldsymbol{a}_c$ and $\boldsymbol{a}_m$ the uncertainty set $\hat{\boldsymbol{\mathcal{U}}}_f(\boldsymbol{a}_c, \boldsymbol{a}_m)$ is convex.

The augmented constrained static linear system is derived from (2.2) and (5.1) as follows. From system (2.2), we have the representation

$$\mathbf{A}_c \boldsymbol{u}_c + \mathbf{A}_f \boldsymbol{u}_f \leq \boldsymbol{b}, \quad \boldsymbol{y}^m = \mathbf{M}_c^m \boldsymbol{u}_c + \mathbf{M}_f^m \boldsymbol{u}_f, \quad \boldsymbol{u}_c \in \boldsymbol{\mathcal{U}}_c, \ \boldsymbol{u}_f \in \boldsymbol{\mathcal{U}}_f,$$

where is it supposed that $\mathcal{M} \neq \emptyset$, $\boldsymbol{\mathcal{U}}_\mathrm{f} \neq \emptyset$, and $\mathrm{rank}(\mathbf{M}_\mathrm{f}^\mathrm{m}) < n_u - |\mathcal{C}|$ hold. For simplicity, we assume that the set of control actions $\boldsymbol{\mathcal{U}}_\mathrm{c}$ and the set of exogenous actions $\boldsymbol{\mathcal{U}}_\mathrm{f}$ influencing the system are both convex polytopes given by

$$\boldsymbol{\mathcal{U}}_\mathrm{c} = \{\boldsymbol{u}_\mathrm{c} \in \mathbb{R}^{|\mathcal{C}|} : \mathbf{Q}_\mathrm{c}\boldsymbol{u}_\mathrm{c} \leq \boldsymbol{q}_\mathrm{c}\}, \quad \boldsymbol{\mathcal{U}}_\mathrm{f} = \{\boldsymbol{u}_\mathrm{f} \in \mathbb{R}^{n_u-|\mathcal{C}|} : \mathbf{Q}_\mathrm{f}\boldsymbol{u}_\mathrm{f} \leq \boldsymbol{q}_\mathrm{f}\},$$

with parameters $\mathbf{Q}_\mathrm{c} \in \mathbb{R}^{l_\mathrm{c}\times|\mathcal{C}|}$, $\mathbf{Q}_\mathrm{f} \in \mathbb{R}^{l_\mathrm{f}\times(n_u-|\mathcal{C}|)}$, $\boldsymbol{q}_\mathrm{c} \in \mathbb{R}^{l_\mathrm{c}}$, and $\boldsymbol{q}_\mathrm{f} \in \mathbb{R}^{l_\mathrm{f}}$. Under this assumption and recalling that $\boldsymbol{u}_\mathrm{c} = \hat{\boldsymbol{u}}_\mathrm{c} + \Delta\boldsymbol{u}_\mathrm{c}$, we obtain the inequality constraints of the augmented system shown in Fig. 5.2 as

$$\begin{aligned}
&\begin{bmatrix}\mathbf{A}_\mathrm{c}\\ \mathbf{Q}_\mathrm{c}\end{bmatrix}(\hat{\boldsymbol{u}}_\mathrm{c} + \Delta\boldsymbol{u}_\mathrm{c}) + \begin{bmatrix}\mathbf{A}_\mathrm{f}\\ \mathbf{0}\end{bmatrix}\boldsymbol{u}_\mathrm{f} \leq \begin{bmatrix}\boldsymbol{b}\\ \boldsymbol{q}_\mathrm{c}\end{bmatrix},\\
\Rightarrow &\begin{bmatrix}\mathbf{A}_\mathrm{c}\\ \mathbf{Q}_\mathrm{c}\end{bmatrix}\hat{\boldsymbol{u}}_\mathrm{c} + \begin{bmatrix}\mathbf{A}_\mathrm{f} & \mathbf{A}_\mathrm{c} & \mathbf{0}\\ \mathbf{0} & \mathbf{Q}_\mathrm{c} & \mathbf{0}\end{bmatrix}\begin{bmatrix}\boldsymbol{u}_\mathrm{f}\\ \Delta\boldsymbol{u}_\mathrm{c}\\ \Delta\boldsymbol{y}^\mathrm{m}\end{bmatrix} \leq \begin{bmatrix}\boldsymbol{b}\\ \boldsymbol{q}_\mathrm{c}\end{bmatrix},\\
\Rightarrow &\hat{\mathbf{A}}_\mathrm{c}\hat{\boldsymbol{u}}_\mathrm{c} + \hat{\mathbf{A}}_\mathrm{f}\hat{\boldsymbol{u}}_\mathrm{f} \leq \hat{\boldsymbol{b}},
\end{aligned} \tag{5.5}$$

where $\hat{\mathbf{A}}_\mathrm{c} \in \mathbb{R}^{\hat{n}_z\times|\mathcal{C}|}$, $\hat{\mathbf{A}}_\mathrm{f} \in \mathbb{R}^{\hat{n}_z\times(n_u+|\mathcal{M}|)}$, and $\hat{\boldsymbol{b}} \in \mathbb{R}^{\hat{n}_z}$, $\hat{n}_z = n_z + l_\mathrm{c}$, and n_z is the number of rows of the matrix $\mathbf{A}_\mathrm{c}$.

In a similar fashion and recalling that $\hat{\boldsymbol{y}}^\mathrm{m} = \boldsymbol{y}^\mathrm{m} + \Delta\boldsymbol{y}^\mathrm{m}$, the observation model for the augmented system is given in terms of $\hat{\boldsymbol{u}}_\mathrm{c}$, $\hat{\boldsymbol{u}}_\mathrm{f}$, and the matrices $\mathbf{M}_\mathrm{c}^\mathrm{m}$ and $\mathbf{M}_\mathrm{f}^\mathrm{m}$ by

$$\begin{aligned}
\hat{\boldsymbol{y}}^\mathrm{m} &= \boldsymbol{y}^\mathrm{m} + \Delta\boldsymbol{y}^\mathrm{m}\\
&= \mathbf{M}_\mathrm{c}^\mathrm{m}\boldsymbol{u}_\mathrm{c} + \mathbf{M}_\mathrm{f}^\mathrm{m}\boldsymbol{u}_\mathrm{f} + \Delta\boldsymbol{y}^\mathrm{m}\\
&= \mathbf{M}_\mathrm{c}^\mathrm{m}(\hat{\boldsymbol{u}}_\mathrm{c} + \Delta\boldsymbol{u}_\mathrm{c}) + \mathbf{M}_\mathrm{f}^\mathrm{m}\boldsymbol{u}_\mathrm{f} + \Delta\boldsymbol{y}^\mathrm{m}\\
&= \mathbf{M}_\mathrm{c}^\mathrm{m}\hat{\boldsymbol{u}}_\mathrm{c} + \mathbf{M}_\mathrm{c}^\mathrm{m}\Delta\boldsymbol{u}_\mathrm{c} + \mathbf{M}_\mathrm{f}^\mathrm{m}\boldsymbol{u}_\mathrm{f} + \Delta\boldsymbol{y}^\mathrm{m}\\
&= \mathbf{M}_\mathrm{c}^\mathrm{m}\hat{\boldsymbol{u}}_\mathrm{c} + \begin{bmatrix}\mathbf{M}_\mathrm{f}^\mathrm{m} & \mathbf{M}_\mathrm{c}^\mathrm{m} & \mathbf{I}\end{bmatrix}\begin{bmatrix}\boldsymbol{u}_\mathrm{f}\\ \Delta\boldsymbol{u}_\mathrm{c}\\ \Delta\boldsymbol{y}^\mathrm{m}\end{bmatrix}\\
&= \mathbf{M}_\mathrm{c}^\mathrm{m}\hat{\boldsymbol{u}}_\mathrm{c} + \hat{\mathbf{M}}_\mathrm{f}^\mathrm{m}\hat{\boldsymbol{u}}_\mathrm{f}\\
&= \mathbf{M}_\mathrm{c}^\mathrm{m}\hat{\boldsymbol{u}}_\mathrm{c} + \hat{\boldsymbol{y}}_\mathrm{f}^\mathrm{m}.
\end{aligned} \tag{5.6}$$

From expressions (5.4), (5.5) and (5.6), we readily obtain a constrained static system compatible with the representation (2.2).

5.2 Computing Admissible Control Laws

The goal of the controller is now to find a control law $\hat{\boldsymbol{u}}_\mathrm{c} = \boldsymbol{k}(\hat{\boldsymbol{y}}^\mathrm{m})$ that guarantees a feasible system state for all possible realizations of the (augmented) exogenous action $\hat{\boldsymbol{u}}_\mathrm{f} \in \hat{\boldsymbol{\mathcal{U}}}_\mathrm{f}(\boldsymbol{a}_\mathrm{c}, \boldsymbol{a}_\mathrm{m})$, with $\boldsymbol{a}_\mathrm{c}$ and $\boldsymbol{a}_\mathrm{m}$ being subject to (5.2). Here it is important to note that the value of $\hat{\boldsymbol{u}}_\mathrm{c} \in \hat{\boldsymbol{\mathcal{U}}}_\mathrm{c} \subseteq \mathbb{R}^{|\mathcal{C}|}$ is not necessarily in the control action space $\boldsymbol{\mathcal{U}}_\mathrm{c}$. This

is because we are looking for artificial control actions in $\hat{\boldsymbol{\mathcal{U}}}_{\mathrm{c}}$ which *after their possible distortion* correspond to valid control actions in $\boldsymbol{\mathcal{U}}_{\mathrm{c}}$.

As we know from Chapters 2 and 3, we can re-express the control law $\hat{\boldsymbol{u}}_{\mathrm{c}} = \boldsymbol{k}(\hat{\boldsymbol{y}}^{\mathrm{m}})$ as a function of $\hat{\boldsymbol{y}}_{\mathrm{f}}^{\mathrm{m}}$, i.e., as a mapping $\hat{\boldsymbol{u}}_{\mathrm{c}} = \hat{\boldsymbol{k}}(\hat{\boldsymbol{y}}_{\mathrm{f}}^{\mathrm{m}})$ for which the admissibility conditions are simpler to analyze and do not involve recursion. In the following, we explain how to compute an admissible control law $\hat{\boldsymbol{u}}_{\mathrm{c}} = \hat{\boldsymbol{k}}(\hat{\boldsymbol{y}}_{\mathrm{f}}^{\mathrm{m}})$ under the assumption that such a mapping exists. We also limit our analysis to the particular case where the actuator attack vector $\boldsymbol{a}_{\mathrm{c}}$ is known to the controller, but the observation attack vector $\boldsymbol{a}_{\mathrm{m}}$ is unknown. The reason for this assumption is clarified later.

The computation of the control law $\hat{\boldsymbol{u}}_{\mathrm{c}} = \hat{\boldsymbol{k}}(\hat{\boldsymbol{y}}_{\mathrm{f}}^{\mathrm{m}})$ takes place in two steps and is derived from the two-stage online control law proposed in Section 3.3.1. Following the explanation given there, the first step consist of finding those worst-case realizations of the augmented exogenous action $\hat{\boldsymbol{u}}_{\mathrm{f}} \in \hat{\boldsymbol{\mathcal{U}}}_{\mathrm{f}}(\boldsymbol{a}_{\mathrm{c}}, \boldsymbol{a}_{\mathrm{m}})$ that maximize the impact on each constraint of the system and are also consistent with the observation $\hat{\boldsymbol{y}}_{\mathrm{f}}^{\mathrm{m}}$. Based on that information, a suitable control action $\hat{\boldsymbol{u}}_{\mathrm{c}}$ is computed in the second step. In the following, we describe these two steps in more detail.

We start by introducing the non-negative integer $\mathsf{k}_{\mathrm{c}} \in \mathbb{Z}_{\geq 0}$ with $\mathbf{1}^{\mathrm{T}}\boldsymbol{a}_{\mathrm{c}} \leq \mathsf{k}_{\mathrm{c}} \leq \mathsf{k}$, which represents the maximum possible number of attacked actuators that the control center can tolerate. As mentioned above, we assume in this thesis that the actuator attack vector $\boldsymbol{a}_{\mathrm{c}}$ is known, i.e., the control center is aware of those actuators that may possibly be distorted by exogenous agents. By using this knowledge, the controller can fix the value of k_{c}, namely $\mathsf{k}_{\mathrm{c}} = \mathbf{1}^{\mathrm{T}}\boldsymbol{a}_{\mathrm{c}}$.

Likewise, we now introduce the non-negative integer $\mathsf{k}_{\mathrm{m}} \in \mathbb{Z}_{\geq 0}$ that fulfills the inequalities $\mathbf{1}^{\mathrm{T}}\boldsymbol{a}_{\mathrm{m}} \leq \mathsf{k}_{\mathrm{m}} \leq \mathsf{k}$ and symbolizes the maximum number of entries of $\hat{\boldsymbol{y}}^{\mathrm{m}}$ (the observation available to the control center) that may unexpectedly be completely off due to either technical errors during transmission or malicious attacks on parts of the system. Since both k and k_{c} are fixed by the controller, the integer k_{m} is simply the difference between k and k_{c}, i.e., $\mathsf{k}_{\mathrm{m}} = \mathsf{k} - \mathsf{k}_{\mathrm{c}}$. Although we assume that the value of the observation attack vector $\boldsymbol{a}_{\mathrm{m}}$ unknown to the controller, we still suppose that it fulfills $\mathbf{1}^{\mathrm{T}}\boldsymbol{a}_{\mathrm{m}} \leq \mathsf{k}_{\mathrm{m}}$.

The desired admissible control law $\hat{\boldsymbol{u}}_{\mathrm{c}} = \hat{\boldsymbol{k}}(\hat{\boldsymbol{y}}_{\mathrm{f}}^{\mathrm{m}})$ should thus be able to tolerate the distortion of at most k_{c} actuators and k_{m} sensors—without the need to know or identify the exact subset of disturbed sensors. Note that, while not being in the scope of this thesis, the method proposed below can be applied to solve problem instances where, e.g., noise or smaller measurement errors are present.

As explained in Section 3.3.1, the first stage of the control law determines the maximum impact on each constraint of the system caused by those realizations of $\hat{\boldsymbol{u}}_{\mathrm{f}} \in \hat{\boldsymbol{\mathcal{U}}}_{\mathrm{f}}(\boldsymbol{a}_{\mathrm{c}}, \boldsymbol{a}_{\mathrm{m}})$ that also are consistent with the current value of the observation $\hat{\boldsymbol{y}}_{\mathrm{f}}^{\mathrm{m}}$. Note that, if the value of the observation attack vector $\boldsymbol{a}_{\mathrm{m}}$ were known, such maximum

impacts could be computed by solving, for all $j = \{1, ..., \hat{n}_z\}$,

$$\begin{aligned} \max_{\hat{\boldsymbol{u}}_\mathrm{f} \in \hat{\boldsymbol{\mathcal{U}}}_\mathrm{f}(\boldsymbol{a}_\mathrm{c}, \boldsymbol{a}_\mathrm{m})} \quad & \hat{\mathbf{A}}_\mathrm{f}^{\,j} \hat{\boldsymbol{u}}_\mathrm{f} \\ \text{s.t. } & \hat{\mathbf{M}}_\mathrm{f}^\mathrm{m} \hat{\boldsymbol{u}}_\mathrm{f} = \hat{\boldsymbol{y}}_\mathrm{f}^\mathrm{m}, \end{aligned} \tag{5.7}$$

where $\hat{\mathbf{A}}_\mathrm{f}^{\,j}$ represents the jth row of $\hat{\mathbf{A}}_\mathrm{f}$. As the uncertainty set $\hat{\boldsymbol{\mathcal{U}}}_\mathrm{f}(\boldsymbol{a}_\mathrm{c}, \boldsymbol{a}_\mathrm{m})$ is convex for fixed $\boldsymbol{a}_\mathrm{c}$ and $\boldsymbol{a}_\mathrm{m}$, the above maximization problem is a LP.

For the case where the value of $\boldsymbol{a}_\mathrm{m}$ unknown, which is the focus in this thesis, we can extend the above formulation by considering the observation attack vector $\boldsymbol{a}_\mathrm{m}$ as an additional binary optimization variable. Concretely, the maximum impact on the jth constraint of the system due to an augmented exogenous action $\hat{\boldsymbol{u}}_\mathrm{f} \in \hat{\boldsymbol{\mathcal{U}}}_\mathrm{f}(\boldsymbol{a}_\mathrm{c}, \boldsymbol{a}_\mathrm{m})$ that is consistent with the observation $\hat{\boldsymbol{y}}_\mathrm{f}^\mathrm{m}$ can be found by solving, for all $j \in \{1, ..., \hat{n}_z\}$, the mixed-integer linear optimization problem

$$\begin{aligned} \check{z}_j(\hat{\boldsymbol{y}}_\mathrm{f}^\mathrm{m}) = \max_{\substack{\boldsymbol{u}_\mathrm{f} \in \mathbb{R}^{n_u - |\mathcal{C}|}, \boldsymbol{a}_\mathrm{m} \in \{0,1\}^{|\mathcal{C}|} \\ \Delta \boldsymbol{y}_\mathrm{f}^\mathrm{m} \in \mathbb{R}^{|\mathcal{M}|}, \Delta \boldsymbol{u}_\mathrm{c} \in \mathbb{R}^{|\mathcal{C}|}}} \quad & \hat{\mathbf{A}}_\mathrm{ff}^{\,j} \boldsymbol{u}_\mathrm{f} + \hat{\mathbf{A}}_\mathrm{fc}^{\,j} \Delta \boldsymbol{u}_\mathrm{c} + \hat{\mathbf{A}}_\mathrm{fm}^{\,j} \Delta \boldsymbol{y}^\mathrm{m} \\ \text{s.t. } & \mathbf{M}_\mathrm{f}^\mathrm{m} \boldsymbol{u}_\mathrm{f} + \mathbf{M}_\mathrm{c}^\mathrm{m} \Delta \boldsymbol{u}_\mathrm{c} + \Delta \boldsymbol{y}_\mathrm{f}^\mathrm{m} = \hat{\boldsymbol{y}}_\mathrm{f}^\mathrm{m}, \\ & \mathbf{1}^\mathrm{T} \boldsymbol{a}_\mathrm{m} \leq \mathsf{k}_\mathrm{m}, \\ & \underline{\Delta \boldsymbol{y}_\mathrm{f}^\mathrm{m}} \circ \boldsymbol{a}_\mathrm{m} \leq \Delta \boldsymbol{y}_\mathrm{f}^\mathrm{m} \leq \overline{\Delta \boldsymbol{y}_\mathrm{f}^\mathrm{m}} \circ \boldsymbol{a}_\mathrm{m}, \\ & \underline{\Delta \boldsymbol{u}_\mathrm{c}} \circ \boldsymbol{a}_\mathrm{c} \leq \Delta \boldsymbol{u}_\mathrm{c} \leq \overline{\Delta \boldsymbol{u}_\mathrm{c}} \circ \boldsymbol{a}_\mathrm{c}, \\ & \mathbf{Q}_\mathrm{f} \boldsymbol{u}_\mathrm{f} \leq \boldsymbol{q}_\mathrm{f}. \end{aligned} \tag{5.8}$$

The above MILP is derived from LP (5.7) by replacing the augmented exogenous action $\hat{\boldsymbol{u}}_\mathrm{f}$ and its associated uncertainty set $\hat{\boldsymbol{\mathcal{U}}}_\mathrm{f}(\boldsymbol{a}_\mathrm{c}, \boldsymbol{a}_\mathrm{m})$ with their explicit representations in terms of $\boldsymbol{u}_\mathrm{f}$, $\Delta \boldsymbol{u}_\mathrm{c}$, and $\Delta \boldsymbol{y}^\mathrm{m}$. Note in MILP (5.8) that the row vectors $\hat{\mathbf{A}}_\mathrm{ff}^{\,j} \in \mathbb{R}^{1 \times (n_u - |\mathcal{C}|)}$, $\hat{\mathbf{A}}_\mathrm{fc}^{\,j} \in \mathbb{R}^{1 \times |\mathcal{C}|}$, and $\hat{\mathbf{A}}_\mathrm{fm}^{\,j} \in \mathbb{R}^{1 \times |\mathcal{M}|}$ correspond to the partitions of the jth row of $\hat{\mathbf{A}}_\mathrm{f}$ associated to $\boldsymbol{u}_\mathrm{f}$, $\Delta \boldsymbol{u}_\mathrm{c}$, and $\Delta \boldsymbol{y}^\mathrm{m}$, respectively.

After computing all entries of mapping $\check{\boldsymbol{z}}(\hat{\boldsymbol{y}}_\mathrm{f}^\mathrm{m})$ via MILP (5.8), the control action $\hat{\boldsymbol{u}}_\mathrm{c}$ is computed by solving the second-stage LP

$$\begin{aligned} \hat{\boldsymbol{u}}_\mathrm{c} = \hat{\boldsymbol{k}}(\hat{\boldsymbol{y}}_\mathrm{f}^\mathrm{m}) = \min_{\hat{\boldsymbol{u}}_\mathrm{c} \in \mathbb{R}^{|\mathcal{C}|}, \eta \in \mathbb{R}} \quad & \eta \\ \text{s.t. } & \hat{\mathbf{A}}_\mathrm{c} \hat{\boldsymbol{u}}_\mathrm{c} + \check{\boldsymbol{z}}(\hat{\boldsymbol{y}}_\mathrm{f}^\mathrm{m}) \leq \hat{\boldsymbol{b}} + \eta \mathbf{1}. \end{aligned} \tag{5.9}$$

Under the assumption that there exists an admissible control law $\hat{\boldsymbol{u}}_\mathrm{c} = \hat{\boldsymbol{k}}(\hat{\boldsymbol{y}}_\mathrm{f}^\mathrm{m})$ for the augmented system, the feasibility indicator η fulfills $\eta \leq 0$ for all possible observations $\hat{\boldsymbol{y}}_\mathrm{f}^\mathrm{m} \in \hat{\mathbf{M}}_\mathrm{f}^\mathrm{m}(\hat{\boldsymbol{\mathcal{U}}}_\mathrm{f}(\boldsymbol{a}_\mathrm{c}, \boldsymbol{a}_\mathrm{m}))$. In other words, the control action $\hat{\boldsymbol{u}}_\mathrm{c}$ mapped via the two-stage online approach (5.8)–(5.9) always guarantees the feasibility of the full system state with respect to the constraints of the system.

The two-stage online control law (5.8)–(5.9) involves solving a total of $\hat{n}_z$ MILPs and one LP. Although mixed-integer linear programming has by definition worst-case exponential time complexity, we verify experimentally that MILP (5.8) performs efficiently in practice for $\mathsf{k}_\mathrm{m} \in \{1, 2\}$ as we illustrate in Chapter 7. Studies with experiments using larger instances of k_m are postponed for future work.

Remark 8. The first-stage MILP (5.8) can be easily extended to consider unknown realizations of the actuator attack vector $\boldsymbol{a}_\mathrm{c}$ by setting $\boldsymbol{a}_\mathrm{c}$ also as a binary decision variable and replacing the constraint $\mathbf{1}^\mathrm{T}\boldsymbol{a}_\mathrm{m} \leq \mathsf{k}_\mathrm{m}$ with $\mathbf{1}^\mathrm{T}\boldsymbol{a}_\mathrm{c} + \mathbf{1}^\mathrm{T}\boldsymbol{a}_\mathrm{m} \leq \mathsf{k}$. However, such approach complicates the second-stage LP (5.9) when computing the control action $\hat{\boldsymbol{u}}_\mathrm{c}$. This is because, when $\boldsymbol{a}_\mathrm{c}$ is unknown, the entries of $\check{\boldsymbol{z}}(\hat{\boldsymbol{y}}_\mathrm{f}^\mathrm{m})$ are determined by $\hat{n}_z$ possibly different realizations of $\boldsymbol{a}_\mathrm{c}$. In that case, there is no guarantee that the control action $\hat{\boldsymbol{u}}_\mathrm{c}$ computed via LP (5.9) will result in a valid control action in $\boldsymbol{u}_\mathrm{c} \in \boldsymbol{\mathcal{U}}_\mathrm{c}$ after being affected by a $\Delta\boldsymbol{u}_\mathrm{c}$ associated to a unique instance of $\boldsymbol{a}_\mathrm{c}$. The extension of second stage LP to the case where $\boldsymbol{a}_\mathrm{c}$ is unknown to the controller certainly represents an interesting direction for future research.

Remark 9. Although MILP (5.8) already provides an efficient method to tackle at most k_m unknown corrupted measurements, it can be computationally demanding for large dimensions of $\hat{\boldsymbol{u}}_\mathrm{f}$. To improve the efficiency of the algorithm, we can approximate the uncertainty set $\Delta\boldsymbol{\mathcal{Y}}_\mathrm{f}^\mathrm{m}(\boldsymbol{a}_\mathrm{m})$ by relaxing the integer constraint $\boldsymbol{a}_\mathrm{m} \in \{0,1\}^{|\mathcal{M}|}$ to the box constraints $\mathbf{0} \leq \boldsymbol{a}_\mathrm{m} \leq \mathbf{1}$. In this manner, we can approximate the mapping $\check{z}_j(\hat{\boldsymbol{y}}_\mathrm{f}^\mathrm{m})$ for all $j \in \{1, ..., \hat{n}_z\}$ via the LP formulation

$$
\begin{aligned}
\max_{\substack{\boldsymbol{u}_\mathrm{f}\in\mathbb{R}^{n_u-|\mathcal{C}|},\boldsymbol{a}_\mathrm{m}\in[0,1]^{|\mathcal{C}|} \\ \Delta\boldsymbol{y}_\mathrm{f}^\mathrm{m}\in\mathbb{R}^{|\mathcal{M}|},\Delta\boldsymbol{u}_\mathrm{c}\in\mathbb{R}^{|\mathcal{C}|}}} \quad & \hat{\mathbf{A}}_\mathrm{ff}^{j}\boldsymbol{u}_\mathrm{f} + \hat{\mathbf{A}}_\mathrm{fc}^{j}\Delta\boldsymbol{u}_\mathrm{c} + \hat{\mathbf{A}}_\mathrm{fm}^{j}\Delta\boldsymbol{y}^\mathrm{m} \\
\text{s.t.} \quad & \mathbf{M}_\mathrm{f}^\mathrm{m}\boldsymbol{u}_\mathrm{f} + \mathbf{M}_\mathrm{c}^\mathrm{m}\Delta\boldsymbol{u}_\mathrm{c} + \Delta\boldsymbol{y}_\mathrm{f}^\mathrm{m} = \hat{\boldsymbol{y}}_\mathrm{f}^\mathrm{m}, \\
& \mathbf{1}^\mathrm{T}\boldsymbol{a}_\mathrm{m} \leq \mathsf{k}_\mathrm{m}, \\
& \underline{\Delta\boldsymbol{y}_\mathrm{f}^\mathrm{m}} \circ \boldsymbol{a}_\mathrm{m} \leq \Delta\boldsymbol{y}_\mathrm{f}^\mathrm{m} \leq \overline{\Delta\boldsymbol{y}_\mathrm{f}^\mathrm{m}} \circ \boldsymbol{a}_\mathrm{m}, \\
& \underline{\Delta\boldsymbol{u}_\mathrm{c}} \circ \boldsymbol{a}_\mathrm{c} \leq \Delta\boldsymbol{u}_\mathrm{c} \leq \overline{\Delta\boldsymbol{u}_\mathrm{c}} \circ \boldsymbol{a}_\mathrm{c}, \\
& \mathbf{Q}_\mathrm{f}\boldsymbol{u}_\mathrm{f} \leq \boldsymbol{q}_\mathrm{f}.
\end{aligned}
\tag{5.10}
$$

After solving the above LP for all $j \in \{1, ..., \hat{n}_z\}$, we obtain an upper bound for each entry of the vector mapped by $\check{\boldsymbol{z}}(\hat{\boldsymbol{y}}_\mathrm{f}^\mathrm{m})$. The control action $\hat{\boldsymbol{u}}_\mathrm{c}$ resulting from using these upper bounds in LP (5.9) is therefore more conservative compared to using the mapping $\check{\boldsymbol{z}}(\hat{\boldsymbol{y}}_\mathrm{f}^\mathrm{m})$ per se. However, the LP relaxation has worst-case polynomial complexity and is thus more efficient than MILP (5.8).

5.3 Discussion

This chapter showed how to compute admissible control laws $\hat{\boldsymbol{u}}_{\mathrm{c}} = \hat{\boldsymbol{k}}(\hat{\boldsymbol{y}}_{\mathrm{f}}^{\mathrm{m}})$ that, under some assumptions, not only handle uncertain exogenous actions, but also the unknown, undesired manipulation of at most k actuator and sensor signals. Those admissible control laws can be computed online by applying the framework and techniques proposed in Chapters 2 and 3. In particular, the two-stage online control law (2.14)–(3.29) has been extended to manage special observation-dependent uncertainty sets with distorted actuators and sensors via mixed-integer linear optimization techniques.

Here we remark that the control law (2.14)–(3.29) has been designed under the assumption that there exists an admissible control law $\hat{\boldsymbol{u}}_{\mathrm{c}} = \hat{\boldsymbol{k}}(\hat{\boldsymbol{y}}_{\mathrm{f}}^{\mathrm{m}})$ for the augmented system. In order to verify the existence of an admissible control law $\hat{\boldsymbol{u}}_{\mathrm{c}} = \hat{\boldsymbol{k}}(\hat{\boldsymbol{y}}_{\mathrm{f}}^{\mathrm{m}})$ prior to its actual implementation, a verification algorithm based on the QCQP proposed in Chapter 3 is still to be derived.

We identified several further venues for future investigations. The techniques proposed in this chapter can be extended to manage partially structured control laws, e.g., a setup where some actuators are controlled according to an affine control law and the remaining ones are controlled via online optimization. Another possible research direction is the incorporation of more complex attack models for the actuator and sensor signals, for instance a distortion model of the form $\boldsymbol{u}_{\mathrm{c}} = \boldsymbol{\Pi}\hat{\boldsymbol{u}}_{\mathrm{c}} + \Delta\boldsymbol{u}_{\mathrm{c}}$, or even a non-linear model $\boldsymbol{u}_{\mathrm{c}} = \varphi(\hat{\boldsymbol{u}}_{\mathrm{c}})$. While this thesis assumes that the non-negative integer k is known, the question of how to efficiently find the maximum possible value of k for which an admissible control exists still remains an open issue.

6 Stability of the Closed-loop Dynamics

The theory introduced in Chapter 2 characterizes admissible control laws for constrained static linear systems. This chapter investigates the synthesis of affine output feedback control laws for constrained LTI dynamic systems. More specifically, the desired control law has to guarantee the asymptotic stability of the resulting closed-loop system and also fulfill a set of operational constraints at steady state. We establish that such steady state constraints can be modeled based on the theory of Chapter 2. We also show that the synthesis of the desired affine output feedback control law can be achieved by integrating conditions for the asymptotic stability of the closed-loop system as additional constraints into the verification algorithms proposed in Chapter 3.

In the context of dynamic systems, the notions of *controllability* and *observability* introduced by Kalman in [121] are crucial for the design of modern control systems. Generally speaking, controllable systems can be steered from any initial state to any desired state in a finite time interval. Observable systems similarly allow the reconstruction of the exact initial state by observing the output of the system for a finite period of time.[1] While generally desirable, these conditions may often not be achievable for large, distributed systems, especially in situations with limited communication resources. Such situations might, for example, arise in smart power grids.

In this chapter, we investigate minimal realizations of affine output feedback control laws for continuous-time LTI dynamic systems. The affine control law has to guarantee the asymptotic stability of the resulting closed-loop system, i.e., that a steady state of the system is approached for constant external conditions. Instead of steering the final state to a single target point, we define a larger target region and guarantee that the steady state is within this region, without being able to exactly identify the final state given the available measurement information, see Fig. 6.1. The target region is defined through a set of linear inequalities. The inputs to the system, both the controlled ones as well as the disturbance inputs, are assumed to be bounded.

[1] Formal definitions for this notions are provided in the following.

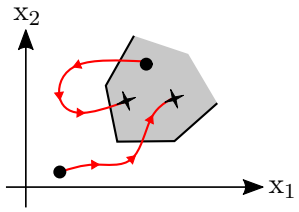

Figure 6.1: From any (typically unknown) starting point (circles), the closed-loop system converges for fixed external conditions to a steady state (crosses) guaranteed to be within the convex polyhedron (shaded).

Existing Approaches. Remarkably, a parametrization of all linear output feedback control laws which, if possible, asymptotically stabilize a given unconstrained, linear time-invariant system was obtained in [122]. A similar result for all $\mathcal{H}_\infty$ state feedback stabilization controllers for unconstrained LTI system was derived in [123].[2]

While traditional $\mathcal{H}_\infty$ output feedback synthesis methods already allow to balance stability and reference-tracking performance [124], they cannot straightforwardly integrate state or input constraints. This also applies to control energy minimizing approaches [60, 104]. When constraints are given, (stochastic) Model Predictive Control (MPC) methods are often used to compute state feedback policies that minimize a given cost function over time [125, 126]. MPC is usually combined with observers that estimate the state of the system based on measured outputs. In contrast, this thesis focuses on affine output feedback control laws not requiring observers.

Contrary to available control techniques based on invariant sets [71, 72], we do not restrict the state of the system to be within a pre-specified target region at all times, but only under steady state conditions. This may allow to design a control law requiring much fewer resources. Nevertheless, our design target is reasonable in many practical situations. For instance, in power systems, short-term violations of generator, transformer, or line capacity constraints are often be acceptable if the steady states are admissible [127, 128].

As indicated in Chapter 1, our investigations are also related to the field of process control. The idea of real-time optimization, dating from the 1990's, consists of designing a high-level controller that periodically computes economic optimal set points for lower-level controllers based on steady state system models [74, 30]. The optimal set points are computed by solving a constrained optimization problem that incorporates feedback information. The approach assumes that the plant (also known as the process) is asymptotically stable, i.e., a steady state exists, and that the time interval between to consecutive optimization steps is large enough for the plant to reach the steady state before the set points are recomputed [30]. RTO has been combined in multiple ways with MPC approaches [129, 130, 131], and recently with machine learning techniques [132, 133]. As

[2] In the field of robust control, $\mathcal{H}_\infty$ stabilization controllers are feedback control laws that not only guarantee the asymptotic stability of the resulting closed-loop system, but also minimize the performance criterion $\sup_{\mathbf{u}_\mathrm{f}(t)\neq 0}(\int_0^\infty \boldsymbol{\zeta}^\mathrm{T}(t)\boldsymbol{\zeta}(t)dt)(\int_0^\infty \mathbf{u}_\mathrm{f}^\mathrm{T}(t)\mathbf{u}_\mathrm{f}(t)dt)^{-1}$, which is specified in terms of the exogenous action $\mathbf{u}_\mathrm{f}(t)$ and the so-called performance outputs $\boldsymbol{\zeta}(t)$.

we will see below, we are not interested in determining optimal set points for the controllable quantities, but on verifying the existence of affine output feedback control laws that result in asymptotically stable closed-loop systems which always fulfill a set of operational constraints at steady state.

Another related line of work aims at bringing the output of the system to a steady state that is the solution of an optimization problem. Such methods encode the KKT conditions of the optimization problem as a dynamic system [134, 135], which allows to transform the optimal steady state problem into a closed-loop stabilization problem. This technique has been recently named *(linear-convex) Optimal Steady State (OSS) control* [136].

To close our brief review, we highlight recent developments in the field of *autonomous optimization* [137]. The idea of this online, almost model-free feedback optimization consist of collecting real-time state measurements at each time step, and then use them as feedback to a controller that incrementally drives the controllable quantities towards optimal set-points. The online optimization technique is based on projected primal-dual gradient flows [138, 139]. Autonomous optimization has already found potential applications in power systems [140].

In the following, we introduce the state space description of linear time-invariant systems controlled by affine output feedback control laws. We then study how to design the control law such that the resulting closed-loop system is asymptotically stable, and in addition fulfills a set of steady state operational constraints for constant external conditions. We show that the steady state requirements can be modeled by applying the ideas presented in Chapters 2 and 3.

6.1 Linear Time-Invariant Systems

Consider the continuous-time,[3] linear time-invariant (LTI) dynamic system

$$\begin{aligned} \dot{\mathbf{x}}(t) &= \mathbf{\Lambda}\mathbf{x}(t) + \mathbf{B}\mathbf{u}(t), \quad \mathbf{x}(0) = \mathbf{x}_0, \\ \mathbf{y}(t) &= \mathbf{C}\mathbf{x}(t), \end{aligned} \tag{6.1}$$

with time $t \in \mathbb{R}_{\geq 0}$, state $\mathbf{x} \in \mathbb{R}^{n_x}$, action $\mathbf{u} \in \mathbb{R}^{n_u}$, measurable output $\mathbf{y} \in \mathbb{R}^{n_y}$, and a priori known matrices $\mathbf{\Lambda} \in \mathbb{R}^{n_x \times n_x}$, $\mathbf{B} \in \mathbb{R}^{n_x \times n_u}$, and $\mathbf{C} \in \mathbb{R}^{n_y \times n_x}$.[4] We assume that the matrix $\mathbf{\Lambda}$ is invertible and that the pairs $(\mathbf{\Lambda}, \mathbf{B})$ and $(\mathbf{\Lambda}, \mathbf{C})$ are controllable and observable, respectively.

[3] While being out of the scope of this thesis, the controller design techniques proposed in the following are straightforwardly extendable to discrete-time LTI systems.

[4] Although we restrict our investigation to systems without feed-through terms (i.e., the observation $\mathbf{y}(t)$ does not depend explicitly on the action $\mathbf{u}(t)$), it is possible to extend the controller synthesis methods proposed below to such system class.

The LTI system (6.1) or the pair $(\mathbf{\Lambda}, \mathbf{B})$ is said to be controllable if, for every initial state $\mathbf{x}(0)$ and any final state $\mathbf{x}(T)$ with $T \in \mathbb{R}_{>0}$, there exists a trajectory for the input $\mathbf{u}(t)$ with $t \in [0, T]$ which transfers $\mathbf{x}(0)$ to $\mathbf{x}(T)$ for some time T.

Similarly, the system (6.1) or the pair $(\mathbf{\Lambda}, \mathbf{C})$ is said to be observable if any inital state $\mathbf{x}(0)$ can be uniquely determined from the knowledge of the output $\mathbf{y}(t)$ and the input $\mathbf{u}(t)$ for $t \in [0, T]$, where $T \in \mathbb{R}_{>0}$ is some finite time.

The controllability and observability of LTI systems can be verified by using the Kalman rank conditions [121]. Concretely, LTI system (6.1) is controllable and observable if and only if

$$\text{rank}\left(\begin{bmatrix}\mathbf{B} & \mathbf{\Lambda B} & \mathbf{\Lambda}^2\mathbf{B} & \dots & \mathbf{\Lambda}^{n_x-1}\mathbf{B}\end{bmatrix}\right) = n_x, \quad \text{rank}\left(\begin{bmatrix}\mathbf{C} \\ \mathbf{C\Lambda} \\ \mathbf{C\Lambda}^2 \\ \dots \\ \mathbf{C\Lambda}^{n_x-1}\end{bmatrix}\right) = n_x,$$

respectively. Since we assume that system is (6.1) controllable and observable, the pairs $(\mathbf{\Lambda}, \mathbf{B})$ and $(\mathbf{\Lambda}, \mathbf{C})$ fulfill the above conditions.

Following the approach introduced in Chapter 2, we now partition the action $\mathbf{u}$ into the control action $\mathbf{u}_\text{c}$, which is determined by the controller via a suitable control law, and the exogenous action $\mathbf{u}_\text{f}$, which is determined by other (cooperative or malicious) users. The indexes of those entries of vector $\mathbf{u}$ associated to the control action $\mathbf{u}_\text{c}$ are in the actuator set $\mathcal{C} \subseteq \{1, ..., n_u\}$. The dimensions of both $\mathbf{u}_\text{c}$ and $\mathbf{u}_\text{f}$ are thus given in terms of the total number of actuators available to the controller, i.e., $\mathbf{u}_\text{c} \in \mathbb{R}^{|\mathcal{C}|}$ and $\mathbf{u}_\text{f} \in \mathbb{R}^{n_u-|\mathcal{C}|}$. Similarly, we partition vector $\mathbf{y}$ into the measured output $\mathbf{y}^\text{m}$, which is used by the controller to determine the control action $\mathbf{u}_\text{c}$, and the unmeasured output $\mathbf{y}^\text{u}$, which is not required by the controller and may (not) be recorded in practice. The indexes of those entries of $\mathbf{y}$ associated to the measured output $\mathbf{y}^\text{m}$ are in the sensor set $\mathcal{M} \subseteq \{1, ..., n_y\}$. The dimensions of both $\mathbf{y}^\text{m}$ and $\mathbf{y}^\text{u}$ are hence determined by the total number of sensors accessible by the controller, i.e., $\mathbf{y}^\text{m} \in \mathbb{R}^{|\mathcal{M}|}$ and $\mathbf{y}^\text{m} \in \mathbb{R}^{n_y-|\mathcal{M}|}$.

The defined partitions of $\mathbf{u}$ and $\mathbf{y}$ allow us to partition matrices $\mathbf{B}$ and $\mathbf{C}$ along their columns or rows as well, yielding the LTI system representation

$$\begin{aligned}\dot{\mathbf{x}}(t) &= \mathbf{\Lambda}\mathbf{x}(t) + \mathbf{B}_\text{c}\mathbf{u}_\text{c}(t) + \mathbf{B}_\text{f}\mathbf{u}_\text{f}(t), \quad \mathbf{x}(0) = \mathbf{x}_0, \\ \begin{bmatrix}\mathbf{y}^\text{m}(t) \\ \mathbf{y}^\text{u}(t)\end{bmatrix} &= \begin{bmatrix}\mathbf{C}^\text{m}\mathbf{x}(t) \\ \mathbf{C}^\text{u}\mathbf{x}(t)\end{bmatrix},\end{aligned} \tag{6.2}$$

where the pair $(\mathbf{\Lambda}, \mathbf{B}_\text{c})$ is not necessarily controllable or the pair $(\mathbf{\Lambda}, \mathbf{C}^\text{m})$ observable.[5]

[5]Note that the existence of a stabilizing linear output feedback is guaranteed iff the pair $(\mathbf{\Lambda}, \mathbf{B}_\text{c})$ is *stabilizable* (i.e., the uncontrollable modes of the system are stable) and the pair $(\mathbf{\Lambda}, \mathbf{C}^\text{m})$ *detectable* (i.e., the unobservable modes of the system are stable) [141, 122]. This is a consequence of the separation principle valid for LTI systems [18].

At this point, we make the key assumption that the exogenous action $\mathbf{u}_{\mathrm{f}}(t)$ is constant, which by using the notation introduced in Chapter 2 means that $\mathbf{u}_{\mathrm{f}}(t) = \boldsymbol{u}_{\mathrm{f}}$. Further, we assume that the exogenous action $\boldsymbol{u}_{\mathrm{f}}$ is bounded by the convex polytope $\boldsymbol{\mathcal{U}}_{\mathrm{f}} = \{\boldsymbol{u}_{\mathrm{f}} \in \mathbb{R}^{n_u - |\mathcal{C}|} : \mathbf{Q}_{\mathrm{f}}\boldsymbol{u}_{\mathrm{f}} \leq \boldsymbol{q}_{\mathrm{f}}\}$, with parameters $\mathbf{Q}_{\mathrm{f}} \in \mathbb{R}^{l_{\mathrm{f}} \times (n_u - |\mathcal{C}|)}$ and $\boldsymbol{q}_{\mathrm{f}} \in \mathbb{R}^{l_{\mathrm{f}}}$. Although the exact value of the exogenous action $\boldsymbol{u}_{\mathrm{f}} \in \boldsymbol{\mathcal{U}}_{\mathrm{f}}$ is supposed to be unknown to the controller, we assume that the controller has knowledge of the set $\boldsymbol{\mathcal{U}}_{\mathrm{f}} \subset \mathbb{R}^{n_u - |\mathcal{C}|}$.

In this thesis, we restrict our analysis to the special case when the controller implements an affine output feedback control law of the form

$$\mathbf{u}_{\mathrm{c}}(t) = \mathbf{K}\mathbf{y}^{\mathrm{m}}(t) + \boldsymbol{w}. \tag{6.3}$$

with controller parameters $\mathbf{K} \in \mathbb{R}^{|\mathcal{C}| \times |\mathcal{M}|}$ and $\boldsymbol{w} \in \mathbb{R}^{|\mathcal{C}|}$.[6] The controller parameters $(\mathbf{K}, \boldsymbol{w})$ are to be chosen such that the resulting closed-loop system is asymptotically stable and the associated steady states are always feasible. A more detailed description of the meaning of these design requirements is provided next.

6.2 Asymptotic Stability in Closed-loop

The control law (6.3) has to guarantee the asymptotic stability of the closed-loop system that results from inserting (6.3) into LTI system (6.2), i.e.,

$$\begin{aligned} \dot{\mathbf{x}}(t) &= \tilde{\boldsymbol{\Lambda}}(\mathbf{K})\mathbf{x}(t) + \mathbf{B}_{\mathrm{c}}\boldsymbol{w} + \mathbf{B}_{\mathrm{f}}\boldsymbol{u}_{\mathrm{f}}, \quad \mathbf{x}(0) = \mathbf{x}_0, \\ \mathbf{y}^{\mathrm{m}}(t) &= \mathbf{C}^{\mathrm{m}}\mathbf{x}(t), \end{aligned} \tag{6.4}$$

where $\tilde{\boldsymbol{\Lambda}}(\mathbf{K}) = \boldsymbol{\Lambda} + \mathbf{B}_{\mathrm{c}}\mathbf{K}\mathbf{C}^{\mathrm{m}}$. Roughly speaking, the above closed-loop system is asymptotically stable if the trajectory of the state $\mathbf{x}(t)$ starting from $\mathbf{x}_0$ converges to a steady state $\boldsymbol{x} \in \mathbb{R}^{n_x}$, i.e., $\lim_{t\to\infty} \mathbf{x}(t) = \boldsymbol{x}$, independently of the value of the initial state $\mathbf{x}_0$ and of the constant actions $\boldsymbol{w}$ and $\boldsymbol{u}_{\mathrm{f}}$. The literature of dynamic systems and control offers a rich variety of criteria to verify the asymptotic stability of LTI systems, see for instance [142] and references therein for a detailed overview of current techniques. In this thesis, we focus on conditions for asymptotic stability in the time-domain. Concretely, we consider the asymptotic stability conditions established by Lyapunov [19] and as well as a condition based on the eigenvalues of the system matrix $\tilde{\boldsymbol{\Lambda}}(\mathbf{K})$. Investigations based on stability conditions defined in the Laplace-domain or the frequency-domain, i.e., those using transfer function matrix representations of LTI systems (e.g., Routh-Hurwitz criterion and Nyquist criterion [18], Popov criterion [143], among others), are thus not covered in the following and postponed to future research.[7]

[6] The matrix $\mathbf{K}$ is usually known in the literature of dynamic systems and control as the *gain matrix*. Likewise, the vector $\boldsymbol{w}$ is typically known as the *reference input*.

[7] A transfer function matrix describes the input-output behavior of a Multiple Input, Multiple Output (MIMO) LTI system in the Laplace domain. It is obtained by applying the Laplace transform to the differential equation (6.1) and assuming zero initial conditions, i.e., $\mathbf{x}_0 = \mathbf{0}$.

Theorem 11 ([144])**.** The autonomous system $\dot{\mathbf{x}}(t) = \tilde{\mathbf{\Lambda}}(\mathbf{K})\mathbf{x}(t)$ is asymptotically stable if and only if

$$\exists \mathbf{P} \in \mathbb{R}^{n_x \times n_x} : \mathbf{P} \succ \mathbf{0} \ \wedge \ \mathbf{P}\tilde{\mathbf{\Lambda}}(\mathbf{K}) + \tilde{\mathbf{\Lambda}}^{\mathrm{T}}(\mathbf{K})\mathbf{P} \prec \mathbf{0}. \tag{6.5}$$

The notation $\mathbf{P} \prec \mathbf{0}$ means that the matrix $\mathbf{P}$ is symmetric and negative definite, i.e., it is a symmetric matrix whose eigenvalues are all real, negative numbers. Similarly, the expression $\mathbf{P} \succ \mathbf{0}$ means that $\mathbf{P}$ is a symmetric, positive definite matrix.[8] Verifying the asymptotic stability of the closed-loop system (6.4) by applying Theorem 11 is in general a challenging task when the matrix $\mathbf{K}$ is unknown due to the bilinear form implied by inequalities (6.5). Moreover, the dimension of the above inequalities grows quadratically with the dimension of the state vector which in general limits the applicability of this technique to small- to medium-sized problem instances depending on the available computing equipment.[9]

An alternative to the aforementioned Lyapunov method is to verify the asymptotic stability of the closed-loop system (6.4) by using a condition given in terms of the *spectral abscissa* $\alpha(\mathbf{K}) : \mathbb{R}^{|\mathcal{C}|\times|\mathcal{M}|} \to \mathbb{R}$, which is defined according to [149] by

$$\alpha(\mathbf{K}) = \max_i \Re(\boldsymbol{\lambda}_i(\tilde{\mathbf{\Lambda}}(\mathbf{K}))), \tag{6.6}$$

where $\Re : \mathbb{C} \to \mathbb{R}$ is the real part operator and $\boldsymbol{\lambda}_i \in \mathbb{C}$ symbolizes the ith eigenvalue of $\tilde{\mathbf{\Lambda}}(\mathbf{K})$, with $i \in \{1, ..., n_x\}$.

Theorem 12 ([149])**.** The autonomous closed-loop system (6.4) is asymptotically stable if and only if the real part of the eigenvalues of $\tilde{\mathbf{\Lambda}}(\mathbf{K})$ is negative, i.e., $\alpha(\mathbf{K}) < 0$.

It has been shown that the spectral abscissa $\alpha(\mathbf{K})$ is a non-convex, non-smooth function of $\mathbf{K}$, which turns the design of a matrix $\mathbf{K}$ fulfilling $\alpha(\mathbf{K}) < 0$ into a challenging feasibility problem from a computational point of view. However, the feasibility problem can still be solved locally by using subgradient optimization algorithms like the Broyden–Fletcher–Goldfarb–Shanno (BFGS) algorithm [150], which has been shown to perform efficiently in many cases [149].

6.3 Steady State Admissibility

Additional to being asymptotically stable, the closed-loop LTI system (6.4) parametrized by $(\mathbf{K}, \boldsymbol{w})$ should fulfill a set of operational requirements at steady state (i.e., $\dot{\mathbf{x}}(t) = \mathbf{0}$).

To this end, first note that—under the assumption that the resulting closed-loop system is asymptotically stable and the exogenous action $\mathbf{u}_{\mathrm{f}}(t)$ is constant—the trajectories

[8] In order to test condition (6.5) by using numerical methods, we will consider the equivalent condition $\exists \mathbf{P} \in \mathbb{R}^{n_x \times n_x} : \mathbf{P} \succeq \epsilon\mathbf{I} \ \wedge \ \mathbf{P}\tilde{\mathbf{\Lambda}}(\mathbf{K}) + \tilde{\mathbf{\Lambda}}^{\mathrm{T}}(\mathbf{K})\mathbf{P} \preceq -\rho\mathbf{I}$ for some small $\epsilon, \rho \in \mathbb{R}_{>0}$.

[9] Note that, under appropriate assumptions, large-scale Lyapunov equations arising from, for instance, the Linear-Quadratic Regulator (LQR) problem [145], can be solved efficiently [146, 147, 148].

of the state $\mathbf{x}(t)$, the output $\mathbf{y}^{\mathrm{m}}(t)$, and the control action $\mathbf{u}_{\mathrm{c}}(t)$, will converge to constant values, i.e.,

$$\begin{aligned}\lim_{t\to\infty} \mathbf{x}(t) &= \boldsymbol{x},\\ \lim_{t\to\infty} \mathbf{y}^{\mathrm{m}}(t) &= \mathbf{C}^{\mathrm{m}}\boldsymbol{x} = \boldsymbol{y}^{\mathrm{m}},\\ \lim_{t\to\infty} \mathbf{u}_{\mathrm{c}}(t) &= \boldsymbol{u}_{\mathrm{c}} = \mathbf{K}\boldsymbol{y}^{\mathrm{m}} + \boldsymbol{w},\end{aligned}$$

where $\boldsymbol{y}^{\mathrm{m}} \in \mathbb{R}^{|\mathcal{M}|}$, and $\boldsymbol{u}_{\mathrm{c}} \in \mathbb{R}^{|\mathcal{C}|}$ represent the steady state values of $\mathbf{y}^{\mathrm{m}}$ and $\mathbf{u}_{\mathrm{c}}$, respectively. We can then constraint the steady state $\boldsymbol{x}$ of the closed-loop system to be always within the polyhedral region $\boldsymbol{\mathcal{X}} \subseteq \mathbb{R}^{n_x}$ defined by

$$\boldsymbol{\mathcal{X}} = \{\boldsymbol{x} \in \mathbb{R}^{n_x} : \mathbf{E}\boldsymbol{x} \leq \boldsymbol{b}\},$$

where the parameters $\mathbf{E} \in \mathbb{R}^{n_z \times n_x}$ and $\boldsymbol{b} \in \mathbb{R}^{n_z}$ are supposed to be known. If the system's steady state $\boldsymbol{x}$ fulfills this condition, then we say that $\boldsymbol{x}$ is feasible. Following the ideas proposed in Chapter 2, we now transform the feasibility condition on the steady state into admissibility conditions for the affine control law (6.3) at steady state as follows.

Since we assume that the exogenous action is constant ($\mathbf{u}_{\mathrm{f}}(t) = \boldsymbol{u}_{\mathrm{f}}$) and bounded by $\boldsymbol{\mathcal{U}}_{\mathrm{f}}$, and that the system matrix $\boldsymbol{\Lambda}$ is invertible, we can always express the steady state $\boldsymbol{x}$ in terms of the constant actions $(\boldsymbol{u}_{\mathrm{c}}, \boldsymbol{u}_{\mathrm{f}})$. This is because from the steady state condition $\dot{\mathbf{x}}(t) = \mathbf{0}$ we readily derive

$$\boldsymbol{x} = -\boldsymbol{\Lambda}^{-1}(\mathbf{B}_{\mathrm{c}}\boldsymbol{u}_{\mathrm{c}} + \mathbf{B}_{\mathrm{f}}\boldsymbol{u}_{\mathrm{f}}) \tag{6.7}$$

The steady state condition (6.7) can now be exploited to express the linear inequalities $\mathbf{E}\boldsymbol{x} \leq \boldsymbol{b}$ defining the feasible region $\boldsymbol{\mathcal{X}}$ as well as the steady state observation $\boldsymbol{y}^{\mathrm{m}}$ uniquely in terms of the constant actions $(\boldsymbol{u}_{\mathrm{c}}, \boldsymbol{u}_{\mathrm{f}})$, i.e.,

$$\begin{aligned}\mathbf{E}\boldsymbol{x} \leq \boldsymbol{b} \Rightarrow \underbrace{-\mathbf{E}\boldsymbol{\Lambda}^{-1}\mathbf{B}_{\mathrm{c}}}_{\mathbf{A}_{\mathrm{c}}}\boldsymbol{u}_{\mathrm{c}} + \underbrace{(-\mathbf{E}\boldsymbol{\Lambda}^{-1}\mathbf{B}_{\mathrm{f}})}_{\mathbf{A}_{\mathrm{f}}}\boldsymbol{u}_{\mathrm{f}} \leq \boldsymbol{b},\\ \boldsymbol{y}^{\mathrm{m}} = \mathbf{C}^{\mathrm{m}}\boldsymbol{x} = \underbrace{(-\mathbf{C}^{\mathrm{m}}\boldsymbol{\Lambda}^{-1}\mathbf{B}_{\mathrm{c}})}_{\mathbf{M}^{\mathrm{m}}_{\mathrm{c}}}\boldsymbol{u}_{\mathrm{c}} + \underbrace{(-\mathbf{C}^{\mathrm{m}}\boldsymbol{\Lambda}^{-1}\mathbf{B}_{\mathrm{f}})}_{\mathbf{M}^{\mathrm{m}}_{\mathrm{f}}}\boldsymbol{u}_{\mathrm{f}}.\end{aligned} \tag{6.8}$$

Observe how the above steady state representation matches the constrained linear system representation introduced in Chapter 2.

Remark 10. For singular $\boldsymbol{\Lambda}$, the approach can be extended via the Moore–Penrose pseudo inverse $\boldsymbol{\Lambda}^{+}$, if the kernel of $\boldsymbol{\Lambda}$ is also in the kernel of $\mathbf{C}^{\mathrm{m}}$ and $\mathbf{E}$. This assumption is fulfilled, e.g., for the power system application examples of Chapter 7.

From the above algebraic manipulations, we conclude that constraining the steady state $\boldsymbol{x}$ to always lie in the convex polyhedron $\boldsymbol{\mathcal{X}}$ is equivalent to restrict the controller parameters $(\mathbf{K}, \boldsymbol{w})$ to fulfill the condition

$$\forall \boldsymbol{u}_{\mathrm{f}} \in \boldsymbol{\mathcal{U}}_{\mathrm{f}} : \mathbf{A}_{\mathrm{c}}\mathbf{K}\boldsymbol{y}^{\mathrm{m}} + \mathbf{A}_{\mathrm{c}}\boldsymbol{w} + \mathbf{A}_{\mathrm{f}}\boldsymbol{u}_{\mathrm{f}} \leq \boldsymbol{b} \ \wedge \mathbf{K}\boldsymbol{y}^{\mathrm{m}} + \boldsymbol{w} \in \boldsymbol{\mathcal{U}}_{\mathrm{c}}, \tag{6.9}$$

where $\boldsymbol{y}^{\mathrm{m}} = \mathbf{M}_{\mathrm{c}}^{\mathrm{m}}\mathbf{K}\boldsymbol{y}^{\mathrm{m}} + \mathbf{M}_{\mathrm{c}}^{\mathrm{m}}\boldsymbol{w} + \mathbf{M}_{\mathrm{f}}^{\mathrm{m}}\boldsymbol{u}_{\mathrm{f}}$ and $\boldsymbol{\mathcal{U}}_{\mathrm{c}} \subset \mathbb{R}^{|\mathcal{C}|}$ is a pre-specified set containing all admissible values for the control action at steady state. Observe that condition (6.9) is exactly the same as the presented in Corollary 4. As we know from the theory of admissible control laws proposed in Chapter 2, we can map the steady state control law $\boldsymbol{u}_{\mathrm{c}} = \mathbf{K}\boldsymbol{y}^{\mathrm{m}} + \boldsymbol{w}$ to an equivalent steady state control law of the form $\boldsymbol{u}_{\mathrm{c}} = \hat{\mathbf{K}}\mathbf{M}_{\mathrm{f}}^{\mathrm{m}}\boldsymbol{u}_{\mathrm{f}} + \hat{\boldsymbol{w}}$, namely,

$$\begin{aligned} & \boldsymbol{u}_{\mathrm{c}} = \mathbf{K}\boldsymbol{y}^{\mathrm{m}} + \boldsymbol{w}, \\ \Rightarrow\ & \boldsymbol{u}_{\mathrm{c}} = \mathbf{K}(\mathbf{M}_{\mathrm{c}}^{\mathrm{m}}\boldsymbol{u}_{\mathrm{c}} + \mathbf{M}_{\mathrm{f}}^{\mathrm{m}}\boldsymbol{u}_{\mathrm{f}}) + \boldsymbol{w}, \\ \Rightarrow\ & \boldsymbol{u}_{\mathrm{c}} = \hat{\mathbf{K}}\underbrace{\mathbf{M}_{\mathrm{f}}^{\mathrm{m}}\boldsymbol{u}_{\mathrm{f}}}_{\boldsymbol{y}_{\mathrm{f}}^{\mathrm{m}}} + \hat{\boldsymbol{w}}. \end{aligned}$$

with

$$\hat{\mathbf{K}} = (\mathbf{I} - \mathbf{K}\mathbf{M}_{\mathrm{c}}^{\mathrm{m}})^{-1}\mathbf{K}, \quad \hat{\boldsymbol{w}} = (\mathbf{I} - \mathbf{K}\mathbf{M}_{\mathrm{c}}^{\mathrm{m}})^{-1}\boldsymbol{w}, \tag{6.10}$$

and $(\mathbf{I} - \mathbf{K}\mathbf{M}_{\mathrm{c}}^{\mathrm{m}})^{-1}$ supposed to be an invertible matrix. Condition (6.9) is thus equivalent to the more simpler condition

$$\forall \boldsymbol{u}_{\mathrm{f}} \in \boldsymbol{\mathcal{U}}_{\mathrm{f}} :\ (\mathbf{A}_{\mathrm{c}}\hat{\mathbf{K}}\mathbf{M}_{\mathrm{f}}^{\mathrm{m}} + \mathbf{A}_{\mathrm{f}})\boldsymbol{u}_{\mathrm{f}} + \mathbf{A}_{\mathrm{c}}\hat{\boldsymbol{w}} \leq \boldsymbol{b}\ \wedge\ \hat{\mathbf{K}}\mathbf{M}_{\mathrm{f}}^{\mathrm{m}}\boldsymbol{u}_{\mathrm{f}} + \hat{\boldsymbol{w}} \in \boldsymbol{\mathcal{U}}_{\mathrm{c}}. \tag{6.11}$$

which is exactly the same as condition (3.1).

6.4 Controller Synthesis

With the conditions introduced in Sections 6.2 and 6.3 we now address the problem of finding suitable controller parameters $(\mathbf{K}, \boldsymbol{w})$ for which the affine output feedback control law (6.3) always guarantees the asymptotic stability of the resulting closed-loop system and also a feasible steady state.[10] To this end, we propose to solve the following non-convex, infinite dimensional feasibility problem

Problem 2. Find, if possible, $\mathbf{K} \in \mathbb{R}^{|\mathcal{C}|\times|\mathcal{M}|}$ and $\boldsymbol{w} \in \mathbb{R}^{|\mathcal{C}|}$ such that

$$\begin{aligned} & \dot{\mathbf{x}}(t) = \tilde{\boldsymbol{\Lambda}}(\mathbf{K})\mathbf{x}(t) \text{ is asymptotically stable } \wedge \\ & \mathbf{K}\boldsymbol{y}^{\mathrm{m}} + \boldsymbol{w} \in \boldsymbol{\mathcal{U}}_{\mathrm{c}}, \quad \forall \boldsymbol{u}_{\mathrm{f}} \in \boldsymbol{\mathcal{U}}_{\mathrm{f}} \wedge \\ & \mathbf{A}_{\mathrm{c}}\mathbf{K}\boldsymbol{y}^{\mathrm{m}} + \mathbf{A}_{\mathrm{c}}\boldsymbol{w} + \mathbf{A}_{\mathrm{f}}\boldsymbol{u}_{\mathrm{f}} \leq \boldsymbol{b}, \quad \forall \boldsymbol{u}_{\mathrm{f}} \in \boldsymbol{\mathcal{U}}_{\mathrm{f}}. \end{aligned}$$

with $\boldsymbol{y}^{\mathrm{m}} = \mathbf{M}_{\mathrm{c}}^{\mathrm{m}}\mathbf{K}\boldsymbol{y}^{\mathrm{m}} + \mathbf{M}_{\mathrm{c}}^{\mathrm{m}}\boldsymbol{w} + \mathbf{M}_{\mathrm{f}}^{\mathrm{m}}\boldsymbol{u}_{\mathrm{f}}$.

Although the above feasibility problem is computationally challenging, we show in the following that under some assumptions it can be solved at least locally. Concretely,

[10] Although having both a stabilizable pair $(\boldsymbol{\Lambda}, \mathbf{B}_{\mathrm{c}})$ and a detectable pair $(\boldsymbol{\Lambda}, \mathbf{C}^{\mathrm{m}})$ guarantees the existence of a gain matrix $\mathbf{K}$ for which the resulting closed-loop system is asymptotically stable, this does not necessarily imply the existence of a gain matrix for which the closed-loop system additionally fulfills the steady state constraints.

we consider the particular case where the sets $\boldsymbol{\mathcal{U}}_{\mathrm{c}}$ and $\boldsymbol{\mathcal{U}}_{\mathrm{f}}$ are hypercubes, i.e.,

$$\boldsymbol{\mathcal{U}}_{\mathrm{c}} = \{\boldsymbol{u}_{\mathrm{c}} \in \mathbb{R}^{|\mathcal{C}|} : \underline{\boldsymbol{u}}_{\mathrm{c}} \leq \boldsymbol{u}_{\mathrm{c}} \leq \overline{\boldsymbol{u}}_{\mathrm{c}}\},$$
$$\boldsymbol{\mathcal{U}}_{\mathrm{f}} = \{\boldsymbol{u}_{\mathrm{f}} \in \mathbb{R}^{n_u - |\mathcal{C}|} : \underline{\boldsymbol{u}}_{\mathrm{f}} \leq \boldsymbol{u}_{\mathrm{f}} \leq \overline{\boldsymbol{u}}_{\mathrm{f}}\}.$$

This allows us to extend the LP verification algorithm (3.18) to consider also the asymptotic stability of the closed-loop system. Here it is important to note that the problem formulations presented below can also be extended to other shapes of $\boldsymbol{\mathcal{U}}_{\mathrm{c}}$ or $\boldsymbol{\mathcal{U}}_{\mathrm{f}}$, e.g., arbitrary convex polytopes or p-norm-shaped sets. To this end, the methods proposed in Section 3.1 can be used as a starting point.

6.4.1 Synthesis Algorithm Based on Lyapunov Stability Conditions

We now present an algorithm that solves Problem 2 when the Lyapunov condition (6.5) for the asymptotic stability of the closed-loop dynamics is used. Similar to the techniques presented in Chapter 3, we first introduce the feasibility indicator $\eta \in \mathbb{R}$ and formulate Problem 2 as an optimization problem. By incorporating inequalities (6.5) together with the expressions (6.10) into problem (3.4), we obtain the infinite dimensional feasibility problem

$$\begin{aligned}
\min_{\mathbf{K},\boldsymbol{w},\hat{\mathbf{K}},\hat{\boldsymbol{w}},\mathbf{P},\eta} \quad & \eta \\
\text{s.t. } & \mathbf{P}\tilde{\boldsymbol{\Lambda}}(\mathbf{K}) + \tilde{\boldsymbol{\Lambda}}^{\mathrm{T}}(\mathbf{K})\mathbf{P} \preceq \mathbf{0}, \\
& (\mathbf{A}_{\mathrm{c}}\hat{\mathbf{K}}\mathbf{M}_{\mathrm{f}}^{\mathrm{m}} + \mathbf{A}_{\mathrm{f}})\boldsymbol{u}_{\mathrm{f}} + \mathbf{A}_{\mathrm{c}}\hat{\boldsymbol{w}} \leq \boldsymbol{b} + \eta\mathbf{1}, \quad \forall \boldsymbol{u}_{\mathrm{f}} \in \boldsymbol{\mathcal{U}}_{\mathrm{f}}, \\
& \hat{\mathbf{K}}\mathbf{M}_{\mathrm{f}}^{\mathrm{m}}\boldsymbol{u}_{\mathrm{f}} + \hat{\boldsymbol{w}} \in \boldsymbol{\mathcal{U}}_{\mathrm{c}}, \quad \forall \boldsymbol{u}_{\mathrm{f}} \in \boldsymbol{\mathcal{U}}_{\mathrm{f}}, \\
& (\mathbf{I} - \mathbf{K}\mathbf{M}_{\mathrm{c}}^{\mathrm{m}})\hat{\mathbf{K}} = \mathbf{K}, \\
& (\mathbf{I} - \mathbf{K}\mathbf{M}_{\mathrm{c}}^{\mathrm{m}})\hat{\boldsymbol{w}} = \boldsymbol{w}, \\
& \mathbf{P} \succeq \mathbf{0}, \\
& \mathbf{P} \in \mathbb{R}^{n_x \times n_x}, \quad \mathbf{K}, \hat{\mathbf{K}} \in \mathbb{R}^{|\mathcal{C}| \times |\mathcal{M}|}, \quad \boldsymbol{w}, \hat{\boldsymbol{w}} \in \mathbb{R}^{|\mathcal{C}|}, \quad \eta \in \mathbb{R}.
\end{aligned} \tag{6.12}$$

If $\eta \leq 0$ holds, then the existence of an affine output feedback control law solving Problem 2 is guaranteed. The above non-convex problem is an infinite dimensional bilinear matrix inequality. It can, however, be solved locally as we show next.

Under the assumption that both $\boldsymbol{\mathcal{U}}_{\mathrm{c}}$ and $\boldsymbol{\mathcal{U}}_{\mathrm{f}}$ are hypercubes, we now propose an algorithm that determines, if possible, the controller parameters $\mathbf{K}$ and $\boldsymbol{w}$. The algorithm is schematically represented in Fig. 6.2.

First, we ignore the constraints related to the asymptotic stability of the closed-loop system, i.e., we solve LP (3.18) and compute the value of the controller parameters $(\mathbf{K}, \boldsymbol{w})$ afterwards via expressions (6.10). Note that computing the affine control law via the LP (3.18) does not guarantee the asymptotic stability of the resulting closed-loop system as can be shown by counterexample. However, the obtained solution can be used to check for the largest real part of the eigenvalues of $\tilde{\boldsymbol{\Lambda}}(\mathbf{K})$. If the resulting

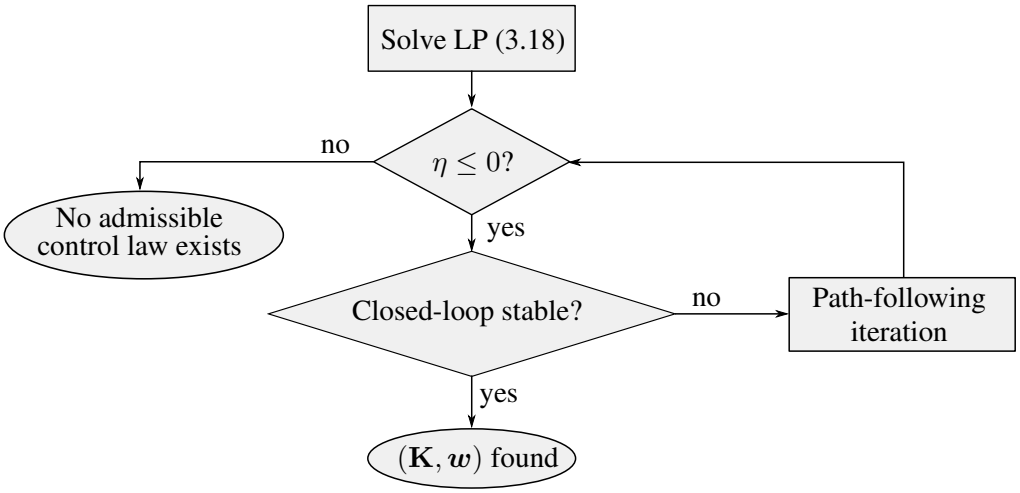

Figure 6.2: Proposed algorithm for the design of an admissible affine control law.

closed-loop system results asymptotically stable, then we stop the algorithm since the solution of LP (3.18) already solves Problem 2. In our simulation experiments we verified that asymptotically stable configurations are obtained in many cases, specially if the autonomous system $\dot{\mathbf{x}}(t) = \mathbf{\Lambda}\mathbf{x}(t)$ is already asymptotically stable.

For those cases where the resulting closed-loop system is not asymptotically stable, we can still use the solution of LP (3.18) as an starting point for solving the BMI

$$
\begin{aligned}
\min_{\mathbf{K},\boldsymbol{w},\hat{\mathbf{K}},\hat{\boldsymbol{w}},\mathbf{H},\mathbf{P},\eta} \quad & \eta \\
\text{s.t. } & \mathbf{H}\mathbf{1} + \tilde{\mathbf{A}}_{\mathrm{c}}\hat{\boldsymbol{w}} \leq \tilde{\boldsymbol{b}} + \eta\mathbf{1}, \\
& H_{ij} \geq \tilde{A}_{ij}(\hat{\mathbf{K}})\overline{u}_{\mathrm{f}j}, \quad \forall i \in \{1,...,\hat{n}_z\},\ \forall j \in \{1,...,n_u - |\mathcal{C}|\}, \\
& H_{ij} \geq \tilde{A}_{ij}(\hat{\mathbf{K}})\underline{u}_{\mathrm{f}j}, \quad \forall i \in \{1,...,\hat{n}_z\},\ \forall j \in \{1,...,n_u - |\mathcal{C}|\}, \\
& (\mathbf{I} - \mathbf{K}\mathbf{M}_{\mathrm{c}}^{\mathrm{m}})\hat{\mathbf{K}} = \mathbf{K}, \\
& (\mathbf{I} - \mathbf{K}\mathbf{M}_{\mathrm{c}}^{\mathrm{m}})\hat{\boldsymbol{w}} = \boldsymbol{w}, \\
& \mathbf{P}\tilde{\mathbf{\Lambda}}(\mathbf{K}) + \tilde{\mathbf{\Lambda}}^{\mathrm{T}}(\mathbf{K})\mathbf{P} \preceq \mathbf{0}, \\
& \mathbf{P} \succeq \mathbf{0}, \\
& \mathbf{P} \in \mathbb{R}^{n_x \times n_x}, \quad \mathbf{K}, \hat{\mathbf{K}} \in \mathbb{R}^{|\mathcal{C}| \times |\mathcal{M}|}, \quad \boldsymbol{w}, \hat{\boldsymbol{w}} \in \mathbb{R}^{|\mathcal{C}|}, \\
& \mathbf{H} \in \mathbb{R}^{\hat{n}_z \times (n_u - |\mathcal{C}|)}, \quad \eta \in \mathbb{R},
\end{aligned}
\tag{6.13}
$$

with $\hat{n}_z = n_z + 2|\mathcal{C}|$, $\tilde{\mathbf{A}}(\hat{\mathbf{K}}) = \tilde{\mathbf{A}}_{\mathrm{c}}\hat{\mathbf{K}}\mathbf{M}_{\mathrm{f}}^{\mathrm{m}} + \tilde{\mathbf{A}}_{\mathrm{f}}$ and

$$
\tilde{\mathbf{A}}_{\mathrm{c}} = \begin{bmatrix} \mathbf{A}_{\mathrm{c}} \\ \mathbf{I} \\ -\mathbf{I} \end{bmatrix}, \quad \tilde{\mathbf{A}}_{\mathrm{f}} = \begin{bmatrix} \mathbf{A}_{\mathrm{f}} \\ \mathbf{0} \\ \mathbf{0} \end{bmatrix}, \quad \tilde{\boldsymbol{b}} = \begin{bmatrix} \boldsymbol{b} \\ \overline{\boldsymbol{u}}_{\mathrm{c}} \\ -\underline{\boldsymbol{u}}_{\mathrm{c}} \end{bmatrix}. \tag{6.14}
$$

Note that the above formulation is obtained simply by including the Lyapunov inequalities (6.5) into LP (3.18).

BMI (6.13) is in general a difficult optimization task due to the non-convexity of 1) the Lyapunov stability inequalities in $\mathbf{P}$ and $\mathbf{K}$, and 2) the equality constraints associated to the gain matrices $\mathbf{K}$ and $\hat{\mathbf{K}}$. However, it can still be optimized locally. To this end, methods like the P-K iteration [142] or path-following [151], have been proposed in the literature. Note there are some special cases in which the BMI condition (6.5) can be reduced to a sufficient but not necessary LMI [152]. The interested reader is referred to [142] and the references therein for detailed information about output feedback stabilization techniques.

In this work, we adapt the *path-following* method proposed by [151] and iteratively improve the stability of the closed-loop system. The method assumes that the actuators have limited authority, and hence shift the eigenvalues of the system only slightly in one step. This enables us to solve a linearized form of (6.13) in each iteration as a convex linear matrix inequality (LMI).

First, we take the solution of LP (3.18) as initial guess, obtaining the initial values $\hat{\mathbf{K}}_0$, $\hat{\boldsymbol{w}}_0$. Using equations (6.10), we then compute initial values for the controller parameters $\mathbf{K}_0$ and $\boldsymbol{w}_0$. Next, we analyze the effect of *small* perturbations around $\hat{\mathbf{K}}_0$, $\hat{\boldsymbol{w}}_0$, $\mathbf{K}_0$, and $\boldsymbol{w}_0$ on equations (6.10). We thus consider the substitutions

$$\begin{aligned} \hat{\mathbf{K}} &= \hat{\mathbf{K}}_0 + \delta\hat{\mathbf{K}}, \qquad & \mathbf{K} &= \mathbf{K}_0 + \delta\mathbf{K}, \\ \hat{\boldsymbol{w}} &= \hat{\boldsymbol{w}}_0 + \delta\hat{\boldsymbol{w}}, \qquad & \boldsymbol{w} &= \boldsymbol{w}_0 + \delta\boldsymbol{w}, \end{aligned} \tag{6.15}$$

where the δ-terms represent such small perturbations. By applying substitutions (6.15) on equations (6.10), we obtain linear relations with respect to the perturbation terms, i.e.,

$$\begin{aligned} (\mathbf{I} - \mathbf{K}_0\mathbf{M}_{\mathrm{c}}^{\mathrm{m}})\delta\hat{\mathbf{K}} &= \delta\mathbf{K}(\mathbf{I} + \mathbf{M}_{\mathrm{c}}^{\mathrm{m}}\hat{\mathbf{K}}_0), \\ \mathbf{K}_0\mathbf{M}_{\mathrm{c}}^{\mathrm{m}}\delta\hat{\boldsymbol{w}} &= -\delta\mathbf{K}\mathbf{M}_{\mathrm{c}}^{\mathrm{m}}\hat{\boldsymbol{w}}_0. \end{aligned} \tag{6.16}$$

Although $\mathbf{K}_0$ yields initially an unstable closed-loop system $\tilde{\mathbf{\Lambda}}_0 = \tilde{\mathbf{\Lambda}}(\mathbf{K}_0)$, we can still find a Lyapunov matrix $\mathbf{P}_0 \in \mathbb{R}^{n_x \times n_x}$ that proofs its largest growth rate, which is determined by the maximum real part over all eigenvalues of $\tilde{\mathbf{\Lambda}}_0$, here denoted by $\rho_0 \in \mathbb{R}$. For small $\epsilon > 0$ we can find $\mathbf{P}_0$ by solving the LMI [151]

$$\begin{aligned} \min_{\kappa \in \mathbb{R}_{\geq 0}, \mathbf{P}_0 \in \mathbb{R}^{n_x \times n_x}} \quad & \kappa \\ \text{s.t. } & \mathbf{I} \preceq \mathbf{P}_0 \preceq \kappa\mathbf{I}, \\ & \tilde{\mathbf{\Lambda}}_0^{\mathrm{T}}\mathbf{P}_0 + \mathbf{P}_0\tilde{\mathbf{\Lambda}}_0 \preceq -2(\rho_0 - \epsilon)\mathbf{P}_0, \end{aligned}$$

where the scalar optimization variable κ ensures that the obtained $\mathbf{P}_0$ has the smallest condition number.[11] We can now linearize Lyapunov inequality (6.5) by introducing the

[11] The condition number of a matrix $\mathbf{P}$ is defined by $\sigma_{\max}(\mathbf{P})/\sigma_{\min}(\mathbf{P})$, where $\sigma_{\max}(\mathbf{P})$ and $\sigma_{\min}(\mathbf{P})$ are the maximal and minimal singular values of $\mathbf{P}$, respectively

substitutions $\mathbf{P} = \mathbf{P}_0 + \delta\mathbf{P}$, $\rho = \rho_0 + \delta\rho$, and neglecting second order perturbation terms. We obtain

$$\begin{aligned}&\tilde{\mathbf{\Lambda}}_0^{\mathrm{T}}(\mathbf{P}_0 + \delta\mathbf{P}) + (\mathbf{P}_0 + \delta\mathbf{P})\tilde{\mathbf{\Lambda}}_0^{\mathrm{T}} + \mathbf{P}_0\mathbf{B}_{\mathrm{c}}\delta\mathbf{K}\mathbf{C}^{\mathrm{m}} + \\ &(\mathbf{B}_{\mathrm{c}}\delta\mathbf{K}\mathbf{C}^{\mathrm{m}})^{\mathrm{T}}\mathbf{P}_0 \preceq -2\rho(\mathbf{P}_0 + \delta\mathbf{P}) - 2\delta\rho\ \delta\mathbf{P}_0.\end{aligned} \tag{6.17}$$

where $\delta\rho$ is fixed and chosen to be *small*.

This results in the following semidefinite feasibility program

$$\begin{aligned}\min_{\eta,\mathbf{H},\delta\hat{\mathbf{K}},\delta\hat{\boldsymbol{w}},\delta\mathbf{K},\delta\mathbf{P}}\quad & \eta \\ \text{s.t. } & \mathbf{H}\mathbf{1} + \tilde{\mathbf{A}}_{\mathrm{c}}\hat{\boldsymbol{w}} \leq \tilde{\boldsymbol{b}} + \eta\mathbf{1}, \\ & H_{ij} \geq \tilde{A}_{ij}(\hat{\mathbf{K}})\overline{u}_{\mathrm{f}j}, \quad \forall i \in \{1,...,\hat{n}_z\},\ \forall j \in \{1,...,n_u - |\mathcal{C}|\}, \\ & H_{ij} \geq \tilde{A}_{ij}(\hat{\mathbf{K}})\underline{u}_{\mathrm{f}j}, \quad \forall i \in \{1,...,\hat{n}_z\},\ \forall j \in \{1,...,n_u - |\mathcal{C}|\}, \\ & \text{Equalities (6.16)}, \\ & \text{Inequality (6.17)}, \\ & \mathbf{P}_0 + \delta\mathbf{P} \succeq \mathbf{0}.\end{aligned} \tag{6.18}$$

In case we obtain an admissible solution, i.e., $\eta \leq 0$, we update the controller parameters according to the obtained perturbations. This process is repeated iteratively until an asymptotically stable closed-loop system is obtained. If LMI (6.18) is infeasible or the optimal value of η fulfills $\eta > 0$, the process is stopped since there is no affine control law solving Problem 2. In (6.13), the size of the matrix $\mathbf{P}$ and of its associated nonconvex (bi)linear matrix inequalities grows quadratically with the dimension of the state $\mathbf{x}$, which makes the proposed algorithm suited only for small- to medium-sized instances of Problem 2 depending on the computing equipment.

6.4.2 Simplifying the Synthesis Algorithm

The design technique proposed in the previous section can be simplified by designing the affine controller entirely in terms of the transformed parameters $\hat{\mathbf{K}}$ and $\hat{\boldsymbol{w}}$, and then recover the original parameters $\mathbf{K}$ and $\boldsymbol{w}$ via equations (6.10) only afterwards. Such approach will remove the variables $\mathbf{K}$ and $\boldsymbol{w}$ together with the equalities (6.10) from the optimization algorithm. However, to this end, we have to find a closed-loop system representation depending linearly on $\hat{\mathbf{K}}$, so that the resulting Lyapunov stability conditions can then be used in the path-following stage of the algorithm shown in Fig. 6.2.

In the following, we show that the relation between the gain matrices $\mathbf{K}$ and $\hat{\mathbf{K}}$ given in (6.10) can be exploited to obtain an autonomous closed-loop system that depends linearly on $\hat{\mathbf{K}}$ and is asymptotically stable if and only if the autonomous closed-loop system $\dot{\mathbf{x}}(t) = (\mathbf{\Lambda} + \mathbf{B}_{\mathrm{c}}\mathbf{K}\mathbf{C}^{\mathrm{m}})\mathbf{x}(t)$ is asymptotically stable, and vice versa.

This finding is based on the following well-known results.

Lemma 1. Let $\mathbf{W} \in \mathbb{R}^{n_x \times n_x}$ be an invertible matrix. Then,

- The eigenvalues of $\mathbf{W}^{-1}$ correspond to the reciprocal eigenvalues of $\mathbf{W}$.
- Both $\mathbf{W}$ and $\mathbf{W}^{-1}$ have the same eigenvectors.

Proof. Let $\boldsymbol{\lambda} \in \mathbb{C}$ be an eigenvalue of $\mathbf{W}$ with associated eigenvector $\boldsymbol{v} \in \mathbb{C}^{n_x}$. Note that $\boldsymbol{\lambda} = 0$ is impossible since the matrix $\mathbf{W}$ is invertible. Thus, by definition

$$\mathbf{W}\boldsymbol{v} = \boldsymbol{\lambda}\boldsymbol{v} \iff \boldsymbol{v} = \boldsymbol{\lambda}\mathbf{W}^{-1}\boldsymbol{v} \iff \frac{1}{\boldsymbol{\lambda}}\boldsymbol{v} = \mathbf{W}^{-1}\boldsymbol{v}.$$

We clearly observe that $1/\boldsymbol{\lambda}$ is an eigenvalue of $\mathbf{W}^{-1}$, with $\boldsymbol{v}$ as associated eigenvector. □

Lemma 2. Let $\boldsymbol{\lambda} \in \mathbb{C}$. Then $\operatorname{sign}(\Re(\boldsymbol{\lambda})) = \operatorname{sign}(\Re(1/\boldsymbol{\lambda}))$.

Proof. Let $\boldsymbol{\lambda} = a + \mathrm{j}c$ with $a, c \in \mathbb{R}$, and $\mathrm{j} = \sqrt{-1}$. Then, $1/\boldsymbol{\lambda} = 1/(a + \mathrm{j}c) = (a - \mathrm{j}c)/(a^2 + c^2)$. The sign of the real parts of $\boldsymbol{\lambda}$ and $1/\boldsymbol{\lambda}$ is thus determined by the sign of a, i.e., $\operatorname{sign}(\Re(\boldsymbol{\lambda})) = \operatorname{sign}(a) = \operatorname{sign}(\Re(1/\boldsymbol{\lambda}))$. □

Lemmas 1 and 2 allow us to map a closed-loop LTI system given in terms of the gain matrix $\mathbf{K}$ to an equivalent closed-loop system that depends linearly on the gain matrix $\hat{\mathbf{K}}$.

Theorem 13. Let $\hat{\mathbf{K}} = (\mathbf{I} - \mathbf{K}\mathbf{M}_{\mathrm{c}}^{\mathrm{m}})^{-1}\mathbf{K}$. The autonomous closed-loop system

$$\dot{\mathbf{x}}(t) = (\boldsymbol{\Lambda} + \mathbf{B}_{\mathrm{c}}\mathbf{K}\mathbf{C}^{\mathrm{m}})\mathbf{x}(t) \tag{6.19}$$

is asymptotically stable if and only if the autonomous closed-loop system

$$\frac{d\hat{\mathbf{x}}(t)}{dt} = (\boldsymbol{\Lambda}^{-1} - \boldsymbol{\Lambda}^{-1}\mathbf{B}_{\mathrm{c}}\hat{\mathbf{K}}\mathbf{C}^{\mathrm{m}}\boldsymbol{\Lambda}^{-1})\hat{\mathbf{x}}(t) \tag{6.20}$$

is asymptotically stable.

Proof. First, we rewrite (6.19) into a form that involves the inverse system matrix given in (6.20). Then, we use Lemmas 1 and 2 to show that the asymptotic stability of (6.19) implies the asymptotic stability of the closed-loop system (6.20) and vice versa.

From (6.10) we know that

$$\hat{\mathbf{K}} = (\mathbf{I} - \mathbf{K}\mathbf{M}_{\mathrm{c}}^{\mathrm{m}})^{-1}\mathbf{K} = (\mathbf{I} + \mathbf{K}\mathbf{C}^{\mathrm{m}}\boldsymbol{\Lambda}^{-1}\mathbf{B}_{\mathrm{c}})^{-1}\mathbf{K}$$

which solving for $\hat{\mathbf{K}}$ turns into

$$\begin{aligned}(\mathbf{I} + \mathbf{K}\mathbf{C}^{\mathrm{m}}\boldsymbol{\Lambda}^{-1}\mathbf{B}_{\mathrm{c}})\hat{\mathbf{K}} = \mathbf{K} &\Rightarrow \hat{\mathbf{K}} + \mathbf{K}\mathbf{C}^{\mathrm{m}}\boldsymbol{\Lambda}^{-1}\mathbf{B}_{\mathrm{c}}\hat{\mathbf{K}} = \mathbf{K} \\ &\Rightarrow \hat{\mathbf{K}} = \mathbf{K} - \mathbf{K}\mathbf{C}^{\mathrm{m}}\boldsymbol{\Lambda}^{-1}\mathbf{B}_{\mathrm{c}}\hat{\mathbf{K}} \\ &\Rightarrow \hat{\mathbf{K}} = \mathbf{K}(\mathbf{I} - \mathbf{C}^{\mathrm{m}}\boldsymbol{\Lambda}^{-1}\mathbf{B}_{\mathrm{c}}\hat{\mathbf{K}}) \\ &\Rightarrow \mathbf{K} = \hat{\mathbf{K}}(\mathbf{I} - \mathbf{C}^{\mathrm{m}}\boldsymbol{\Lambda}^{-1}\mathbf{B}_{\mathrm{c}}\hat{\mathbf{K}})^{-1}.\end{aligned}$$

This enables us to express system (6.19) in terms of the transformed gain matrix $\hat{\mathbf{K}}$:

$$\dot{\mathbf{x}}(t) = (\mathbf{\Lambda} + \mathbf{B}_{\mathrm{c}}\hat{\mathbf{K}}(\mathbf{I} - \mathbf{C}^{\mathrm{m}}\mathbf{\Lambda}^{-1}\mathbf{B}_{\mathrm{c}}\hat{\mathbf{K}})^{-1}\mathbf{C}^{\mathrm{m}})\mathbf{x}(t). \tag{6.21}$$

Now consider the matrix $(-\mathbf{\Lambda} + \mathbf{B}_{\mathrm{c}}\hat{\mathbf{K}}\mathbf{C}^{\mathrm{m}})^{-1}$. By applying the Woodbury identity for inverses [153], we obtain

$$(-\mathbf{\Lambda} + \mathbf{B}_{\mathrm{c}}\hat{\mathbf{K}}\mathbf{C}^{\mathrm{m}})^{-1} = -\mathbf{\Lambda}^{-1} - \mathbf{\Lambda}^{-1}\mathbf{B}_{\mathrm{c}}\hat{\mathbf{K}}(\mathbf{I} - \mathbf{C}^{\mathrm{m}}\mathbf{\Lambda}^{-1}\mathbf{B}_{\mathrm{c}}\hat{\mathbf{K}})^{-1}\mathbf{C}^{\mathrm{m}}\mathbf{\Lambda}^{-1}.$$

Subsequently, by left- and right-multiplying both sides of the above expression by $\mathbf{\Lambda}$, and changing the sign, we obtain

$$-\mathbf{\Lambda}(-\mathbf{\Lambda} + \mathbf{B}_{\mathrm{c}}\hat{\mathbf{K}}\mathbf{C}^{\mathrm{m}})^{-1}\mathbf{\Lambda} = \mathbf{\Lambda} + \mathbf{B}_{\mathrm{c}}\hat{\mathbf{K}}(\mathbf{I} - \mathbf{C}^{\mathrm{m}}\mathbf{\Lambda}^{-1}\mathbf{B}_{\mathrm{c}}\hat{\mathbf{K}})^{-1}\mathbf{C}^{\mathrm{m}},$$

which corresponds to the system matrix of system (6.21). This expression allows us to rewrite the autonomous closed-loop system (6.19) as

$$\begin{aligned}\dot{\mathbf{x}}(t) &= (\mathbf{\Lambda} + \mathbf{B}_{\mathrm{c}}\mathbf{K}\mathbf{C}^{\mathrm{m}})\mathbf{x}(t)\\ &= -\mathbf{\Lambda}(-\mathbf{\Lambda} + \mathbf{B}_{\mathrm{c}}\hat{\mathbf{K}}\mathbf{C}^{\mathrm{m}})^{-1}\mathbf{\Lambda}\mathbf{x}(t)\\ &= (\mathbf{\Lambda}^{-1} - \mathbf{\Lambda}^{-1}\mathbf{B}_{\mathrm{c}}\hat{\mathbf{K}}\mathbf{C}^{\mathrm{m}}\mathbf{\Lambda}^{-1})^{-1}\mathbf{x}(t).\end{aligned}$$

Clearly, $\mathbf{\Lambda} + \mathbf{B}_{\mathrm{c}}\mathbf{K}\mathbf{C}^{\mathrm{m}} = (\mathbf{\Lambda}^{-1} - \mathbf{\Lambda}^{-1}\mathbf{B}_{\mathrm{c}}\hat{\mathbf{K}}\mathbf{C}^{\mathrm{m}}\mathbf{\Lambda}^{-1})^{-1}$ holds. According to Lemma 1, the eigenvalues of the matrix $\mathbf{A} + \mathbf{B}_{\mathrm{c}}\mathbf{K}\mathbf{C}^{\mathrm{m}}$ correspond to the reciprocal eigenvalues of the matrix $\mathbf{\Lambda}^{-1} - \mathbf{\Lambda}^{-1}\mathbf{B}_{\mathrm{c}}\hat{\mathbf{K}}\mathbf{C}^{\mathrm{m}}\mathbf{\Lambda}^{-1}$. Lemma 2 ensures that the system (6.19) is asymptotically stable iff the system (6.20) is asymptotically stable. □

As a consequence of Theorem 13, we can design the affine output feedback controller (6.3) entirely in terms of the transformed parameters $\hat{\mathbf{K}}$ and $\hat{\boldsymbol{w}}$. Once $\hat{\mathbf{K}}$ and $\hat{\boldsymbol{w}}$ are found, the original controller parameters $\mathbf{K}$ and $\boldsymbol{w}$ can be recovered by solving equations (6.10). Solving BMI (6.12) is thus equivalent to solving the BMI

$$\begin{aligned}\min_{\hat{\mathbf{K}},\hat{\boldsymbol{w}},\hat{\mathbf{P}},\eta}\ & \eta\\ \text{s.t. } & \hat{\mathbf{P}}(\mathbf{\Lambda}^{-1} - \mathbf{\Lambda}^{-1}\mathbf{B}_{\mathrm{c}}\hat{\mathbf{K}}\mathbf{C}^{\mathrm{m}}\mathbf{\Lambda}^{-1}) + (\mathbf{\Lambda}^{-1} - \mathbf{\Lambda}^{-1}\mathbf{B}_{\mathrm{c}}\hat{\mathbf{K}}\mathbf{C}^{\mathrm{m}}\mathbf{\Lambda}^{-1})^{\mathrm{T}}\hat{\mathbf{P}} \preceq \mathbf{0},\\ & (\mathbf{A}_{\mathrm{c}}\hat{\mathbf{K}}\mathbf{M}_{\mathrm{f}}^{\mathrm{m}} + \mathbf{A}_{\mathrm{f}})\boldsymbol{u}_{\mathrm{f}} + \mathbf{A}_{\mathrm{c}}\hat{\boldsymbol{w}} \leq \boldsymbol{b} + \eta\mathbf{1}, \quad \forall \boldsymbol{u}_{\mathrm{f}} \in \boldsymbol{\mathcal{U}}_{\mathrm{f}},\\ & \hat{\mathbf{K}}\mathbf{M}_{\mathrm{f}}^{\mathrm{m}}\boldsymbol{u}_{\mathrm{f}} + \hat{\boldsymbol{w}} \in \boldsymbol{\mathcal{U}}_{\mathrm{c}}, \quad \forall \boldsymbol{u}_{\mathrm{f}} \in \boldsymbol{\mathcal{U}}_{\mathrm{f}},\\ & \hat{\mathbf{P}} \succeq \mathbf{0}.\end{aligned} \tag{6.22}$$

Observe that the techniques presented in Section 6.4.1 can also be used here to reduce BMI (6.22) to finite dimensional feasibility problem for the special case where the sets $\boldsymbol{\mathcal{U}}_{\mathrm{c}}$ and $\boldsymbol{\mathcal{U}}_{\mathrm{f}}$ are hypercubes. Notwithstanding, we recall that the algorithms proposed in this chapter can also be extended another shapes of $\boldsymbol{\mathcal{U}}_{\mathrm{c}}$ or $\boldsymbol{\mathcal{U}}_{\mathrm{f}}$, for instance an arbitrary convex polytope or a p-norm-shaped set, cf. Section 2.4.

Given that $(\boldsymbol{\mathcal{U}}_{\mathrm{c}}, \boldsymbol{\mathcal{U}}_{\mathrm{f}})$ are convex polytopes, BMI (6.13) turns into

$$
\begin{aligned}
\min_{\hat{\mathbf{K}},\hat{\boldsymbol{w}},\mathbf{H},\hat{\mathbf{P}},\eta} \quad & \eta \\
\text{s.t. } & \hat{\mathbf{P}}(\boldsymbol{\Lambda}^{-1} - \boldsymbol{\Lambda}^{-1}\mathbf{B}_{\mathrm{c}}\hat{\mathbf{K}}\mathbf{C}^{\mathrm{m}}\boldsymbol{\Lambda}^{-1}) + (\boldsymbol{\Lambda}^{-1} - \boldsymbol{\Lambda}^{-1}\mathbf{B}_{\mathrm{c}}\hat{\mathbf{K}}\mathbf{C}^{\mathrm{m}}\boldsymbol{\Lambda}^{-1})^{\mathrm{T}}\hat{\mathbf{P}} \preceq \mathbf{0}, \\
& \mathbf{H}\mathbf{1} + \tilde{\mathbf{A}}_{\mathrm{c}}\hat{\boldsymbol{w}} \leq \tilde{\boldsymbol{b}} + \eta\mathbf{1}, \\
& H_{ij} \geq \tilde{A}_{ij}(\hat{\mathbf{K}})\overline{u}_{\mathrm{f}j}, \quad \forall i \in \{1, ..., \hat{n}_z\},\ \forall j \in \{1, ..., n_u - |\mathcal{C}|\}, \\
& H_{ij} \geq \tilde{A}_{ij}(\hat{\mathbf{K}})\underline{u}_{\mathrm{f}j}, \quad \forall i \in \{1, ..., \hat{n}_z\},\ \forall j \in \{1, ..., n_u - |\mathcal{C}|\}, \\
& \hat{\mathbf{P}} \succeq \mathbf{0}, \\
& \hat{\mathbf{P}} \in \mathbb{R}^{n_x \times n_x}, \quad \hat{\mathbf{K}} \in \mathbb{R}^{|\mathcal{C}|\times|\mathcal{M}|}, \quad \hat{\boldsymbol{w}} \in \mathbb{R}^{|\mathcal{C}|}, \\
& \mathbf{H} \in \mathbb{R}^{\hat{n}_z \times (n_u - |\mathcal{C}|)}, \quad \eta \in \mathbb{R},
\end{aligned}
\tag{6.23}
$$

where $\tilde{\mathbf{A}}(\hat{\mathbf{K}}) = \tilde{\mathbf{A}}_{\mathrm{c}}\hat{\mathbf{K}}\mathbf{M}_{\mathrm{f}}^{\mathrm{m}} + \tilde{\mathbf{A}}_{\mathrm{f}}$, and $\tilde{\mathbf{A}}_{\mathrm{c}}$ and $\tilde{\mathbf{A}}_{\mathrm{f}}$ are given as in (6.14). Similar to BMI (6.13), the above BMI can be solved locally by employing the algorithm depicted in Fig. 6.2. Once a solution for BMI (6.23) is found, we can recover the controller parameters $\mathbf{K}$ and $\boldsymbol{w}$ via equations (6.10). As the size of the auxiliary matrix $\hat{\mathbf{P}}$ and of its associated non-convex (bi)linear matrix inequalities grows quadratically with the dimension of the state vector, solving this particular instance of Problem 2 by means of BMI (6.23) is adequate for small- to medium-sized problem instances only.

6.4.3 Synthesis Algorithm Based on the Spectral Abscissa

In large-scale problem instances, testing the asymptotic stability of closed-loop LTI systems by using Lyapunov methods is computationally prohibitive as the number of optimization variables and constraints grows quadratically with the dimension of the state vector $\mathbf{x}$. An alternative to reduce the computational burden is to obtain a mathematical problem formulation whose stability constraints are given in terms of the control actions inputs $\mathbf{u}_{\mathrm{c}}$ and the outputs $\mathbf{y}^{\mathrm{m}}$ only, e.g., the spectral abscissa defined in Section 6.2. This is beneficial for a plant whose control system employs a small number of actuators and sensors. Consider the following equivalent formulation of Problem 2 that uses the closed-loop representation $d\hat{\mathbf{x}}(t)/dt = (\boldsymbol{\Lambda}^{-1} - \boldsymbol{\Lambda}^{-1}\mathbf{B}_{\mathrm{c}}\hat{\mathbf{K}}\mathbf{C}^{\mathrm{m}}\boldsymbol{\Lambda}^{-1})\hat{\mathbf{x}}(t)$ obtained from Theorem 13,

$$
\begin{aligned}
\min_{\hat{\mathbf{K}}\in\mathbb{R}^{|\mathcal{C}|\times|\mathcal{M}|},\hat{\boldsymbol{w}}\in\mathbb{R}^{|\mathcal{C}|},\eta\in\mathbb{R}} \quad & \eta \\
\text{s.t. } & \alpha(\hat{\mathbf{K}}) \leq 0, \\
& (\mathbf{A}_{\mathrm{c}}\hat{\mathbf{K}}\mathbf{M}_{\mathrm{f}}^{\mathrm{m}} + \mathbf{A}_{\mathrm{f}})\boldsymbol{u}_{\mathrm{f}} + \mathbf{A}_{\mathrm{c}}\hat{\boldsymbol{w}} \leq \boldsymbol{b} + \eta\mathbf{1}, \quad \forall \boldsymbol{u}_{\mathrm{f}} \in \boldsymbol{\mathcal{U}}_{\mathrm{f}}, \\
& \hat{\mathbf{K}}\mathbf{M}_{\mathrm{f}}^{\mathrm{m}}\boldsymbol{u}_{\mathrm{f}} + \hat{\boldsymbol{w}} \in \boldsymbol{\mathcal{U}}_{\mathrm{c}}, \quad \forall \boldsymbol{u}_{\mathrm{f}} \in \boldsymbol{\mathcal{U}}_{\mathrm{f}}, \\
& \alpha(\hat{\mathbf{K}}) = \max_i \Re(\boldsymbol{\lambda}_i(\boldsymbol{\Lambda}^{-1} - \boldsymbol{\Lambda}^{-1}\mathbf{B}_{\mathrm{c}}\hat{\mathbf{K}}\mathbf{C}^{\mathrm{m}}\boldsymbol{\Lambda}^{-1})).
\end{aligned}
\tag{6.24}
$$

While being not everywhere differentiable and even not everywhere Lipschitz continuous,[12] recent developments indicate that a suboptimal solution for the spectral abscissa $\alpha(\hat{\mathbf{K}})$ can be found by employing non-convex optimization techniques derived from a combination of the BFGS algorithm [150] and an adaptive gradient sampling technique [149]. Particularly, the software tool HIFOO ($\mathcal{H}_\infty - \mathcal{H}_2$ Fixed Order Optimization) contains a series of Matlab packages for output feedback stabilization of LTI systems [149]. Alternatively, the spectral abscissa can be *smoothed* [154], i.e., turning it into a still non-convex, but differentiable function which allows for a gradient-based optimization algorithm. For the special case of having both $\boldsymbol{\mathcal{U}}_\mathrm{c}$ and $\boldsymbol{\mathcal{U}}_\mathrm{f}$ given as hypercubes, the infinite dimensional feasibility problem (6.24) is given as

$$
\begin{aligned}
&\min_{\hat{\mathbf{K}},\hat{\boldsymbol{w}},\mathbf{H},\eta} \quad \eta \\
&\quad \text{s.t. } \alpha(\hat{\mathbf{K}}) \leq 0, \\
&\qquad \mathbf{H}\mathbf{1} + \tilde{\mathbf{A}}_\mathrm{c}\hat{\boldsymbol{w}} \leq \tilde{\boldsymbol{b}} + \eta\mathbf{1}, \\
&\qquad H_{ij} \geq \tilde{A}_{ij}(\hat{\mathbf{K}})\overline{u}_{\mathrm{f}j}, \quad \forall i \in \{1,...,\hat{n}_z\},\ \forall j \in \{1,...,n_u - |\mathcal{C}|\}, \\
&\qquad H_{ij} \geq \tilde{A}_{ij}(\hat{\mathbf{K}})\underline{u}_{\mathrm{f}j}, \quad \forall i \in \{1,...,\hat{n}_z\},\ \forall j \in \{1,...,n_u - |\mathcal{C}|\}, \\
&\qquad \alpha(\hat{\mathbf{K}}) = \max_i \Re(\boldsymbol{\lambda}_i(\boldsymbol{\Lambda}^{-1} - \boldsymbol{\Lambda}^{-1}\mathbf{B}_\mathrm{c}\hat{\mathbf{K}}\mathbf{C}^\mathrm{m}\boldsymbol{\Lambda}^{-1})), \\
&\qquad \hat{\mathbf{K}} \in \mathbb{R}^{|\mathcal{C}|\times|\mathcal{M}|}, \quad \hat{\boldsymbol{w}} \in \mathbb{R}^{|\mathcal{C}|}, \quad \mathbf{H} \in \mathbb{R}^{\hat{n}_z\times(n_u-|\mathcal{C}|)},
\end{aligned}
\tag{6.25}
$$

where $\tilde{\mathbf{A}}(\hat{\mathbf{K}}) = \tilde{\mathbf{A}}_\mathrm{c}\hat{\mathbf{K}}\mathbf{M}_\mathrm{f}^\mathrm{m} + \tilde{\mathbf{A}}_\mathrm{f}$, and $\tilde{\mathbf{A}}_\mathrm{c}$ and $\tilde{\mathbf{A}}_\mathrm{f}$ are given as in (6.14). The non-convex, non-smooth feasibility problem (6.25) can be solved via BFGS optimization. To this end, the analytical expressions for the gradient of each constraint w.r.t. each optimization variable have to be precomputed. The number of optimization variables and constraints is dominated by the auxiliary matrix $\mathbf{H}$, whose number of entries grows quadratically with the number $\hat{n}_z(n_u - |\mathcal{C}|)$. The approach is thus recommended for problem instances for which the dimension of $\boldsymbol{u}_\mathrm{f}$ is small or the number of constraints is small. In that case, the number of precomputed gradients will also be small.

6.5 Discussion

The computation of affine output feedback control laws guaranteeing 1) the asymptotic stability of the resulting closed-loop system and 2) the fulfillment of set of polyhedral operational constraints at steady state is in general a difficult task. The obtained formulations are non-convex or (even non-smooth) due to the form of the conditions for asymptotically stability. However, we provide local optimization approaches relying on sequential linearizations of the non-convex constraints. As a potential research direction for future

[12] The function $f : \mathbb{R} \to \mathbb{R}$ is Lipschitz continuous if there exists a positive real constant C such that, for all $x_1, x_2 \in \mathbb{R}$, the inequality $|f(x_1) - f(x_2)| \leq C|x_1 - x_2|$ holds.

work, one may employ a time discretization and render the problem into a finite-horizon formulation with terminal constraints.

A natural extension of the synthesis algorithms proposed above is the design of the transient response of the closed-loop system. If the existence of a steady state admissible, affine output feedback control law is guaranteed, then this can be achieved by, for instance, replacing the objective η in problem 6.22 with a linear or (convex) quadratic function of $\boldsymbol{u}_{\mathrm{c}}$ expressed in terms of the gain matrix.

Concerning both continuous- and discrete-time LTI systems, future work will investigate under which conditions we can guarantee the existence of PWA output feedback control laws for which the resulting closed-loop system is asymptotically stable and also fulfills a set of operational requirements (at steady state). We also are interested in extending the ideas proposed in this chapter to more complex dynamic system representations, e.g., linear time-varying systems or Markov decision processes [155].

To conclude this chapter, we highlight that, for the special case where the sets $\boldsymbol{\mathcal{U}}_{\mathrm{c}}$ and $\boldsymbol{\mathcal{U}}_{\mathrm{f}}$ are hypercubes, we can straightforwardly extend the hill climbing optimization approach proposed in Chapter 4 to determine an upper bound for the minimal actuator and sensor sets fulfilling the design specifications considered in this chapter. The derivation of a branch-and-bound [156] solvable problem formulation is in this regard matter of further investigations.

7 Applications to Power Systems

The algorithms developed in previous chapters are general and suitable for the control of constrained static linear systems under uncertainty. The goal of this chapter is to illustrate the potential of these control algorithms in the context of electrical power networks. In particular, we demonstrate how to apply our methods to the following power flow control tasks:

- Identification of critical actuator and sensor devices for robust active power flow control in transmission networks
- Robust voltage/VAr regulation in distribution networks

After a brief mathematical description of the adopted models for electrical power networks with constraints, the above listed power flow problems are solved for 1) simple power networks with a few number of nodes/lines and 2) modified versions of some IEEE test cases.

The simulation experiments were performed using an i5 notebook with 8 GB of RAM. The algorithms were implemented in Matlab R2018b, using YALMIP [157] as modeling language, CPLEX 12.9 as LP and MILP solver, Gurobi 9.2 as QCQP solver, and MOSEK as SDP solver.

7.1 Power Flow as a Set of Linear Equations

7.1.1 AC Power Flow

We consider a three-phase electrical power network with $N \in \mathbb{N}^+$ electrical buses connected by $T \in \mathbb{N}^+$ transmission lines. The network is assumed to have balanced generation and consumption values on each phase, which allows us to analyze a *single-phase* representation of the network instead of the three-phase description. The transmission line connected between buses $i \in \mathbb{N}^+$ and $j \in \mathbb{N}^+$ is modeled as the series connection of an electrical conductance $g_{ij} \in \mathbb{R}_{\geq 0}$ and an electrical susceptance $b_{ij} \in \mathbb{R}_{\geq 0}$. The voltage levels across the network are determined by the active and reactive power injected at each bus. Let $p_i \in \mathbb{R}$ and $q_i \in \mathbb{R}$ denote the active and reactive power injected at bus i. As the

voltage level at bus i is modeled as a phasor described entirely by its magnitude $|V_i| \geq 0$ and phase $\theta_i \in \mathbb{R}$, the power flow equations at steady state read, for $i = 1, ..., N$,

$$\begin{aligned} p_i &= \sum_{j=1}^{N} p_{ij} = \sum_{j=1}^{N} |V_i||V_j|\big(g_{ij}\cos(\theta_i - \theta_j) + b_{ij}\sin(\theta_i - \theta_j)\big), \\ q_i &= \sum_{j=1}^{N} q_{ij} = \sum_{j=1}^{N} |V_i||V_j|\big(g_{ij}\cos(\theta_i - \theta_j) - b_{ij}\sin(\theta_i - \theta_j)\big). \end{aligned} \tag{7.1}$$

Thereby, the terms p_{ij} and q_{ij} correspond to the active and reactive power flowing through the line connecting buses i and j, respectively. The above set of non-linear equations are known in the literature as the *AC power flow equations* and are widely used in many numerical analysis, e.g., in AC optimal power flow (AC-OPF) studies [26]. The electrical parameters g_{ij}, b_{ij} as well as the voltage magnitudes are usually given in the per-unit system, which facilitates the analysis of the power flows and improves the numerical performance of the numerical methods of solving (7.1).

7.1.2 DC Power Flow

The AC power flow equations (7.1) model the steady state of a power network accurately. When using them for optimization purposes, e.g., optimal dispatch, the resulting formulations are typically non-convex [26] and, therefore, difficult to solve. A common technique to obtain convex formulations is to linearize the AC power flow equations. Particularly for transmission networks, the following assumptions can be done for the linearization [81]:

- The voltage magnitude is equal for all buses, i.e., $|V_i| \approx 1$ p.u..
- The voltage angle differences between neighboring buses are small, which results in the linearizations: $\sin(\theta_i - \theta_j) \approx \theta_i - \theta_j$, $\cos(\theta_i - \theta_j) \approx 1$.
- The network has no losses, implying that the electrical parameters of the transmission lines are simplified: $g_{ij} \approx 0$.
- The reactive power flowing through the network can be neglected compared to the flow of active power, i.e., $q_{ij} \ll p_{ij}$.

Under the above assumptions and using vector notation, the voltage phase angles $\boldsymbol{\theta} \in \mathbb{R}^N$ determine the nodal active power injections $\boldsymbol{p} \in \mathbb{R}^N$ and the active power line flows $\boldsymbol{p}_{\mathrm{F}} \in \mathbb{R}^T$ as

$$\boldsymbol{p} = \mathbf{B}_{\mathrm{I}}\boldsymbol{\theta}, \quad \boldsymbol{p}_{\mathrm{F}} = \mathbf{B}_{\mathrm{F}}\boldsymbol{\theta},$$

where the entries of $\mathbf{B}_{\mathrm{I}} \in \mathbb{R}^{N\times N}$ and $\mathbf{B}_{\mathrm{F}} \in \mathbb{R}^{T\times N}$ are defined element-wise as $B_{\mathrm{I},ij} = -b_{ij}$ if $i \neq j$, $B_{\mathrm{I},ii} = \sum_{j=1}^{N} b_{ij}$ and $B_{\mathrm{F},ij} = b_{ij}$, with b_{ij} the susceptance of the line

connecting buses i and j. The above linear equations are known as the *DC power flow* equations [26].

Without loss of generality, we assume that exactly one generator or load is connected to each bus, with an externally defined active power set point u_i. If the sum of the set points in the grid is not balanced, a *droop-based primary control* scheme [81] adjusts power injections $\boldsymbol{p}$ under adaptation of the frequency to achieve this balance, such that at steady state we obtain

$$\boldsymbol{p} = \boldsymbol{u} - \mathbf{k}\Delta\omega.$$

Here, $\mathbf{k} \in \mathbb{R}^N$ represents the vector of droop constants, $\mathrm{k}_i \geq 0$ and $\sum_{i=1}^{N} \mathrm{k}_i > 0$, and $\Delta\omega \in \mathbb{R}$ the frequency deviation with respect to its nominal value.[1]

This common setup implies that the measurable quantities $\boldsymbol{p}$, $\boldsymbol{p}_\mathrm{F}$, and $\Delta\omega$ are linearly determined by the power set points $\boldsymbol{u} \in \mathbb{R}^N$. The kernel of the Laplacian matrix $\mathbf{B}_\mathrm{I}$ contains only the constant vectors for connected graphs,[2] that is, a constant shift of the phase angles has no impact on $\boldsymbol{p}$. We thus fix $\theta_1 = 0$ and delete the first column of $\mathbf{B}_\mathrm{I}$ to obtain $\tilde{\mathbf{B}}_\mathrm{I}$. The remaining dimensions of $\boldsymbol{\theta}$ are denoted by $\tilde{\boldsymbol{\theta}}$. We similarly reduce $\mathbf{B}_\mathrm{F}$ to $\tilde{\mathbf{B}}_\mathrm{F}$. The image of $\tilde{\mathbf{B}}_\mathrm{I}$ moreover contains all vectors with balanced nodal injections. To handle unbalanced set points $\boldsymbol{u}$, we add $\mathbf{k}$ as the last column, This lets us compute

$$\begin{bmatrix} \boldsymbol{p} \\ \boldsymbol{p}_\mathrm{F} \\ \Delta\omega \end{bmatrix} = \begin{bmatrix} \tilde{\mathbf{B}}_\mathrm{I} & \mathbf{0} \\ \tilde{\mathbf{B}}_\mathrm{F} & \mathbf{0} \\ \mathbf{0} & 1 \end{bmatrix} \begin{bmatrix} \tilde{\boldsymbol{\theta}} \\ \Delta\omega \end{bmatrix} = \begin{bmatrix} \tilde{\mathbf{B}}_\mathrm{I} & \mathbf{0} \\ \tilde{\mathbf{B}}_\mathrm{F} & \mathbf{0} \\ \mathbf{0} & 1 \end{bmatrix} \begin{bmatrix} \tilde{\mathbf{B}}_\mathrm{I} & \mathbf{k} \end{bmatrix}^{-1} \boldsymbol{u}. \tag{7.2}$$

From expression (7.2), we can consider vector $\boldsymbol{u}$ as the *action* since it uniquely determines the value of the power flows and the frequency deviation. The state of the system may be determined by observing some elements of $\boldsymbol{p}$ or $\boldsymbol{p}_\mathrm{F}$, or the frequency deviation $\Delta\omega$. In real systems the nodal injections $\boldsymbol{p}$ will be limited above and below by the technical capabilities of the connected generator or load. Valid set points $\boldsymbol{u}$ might additionally be restricted to smaller intervals than vector $\boldsymbol{p}$ to leave some space for power generation scheduled by the primary controller. Similarly, line power flows $\boldsymbol{p}_\mathrm{F}$ and the frequency deviation $\Delta\omega$ are typically subject to upper and lower bounds.

7.1.3 Branch Flow Models

Contrary to the model exposed in the previous section, the so-called *branch flow* models [26] assume a directed graph to describe the power flows and voltages across the network. As before, we consider an electrical power network consisting of N buses

[1] The tuning of the vector of droop constants $\mathbf{k}$ is usually done locally by trial an error, by following some practical heuristic, or by using models [158].

[2] Conceptually, the $\mathbf{B}_\mathrm{I}$ is a Laplacian matrix because it encodes the undirected graph associated to the topology of the power grid. For an undirected graph $\mathcal{G} = (\mathcal{V}, \mathcal{E})$ with vertices in $\mathcal{V}$ and edges in $\mathcal{E}$, the Laplacian matrix $\mathbf{L} = \mathbf{D} - \mathbf{A}$ is determined by the *degree* matrix $\mathbf{D} \in \mathbb{R}^{|\mathcal{V}|\times|\mathcal{V}|}$ and the *adjancency* matrix $\mathbf{A} \in \mathbb{R}^{|\mathcal{V}|\times|\mathcal{V}|}$ of the graph [159].

connected by T transmission lines. However, the topology of the network is presupposed to be acyclic, i.e., the network has a tree structure with $T = N - 1$. This makes the model specially suitable for the analysis of distribution networks. The line connecting buses i and j is modeled by the series impedance parametrized by the electrical resistance $r_{ij} \in \mathbb{R}_{\geq 0}$ and the electrical reactance $\mathrm{x}_{ij} \in \mathbb{R}_{\geq 0}$. Let $|I_{ij}|$ denote the magnitude of the electrical current flowing throw the transmission line connected to the buses i and j. Also let $v_i = |V_i|^2$ and $\ell_{ij} = |I_{ij}|^2$. The power injected at each bus determines the power flows, the voltage levels, and the line losses in the network according to the non-linear equations, for $i, j = 1, ..., N$

$$\begin{aligned} p_{ij} &= r_{ij}\ell_{ij} - p_j + \sum_{k:j\to k} p_{jk}, \\ q_{ij} &= \mathrm{x}_{ij}\ell_{ij} - q_j + \sum_{k:j\to k} q_{jk}, \\ v_j &= v_i - 2(r_{ij}p_{ij} + \mathrm{x}_{ij}q_{ij}) + (r_{ij}^2 + \mathrm{x}_{ij}^2)\ell_{ij}, \\ \ell_{ij}v_i &= p_{ij}^2 + q_{ij}^2. \end{aligned} \tag{7.3}$$

The notation $k : j \to k$ refers to the set of transmission lines starting at bus j, i.e., the out neighbors of j. The above equations are known as the *DistFlow* model and can be solved recursively. The DistFlow model is utilized extensively in the literature and can also be extended to consider non-balanced three-phase distribution systems [160].

7.1.4 Linear *DistFlow* Model

For radial distribution networks with negligible losses, the term ℓ_{ij} in equations (7.3) is set to zero and we obtain the following set of linear equalities, for $i, j = 1, ..., N$

$$p_{ij} = -p_j + \sum_{k:j\to k} p_{jk}, \quad q_{ij} = -q_j + \sum_{k:j\to k} q_{jk}, \quad v_j = v_i - 2(r_{ij}p_{ij} + \mathrm{x}_{ij}q_{ij}) + s_i.$$

In the above model, we additionally include the term s_i to represent the effect of a voltage regulator at node i. If there is no voltage regulator at node i, we set $s_i = 0$ throughout. The above equations are linear and the power flows (p_{ij}, q_{ij}) and nodal voltages v_i are determined uniquely by the combination of the power injections (p_j, q_j) at the non-root nodes, the voltage v_0 at the root node, and the voltage impacts s_i of the installed voltage regulators. The state of the system is defined by the voltages $v_1, ..., v_n$, since it is determined by both the voltage v_0 and the nodal active and reactive power injections.

In distribution grids, nodal voltages v_i are typically required to be maintained within the range of [0.9, 1.1] p.u.. In order to guarantee such a feasible system operation, the On-Load Tap Changer (OLTC) of the distribution transformer at the root node can be controlled to set a voltage value v_0.[3] Moreover, the reactive power injections q_j of some

[3]The OLTC is a controllable mechanism that manipulates the turn ratios of the transformer by using taps. Contrary to reality where the tap positions are set in discrete steps, we approximate the tap actions by using a continuous, interval-bounded action space.

of the decentralized generators may also be available for actuation. These control actions can be determined based on local measurements at the root node, i.e., the total power supplied (p_0, q_0), as well as information from some points throughout the grid, e.g., nodal voltage measurements v_i at some of the nodes with decentralized generators. All state variables have physical limitations in the form of interval constraints. Note that non-linear constraints, e.g., conservation voltage reduction, can be modeled with the help of piecewise linear functions. Additional constraints may apply in certain situations as outlined in Sections 7.4.3 and 7.4.4.

7.2 Minimal Admissible Power Flow in Transmission Networks

The algorithms developed in Chapter 4 are now applied to find the minimal admissible setting of actuators and sensors for two exemplary power systems. We first demonstrate our setup and typical effects on a simple microgrid of 4 buses connected in a line. Subsequently, a modified version of the IEEE 118 bus test case is studied.

7.2.1 Introductory Microgrid

Fig. 7.1 shows the considered microgrid consisting of three generators supplying a demand of 5 MW. It gives the topology of the grid together with the capacity limits of each transmission line and each generator/load. The generator located at bus 4 provides primary reserve, initially with a droop of 12 MW/Hz and later with 4 MW/Hz. The maximum allowed frequency deviation is ± 0.1 Hz. We first assume that all transmission lines have a power transfer capacity of ± 10 MW, which is adequate to avoid grid limitations. In scenario (d) we add an active line constraint in the middle.

In scenario (a) where only the power set point at each bus may be measured, it is sufficient to control the large generator located at bus 4 for achieving feasible grid operation. The set points of the remaining smaller generators can be chosen freely by other system users and no additional measurement devices are required.

In scenario (b) we reduce the droop of the generator at bus 4 to 4 MW/Hz. This makes the measurement of the power injections at buses 1 and 2 necessary. Although the power injections at buses 1 and 2 can be chosen arbitrarily, they must be monitored so that the power produced by the generator located at bus 4 can be set appropriately to balance the system within the given frequency tolerance.

In scenarios (a) and (b), where $\mathbf{M} = \mathbf{I}$, the solutions of MILP (4.13) were admissible (and optimal) without further adaptation of the actuator and sensor sets $(\mathcal{C}, \mathcal{M})$ and the greedy approach, starting from empty sets, produced the same results.

In scenario (c) the measurement of the line flows and the grid frequency is added to the set of possible measurements when performing both the MILP (4.9) and the greedy

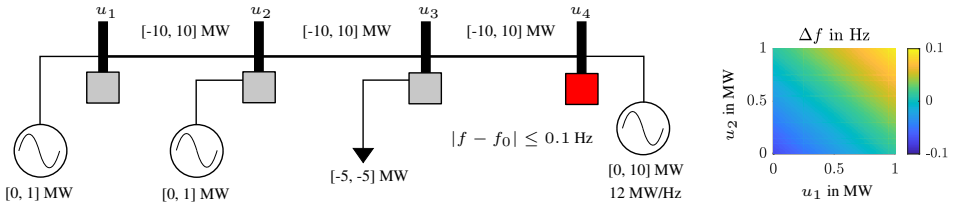

(a) $\boldsymbol{u}_\mathrm{c} = u_4;\ \boldsymbol{u}_\mathrm{f} = \begin{bmatrix} u_1 & u_2 & u_3 \end{bmatrix}^\mathrm{T};\ \hat{\mathbf{S}} = \emptyset;\ \mathbf{M}_\mathrm{f}^\mathrm{m} = \emptyset;\ \hat{\boldsymbol{w}} = 4.1.$

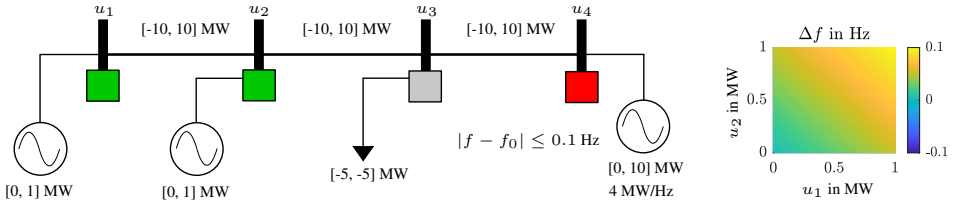

(b) $\boldsymbol{u}_\mathrm{c} = u_4;\ \boldsymbol{u}_\mathrm{f} = \begin{bmatrix} u_1 & u_2 & u_3 \end{bmatrix}^\mathrm{T};\ \hat{\mathbf{S}} = -0.81 \begin{bmatrix} 1 & 1 \end{bmatrix};\ \mathbf{M}_\mathrm{f}^\mathrm{m} = \begin{bmatrix} 1 & 0 & 0 \\ 0 & 1 & 0 \end{bmatrix};\ \hat{\boldsymbol{w}} = 5.$

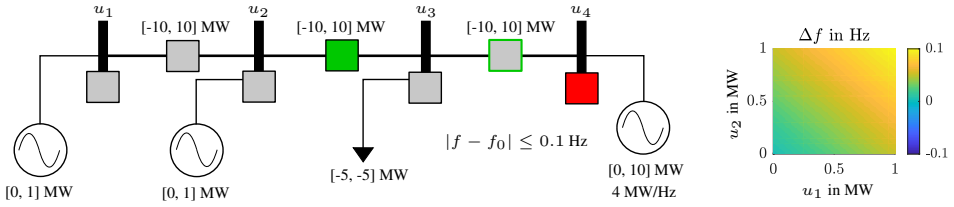

(c) $\boldsymbol{u}_\mathrm{c} = u_4;\ \boldsymbol{u}_\mathrm{f} = \begin{bmatrix} u_1 & u_2 & u_3 \end{bmatrix}^\mathrm{T};\ \hat{\mathbf{S}} = -0.81;\ \mathbf{M}_\mathrm{f}^\mathrm{m} = \begin{bmatrix} 1 & 1 & 0 \end{bmatrix};\ \hat{\boldsymbol{w}} = 5.$

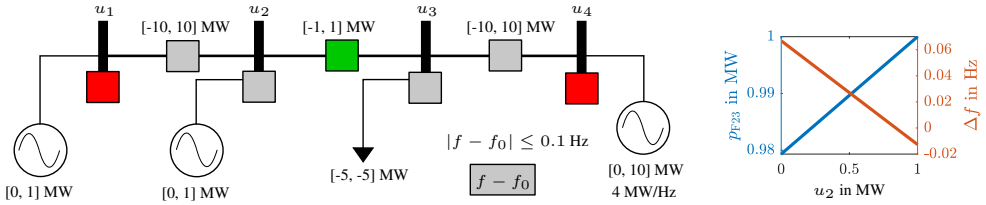

(d) $\boldsymbol{u}_\mathrm{c} = \begin{bmatrix} u_1 \\ u_4 \end{bmatrix};\ \boldsymbol{u}_\mathrm{f} = \begin{bmatrix} u_2 \\ u_3 \end{bmatrix};\ \mathbf{M}_\mathrm{f}^\mathrm{m} = \begin{bmatrix} 1 & 0 \end{bmatrix};\ \hat{\mathbf{S}} = -\begin{bmatrix} 0.98 \\ 0.34 \end{bmatrix};\ \hat{\boldsymbol{w}} = \begin{bmatrix} 0.98 \\ 4.29 \end{bmatrix}.$

Figure 7.1: Minimal sets of $\mathcal{C}$ and $\mathcal{M}$ for a simple microgrid. The gray squares represent potential controller/measurement locations. The selected controllers and measurements are highlighted in red and green, respectively. Scenarios (a) and (b) have $\mathbf{M} = \mathbf{I}$, whereas line flows and frequency deviation can also be measured in (c) and (d). For each scenario, the resulting (non-unique) affine control realization is provided below together with the behavior of the potentially active constraints for all $\boldsymbol{u}_\mathrm{f} \in \boldsymbol{\mathcal{U}}_\mathrm{f}$ on the right. For scenario (c) with multiple, equivalent optimal solutions, the colored frames denote alternative optimal solutions. The rationale behind the scenarios is as follows: In (b) the primary control droop is reduced compared to (a). In (c) we allow for additional measurements. In (d) we reduce the transfer capacity of the middle link to form an additional active constraint.

optimization. This allows us to reduce the number of measurements to only one. For this scenario the solution is not unique: one possibility is to take the measurement of the frequency deviation as feedback to the controller, yielding an adapted primary control scheme. An alternative solution that is shown in Fig. 7.1 (c) is to monitor the sum of the outputs of generators 1 and 2 by measuring the line flow between bus 2 and 3 for

Scenario	MILP	HC (empty sets)	HC ($\mathcal{C}$ from MILP)
(a)	77 ms	160 ms	100 ms
(b)	78 ms	233 ms	135 ms
(c)	97 ms	277 ms	171 ms
(d)	101 ms	330 ms	176 ms

Table 7.1: Total solver time for the proposed optimization algorithms applied to the simple microgrid.

controlling the set point of the generator at bus 4. This situation will be very common in future active distribution grids, where individual small scale loads or generators are not able to violate local grid constraints, but their aggregated effect is important to the system. Since the load is fixed, measuring the line between buses 3 and 4 would be equally informative. The admissibility of all these solution candidates was verified via LP (3.18), obtaining valid affine controller realizations in all cases.

In scenario (d), we constrain the capacity of the transmission line connecting buses 2 and 3 to the interval $[-1, 1]$ MW. This represents an active grid constraint if the generators at buses 1 and 2 produce at maximum power. The solution obtained via MILP (4.9) as well as hill climbing optimization consists of additionally controlling the power injection at bus 1. Again, several alternative solutions are possible.

In scenarios (a), (b), and (c), the frequency deviation represents an active constraint to the operation of the system. Observe in Fig. 7.1 how in each case the resulting affine control law keeps the frequency deviation inside the feasible region for all values of the non-controlled injections. In scenario (d), the designed controller also ensures feasible system operation despite the limited power capacity of the middle line.

While for the demonstrated example all solutions can readily be verified manually, it shows that the situation may become much more complex in larger grids. The topological location of generators and loads in the grid is important as well as their capacity and their neighborhood. An automated algorithm for selecting critical elements to control and/or measure is thus very beneficial for complex networks with distributed generation and transmission lines that are operated close to their technical limits.

In scenarios (c) and (d) we also test the greedy approach 1) starting with empty sets, and 2) using the solution of MILP (4.13) for $\mathcal{C}$ as starting point. In both cases the same optimal objective function value is obtained. The solutions for $\mathcal{M}$ and $\mathcal{C}$ did not always agree exactly, but could be shown to be equally optimal.

The total solver time for all scenarios is shown in Table 7.1. As expected, MILP (4.13) performs faster than the hill climbing optimization for the same instances. When computing the optimal sets for scenarios (a) and (b), the MILP algorithm was more than 2 times faster than the hill climbing with empty sets. It was also ca. 1.2 times faster than the hill climbing that uses the solution of MILP (4.13) for $\mathcal{C}$ as initial guess, which corroborates the benefits of such concatenated optimization procedure.

7.2.2 Modified IEEE 118 bus test case

We now analyze the modified version of the IEEE 118 bus test case, see Fig. 7.2. This power system is composed of 54 generators, 99 loads, and 186 transmission lines. The topology of the power system, the load values and the line and generator capacities were taken from [161]. We assume that each generator can be scheduled in the range of 10–90 % of its available capacity. In addition, we admit 10% of uncertainty for each load in both directions. The maximum allowed frequency deviation is taken as ± 0.2 Hz.

We first consider the case when only the power set points may be measured, i.e., $\mathbf{M} = \mathbf{I}$, see Fig. 7.2 (a). We obtain an optimal set of 12 actuator and 20 sensor devices that guarantee feasible grid operation. The remaining 96 injections can be left operating free and/or be manipulated deliberately and do not require any monitoring equipment.

To obtain this result, we first use MILP (4.13) and then validate its solution via LP (3.18). The obtained feasibility indicator η is smaller than zero, thereby proving the admissibility and optimality of the MILP solution. When we initialize the greedy search with empty sets, we obtain an admissible solution consisting of 23 actuators and 9 sensors. As expected, the obtained solution in this case is larger than the one provided via MILP optimization. This confirms that taking the MILP solution as initial guess is beneficial for the greedy search.

We now include sensors for the line flows as well as the frequency deviation as possible measurements, see Fig. 7.2 (b). This yields in total 305 possible sensor devices. We first apply MILP (4.13) and then the greedy optimization approach, starting with the actuators identified via the MILP. As expected, the solution is much sparser than before. The total number of required sensors is reduced from 20 to 3. The selected line flows confer a large amount of information that help avoiding grid capacity violations.

It is insightful to observe the progress of the hill climbing procedure: buses with major generators connected are selected as controlled nodes first. The procedure is thus initially reducing the impact of the exogenous actions on the system by controlling the highest uncertain power injections first. When enough controlled nodes were selected, the selection of sensors starts to be significant for the minimization of the cost function. Selected sensors are often related to nodes connected either to large non-controlled generators or to high uncertain loads. Remaining buses with smaller injections are mostly left unobserved.

Table 7.2 shows the obtained solver time for all studied cases. The solution for case (a) using MILP optimization was found in about 2.57 minutes. Observe that the solution for case (b) was computed in about 28 min for the concatenated execution of both algorithms, compared to the ca. 154 minutes needed by the solver when starting hill climbing with empty sets. A single verification step using LP (3.18) took less than a second.

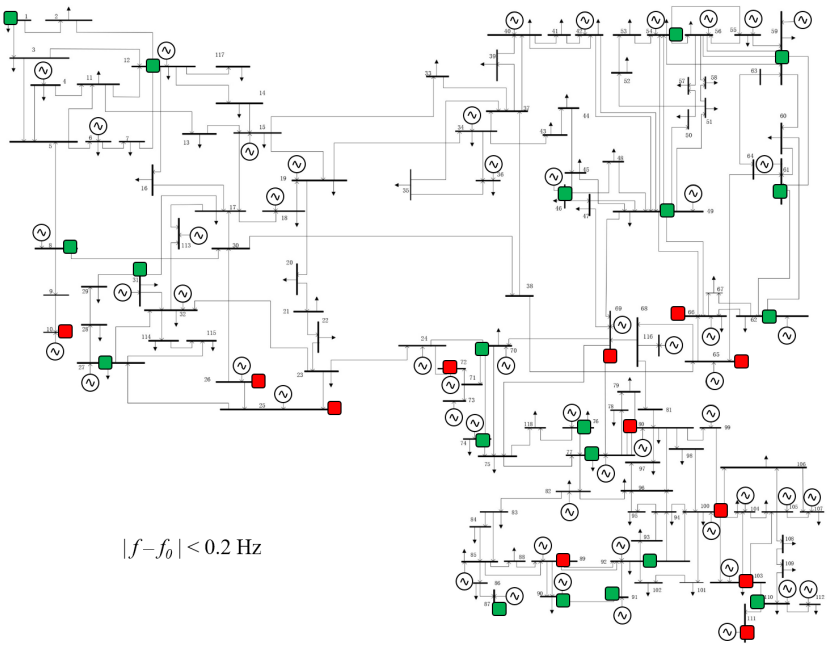

(a)

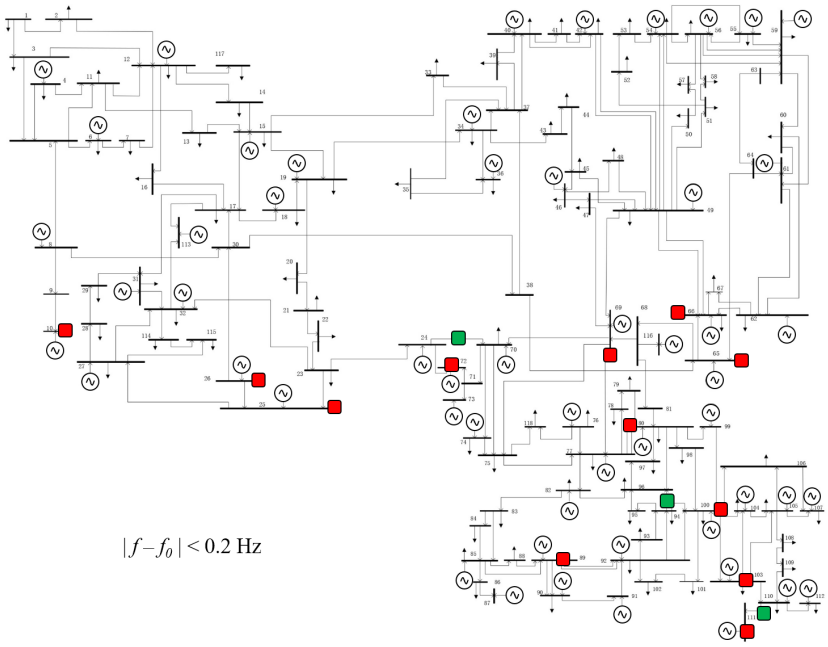

(b)

Figure 7.2: Minimal sets of actuators and sensors for the modified IEEE 118 bus test case. The selected actuators and sensors are highlighted in red and green, respectively. (a) Only the nodal power set points may be measured. In this scenario, only 12 actuators and 20 sensors are required to guarantee feasible grid operation. (b) The measurement of line power flows and grid frequency deviation are additionally considered as possible. In this case only 3 sensors are required.

Scenario	MILP	HC (empty sets)	HC ($\mathcal{C}$ from MILP)
(a)	2.57 min	13 min	5.78 min
(b)	-	154 min	28 min

Table 7.2: Total solver time for the proposed optimization algorithms applied to the modified IEEE 118 bus test case.

The computation time could further be improved, e.g., by testing not all possible set extensions in each step of the greedy search but using only a representative subset, selected by proximity in the graph. Another idea would be to add more than one element in each iteration. For the control design task described in this paper, however, the achieved computation time seemed acceptable even without these extensions.

7.3 Stability in Closed-loop Linearized Power Networks

In this section, we show the potential of the above developed algorithms to design wide-area controllers for electrical power systems. After a brief description of the dynamics of power systems in the linear regime, we present the designs for 1) the introductory microgrid of Section 7.2.1 and 2) a modified version of the IEEE 57 bus test case.

7.3.1 Power Grids as LTI Systems

We analyze electrical transmission networks with N electrical buses connected by T transmission lines under the *DC power flow* assumptions introduced in Section 7.1.2. The power grid with integrated primary control action can then be modeled around its nominal operating point as a network of coupled oscillators subject to the linear swing equation

$$\mathbf{J}\ddot{\boldsymbol{\theta}}(t) + \mathbf{K}\dot{\boldsymbol{\theta}}(t) + \mathbf{B}_{\mathrm{I}}\boldsymbol{\theta}(t) = \mathbf{p}(t), \tag{7.4}$$

where $\boldsymbol{\theta}(t) \in \mathbb{R}^N$ symbolizes the vector of voltage angles, and $\mathbf{p}(t) \in \mathbb{R}^N$ the vector of set points for the active power injections. We assume that both the inertia $\mathbf{J} \in \mathbb{R}^{N\times N}$ and primary control $\mathbf{K} \in \mathbb{R}^{N\times N}$ matrices are diagonal. Moreover, it is supposed that $\mathbf{J} \succ \mathbf{0}$ and $\mathbf{K} \succeq \mathbf{0}$. The coupling matrix $\mathbf{B}_{\mathrm{I}} \in \mathbb{R}^{N\times N}$ is given element-wise as in Section 7.1.2.

By defining $\mathbf{x}(t) = \begin{bmatrix}\boldsymbol{\theta}^{\mathrm{T}}(t) & \dot{\boldsymbol{\theta}}^{\mathrm{T}}(t)\end{bmatrix}^{\mathrm{T}}$ and $\mathbf{u}(t) = \mathbf{p}(t)$, the state space representation of (7.4) is given by

$$\dot{\mathbf{x}}(t) = \underbrace{\begin{bmatrix}\mathbf{0} & \mathbf{I} \\ -\mathbf{J}^{-1}\mathbf{B}_{\mathrm{I}} & -\mathbf{J}^{-1}\mathbf{K}\end{bmatrix}}_{\mathbf{A}}\mathbf{x}(t) + \underbrace{\begin{bmatrix}\mathbf{0} \\ \mathbf{J}^{-1}\end{bmatrix}}_{\mathbf{B}}\mathbf{u}(t), \tag{7.5}$$

where we use $\mathbf{0}$ to denote a matrix of zeros with suitable dimensions. Quantities like the active power injected by generators or consumed by loads, the nodal frequencies, and the line power flows are considered as measurable quantities that can be determined

linearly from the knowledge of $\mathbf{x}(t)$. The nodal power injections will be limited above and below by the technical capabilities of the connected generator or load. Similarly, line power flows and the grid frequency are typically subject to upper and lower bounds. This reasoning lets us define the structure of the linear inequalities $\mathbf{E}\boldsymbol{x} \leq \boldsymbol{b}$, cf. Chapter 6.

7.3.2 Introductory Microgrid

The considered microgrid consists of 3 generators supplying a demand of 5 MW. Fig. 7.1 (a) shows the topology of the grid together with the capacity limits of each transmission line and each generator/load. The generator located at bus 4 provides primary reserve, with a droop of 4 MW/Hz. Nodal frequency deviations must not exceed ± 0.1 Hz.

We initially assume that all transmission lines have a power transfer capacity of ± 10 MW, which is adequate to avoid grid limitations. It is presupposed that both the nodal power injections and the line flows are measurable quantities. Nodal frequencies are not monitored. In this scenario, it is sufficient to control the generator located at bus 4 based on the power flowing between buses 2 and 3, in order to fulfill the steady state requirements. For this setup, the system is neither controllable nor observable, since both the observability and the controllability matrices have insufficient rank. We further simulate the dynamics of the network assuming that the exogenous actions are manipulated at fixed time intervals, uniformly at random, and low-pass filtered. Fig. 7.3 shows how the resulting affine control law maintains the frequency deviations within the desired region at steady state, while occasional violations during the transition period can be observed.

Now we constrain the power flowing between buses 2 and 3 to be within the interval $[-1, 1]$ MW. In this scenario, the resulting minimal sets $\mathcal{C}$ and $\mathcal{M}$ are shown in Fig. 7.1 (d). We see that the injection at bus 2 must additionally be controlled. As mentioned in Section 7.2.1, the system admits multiple equivalent minimal actuator and sensor sets. When controlling the injection at bus 1 instead of the injection at bus 2, the solution of

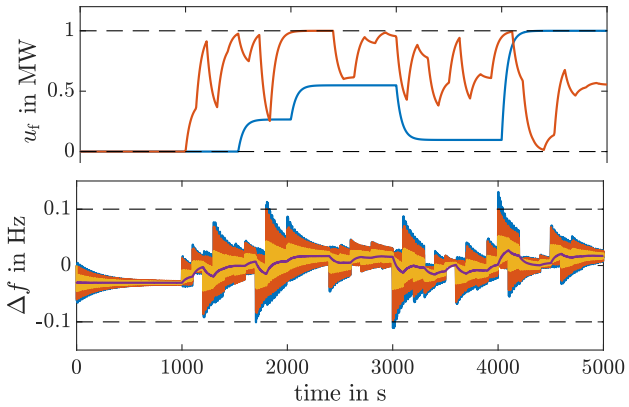

Figure 7.3: Simple microgrid without active steady state constraints on the transmission lines. Top: Trajectories of the exogenous action $\mathbf{u}_\mathrm{f}(t)$, i.e., the injections at buses 1 (blue) and 2 (red). Bottom: Resulting transient frequency deviations for all 4 buses.

LP (3.18) yields an affine control law for which the resulting closed-loop is unstable. The system can, however, be stabilized with only one iteration of the path-following algorithm. Here we remark that when computing the minimal admissible actuator and sensor sets via hill climbing optimization, we rarely required the stability improvement procedure.

7.3.3 Modified IEEE 57 bus test case

We now design a minimal admissible affine output feedback controller for the modified IEEE 57 bus power system shown in Fig. 7.4 (a). It has 28 generators, 29 loads, and 80 transmission lines. The topology of the power system, the nominal load values, and generator capacities for producers located at buses $\{1, 2, 3, 6, 8, 9, 12\}$ were taken from [161]. The capacity of the remaining generators are drawn from a uniform distribution within the interval [0, 150] MW, and the capacity of the transmission lines is set to ± 100 MW. It is also supposed that the power injections as well as the line flows are available as possible measurements. In addition, we admit 5% of uncertainty for each load in both directions. The maximum allowed frequency deviation is ± 0.2 Hz.

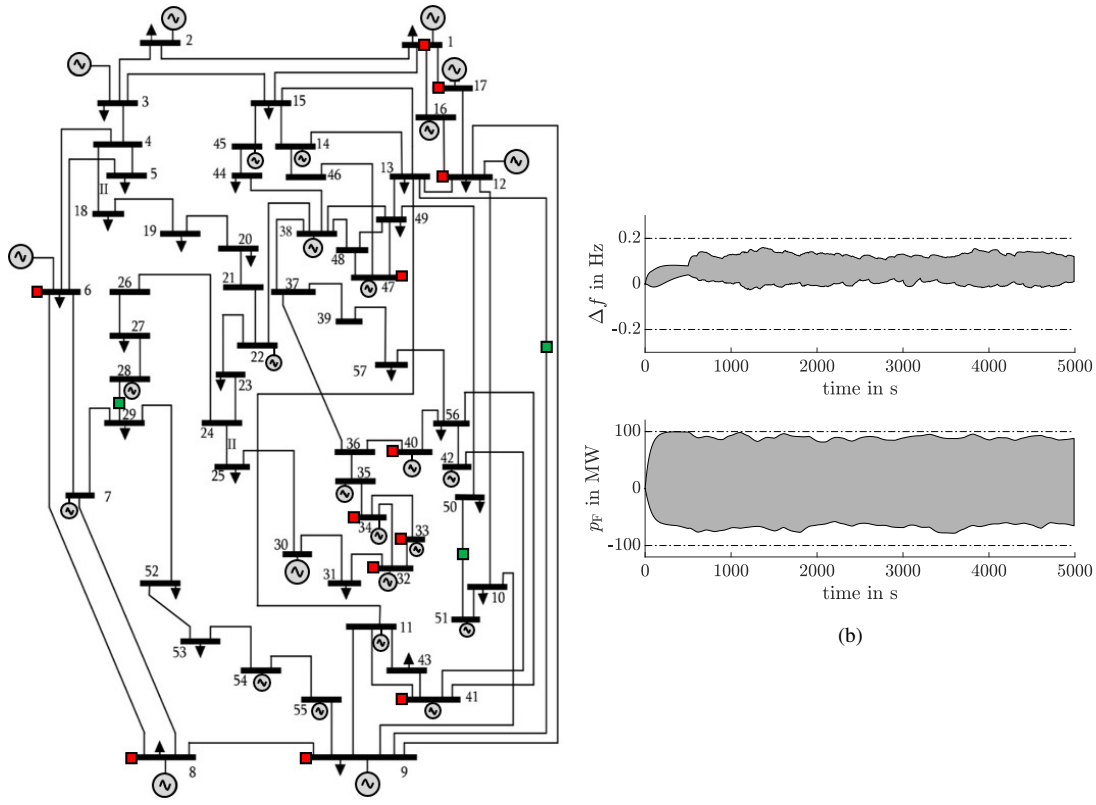

(a) (b)

Figure 7.4: (a) Minimal sets $\mathcal{C}$ and $\mathcal{M}$ for the modified IEEE 57 bus power system. The location of the selected actuators and sensors is marked in red and green, respectively. (b) Time behavior of the transient frequency deviations (top) and the line flows (down) when the remaining non-controlled generators and loads are manipulated randomly within their operating limits. The area in gray encloses the time trajectories of all nodal frequencies and all line flows, the dashed lines mark their allowed range.

The obtained minimal admissible sets $(\mathcal{C}, \mathcal{M})$ are shown in Fig. 7.4 (a). We obtain that 12 generators must be controlled based on 3 line flow measurements in order to fulfill the two design specifications. Next, we simulate the time behavior of the system, manipulating the set-points of the non-controlled generators and loads as before, at fixed time intervals according to a uniform distribution and applying low-pass filtering. Fig. 7.4 (b) shows that the local frequency deviations and the line flows remain within the desired region throughout the simulation time.

7.4 Voltage Regulation in Distribution Networks

The massive integration of decentralized energy resources into power distribution systems implies new challenges for distribution system operators in order to guarantee feasible system operation at all times [162]. In particular, the nodal voltage levels in the network are affected by decentralized generation and need to be actively regulated. The problem is known as the *voltage regulation* or the *Voltage VAr Control* (VVC) problem. It is challenging because the grid state is often highly uncertain due to the low number of sensors in the grid, which may or may not be connected to the control center.

VVC has been widely studied in recent years and, with respect to the assumed degree of observability of the distribution grid, these works can be structured as follows. Many different actuators such as the OLTC of the substation transformer, reactive power contributions of decentralized generators and capacitor banks, or voltage regulators can be controlled by solving central optimization problems targeting voltage feasibility at minimal losses and minimal switching frequency of the OLTC [163, 164]. The grid state is assumed to be fully known in these works. The authors in [165] estimate the grid state and accommodates for prediction errors by employing additional security margins for the controlled voltage levels. A stochastic optimization approach is followed in [166]. Robust control is considered in [167]. The considered uncertainty sets, however, are fixed and not adaptive to available measurement values. This means that the uncertainty set has to be larger than necessary and the control action more conservative.

In the following, we design robust control policies for the VVC problem. We make use of measurement-dependent uncertainty sets which allows us to balance robustness and performance. Not only incomplete observability and measurement errors can be considered as sources of uncertainty but also the large-scale failure of a small number of sensors, e.g., due to outages or malicious distortions.

In the following, we formulate the VVC problem by using the abstract constrained static linear system representation proposed in this thesis. However, we do not restrict ourselves to affine controller structures but propose to use the admissible PWA control law proposed in Section 3.3. Given current values for the measured quantities we can quickly check whether an adaption is necessary, and otherwise save multiple costly OLTC switching events. Here we note that our automated design approach can quickly adapt to

changing system environments, e.g., in case of crises, and thus increases the operational resilience of the system.

The PWA control laws proposed in Section 3.3 is now demonstrated with simulations of active distribution networks. First, three explanatory distribution feeders of small size are studied. Thereafter, the scalability of our admissible PWA controllers is verified using a modified version of the IEEE 123 bus test case.

7.4.1 Simple Distribution Feeder – Online PWA Control Law

Fig. 7.5 (a) shows a simple distribution feeder with two loads and two photovoltaic (PV) units. The setup—although strongly simplified—resembles a typical situation in today distributions with high PV penetration. The impedance of each line segment is assumed to be $0.03+\mathrm{j}0.06$ p.u. High PV-infeeds at low loads lead to voltage rises towards the end of the feeder, and high loads without PV production to voltage drops. Keeping the nodal voltage levels within $[0.9,\ 1.1]$ p.u. thus represents the relevant operational constraint, while transmission limits are not relevant here.

The PV units generate active power depending on the weather conditions, with maximum capacity of 1 p.u. We assume that the geographically closeness of the PV units leads to strong coupling of their production, i.e., both PV units produce the same power in each time step. This behavior is modeled by the interval uncertainty set shown in Fig. 7.5 (b). The maximum load at each node is assumed to be 1 p.u., but we limit the joint demand to 50% of the sum of the individual peak demands, resulting in the uncertainty set shown in Fig. 7.5 (c). The uncertainty set for the combined active power injections is illustrated in Fig. 7.5 (d).

We assume in this example that the PV units do not inject reactive power to the network, leaving the OLTC of the distribution transformer as the unique controllable actuator to regulate the voltage.

We first study the case in which there is no information available online to set the voltage v_0 via the OLTC, meaning that a constant voltage v_0 should be valid for all active power injections in the uncertainty set. For this setup, the maximum impact of the uncertain active power injections on the system constraints is computed via LP (3.28). Subsequently, we solve LP (3.29) and obtain $\eta > 0$. This means that the current actuator/sensor equipment does not allow for the design of an admissible control law, i.e., there is no constant v_0 guaranteeing feasible system operation in all cases.

Now we integrate the measurement of the nodal active power at the root bus into the control system, which is a common local measurement available to OLTC controllers. The new controller setup admits an admissible control law since by applying the proposed two-stage algorithm we can determine a feasible value v_0 for each possible power measurement p_0 in the range $[-2,\ 1]$ p.u., see Fig. 7.5 (e). In case of high PV generation, voltage v_0 is set to its lower bound, independently of the load values. In contrast, when there is no PV generation and one of the loads reaches its peak value, voltage v_0 is set to

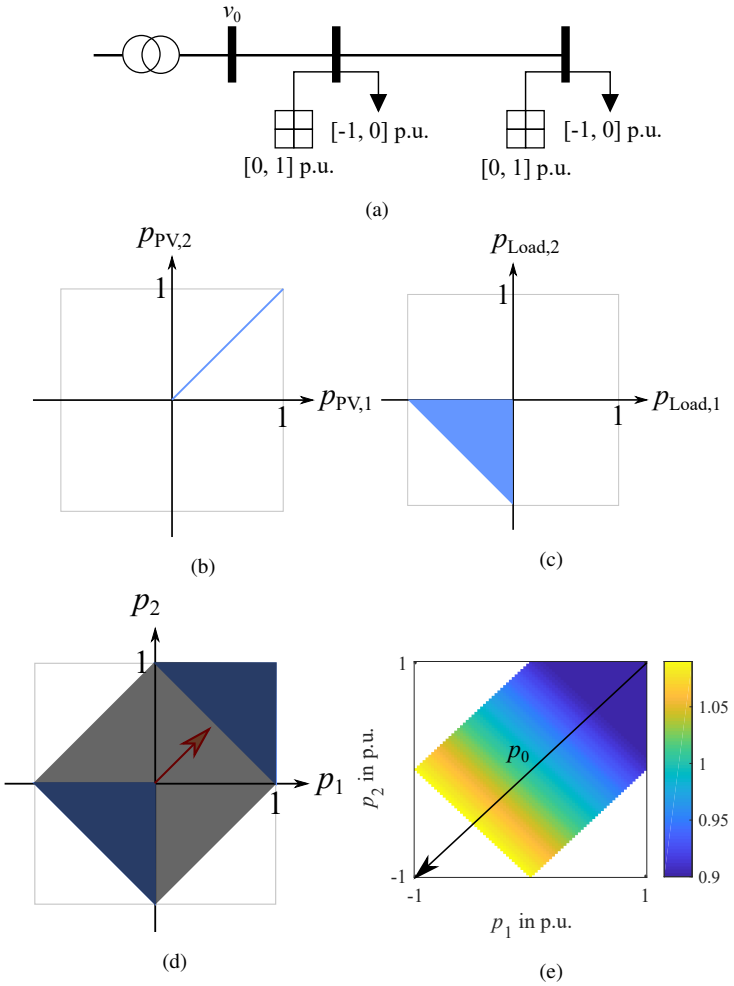

Figure 7.5: Exemplary active distribution feeder subject to uncertain active power loads and coupled PV production. (a) Topology of the network with specified operation limits for loads and PV units. (b) The blue line corresponds to the uncertainty set for the active power generated by the PV units. (c) The blue region models the uncertainty for the loads. (d) The uncertainty set for the active power injections (shaded) is obtained by combining the sets (a) and (b). (e) Optimal voltage set point v_0 as a function of the active power p_0 provided by the distribution transformer.

1.09 p.u., close to its maximum allowed value. As expected, the voltage v_0 increases gradually with the power p_0 provided by the transformer. Unlike the following examples, this small test case could be solved intuitively, but serves to validate the proposed approach.

7.4.2 Simple Distribution Feeder – Offline PWA Control Law

Fig. 7.6 (a) shows the single-line diagram of a simple distribution feeder with a substation transformer and two buses. Each transmission line is parametrized by a series impedance of $0.0153 + \mathrm{j}0.033$ p.u.. The voltage at the substation is fixed at $v_0 = 1$ p.u.. Further, a pure active load as well as a small PV unit are connected to node 1. This PV unit produces power with a power factor of one. The PV unit connected at node 2 has a maximum apparent power capacity of $\overline{S}_2 = 1$ p.u. and is allowed to inject reactive power

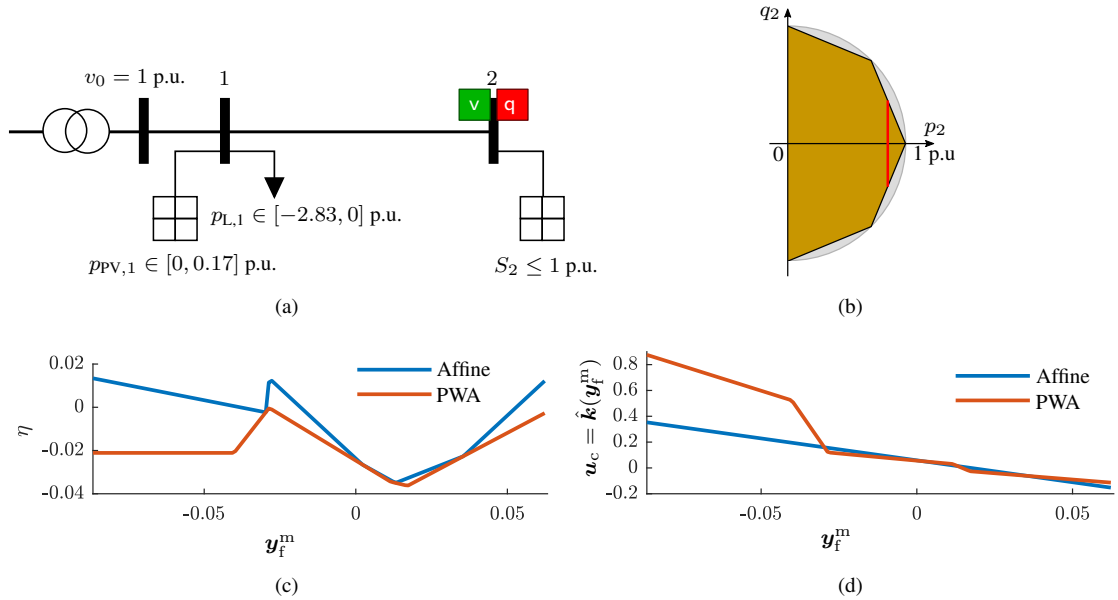

Figure 7.6: A simple active distribution feeder subject to uncertain active power loads and PV generation. (a) Topology of the network with specified operation limits for loads and PV units. (b) Operational constraint for the PV unit at bus 2 approximated via polyhedral constraints. The red line indicates the maximum allowed active power output p_2 that ensures sufficient reactive power capabilities during peak output. (c) Feasibility indicator η over all possible observations obtained for both affine and PWA control laws. While the system does not admit an affine control law, an admissible PWA control law is possible. Note that η as a function of $\boldsymbol{y}_{\mathrm{f}}^{\mathrm{m}}$ is a non-convex PWA mapping. (d) The best possible affine control law cannot cope with all peak load/generation situations, which in contrast are easily handled by an admissible PWA control law.

to the network based on the measurement of the voltage level at node 2. We are thus interested in finding an admissible control law $\boldsymbol{u}_{\mathrm{c}} = \hat{\boldsymbol{k}}(\boldsymbol{y}_{\mathrm{f}}^{\mathrm{m}})$, where $\boldsymbol{u}_{\mathrm{c}} = q_2$ and $\boldsymbol{y}_{\mathrm{f}}^{\mathrm{m}}$ is the observation associated to v_2.

In distribution grid operations, the nodal voltage levels across the network are typically restricted to be within the interval $[0.95,\ 1.05]$ p.u.. Moreover, the reactive power injected by the PV unit at bus 2 has to be chosen such that the maximum power capacity of the PV unit is not exceeded, i.e., for a fixed value of generated active power p_2, the condition $\sqrt{p_2^2 + q_2^2} \leq \overline{S}_2$ must hold. This non-linear constraint can be approximated with the help of polyhedral constraints as illustrated in Fig. 7.6 (b). The maximum active power produced by the PV unit at node 2 is limited to 95% of the maximum apparent power capacity $\overline{S}_2$ in order to still be able to support voltage regulation during peak load situations.

For this system setup, we first check for the existence of an affine mapping using the LP algorithm (3.9). We obtain $\eta^\star = 0.013 > 0$, which means that the power system does not admit an affine control law. We thereafter solve our QCQP (3.27) and obtain $\eta^\star = -3.7 \times 10^{-4} \leq 0$, i.e., an admissible PWA control law exists, namely the PWA function $\boldsymbol{u}_{\mathrm{c}} = \hat{\boldsymbol{k}}(\boldsymbol{y}_{\mathrm{f}}^{\mathrm{m}})$ depicted in Fig. 7.6 (d). The PWA mapping $\boldsymbol{u}_{\mathrm{c}} = \hat{\boldsymbol{k}}(\boldsymbol{y}_{\mathrm{f}}^{\mathrm{m}})$ has a total of 5 pieces, which can be precomputed by employing the two-step technique proposed in

Section 3.3.2. Note in Fig. 7.6 (c) that, as predicted by the solution of QCQP (3.27), the value of the feasibility indicator η over all observations fulfills $\eta \leq 0$. With the hardware specified in above, the admissibility guarantee is obtained in ca. 25 ms.

7.4.3 11 Node Distribution Feeder – Distorted Sensors

Now we apply the control algorithm proposed in Section 3.3 to simulate the operation of the 11 node feeder shown in Fig. 7.7 for one day. The system has active power loads of up to 1 p.u. connected to nodes $\{1, 2, 4, 8, 9\}$, and PV units with capacity of 1 p.u. are connected to nodes $\{3, 5, 6, 7, 10\}$. With exception to the PV unit at node 7, which has a reactive power capacity of ± 0.2 p.u., all remaining PV units operate with a power factor of 1. The impedance of each line segment is assumed as $0.002 + \mathrm{j}0.006$ p.u. The voltage at node 0 is controlled via the OLTC within the operation interval of $[0.9, 1.1]$ p.u. In addition, the reactive power injection of the PV unit at node 7 can also be controlled. The control system has access to the measurement of the nodal voltages at nodes $\{3, 7, 10\}$ as well as the active power provided by the transformer.

As above, the production of the PV units is assumed to be geographically coupled. The PV generation follows the profile of a sunny day as shown in Fig. 7.8 (a). Power consumptions are modeled as individual random processes with uniform distribution. Fig. 7.8 (b) shows the resulting load profiles together with the total load over time. The controller determines new control set points every 5 minutes.

Initially, the controller is designed for the case of having non-corrupted measurements. Using the proposed minimal action control algorithm based on LPs (3.28)–(3.29), we obtain the optimal trajectory for v_0 depicted in Fig. 7.8 (c). In this scenario, the voltage at the distribution transformer has to be adjusted only two times. As expected, the maximum nodal voltage in the network coincides with v_0 during the hours of low PV generation. In contrast, the value of v_0 corresponds to the minimum nodal voltage in the network during the peak PV generation hours. During the day, the lowest nodal voltage levels were reported at nodes $\{0, 1, 2, 4, 8, 9, 10\}$, and the highest at nodes $\{0, 5, 6, 7, 10\}$. This indicates that the identification of critical nodes in the feeder is not trivial when having a high, non-uniformly spread penetration of decentralized generation in the network.

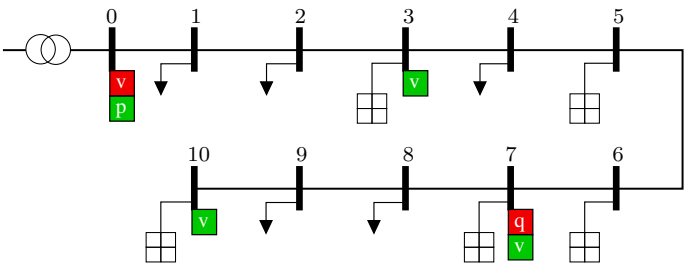

Figure 7.7: 11 node distribution feeder with 5 loads and 5 coupled PV units. The controller sets the OLTC voltage v_0 and the reactive power injection of the PV unit at node 7 (red boxes) based on the available measurements (green boxes).

Subsequently, we design an admissible control law that tolerates the distortion of at most $\mathsf{k} = 1$ sensor, where the position of the distorted sensor is unknown to the DSO, cf. Chapter 5. We now define the interval boundaries of the manipulation signal $\Delta\boldsymbol{\mathcal{Y}}_{\mathrm{f}}^{\mathrm{m}}$ for the voltage measurements as 0.5 p.u. in both directions. To check the validity of the approach, we artificially alter the voltage sensor at bus 10 with a constant offset of 0.3 p.u..

Interestingly, the solution for v_0 obtained based on MILP (5.8) for dealing with corrupted measurements is almost identical as the solution for the undisturbed case. This demonstrates well that our proposed approach is robust to this large distortion. When computing the control actions using the LP relaxation (5.10) for dealing with corrupted measurements, we obtain a slightly different solution for the v_0 values, see Fig. 7.8 (d). Due to the relaxation, the size of the uncertainty set increases and the computed the worst-case upper and lower voltages show a wider corridor than before. This forces the algorithm to adapt the control values more often. Nevertheless, the voltage is adapted only 4 times during the day. Fig. 7.8 (e) shows the resulting trajectories for the reactive power to be injected by the PV unit connected at node 7. By choosing one of the approaches, users can make their preferred choice in the trade-off between the slightly higher computational requirements for MILP (5.8) and its superior solution quality.

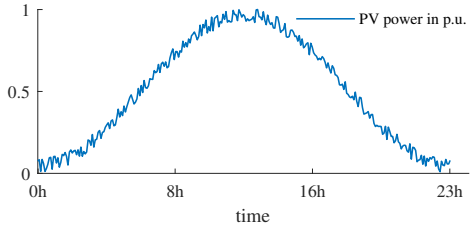

(a) Generation profile for each PV unit during a sunny day.

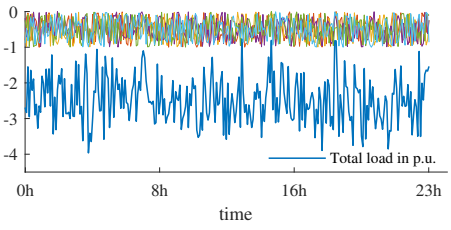

(b) Load profiles taken from a uniform random process.

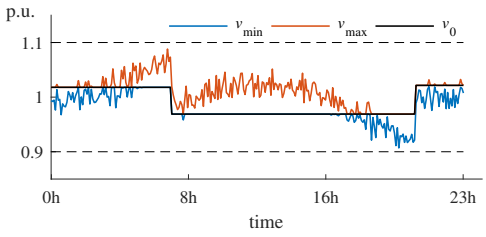

(c) OLTC voltage v_0 and max/min voltages throughout the grid assuming correct, see LP (3.28), or 1 distorted, see MILP (5.8) sensor.

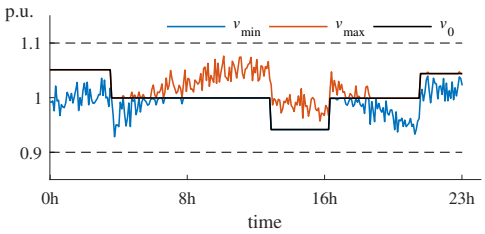

(d) OLTC voltage v_0 and max/min voltages throughout the grid assuming 1 corrupted sensor, see LP (5.10) with $\mathsf{k} = 1$.

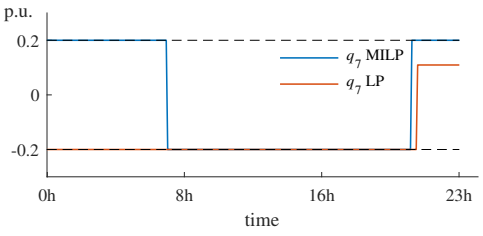

(e) Reactive power set points q_7 related to the plots (c) and (d).

Figure 7.8: Robust voltage regulation for the 11 node distribution feeder of Fig. 7.7 during a sunny day.

7.4.4 Modified IEEE 123 Bus Test Feeder – Distorted Sensors

To validate the scalability of the proposed voltage regulator, we briefly present its application to a modified version of the IEEE 123 bus test case [168], see Fig. 7.9 (a). We install a total of 36 PV units with a capacity of 50 p.u. in the grid, assuming power factor 1 for all of them. The control center is able to control the voltage v_0 at the main tranformer as well as the voltage regulators at nodes 9, 25, and 118. The sensor set consists of the active power at node 0 and the nodal voltages at a few of the PV units that are assumed to be connected to the control center. A maximum of $\mathsf{k} = 2$ sensors are assumed to be subject to exogenous manipulation within the interval-bounded uncertainty set $\Delta\mathcal{Y}_{\mathrm{f}}^{\mathrm{m}}$, cf. Chapter 5. We define interval boundaries of $\Delta\mathcal{Y}_{\mathrm{f}}^{\mathrm{m}}$ for the voltage measurements as 0.5 p.u. in both directions. As before, the PV production assumed to be geographically coupled, i.e., each PV unit follows the generation profile shown in Fig. 7.8 (a).

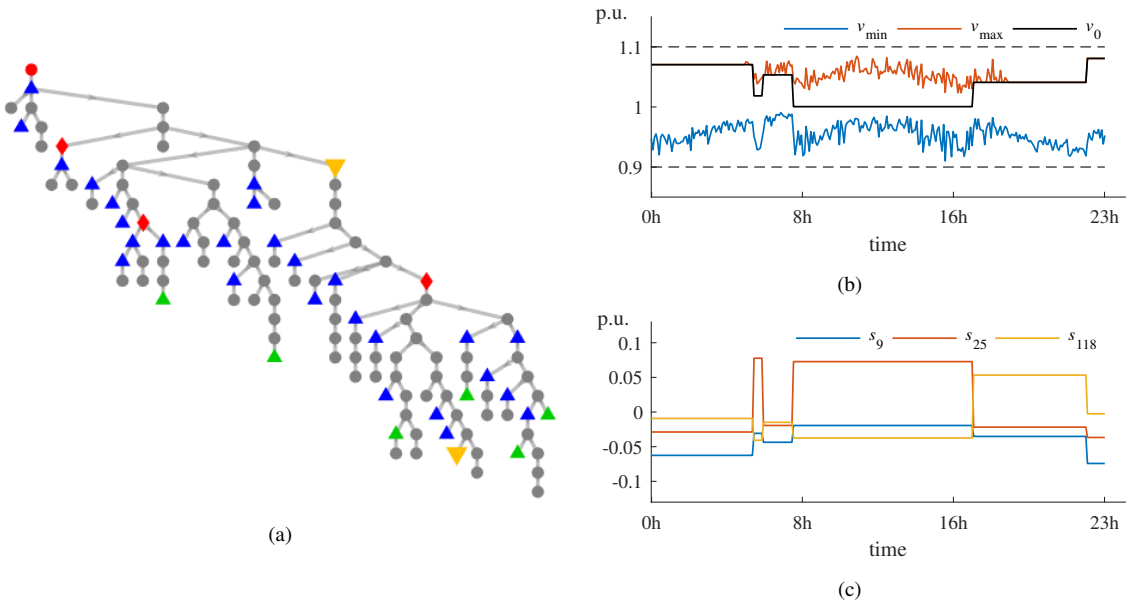

Figure 7.9: Simulation of the VVC control for the modified version of the IEEE 123 bus test case during a sunny day. (a) Topology of the grid.. The red circle represents the root node, whose nodal voltage is controlled and active power measured. Red diamonds symbolize locations of controllable voltage regulators. Nodes with PV units are marked with the blue, green, or orange triangles. Green and orange marks indicate that the local voltage is available to the control center. Orange implies that the measurement is distorted. (b) OLTC voltage v_0 and maximal/minimal possible voltages throughout the grid assuming up to two corrupted measurements, see MILP (5.8) with $\mathsf{k} = 2$. (c) Obtained set points for the voltage regulators at notes $\{9, 25, 118\}$.

The active and reactive power loads are modeled uniformly random, with peak values as specified in [168]. The average total active and reactive loads for the simulation day are 1500 p.u. and 500 p.u., respectively. The simulated voltage measurements available to the controller are manipulated for two sensors, via an offset of 0.4 p.u. The distorted subset of sensors is unknown to the controller.

Every 5 min, the controller determines the value of the control action for the given observation to guarantee nodal voltage levels within the interval $[0.9,\ 1.1]$ p.u.. By applying the proposed minimal action control concept based on MILP (5.8), we obtain the trajectories for the control action depicted in Figs. 7.9 (b) and (c). Observe how the minimum and maximum voltages are closed to the operational limits during almost the whole simulation day. This is achieved by in 5 switching operations of the control actions during the day. The voltage regulators change their value synchronously with v_0. The solver time for each iteration of the control algorithm is about 9 s.

7.4.5 Modified IEEE 123 Distribution Feeder – Verifying the Existence of Admissible Control Laws

We again address a modified version of the IEEE 123 bus test case [168], which is shown in Fig. 7.10. We assume that the system is balanced, allowing us to perform single-line analysis. The system has a total of 86 loads. Each load has active and reactive power components subject to interval bounded uncertainty sets. The peak load at each node is calculated as the sum of the nodal spot load values prespecified in [168]. The system has a total peak load of $\overline{S}_{\text{load}}^{\text{total}} = 14.36 + \text{j}7.84$ p.u..

We now install a total of 35 PV units at those nodes highlighted in yellow and cyan in Fig. 7.10. We assume that the active power injected by each PV unit is uncertain and bounded by an interval uncertainty set. Each PV unit has a maximum power capacity of $\overline{S}_{\text{PV}} = 0.384$ p.u.. The PV units in yellow generate power with a power factor of 1. In contrast, the PV units in cyan are able to inject reactive power into the network and, as in the previous test case, are subject to the operational constraints depicted in Fig. 7.6 (b). We require all voltage levels in the network to lie between 0.9 and 1.1 p.u..

The system operator can control the voltage regulators located at nodes $\{0, 8, 23, 71\}$ together with the reactive power injected by the PV units at nodes $\{74, 105\}$. In addition, the system operator has access to the voltage levels at nodes $\{74, 105\}$. These physical quantities define the variables $\boldsymbol{u}_{\text{c}} \in \mathbb{R}^6$, $\boldsymbol{u}_{\text{f}} \in \mathbb{R}^{211}$, and $\boldsymbol{y}_{\text{f}}^{\text{m}} \in \mathbb{R}^2$. As before, we use the linearized version of the DistFlow equations to derive the static system representation (2.1).

Next, we check whether it is possible to find an admissible affine control law for the system. After solving LP (3.9) in ca. 11.8 s, we obtain $\eta^\star = 0.007 > 0$, i.e., the system does not admit an affine control law. In contrast, the solution of our proposed QCQP (3.27) outputs $\eta^\star = -0.004 < 0$, which confirms the existence of an admissible PWA control law. We remark that QCQP (3.27) is solved to optimality and the admissibility guarantee is obtained in ca. 5.15 s.

We now increase the maximum capacity of the PV units by 10% and check whether there exist an admissible control law for this scenario. After solving QCQP (3.27) we obtain that the system does not admit an PWA control law as $\eta^\star = 0.0082$. QCQP (3.27)

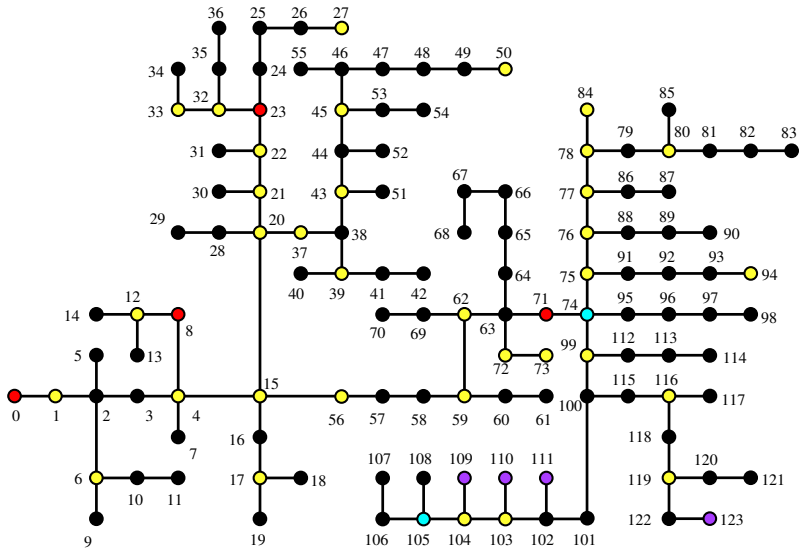

Figure 7.10: Modified version of the IEEE 123 bus test case. The black circles correspond to load nodes and the substation transformer is located at node 0. The red circles indicate the location of voltage regulators. Those PV units that generate with power factor 1 are highlighted in yellow, and those having reactive power control and communication capabilities are colored in cyan. The network has shunt capacitors (purple circles) at nodes {109,110,111,123}.

is solved in approx. 4.15 s. In fact, the optimal value of $\boldsymbol{\alpha}$ indicates that there is an overvoltage at bus 123 (where a large shunt capacitor is injecting reactive power). Such overvoltage is caused by a joint peak PV generation, as we read from the optimal value of $\boldsymbol{u}_{\mathrm{f}}$. This situation cannot be avoided by any choice of the control action computable from the available sensor equipment. Hence, we have to increase the number of actuators and sensors in the system.

We propose to additionally control the active power injected by the PV units at nodes $\{74, 105\}$, as those PV units already have communication capabilities. The solution of QCQP (3.27) then outputs $\eta^\star = -0.007$, corroborating the effectiveness of our proposed measure. QCQP (3.27) is solved to global optimality in about 46.5 s, and an upper bound below zero for the optimal value of $\eta^\star$ is obtained after ca. 18 s. We thus see QCQP (3.27) as a powerful verification tool, which can be implemented efficiently using off-the-shelf optimization software and allows the practitioner to run robust control algorithms with theoretical guarantees in safety critical power flow control applications.

The QCQP algorithm can also be exploited to determine the minimum number of actuators and sensors required for the existence of an admissible PWA control law, e.g., by using hill climbing optimization as introduced in [20] for the case of affine control laws. In addition, the optimal values of $\boldsymbol{\alpha}$ and $\boldsymbol{u}_{\mathrm{f}}$ also provide valuable information about which constraints are critical and which realization of the uncertain variables leads (or may lead) to a (potential) constraint violation. This kind of analysis is paramount in current and future grid operation and grid planning activities.

8 Conclusions & Outlook

The path to the energy transition calls for adaptation of current decision-making algorithms in power flow operations. These novel control algorithms should be efficient and capable of handling the inherent uncertainty introduced by a constantly growing number of decentralized generation units and flexibilities in order to always ensure a feasible grid state. In addition, they should enhance the operational resilience of the grid by overcoming cyber-physical threads and by tolerating low-probability, high-impact events. The broadness of this scientific scope can certainly not be covered by one thesis, but small steps are always key steps for the accomplishment of complex tasks. Let us now recapitulate on the investigations we conducted in this work and on our achievements.

This thesis provides a novel mathematical framework for the characterization and computation of admissible control laws for constrained static linear systems. An admissible control law is a feedback mapping that based on imperfect measured quantities always determines control actions resulting in feasible system states. While directly verifying the existence of an admissible control law is computationally challenging, we provided a set of related admissibility conditions which, in some special cases, can be used to verify the existence of admissible control laws with finite computational efforts. In particular, the existence of admissible affine control laws can in many cases be achieved in polynomial-time, given that the exogenous action is bounded either by a convex polytope, or a p-norm with $\mathsf{p} = 1$ or $\mathsf{p} \to \infty$. However, there are many system instances for which admissible affine control laws are impossible, but admissible PWA control laws exists. The existence of admissible PWA control laws can be verified by solving a non-convex QCQP, provided that both the control action and the exogenous action are bounded by convex polytopes. Although the computational complexity of the proposed QCQP is exponential in the worst-case, the admissibility guarantee can be obtained for realistic use cases with very reasonable efforts as we verified experimentally. The offline verification step is crucially important to apply these kind of controllers in real, safety-critical power grid applications.

Once the existence of an admissible control law has been verified, we can compute one efficiently using off-the-self optimization software. In case the exogenous action is bounded by a convex polytope, admissible affine control laws are computable offline by

solving a linear optimization problem. Moreover, admissible PWA control laws can be computed either online via LP, or offline by solving a two-stage multiparametric linear optimization problem. We remarked that the offline two-stage algorithm is limited to small-sized problem instances as the number of pieces of the PWA mapping grows exponentially with the dimension of the exogenous action. On the other hand, the online optimization algorithm relies on an efficient characterization of the uncertainty in terms of the current observation, which makes the method suitable for application to large-sized problem instances.

Our framework also incorporates algorithms to find the smallest number of actuators and sensors required to guarantee the existence of an admissible control law. Minimal admissible actuator and sensor sets for affine control laws are computable by solving a MILP. However, the method is adequate only in small- and medium-scale applications as the optimization model involves a large number of auxiliary variables and constraints that grows quadratically with the dimension of the exogenous action and the number of operational constraints. A lower bound for the minimal actuator and sensor sets allowing for the existence of PWA admissible control laws can be computed via MILP under the assumption that $\mathbf{M} = \mathbf{I}$. The proposed MILP performs efficiently in practice and also provides minimal admissible actuator and sensor sets in many cases. The solution of the MILP can additionally be utilized as starting point for an optimization routine based on hill climbing techniques.

Furthermore, we established that our framework is compatible with the steady state description of closed-loop LTI dynamic systems controlled via affine output feedback control laws. When using Lyapunov conditions for asymptotic stability in closed-loop, the resulting synthesis algorithm is a BMI, which can be solved at least locally by applying optimization algorithms like path-following. If, instead, stability conditions based on the real part of the eigenvalues of the closed-loop system matrix are used, then a non-convex, non-smooth optimization problem should be solved for the synthesis of the controller. The derivation of efficiently testable asymptotic stability conditions for steady state admissible (PWA) control laws is unquestionably a gap to be closed in future developments.

The potential of the framework and algorithms presented in this thesis has been verified with application examples in the power systems domain. We studied the identification of critical generator and sensor devices for robust active power flow in transmission grids, finding that in many cases a small number of generators and power flow measurements is sufficient for guaranteeing feasible system operation under uncertainty. Besides, we showed how to design robust voltage/VAr control policies for distribution networks having a large amount of photovoltaic generation units. Our policies keep the voltage levels across the network within a desired range of values independently of the power consumption/generation profile at each node. This is achieved by an admissible PWA control law

that adjusts both the OLTC's voltage at the substation transformer and the reactive power injected by a small number of photovoltaic units based on a small number of power and voltage measurements only. The resulting control algorithm also tolerates the exogenous malicious manipulation of some actuator/sensor signals.

Outlook

We identify several directions for additional research on the ideas presented in this thesis.

Stochastic Systems. Instead of taking a deterministic model for the uncertain exogenous actions, we can consider these variables as random and subject to known probability distributions. We can employ techniques like PCE to derive a framework for verifying the existence of admissible control policies that, based on random observations, guarantee a feasible system state for many realizations of the uncertain variables.

Constrained Static Non-linear Systems. In this thesis, we limit out developments to the case where the control action lies in a continuous, bounded and convex action space. However, there are many important cases where either only discrete decisions or a mix of discrete and continuous decisions are possible. Examples of this in power systems are connection/disconnection of a transmission line, load shedding, network topology reconfiguration, among others. The development of new theory and models for this kind of operational decisions under uncertainty thus represent an interesting direction for future research.

Another aspect that demands further work is the incorporation of non-linear observation models and non-convex system constraints into the framework introduced in this thesis. A novel set of admissibility conditions and efficient algorithms for the computation and verification of admissible control laws is to be investigated here.

Minimal Admissible Actuator and Sensor Sets for $N - \mathsf{k}$. The mixed-integer optimization approaches proposed in Chapter 4 can be readily extended to the identification of minimal actuators and sensors sets which guarantee the existence of an admissible control law that tolerates the malfunction/disruption of at most k actuator/sensor elements. However, alternative optimization methods and/or heuristics should be investigated due to the combinatorial explosion of the number of possible contingencies, even for small k. Regarding this, we think that decomposition methods like Benders [169] or Danzig-Wolfe [170] decomposition techniques can be beneficial.

Constrained Dynamic Systems. We believe that our ideas can also be extended to the design of admissible output feedback control laws that guarantee a feasible (but possibly undetermined) state at all times. The ideas presented in Chapter 6 also serve as a

starting point for the derivation of admissible output feedback control laws for discrete-time dynamic systems. Theoretical guarantees for the asymptotic stability of the resulting closed-loop system are to be investigated.

Applications to Power Systems and Beyond. Additional to the use cases studied in this thesis, we sense interesting applications in network expansion planning and sector coupling. For instance, one could apply our framework to maximize the installed power capacity of decentralized generation units in (large) distribution networks. In our opinion, this task is strongly related to the optimal placement of controllable network coupling devices (e.g., DC-DC links), which can be exploited to reroute the power flows and prevent undesired voltages rises.

We further believe that the interactions between the power network with other networks (communication, gas, water, transport, etc.) shall be understood in more detail. What are the key cyber-physical effects that network models should capture? How to design control algorithms with enhanced operational resilience for such large-scale, time-evolving complex networks?

Acknowledgments

This thesis was sponsored by the German Federal Ministry of Education and Research in project *AlgoRes* (grant no. 01|S18066A). It has been performed in the context of the LOEWE center *emergenCITY*.

I would like to express my deepest gratitude to Prof. Florian Steinke for the opportunity of doing research in his lab during the last three years, for the supervision of my Ph.D. thesis, and for the inspiring conversations on both technical and philosophical topics. My sincere gratitude also to Prof. Timm Faulwasser for his willingness to accept and evaluate this thesis, for the fruitful discussions and remarks. I also thank my students and colleagues for the nice time in the lab and all advices leading to the successful completion of this work. Special thanks also go to my friends for the pleasant talks, trips, and experiences together. For their unconditional support and company in the journey of life, I finally express infinite gratitude to my parents Isaura and Jeronimo, my brother Oscar, and my girlfriend Fabiola. Without you, I would not be where I am today.

Erklärungen laut Promotionsordnung

§ 8 Abs. 1 lit. c PromO Ich versichere hiermit, dass die elektronische Version meiner Dissertation mit der schriftlichen Version übereinstimmt.

§ 8 Abs. 1 lit. d PromO Ich versichere hiermit, dass zu einem vorherigen Zeitpunkt noch keine Promotion versucht wurde. In diesem Fall sind nähere Angaben über Zeitpunkt, Hochschule, Dissertationsthema und Ergebnis dieses Versuchs mitzuteilen.

§ 9 Abs. 1 PromO Ich versichere hiermit, dass die vorliegende Dissertation selbstständig und nur unter Verwendung der angegebenen Quellen verfasst wurde.

§ 9 Abs. 2 PromO Die Arbeit hat bisher noch nicht zu Prüfungszwecken gedient.

Darmstadt, den 30.11.2021, Edwin Mora

Edwin Camilo Mora Gil

References

[1] I. E. Agency. *Electricity Information: Overview*. 2020. URL: https://www.iea.org/reports/electricity-information-overview.

[2] F. I. for Solar Energy Systems. *Net Public Electricity Generation in Germany in 2020*. 2020. URL: https://energy-charts.info/downloads.html?l=en&c=DE.

[3] A. Toffler. *The third wave*. Vol. 484. Bantam books New York, 1980.

[4] K. Kostková, Ľ. Omelina, P. Kyčina, and P. Jamrich. "An introduction to load management". In: *Electric Power Systems Research* 95 (2013), pp. 184–191.

[5] C. P. Mediwaththe, E. R. Stephens, D. B. Smith, and A. Mahanti. "A Dynamic Game for Electricity Load Management in Neighborhood Area Networks". In: *IEEE Transactions on Smart Grid* 7.3 (2016), pp. 1329–1336.

[6] M. S. ElNozahy and M. M. A. Salama. "Technical impacts of grid-connected photovoltaic systems on electrical networks—A review". In: *Journal of Renewable and Sustainable Energy* 5.3 (2013), p. 032702.

[7] T. Stetz, F. Marten, and M. Braun. "Improved Low Voltage Grid-Integration of Photovoltaic Systems in Germany". In: *IEEE Transactions on Sustainable Energy* 4.2 (2013), pp. 534–542.

[8] S. Pequito, N. Popli, S. Kar, M. D. Ilić, and A. P. Aguiar. "A framework for actuator placement in large scale power systems: Minimal strong structural controllability". In: *2013 5th IEEE International Workshop on Computational Advances in Multi-Sensor Adaptive Processing (CAMSAP)*. 2013, pp. 416–419.

[9] I. E. Agency. *Solar PV*. 2021. URL: https://www.iea.org/reports/solar-pv.

[10] F. ISE. *Recent Facts about Photovoltaics in Germany*. 2021. URL: https://www.ise.fraunhofer.de/en/publications/studies/recent-facts-about-pv-in-germany.html.

[11] I. E. Agency. *Global EV stock by mode in the Sustainable Development Scenario 2020-2030*. 2021. URL: https://www.iea.org/data-and-statistics/charts/global-ev-stock-by-mode-in-the-sustainable-development-scenario-2020-2030.

[12] F. Pasqualetti, F. Dörfler, and F. Bullo. "Control-Theoretic Methods for Cyber-physical Security: Geometric Principles for Optimal Cross-Layer Resilient Control Systems". In: *IEEE Control Systems Magazine* 35.1 (Feb. 2015), pp. 110–127.

[13] F. Milano, F. Dörfler, G. Hug, D. J. Hill, and G. Verbič. "Foundations and Challenges of Low-Inertia Systems (Invited Paper)". In: *2018 Power Systems Computation Conference (PSCC)*. 2018, pp. 1–25.

[14] *Operation Handbook – Appendix 1: Load frequency control and performance*. Tech. rep. ENTSO-E, 2015. URL: https://eepublicdownloads.entsoe.eu/clean-documents/pre2015/publications/entsoe/Operation_Handbook/Policy_1_Appendix%20_final.pdf.

[15] A. Street, F. Oliveira, and J. M. Arroyo. "Contingency-Constrained Unit Commitment With $n - K$ Security Criterion: A Robust Optimization Approach". In: *IEEE Transactions on Power Systems* 26.3 (2011), pp. 1581–1590.

[16] Q. Wang, J.-P. Watson, and Y. Guan. "Two-stage robust optimization for N-k contingency-constrained unit commitment". In: *IEEE Transactions on Power Systems* 28.3 (2013), pp. 2366–2375.

[17] L. Grigsby. *Power System Stability and Control*. Online access with subscription: Proquest Ebook Central. CRC Press, 2017.

[18] R. C. Dorf and R. H. Bishop. *Modern control systems*. Pearson Prentice Hall, 2008.

[19] A. M. Lyapunov. "The general problem of the stability of motion". In: *International Journal of Control* 55.3 (Mar. 1992), pp. 531–534.

[20] E. Mora and F. Steinke. "On the minimal set of controllers and sensors for linear power flow". In: *Electric Power Systems Research* 190 (2021). Presented at the 21st Power Systems Computation Conference (PSCC) 2020, p. 106647.

[21] E. Mora and F. Steinke. "Verifying the existence of admissible piecewise-affine control policies for constrained linear power flow". In: *22nd Power Systems Computation Conference (PSCC)*. Porto, Portugal, June 2022, pp. 1–7.

[22] E. Mora and F. Steinke. "Computing sparse affine-linear control policies for linear power flow in microgrids". In: *2020 IEEE PES Innovative Smart Grid Technologies Europe (ISGT-Europe)*. 2020, pp. 364–368.

[23] E. Mora and F. Steinke. “Robust voltage regulation for active distribution networks with imperfect observability”. In: *2021 IEEE Madrid PowerTech*. 2021, pp. 1–6.

[24] E. Mora and F. Steinke. “Minimal Control of Constrained, Partially Controllable & Observable Linear Systems”. In: *IFAC-PapersOnLine* 53.2 (2020). Presented at the 21st IFAC World Congress 2020, pp. 4521–4526.

[25] Q. Shafiee, J. M. Guerrero, and J. C. Vasquez. “Distributed Secondary Control for Islanded Microgrids—A Novel Approach”. In: *IEEE Transactions on Power Electronics* 29.2 (2014), pp. 1018–1031.

[26] D. K. Molzahn, F. Dörfler, H. Sandberg, S. H. Low, S. Chakrabarti, R. Baldick, and J. Lavaei. “A Survey of Distributed Optimization and Control Algorithms for Electric Power Systems”. In: *IEEE Transactions on Smart Grid* 8.6 (Nov. 2017), pp. 2941–2962.

[27] J. W. Simpson-Porco, Q. Shafiee, F. Dörfler, J. C. Vasquez, J. M. Guerrero, and F. Bullo. “Secondary Frequency and Voltage Control of Islanded Microgrids via Distributed Averaging”. In: *IEEE Transactions on Industrial Electronics* 62.11 (2015), pp. 7025–7038.

[28] A. Ben-Tal, L. El Ghaoui, and A. Nemirovski. *Robust Optimization*. Princeton Series in Applied Mathematics. Princeton University Press, Oct. 2009.

[29] A. Schrijver. *Combinatorial Optimization - Polyhedra and Efficiency*. Springer, 2003.

[30] S. Engell. “Feedback Control for Optimal Process Operation”. In: *IFAC Proceedings Volumes* 39.2 (2006). 6th IFAC Symposium on Advanced Control of Chemical Processes, pp. 13–26.

[31] X. Bai, L. Qu, and W. Qiao. “Robust AC Optimal Power Flow for Power Networks With Wind Power Generation”. In: *IEEE Transactions on Power Systems* 31.5 (2016), pp. 4163–4164.

[32] X. Wu and A. J. Conejo. “An Efficient Tri-Level Optimization Model for Electric Grid Defense Planning”. In: *IEEE Transactions on Power Systems* 32.4 (2017), pp. 2984–2994.

[33] D. Bertsimas, D. A. Iancu, and P. A. Parrilo. “Optimality of Affine Policies in Multistage Robust Optimization”. In: *Mathematics of Operations Research* 35.2 (2010), pp. 363–394.

[34] Á. Lorca, X. A. Sun, E. Litvinov, and T. Zheng. “Multistage Adaptive Robust Optimization for the Unit Commitment Problem”. In: *Operations Research* 64.1 (2016), pp. 32–51.

[35] S. Boyd and L. Vandenberghe. *Convex Optimization*. Cambridge University Press, Mar. 2004.

[36] A. Mešanović, U. Münz, and C. Ebenbauer. "Robust Optimal Power Flow for Mixed AC/DC Transmission Systems With Volatile Renewables". In: *IEEE Transactions on Power Systems* 33.5 (Sept. 2018), pp. 5171–5182.

[37] E. Roos and D. den Hertog. "Reducing Conservatism in Robust Optimization". In: *INFORMS Journal on Computing* 32.4 (2020), pp. 1109–1127.

[38] J. M. Morales and J. Perez-Ruiz. "Point Estimate Schemes to Solve the Probabilistic Power Flow". In: *IEEE Transactions on Power Systems* 22.4 (2007), pp. 1594–1601.

[39] Z. Q. Xie, T. Y. Ji, M. S. Li, and Q. H. Wu. "Quasi-Monte Carlo Based Probabilistic Optimal Power Flow Considering the Correlation of Wind Speeds Using Copula Function". In: *IEEE Transactions on Power Systems* 33.2 (2018), pp. 2239–2247.

[40] A. Schellenberg, W. Rosehart, and J. Aguado. "Cumulant-based probabilistic optimal power flow (P-OPF) with Gaussian and gamma distributions". In: *IEEE Transactions on Power Systems* 20.2 (2005), pp. 773–781.

[41] T. Mühlpfordt, T. Faulwasser, and V. Hagenmeyer. "A generalized framework for chance-constrained optimal power flow". In: *Sustainable Energy, Grids and Networks* 16 (2018), pp. 231–242.

[42] D. Métivier, M. Vuffray, and S. Misra. "Efficient polynomial chaos expansion for uncertainty quantification in power systems". In: *Electric Power Systems Research* 189 (2020), p. 106791.

[43] K. Margellos, P. Goulart, and J. Lygeros. "On the Road Between Robust Optimization and the Scenario Approach for Chance Constrained Optimization Problems". In: *IEEE Transactions on Automatic Control* 59.8 (2014), pp. 2258–2263.

[44] F. Borrelli, A. Bemporad, and M. Morari. "Geometric Algorithm for Multiparametric Linear Programming". In: *Journal of Optimization Theory and Applications* 118 (3 2003), pp. 515, 540.

[45] C. Jones, M. Barić, and M. Morari. "Multiparametric Linear Programming with Applications to Control". In: *European Journal of Control* 13.2 (2007), pp. 152–170.

[46] V. Dua and E. N. Pistikopoulos. "An algorithm for the solution of multiparametric mixed integer linear programming problems". In: *Annals of operations research* 99.1 (2000), pp. 123–139.

[47] N. A. Diangelakis, I. S. Pappas, and E. N. Pistikopoulos. "On multi-parametric/explicit nmpc for quadratically constrained problems". In: *IFAC-PapersOnLine* 51.20 (2018), pp. 400–405.

[48] A. Bemporad, M. Morari, V. Dua, and E. N. Pistikopoulos. "The explicit linear quadratic regulator for constrained systems". In: *Automatica* 38.1 (2002), pp. 3–20.

[49] A. Bemporad, F. Borrelli, and M. Morari. "Model predictive control based on linear programming - the explicit solution". In: *IEEE Transactions on Automatic Control* 47.12 (2002), pp. 1974–1985.

[50] T. Johansen. "On multi-parametric nonlinear programming and explicit nonlinear model predictive control". In: *Proceedings of the 41st IEEE Conference on Decision and Control, 2002.* Vol. 3. 2002, 2768–2773 vol.3.

[51] A. Alessio and A. Bemporad. "A Survey on Explicit Model Predictive Control". In: *Nonlinear Model Predictive Control: Towards New Challenging Applications*. Berlin, Heidelberg: Springer Berlin Heidelberg, 2009, pp. 345–369.

[52] M. Morari, Y. Arkun, and G. Stephanopoulos. "Studies in the synthesis of control structures for chemical processes: Part I: Formulation of the problem. Process decomposition and the classification of the control tasks. Analysis of the optimizing control structures". In: *AIChE Journal* 26.2 (1980), pp. 220–232.

[53] C. Lin, W. Wu, X. Chen, and W. Zheng. "Decentralized Dynamic Economic Dispatch for Integrated Transmission and Active Distribution Networks Using Multi-Parametric Programming". In: *IEEE Transactions on Smart Grid* 9.5 (2018), pp. 4983–4993.

[54] Y. Ng, S. Misra, L. A. Roald, and S. Backhaus. "Statistical Learning for DC Optimal Power Flow". In: *2018 Power Systems Computation Conference (PSCC)*. 2018, pp. 1–7.

[55] M. van de Wal and B. de Jager. "A review of methods for input/output selection". In: *Automatica* 37.4 (2001), pp. 487–510.

[56] Y.-Y. Liu and A.-L. Barabási. "Control principles of complex systems". In: *Rev. Mod. Phys.* 88 (3 Sept. 2016), p. 035006.

[57] S. Pequito, S. Kar, and A. P. Aguiar. "A Framework for Structural Input/Output and Control Configuration Selection in Large-Scale Systems". In: *IEEE Transactions on Automatic Control* 61.2 (Feb. 2016).

[58] J. A. Taylor, N. Luangsomboon, and D. Fooladivanda. "Allocating Sensors and Actuators via Optimal Estimation and Control". In: *IEEE Transactions on Control Systems Technology* 25.3 (2017), pp. 1060–1067.

[59] J. Li, X. Chen, S. Pequito, G. J. Pappas, and V. M. Preciado. “Structural Target Controllability of Undirected Networks”. In: *2018 IEEE Conference on Decision and Control (CDC)*. IEEE, Dec. 2018.

[60] G. Lindmark and C. Altafini. “Minimum Energy Control for Complex Networks”. In: *Nature - Scientific Reports* 8.1 (Feb. 2018).

[61] F. Pasqualetti, S. Zampieri, and F. Bullo. “Controllability Metrics, Limitations and Algorithms for Complex Networks”. In: *IEEE Transactions on Control of Network Systems* 1.1 (Mar. 2014), pp. 40–52.

[62] T. H. Summers, F. L. Cortesi, and J. Lygeros. “On Submodularity and Controllability in Complex Dynamical Networks”. In: *IEEE Transactions on Control of Network Systems* 3.1 (Mar. 2016), pp. 91–101.

[63] J. Lunze. *Regelungstechnik 2: Mehrgrößensysteme, Digitale Regelung*. 9th ed. Lehrbuch. Berlin: Springer Vieweg, 2016.

[64] C.-Y. Chang, S. Martínez, and J. Cortés. “Co-Optimization of Control and Actuator Selection for Cyber-Physical Systems”. In: *IFAC-PapersOnLine* 51.23 (2018), pp. 118–123.

[65] S. Nugroho, A. F. Taha, T. Summers, and N. Gatsis. “Simultaneous Sensor and Actuator Selection/Placement through Output Feedback Control”. In: *2018 Annual American Control Conference (ACC)*. 2018, pp. 4159–4164.

[66] A. Taha, N. Gatsis, T. Summers, and S. Nugroho. “Time-Varying Sensor and Actuator Selection for Uncertain Cyber-Physical Systems”. In: *IEEE Transactions on Control of Network Systems* 6.2 (June 2019).

[67] F. Lin, M. Fardad, and M. R. Jovanović. “Design of Optimal Sparse Feedback Gains via the Alternating Direction Method of Multipliers”. In: *IEEE Transactions on Automatic Control* 58.9 (2013), pp. 2426–2431.

[68] X. Wu, F. Dörfler, and M. R. Jovanović. “Input-Output Analysis and Decentralized Optimal Control of Inter-Area Oscillations in Power Systems”. In: *IEEE Transactions on Power Systems* 31.3 (2016), pp. 2434–2444.

[69] M. Fardad, F. Lin, and M. R. Jovanović. “Sparsity-promoting optimal control for a class of distributed systems”. In: *Proceedings of the 2011 American Control Conference*. 2011, pp. 2050–2055.

[70] S. A. Nugroho, A. F. Taha, N. Gatsis, T. H. Summers, and R. Krishnan. “Algorithms for joint sensor and control nodes selection in dynamic networks”. In: *Automatica* 106 (2019), pp. 124–133.

[71] E. Kerrigan. “Robust constraint satisfaction: invariant sets and predictive control”. PhD thesis. University of Cambridge, Nov. 2000.

[72] C. E. T. Dorea. “Output-feedback controlled-invariant polyhedra for constrained linear systems”. In: *Proceedings of the 48h IEEE Conference on Decision and Control (CDC) held jointly with 2009 28th Chinese Control Conference*. IEEE, Dec. 2009.

[73] T. E. Marlin, A. N. Hrymak, et al. “Real-time operations optimization of continuous processes”. In: *AIChE Symposium Series*. Vol. 93. 316. New York, NY: American Institute of Chemical Engineers, 1971-c2002. 1997, pp. 156–164.

[74] K. Ariyur and M. Krstic. *Real-Time Optimization by Extremum-Seeking Control*. Wiley-Interscience. Wiley, 2003.

[75] A. Marchetti, B. Chachuat, and D. Bonvin. “Modifier-adaptation methodology for real-time optimization”. In: *Industrial & engineering chemistry research* 48.13 (2009), pp. 6022–6033.

[76] L. S. P. Lawrence, J. W. Simpson-Porco, and E. Mallada. “Linear-Convex Optimal Steady-State Control”. In: *IEEE Transactions on Automatic Control* (2020), pp. 1–1.

[77] W. Karush. “Minima of functions of several variables with inequalities as side conditions.” PhD thesis. Thesis (S.M.)–University of Chicago, Department of Mathematics, Dec. 1939.

[78] H. W. Kuhn and A. W. Tucker. “Nonlinear programming”. In: *Proceedings of the Berkeley Symposium on Mathematical Statistics and Probability*. 1951, pp. 481–492.

[79] S. Boyd, L. El Ghaoui, E. Feron, and V. Balakrishnan. *Linear matrix inequalities in system and control theory*. SIAM, 1994.

[80] D. Bertsekas. *Dynamic programming and optimal control: Volume I*. Vol. 1. Athena scientific, 2012.

[81] P. Kundur, N. Balu, and M. Lauby. *Power System Stability and Control*. EPRI power system engineering series. McGraw-Hill Education, 1994.

[82] K. Ogata. *Modern Control Engineering*. Instrumentation and controls series. Prentice Hall, 2010.

[83] L. A. Wolsey and G. L. Nemhauser. *Integer and combinatorial optimization*. Vol. 55. John Wiley & Sons, 1999.

[84] G. F. Franklin, J. D. Powell, A. Emami-Naeini, and J. D. Powell. *Feedback control of dynamic systems*. Vol. 4. Prentice hall Upper Saddle River, NJ, 2002.

[85] R. S. Sutton and A. G. Barto. *Reinforcement learning: An introduction*. MIT press, 2018.

[86] D. Bertsekas. *Reinforcement learning and optimal control*. Athena Scientific, 2019.

[87] R. E. Kalman. "A New Approach to Linear Filtering and Prediction Problems". In: *Transactions of the ASME–Journal of Basic Engineering* 82.Series D (1960), pp. 35–45.

[88] M. Baran and F. Wu. "Optimal capacitor placement on radial distribution systems". In: *IEEE Transactions on Power Delivery* 4.1 (1989), pp. 725–734.

[89] M. Baran and F. Wu. "Optimal sizing of capacitors placed on a radial distribution system". In: *IEEE Transactions on Power Delivery* 4.1 (1989), pp. 735–743.

[90] D. Donoho. "Compressed sensing". In: *IEEE Transactions on Information Theory* 52.4 (2006), pp. 1289–1306.

[91] R. Isermann. "Feedforward Control". In: *Digital Control Systems: Volume 2: Stochastic Control, Multivariable Control, Adaptive Control, Applications*. Berlin, Heidelberg: Springer Berlin Heidelberg, 1991, pp. 56–67.

[92] M. C. Ferris, O. L. Mangasarian, and S. J. Wright. *Linear programming with MATLAB*. SIAM, 2007.

[93] N. P. Faísca, V. Dua, and E. N. Pistikopoulos. "Multiparametric Linear and Quadratic Programming". In: *Multi-Parametric Programming*. John Wiley & Sons, Ltd, 2007. Chap. 1, pp. 1–23.

[94] M. S. Floater. "One-to-One Piecewise Linear Mappings over Triangulations". In: *Mathematics of Computation* 72.242 (2003), pp. 685–696.

[95] M. Henk, R.-G. Jürgen, and G. Ziegler. "Basic Properties Of Convex Polytopes". In: *Handbook of Discrete and Computational Geometry* (Mar. 1999).

[96] S. Mehrotra. "On the Implementation of a Primal-Dual Interior Point Method". In: *SIAM Journal on Optimization* 2.4 (1992), pp. 575–601.

[97] Gurobi Optimization, LLC. *Gurobi Optimizer Reference Manual*. 2021. URL: `https://www.gurobi.com`.

[98] P. M. Castro. "Tightening piecewise McCormick relaxations for bilinear problems". In: *Computers & Chemical Eng.* 72 (2015), pp. 300–311.

[99] P. Kirst, O. Stein, and P. Steuermann. "An Enhanced Spatial Branch-and-Bound Method in Global Optimization with Nonconvex Constraints [Preprint]". In: *TOP* (2015).

[100] G. Still. "Lectures on parametric optimization: An introduction". In: *Optimization Online* (2018).

[101] M. Herceg, M. Kvasnica, C. Jones, and M. Morari. "Multi-Parametric Toolbox 3.0". In: *Proc. of the European Control Conference*. Zürich, Switzerland, July 2013, pp. 502–510.

[102] A. Abedi, L. Gaudard, and F. Romerio. "Review of major approaches to analyze vulnerability in power system". In: *Reliability Engineering & System Safety* 183 (Mar. 2019), pp. 153–172.

[103] W. Yuan, J. Wang, F. Qiu, C. Chen, C. Kang, and B. Zeng. "Robust Optimization-Based Resilient Distribution Network Planning Against Natural Disasters". In: *IEEE Transactions on Smart Grid* 7.6 (Nov. 2016), pp. 2817–2826.

[104] G. Li, L. Deng, G. Xiao, P. Tang, C. Wen, W. Hu, J. Pei, L. Shi, and H. E. Stanley. "Enabling Controlling Complex Networks with Local Topological Information". In: *Nature - Scientific Reports* 8.4593 (Mar. 2018).

[105] Ching-Tai Lin. "Structural controllability". In: *IEEE Transactions on Automatic Control* 19.3 (June 1974), pp. 201–208.

[106] B. Polyak, M. Khlebnikov, and P. Shcherbakov. "An LMI approach to structured sparse feedback design in linear control systems". In: *2013 European Control Conference (ECC)*. 2013, pp. 833–838.

[107] F. Dörfler, M. R. Jovanović, M. Chertkov, and F. Bullo. "Sparsity-Promoting Optimal Wide-Area Control of Power Networks". In: *IEEE Transactions on Power Systems* 29.5 (2014), pp. 2281–2291.

[108] X.-S. Yang. *Nature-Inspired Optimization Algorithms*. Second Edition. Academic Press, 2021, pp. 111–121.

[109] B. Selman and C. P. Gomes. "Hill-climbing Search". In: *Encyclopedia of Cognitive Science*. American Cancer Society, 2006, pp. 333–336.

[110] D. Bienstock and A. Verma. "The $N - k$ Problem in Power Grids: New Models, Formulations, and Numerical Experiments". In: *SIAM Journal on Optimization* 20.5 (2010), pp. 2352–2380.

[111] M. Ahumada-Paras, K. Sundar, R. Bent, and A. Zlotnik. "N-k interdiction modeling for natural gas networks". In: *Electric Power Systems Research* 190 (2021), p. 106725.

[112] J. Salmeron, K. Wood, and R. Baldick. "Analysis of electric grid security under terrorist threat". In: *IEEE Transactions on Power Systems* 19.2 (2004), pp. 905–912.

[113] A. Pinar, J. Meza, V. Donde, and B. Lesieutre. "Optimization Strategies for the Vulnerability Analysis of the Electric Power Grid". In: *SIAM Journal on Optimization* 20.4 (2010), pp. 1786–1810.

[114] T. Kim, S. J. Wright, D. Bienstock, and S. Harnett. "Analyzing Vulnerability of Power Systems with Continuous Optimization Formulations". In: *IEEE Transactions on Network Science and Engineering* 3.3 (2016), pp. 132–146.

[115] K. Sundar, C. Coffrin, H. Nagarajan, and R. Bent. "Probabilistic N-k failure-identification for power systems". In: *Networks* 71.3 (2018), pp. 302–321.

[116] F. Pasqualetti, F. Dörfler, and F. Bullo. "Attack Detection and Identification in Cyber-Physical Systems". In: *IEEE Transactions on Automatic Control* 58.11 (2013), pp. 2715–2729.

[117] S. Sridhar and M. Govindarasu. "Model-Based Attack Detection and Mitigation for Automatic Generation Control". In: *IEEE Transactions on Smart Grid* 5.2 (2014), pp. 580–591.

[118] S. Soltan, M. Yannakakis, and G. Zussman. "REACT to Cyber Attacks on Power Grids". In: *IEEE Transactions on Network Science and Engineering* 6.3 (2019), pp. 459–473.

[119] S. Braun, S. Albrecht, and S. Lucia. "A Hierarchical Attack Identification Method for Nonlinear Systems". In: *2020 59th IEEE Conference on Decision and Control (CDC)*. 2020, pp. 5035–5042.

[120] J. Giraldo, D. Urbina, A. Cardenas, J. Valente, M. Faisal, J. Ruths, N. O. Tippenhauer, H. Sandberg, and R. Candell. "A Survey of Physics-Based Attack Detection in Cyber-Physical Systems". In: *ACM Comput. Surv.* 51.4 (July 2018).

[121] R. Kalman. "On the general theory of control systems". In: *1st International IFAC Congress on Automatic and Remote Control*. 1960.

[122] T. Iwasaki and R. Skelton. "Parametrization of all stabilizing controllers via quadratic Lyapunov functions". In: *Journal of Optimization Theory and Applications* 85.2 (1995), pp. 291–307.

[123] J. Gadewadikar, F. Lewis, L. Xie, V. Kucera, and M. Abu-Khalaf. "Parameterization of All Stabilizing Hc. Static State-Feedback Gains: Application to Output-Feedback Design". In: *Proceedings of the 45th IEEE Conference on Decision and Control*. 2006, pp. 3566–3571.

[124] I. R. Petersen and R. Tempo. "Robust control of uncertain systems: Classical results and recent developments". In: *Automatica* 50.5 (May 2014), pp. 1315–1335.

[125] G. C. Calafiore and L. Fagiano. "Robust model predictive control via scenario optimization". In: *IEEE Transactions on Automatic Control* 58.1 (Jan. 2013), pp. 219–224.

[126] M. Farina, L. Giulioni, and R. Scattolini. "Stochastic linear model predictive control with chance constraints–A review". In: *Journal of Process Control* 44 (Aug. 2016), pp. 53–67.

[127] I. M. Sanz, P. D. Judge, C. E. Spallarossa, B. Chaudhuri, and T. C. Green. "Dynamic Overload Capability of VSC HVDC Interconnections for Frequency Support". In: *IEEE Transactions on Energy Conversion* 32.4 (Dec. 2017).

[128] G. D. Carne, G. Buticchi, M. Liserre, P. Marinakis, and C. Vournas. "Coordinated frequency and Voltage Overload Control of Smart Transformers". In: *2015 IEEE Eindhoven PowerTech*. IEEE, June 2015.

[129] M. Diehl, H. G. Bock, J. P. Schlöder, R. Findeisen, Z. Nagy, and F. Allgöwer. "Real-time optimization and nonlinear model predictive control of processes governed by differential-algebraic equations". In: *Journal of Process Control* 12.4 (2002), pp. 577–585.

[130] G. De Souza, D. Odloak, and A. C. Zanin. "Real time optimization (RTO) with model predictive control (MPC)". In: *Computers & Chemical Engineering* 34.12 (2010), pp. 1999–2006.

[131] T. Faulwasser, M. Korda, C. N. Jones, and D. Bonvin. "Turnpike and dissipativity properties in dynamic real-time optimization and economic MPC". In: *53rd ieee conference on decision and control*. IEEE. 2014, pp. 2734–2739.

[132] Z. Zhang, Z. Wu, D. Rincon, and P. D. Christofides. "Real-time optimization and control of nonlinear processes using machine learning". In: *Mathematics* 7.10 (2019), p. 890.

[133] B. Powell, D. Machalek, and T. Quah. "Real-time optimization using reinforcement learning". In: *Computers & Chemical Engineering* 143 (2020), p. 107077.

[134] A. Jokic, M. Lazar, and P. P. J. van den Bosch. "On Constrained Steady-State Regulation: Dynamic KKT Controllers". In: *IEEE Transactions on Automatic Control* 54.9 (2009), pp. 2250–2254.

[135] M. Colombino, E. Dall'Anese, and A. Bernstein. "Online Optimization as a Feedback Controller: Stability and Tracking". In: *IEEE Transactions on Control of Network Systems* 7.1 (2020), pp. 422–432.

[136] L. S. P. Lawrence, J. W. Simpson-Porco, and E. Mallada. "Linear-Convex Optimal Steady-State Control". In: *IEEE Transactions on Automatic Control* (2020), pp. 1–1.

[137] A. Hauswirth, S. Bolognani, G. Hug, and F. Dörfler. "Timescale Separation in Autonomous Optimization". In: *IEEE Transactions on Automatic Control* 66.2 (2021), pp. 611–624.

[138] J. Cortés. "Finite-time convergent gradient flows with applications to network consensus". In: *Automatica* 42.11 (2006), pp. 1993–2000.

[139] G. Bianchin, J. Cortes, J. I. Poveda, and E. Dall'Anese. "Time-varying optimization of LTI systems via projected primal-dual gradient flows". In: *arXiv preprint arXiv:2101.01799* (2021).

[140] M. Picallo, S. Bolognani, and F. Dörfler. "Closing the loop: Dynamic state estimation and feedback optimization of power grids". In: *Electric Power Systems Research* 189 (2020), p. 106753.

[141] A. Rantzer. "A separation principle for distributed control". In: *Proceedings of the 45th IEEE Conference on Decision and Control*. IEEE. 2006, pp. 3609–3613.

[142] M. S. Sadabadi and D. Peaucelle. "From static output feedback to structured robust static output feedback: A survey". In: *Annual Reviews in Control* 42 (2016), pp. 11–26.

[143] R. Brockett and J. Willems. "Frequency domain stability criteria–Part I". In: *IEEE Transactions on automatic control* 10.3 (1965), pp. 255–261.

[144] W. J. Rugh. *Linear system theory*. Prentice-Hall, Inc., 1996.

[145] B. D. Anderson and J. B. Moore. *Optimal control: linear quadratic methods*. Courier Corporation, 2007.

[146] P. Benner, J.-R. Li, and T. Penzl. "Numerical solution of large-scale Lyapunov equations, Riccati equations, and linear-quadratic optimal control problems". In: *Numerical Linear Algebra with Applications* 15.9 (2008), pp. 755–777.

[147] V. Simoncini. "A new iterative method for solving large-scale Lyapunov matrix equations". In: *SIAM Journal on Scientific Computing* 29.3 (2007), pp. 1268–1288.

[148] S. Gugercin, D. C. Sorensen, and A. C. Antoulas. "A modified low-rank Smith method for large-scale Lyapunov equations". In: *Numerical Algorithms* 32.1 (2003), pp. 27–55.

[149] J. Burke, D. Henrion, A. Lewis, and M. Overton. "HIFOO - A Matlab Package For Fixed-order Controller Design and $\mathcal{H}_\infty$ Optimization". In: *IFAC Proceedings Volumes* 39.9 (2006). 5th IFAC Symposium on Robust Control Design, pp. 339–344.

[150] C. G. Broyden. "The Convergence of a Class of Double-rank Minimization Algorithms 1. General Considerations". In: *IMA Journal of Applied Mathematics* 6.1 (Mar. 1970), pp. 76–90.

[151] A. Hassibi, J. How, and S. Boyd. "A path-following method for solving BMI problems in control". In: *Proceedings of the 1999 American Control Conference*. IEEE, 1999.

[152] A. Trofino. “Robust stability and domain of attraction of uncertain nonlinear systems”. In: *Proceedings of the 2000 American Control Conference. ACC (IEEE Cat. No.00CH36334)*. Vol. 5. 2000, 3707–3711 vol.5.

[153] L. Guttman. “Enlargement Methods for Computing the Inverse Matrix”. In: *The Annals of Mathematical Statistics* 17.3 (1946), pp. 336–343.

[154] J. Vanbiervliet, B. Vandereycken, W. Michiels, S. Vandewalle, and M. Diehl. “The smoothed spectral abscissa for robust stability optimization”. In: *SIAM Journal on Optimization* 20.1 (2008), pp. 156–171.

[155] R. Bellman. “A Markovian Decision Process”. In: *Indiana Univ. Math. J.* 6 (4 1957), pp. 679–684.

[156] E. L. Lawler and D. E. Wood. “Branch-and-bound methods: A survey”. In: *Operations research* 14.4 (1966), pp. 699–719.

[157] J. Löfberg. “YALMIP : A Toolbox for Modeling and Optimization in MATLAB”. In: *In Proceedings of the CACSD Conference*. Taipei, Taiwan, 2004.

[158] A. Mešanović, U. Münz, A. Szabo, M. Mangold, J. Bamberger, M. Metzger, C. Heyde, R. Krebs, and R. Findeisen. “Structured controller parameter tuning for power systems”. In: *Control Engineering Practice* 101 (2020), p. 104490.

[159] B. Bollobás and B. Bollobas. *Modern graph theory*. Vol. 184. Springer Science & Business Media, 1998.

[160] C. Cheng and D. Shirmohammadi. “A three-phase power flow method for real-time distribution system analysis”. In: *IEEE Transactions on Power Systems* 10.2 (1995), pp. 671–679.

[161] A. R. Al-Roomi. *Power Flow Test Systems Repository*. Halifax, Nova Scotia, Canada, 2015. URL: `https://al-roomi.org/power-flow`.

[162] N. Mahmud and A. Zahedi. “Review of control strategies for voltage regulation of the smart distribution network with high penetration of renewable distributed generation”. In: *Renewable and Sustainable Energy Reviews* 64 (2016), pp. 582–595.

[163] N. Daratha, B. Das, and J. Sharma. “Coordination Between OLTC and SVC for Voltage Regulation in Unbalanced Distribution System Distributed Generation”. In: *IEEE Transactions on Power Systems* 29.1 (2014), pp. 289–299.

[164] P. Li, H. Ji, C. Wang, J. Zhao, G. Song, F. Ding, and J. Wu. “Coordinated Control Method of Voltage and Reactive Power for Active Distribution Networks Based on Soft Open Point”. In: *IEEE Transactions on Sustainable Energy* 8.4 (2017), pp. 1430–1442.

[165] F. Bignucolo, R. Caldon, and V. Prandoni. "Radial MV networks voltage regulation with distribution management system coordinated controller". In: *Electric Power Systems Research* 78.4 (2008), pp. 634–645.

[166] T. Niknam, M. Zare, and J. Aghaei. "Scenario-based multiobjective volt/var control in distribution networks including renewable energy sources". In: *IEEE Transactions on Power Delivery* 27.4 (2012), pp. 2004–2019.

[167] P. Li, C. Zhang, Z. Wu, Y. Xu, M. Hu, and Z. Dong. "Distributed adaptive robust voltage/var control with network partition in active distribution networks". In: *IEEE Transactions on Smart Grid* 11.3 (2019), pp. 2245–2256.

[168] *IEEE 123 Bus Test Case*. URL: `https://site.ieee.org/pes-testfeeders/resources/`.

[169] J. F. Benders. "Partitioning procedures for solving mixed-variables programming problems". In: *Numerische Mathematik* 4.1 (1962), pp. 238–252.

[170] G. B. Dantzig and P. Wolfe. "Decomposition Principle for Linear Programs". In: *Operations Research* 8.1 (1960), pp. 101–111.